CHAPTER I
INTRODUCTION

Total cultivated area of the country is 124.75 Mha, which yields about 259.23 Mt of food grain. This has been achieved through the adoption of improved seeds, fertilizer, irrigation, biological mechanized farming and other chemical and mechanical inputs. One of the biggest challenges before the agricultural sector is to meet the growing demand of the food grains to feed the increasing population. This will require both higher energy inputs and better management of food production systems. The availability of farm power per unit area is considered to be an important parameter in evaluating the level of farm mechanization. In India the present level of mechanization is only 1.84 kW/ha, which is very low compared to that available in some of the advanced countries such as Japan (8.75 kW/ha) and Italy (3.01 kW/ha). India is the largest producer of farm tractors in the world which account for 46 per cent of the total share of mechanical power used in the country (Mehta *et al*., 2014). The tractors manufactured in India are mostly rear wheel driven tractors and they are in the power range of 20 to 45 kW. The agricultural tractors are primarily used to perform drawbar work. Drawbar work is defined by the pull and travel speed. Research shows that about 20-55 per cent of the available tractor energy is wasted at the tyre-soil interface. This energy wears the tyres and compacts the soil to a degree that may cause detrimental crop production (Burt *et al.*, 1982). The farm tractors operation can be made efficient by: (1) maximizing the fuel efficiency of the engine and drive train, (2) maximizing the tractive advantage of the traction devices (tyres), and (3) selecting an optimum travel speed for a given tractor-implement system.

1.1 Agricultural Tractors Drawbar Performance Prediction

People working in the area of farm mechanization such as engineers designing tractors and implements have a need for information relating to the performance of tractors in the field. Tractive performance studies are essential in understanding and quantifying the tractor drawbar power utilization. The official tractor drawbar performance tests conducted on a concrete surface provides a valid comparison between tractors. However, the data do not provide much information about performance under field conditions. This is mainly due to the fact that the performance of the tyres or other traction devices is not same under the hard and soft

soil conditions. This shows that, the empirical models and other tools available in the literature to predict the tractor drawbar performance based on their performance on a hard surface are not suitable for use under different field conditions. This compelled the scientists and engineers to evaluate the traction performance of the traction devices (tyres) used in the tractors under controlled soil bin conditions for assessing the tractor drawbar performance. Traction performance is influenced by tyre parameters, soil condition, implement type, and tractor configuration (Brixius, 1987). Traction prediction equations provide a basis for predicting the tractor performance, when combined with the basic information taken from the official tractor drawbar tests. The tractive characteristics of a tyre depend on tyre geometry (width, diameter, and section height), tyre type (radial & bias), lug design, inflation pressure, dynamic load on axle and soil type and conditions (Gill and Vandenberg, 1968; Upadhyaya, 1986).

1.2 Predicting Tractive Potential of Radial-ply Tyres

The majority of the tractors manufactured in India are in the power range of 20-45 kW and are provided with different sizes of bias-ply tyres ranging from 12.4 - 28 to 16.9 - 28. The use of radial-ply tyres is limited due to their non availability in the local market and higher cost. However, the use of radial-ply tyre is gaining popularity as it is one of the best ways to improve tractive efficiency. Radial-ply tyres have been found to be more efficient than the bias-ply tyres in terms of traction performance as well as in fuel economy (Forrest, 1962; Thaden, 1962; Gee-Clough, 1977; Hausz and Akins, 1980; Hauck *et al.*, 1983). These advantages are due to the construction of this type of tyres. Radial-ply tyres have plies that run at right angles to the tread and may have one or more layers or plies. This results in a tyre with flexible side wall. A belt around the radial ply tire gives it strength and stability. The flexible side wall and stable belt leads to longer tyre-soil contact area and uniform pressure distribution, which results in higher pulling ability of the tyre (Hausz, 1985). Tractive characteristics of the tyres are usually determined by conducting either field experiments or tests under the controlled laboratory soil bin conditions. A traction test under controlled soil bin conditions involves loading the test tyre to a desirable dynamic load and then controlling draft or slip in some predetermined manner. The response of the system consists of input torque and draft for the controlled slip, or slip for the controlled draft.

A pre-requisite for the successful design of a traction device is a sound mathematical model for the soil-traction interaction process. These models allow researchers and designers to investigate many problems related to tractor performance under a wide range of operating conditions with a goal of improving the tractor design to optimize tractor operational parameters and to improve the tractor/implement matching. Relative importance of the factors affecting field performance of a tractor can also be achieved using these models without any expensive field-testing.

Numerous studies have been reported on performance prediction of off-road tyre along the years. Some dealt in analytical approaches and others in semi-empirical approaches. The diversity in the approaches of research on off-road tyre performance points to the complexity of the issue. Each of the above-mentioned approaches has some limitations: the analytical approaches are difficult to use, empirical equations are limited to the tested cases and most semi-empirical methods focus on predicting separate performance in braking and driving modes. Out of these, however, the empirical approaches have proved to be useful in solving many complex engineering problems including the tractive performance prediction.

Many of these empirical wheel-soil traction prediction models based on mobility number approach have been developed in US and European countries to suit the conditions prevailing in those countries. The traction prediction equations developed by Brixius (1987) are most prominently used today and has been accepted by the ASABE Standards. The applicability of these equations in Indian soil conditions is unknown. This calls for a systematic study to investigate the traction performance of the radial-ply tractor tyres used in the country and to develop suitable traction prediction models for Indian operating conditions.

1.3 Scope and Objectives

In developing countries, particularly in India, the use of high hp tractors in the power segment of 37 kW and beyond has been found to be increasing during the last one decade. These tractors are preferred for heavy field and haulage operations where greater amount of traction power is needed. The radial tyres are expected to use in such tractors because they provide better traction requirement and fuel economy as well as comfort in haulage operations compared to bias-ply tyres. It is essential to have suitable traction prediction models for these tyres to help in designing the new

tractors. In this context, many studies were reported in the past, but the model developed by Brixius in 1987 is the most widely used. The applicability of this model for the tyres used in Indian soil conditions is unknown and the tractive performance of these tyres under varying conditions has so far not been conducted in the country and hence their performance has not been documented. In absence of this information the manufacturers have been designing their tractors based on tractive performance data available in the developed countries. The tractors being designed based on outside data have not been found performing up to the desired level and hence a large amount of energy is lost in converting axle power into useful drawbar power. On comparing with the preliminary experimental data obtained at IIT Kharagpur, the Brixius model was found to over predict the tractive efficiency of 14.9 R 28 tyre by 13-50% under different soil conditions. A need was, therefore, felt to study the traction potential of radial-ply tyres under different soil and tyre operating conditions of India. Such models would be of a great help in developing efficient and cost effective tractors and evaluating their drawbar performance in field as well as haulage operations of Indian operating conditions.

It is noted that, evaluation of traction performance of a driving wheel considers the tyre-soil interaction in two interrelated aspects: (i) deflection characteristics and (ii) traction potential. The former is required to select suitable load-inflation pressure combinations to achieve the desired levels of deflection for assessing the traction potential of tyres under different soil conditions.

Keeping the above points in view the present study has been taken up with the following objectives.

Objectives

1. To study the deflection and contact characteristics of radial-ply tractor tyres at different normal loads and inflation pressures.
2. To study the characteristics of the radial-ply tractor tyres at zero condition.
3. To study the influence of soil, tyre and system parameters on the tractive performance of the tyres.
4. To develop empirical models for drawbar performance prediction of radial-ply tractor tyres for Indian operating conditions and to compare them with the prominently used traction prediction models.

In the present investigation an attempt has been made to study the effect of the operating and structural parameters of the radial-ply tyres on their tractive performance in lateritic sandy loam soil under Indian operating conditions. The various studies reported in the literature related to deflection and traction behaviour of pneumatic tyres under deformable and undeformable terrains are presented in the next chapter supporting the scope of the present investigation.

CHAPTER II
REVIEW OF LITERATURE

The interaction mechanics of a powered pneumatic tyre and a yielding soil are complex. The process of interaction between soil and tyre continues to be the main subject of study of researchers in connection with the necessity to considerably improve the performance characteristics of pneumatic tyres in different soil conditions (Lyasko, 1994). Various researchers have proposed a number of theories for predicting the tractive performance of different traction devices.

In this chapter an attempt has been made to discuss various studies related to the deflection and traction behaviour of pneumatic tyres under deformable and undeformable terrains. The major topics included are as follows.

- Tyre deflection characteristics
- Strength of soil
- Techniques for single wheel testing
- Traction prediction approaches
- Tyre soil and system parameters
- Comparison of radial and bias-ply tyre

2.1 Tyre Deflection Characteristics

Agricultural tractor tyres cushion the vehicle over surface irregularities, provide traction for movement and braking, and also allow adequate steering control for directional stability. In the early 1940s, tyre companies began to offer radial-ply pneumatic tyres for farm tractors**.** Generally two types of tyres are used for agricultural tractors: bias and radial-ply tyres. Bias-ply tyres are widely used in India and other Asian countries, while radial-ply tyres have found widespread acceptance in the developed countries.

For most off-road applications, the terrain must deform significantly to produce the stresses required to support the vertical load imposed on the tyre. The tyre also deforms depending primarily on its inflation pressure, normal load and to a lesser extent on its carcass stiffness. A general rule of thumb is that, the average surface contact pressure is slightly higher than the tyre's inflation pressure with the difference

attributable to carcass stiffness. The mean contact pressure multiplied by the contact patch area must equal the applied vertical load. If the inflation pressure is increased at constant vertical load, the tyre's deformation must decrease to decrease the area of contact patch. Or, if the inflation pressure is held constant, decrease in vertical load must also be accompanied by decrease in tyre deflection and contact patch area.

The tyre deflection characteristics have extensively been reviewed and presented as follows

2.1.1 Pneumatic tyre deflection

The vertical load carrying capability of off-road tyres depends on the pressure and volume of the air that they contain. Thus, vertical load capacity increases with inflation pressure and tyre size. The maximum inflation pressure is limited by the tyre construction as expressed by ply rating of pneumatic tyres. Maximum load ratings and tyre dimensions are published by the tyre manufacturers. Tractor tyre load ratings are paired values of inflation pressure and normal load, which yield approximately the same deflection of the tyre on a rigid surface. Thus, all load-inflation pressure combination for a given tyre represents approximately the same deflection of that tyre and hence, the same contact area, on a rigid surface.

Knight *et al.* (1962**)** conducted deflection tests on firm and various test surfaces at different speeds to measure vertical and or lateral deflections of moving tubeless tyres with the help of linear and circular potentiometers. This technique for measuring deflection was also used by Krick (1969) and Li *et al.* (1985). Results showed that the shape of the tyre appeared to be at least a crude indicator of the distribution of forces imparted by the tyre to the surface on which it was operating, as well as an indicator of its ability to travel on that surface.

Freitag and Smith (1966) developed a system which used a linear potentiometer fitted within the tyre cavity to measure radial deformations, and a rotary potentiometer to measure tangential deformations at the centre line of a pneumatic tyre. They investigated the shape of the centre line tyre deformation as affected by inflation pressure, slip level and soil strength. It was found that the tyre deformation depends on inflation pressure, load and soil strength.

Krick (1969) measured the difference between the undeformed and deformed radii directly beneath the wheel axis for indicating the bias-ply tyre deflection on the rigid surface. On the basis of the test results (load range of 200 - 1600 kp and inflation pressures between 0.6 and 2.5 atm.), relationship between the tyre deformation and system parameters was obtained by the dimensional analysis technique in the following form.

$$\frac{\delta}{h} = 0.67\left[\frac{P_g}{W}(d.b)\right]^{-0.8} \tag{2.1}$$

where, δ = tyre deflection, m,
h = tyre section height, m,
b = tyre width, m,
d = tyre diameter, m,
W = normal load on the tyre, kN,
P_g = ground pressure ($p_i + p_c$),
p_c = carcass stiffness, kPa and
p_i = inflation pressure, kPa.

Abeels (1976) conducted deflection and contact studies on agricultural equipment bias-ply tyres on rigid surface. It was found a linear variation in tyre section height with increased load. Contact area was directly related to load and inversely to inflation pressure. Further, the dimensional variations of pneumatic tyre influence the off-road locomotion.

Komandi (1976) made an attempt to find out the empirical equation to express the deflection, the width of contact area and length of contact area as a function of wheel load, tyre diameter, tyre width and inflation pressure. Tests were conducted on concrete pavement under static condition at different loads and inflation pressures. The following relationship was derived for tyre deflection.

$$\delta = C_1 \frac{W^{0.85}}{b^{0.7} d^{0.43} p_i^{0.6}} K \tag{2.2}$$

where, δ = tyre deflection, cm,
W = wheel load, kp,
b = width of tyre, cm,
K = 0.015 b + 0.42,
d = tyre diameter; cm,
p_i = inflation pressure, kp/cm^2 and
C_1 = constant depending on tyre design.

Fujimoto (1977) found a linear relationship between vertical tyre deflection and load. The tyre deflection was expressed as

$$\delta = \delta_0 + k_1 W \quad (2.3)$$

where, δ = tyre deflection,
δ_0 = constant depending on tyre,
k_1 = constant depending on the inflation pressure and
W = load on the wheel.

Abeels (1981) conducted tyre tests on special test rigs for tyre dynamic characteristics and suggested that squash rate of a tyre (variation in height) allows judgment of its deformability while the flattening rate (variation in width) allows judgment of its side wall stiffness. Further, Abeels (1989) described an electro-mechanical device for measuring tyre deformation including the side wall bulging on rigid and deformable surfaces.

Painter (1981) presented deflection model based on simple geometrical theory suitable for fitting experimental data to relate inflation pressure, maximum permissible load and tyre geometry.

Hausz (1985) stated that the traction improvements of a radial tractor tyre result from the deflection characteristics and pressure distribution under the tyre at the tyre-soil interface.

Wulfsohn *et al.* (1988) gave multilinear regression model between tyre deflection (δ, m), vertical load (W, kN) and tyre inflation pressure (P_i, kPa) for 18.4 – 38 tyre.

$$\delta = 0.02 + 0.006 \times W - 1.35 \times 10^{-5} \times W \times p_i \quad (2.4)$$

Lines and Murphy (1991) measured dynamic stiffness of rolling agricultural tractor tyres in the radial direction. It was concluded that inflation pressure, rolling speed, tyre size, and tyre age had larger effect on tyre stiffness compared to variations in tyre load, vibration amplitude, driving torque, ply rating, and frequency. The stiffness of a traction type tyre was estimated by the relationship

$$K_t = 172 - 1.77 d_r + 5.6 t_a + 0.34 b d_r p_i \quad (2.5)$$

where, K_t = tyre stiffness, kN/m,
b = tyre section width, in.,

d_r = rim diameter, in.,
t_a = tyre age, years and
p_i = inflation pressure, bar.

Lyasko (1994) measured the tyre vertical deflection at different normal load and inflation pressure on rigid surface and gave following formula

$$\delta = \frac{C_2 \times W}{2 \times (p_a + p_0)} + \sqrt{\left(\frac{C_2 \times W}{2 \times (p_a + p_0)}\right)^2 + C_1 \times W} \quad (2.6)$$

where, W = Normal load, kN,
p_a = tyre inflation pressure, kPa,
p_0 = conditional pressure for a tyre at zero inflation pressure on hard ground, kPa and
C_1, C_2 = Constant coefficient for a given tyre.

Sharma and Pandey (1996) measured vertical deflection of three bias-ply agricultural tyres (11.2-28, 12.4-28 and 13.6-28) at different normal loads and inflation pressure on rigid surface. The deflection was estimated by

$$\frac{\delta^2}{W} = 0.0838 + 5.9559\frac{\delta}{p_g} \quad (2.7)$$

Taylor *et al.* (2000) calculated tyre deflection at three inflation pressures (41, 83, and 124 kPa) by increasing the static load and measuring the static loaded radius as the tyre rested on a smooth metal plate. The unloaded radius of the tyre was determined from the circumference of the tyre. As load was applied to the tyre, static loaded radius was measured and tyre deflection was calculated as the difference between the unloaded radius and static loaded radius.

Tiwari (2006) measured the tyre deflection on the rigid surface for bias-ply tyres. The normal load was varied from 7.36 kN to 18.64 kN and inflation pressures from 69 kPa to 234 kPa. A relationship between tyre deflection and system parameters was obtained by the dimensional analysis technique in the following form.

$$\frac{\delta}{h} = 1.052 \left[\frac{P_g}{W}(d \times b)\right]^{-1.01} \quad (2.8)$$

where, $\frac{\delta}{h}$ = deflection ratio, %,

b = width of the tyre, m,
d = diameter of the tyre, m,
W = normal load, kN,
p_i = inflation pressure, kPa,
p_c = carcass pressure, kP and
P_g = (p_i + p_c) = ground pressure (W/A), kPa.

Rashidi *et al.* (2013) developed tyre deflection model for four radial-ply tyres (165/65 R13, 185/65 R14, 185/65 R15 and 216/60 R16). The normal load was varied from 5.87 kN to 13.69 kN and inflation pressure from 30 kPa to 38 kPa. The developed model was as follows

$$\delta = 75.67 + 0.104 \times b - 0.107 \times d - 0.758 \times P_i + 3.519 \times W \quad (2.9)$$

where, δ = deflection, mm,
b = width of the tyre, mm,
d = diameter of the tyre, mm,
W = normal load, kN and
p_i = inflation pressure, kPa.

2.1.2 Tyre contact area

Tyre and soil interface can be interpreted in many ways depending on the analysis of the forces involved. The two simplest terms are contact area and contact surface, as shown in Fig. 2.1.

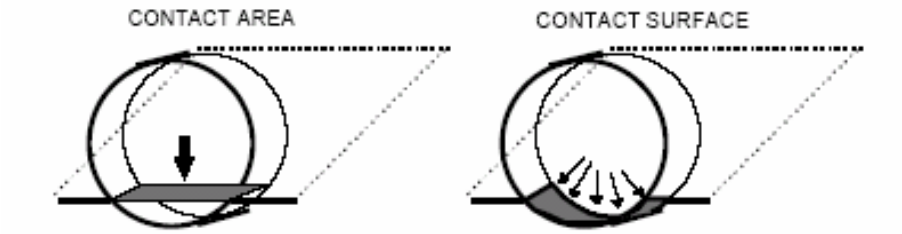

Fig. 2.1 Contact area and contact surface

The performance of a pneumatic tyre depends largely on the nature and distribution of contact normal and tangential stresses over the soil-tyre contact interface. The tyre surface contact area defines the loading area and intensity of applied stresses. It reflects the tyre flexibility with respect to its reaction to the supporting surface. The performance characteristics (pull-to-weight ratio, tractive efficiency, compaction etc.) of a tyre depend to a great degree not only upon the contact stresses but also upon the size and shape of the contact area (Taylor and Burt, 1975; Porterfield and Carpenter, 1986; and Upadhyaya *et al.* 1987).

(a) Experimental techniques for measuring contact area

In general contact area is described by the length and width, which in turn depends on tyre parameters (type and size), inflation pressure, tyre load and soil parameters. Low inflation pressure, high tyre load and soft soil give a larger contact area. Many researchers have used several techniques to measure tyre-rigid surface and tyre-soil contact area. However, all techniques are equally competitive. Some of these techniques are presented below:

Janosi (1961) and Krick (1969) measured tyre contact area in soil by pouring plaster of Paris in the imprints until its depth exceeded the height of lugs by 6 mm. The ground contact area was established by measuring the area enclosed by the contour of the dry plaster cast.

Yong *et al.* (1978) used spray painting technique for measuring the contact area on rigid surface. In this technique, tyre was painted before loading it on a rigid surface and imprinted foot print area was measured. Another technique was used for continuous measurement of contact area. In this technique tyre was placed on a thick plexiglass sheet (a light transparent plastic sheet) with grid lines and camera was placed under the sheet for taking photographs.

Plackett (1984) painted the tyre by black ink before loading it on a piece of white paper on a hard surface to get imprint of contact area. This technique was also used by Romano *et al.* (2008) and Ekinci *et al.* (2011); whereas Upadhyaya and Wulfsohn (1988), Lyasko (1994) and Grecenko (1995) covered the tyre with a carbon coating before loading it on a piece of white paper on a hard surface to get imprint of contact area.

Dexter *et al.* (1988) puffed talcum powder around the edge of the contact area and drove the vehicle off. The remaining footprint was then copied in the field with a felt-tipped pen on a transparent plastic film placed over it and size of contact area was later determined with a planimeter. The author used spray colour for the same purpose. The remaining contact area was photographed with diapositive film with a length scale inserted. Contact area was determined by projecting the slide in appropriate scale on a checked paper and counting squares.

Zbigniew (1990) measured the tyre-soil contact area under static and dynamic conditions. Under static condition, the ground in direct contact with the tyre was sprinkled with talc before the wheel was raised. After the tyre was raised, the position of the line limiting the area was measured.

Upadhyaya and Wulfsohn (1990) used a steel plate covered with white sheet and carbon paper beneath the tyre before the tyre was loaded to desired vertical load using USD single wheel tester (Upadhyaya *et al.*, 1986). The process of pressing the wheel against the steel plate was repeated to obtain a good imprint of tyre contact on the white sheet. Sharma and Pandey (1996) and Tiwari (2006) also used the same technique.

Schwanghart (1991) powdered the edge of the contact area with white calcium carbonate and traced the contact area on transparent paper after removing the wheel. This technique of simulating the conditions of a wheel in motion was also used by Taylor (1988). When tyre was in motion, contact area geometry was determined by measuring radial and longitudinal deflections of the tyre, deflection of the ground and height reached by the soil under the tyre in the rut with the special equipment/instruments designed by the author.

Wulfsohn and Upadhyaya (1992) measured the dynamic three-dimensional contact profile between a tyre and deformable soil using a transducer. The transducer consisted of a thin wire sheathed within a flexible cable lying on the surface of the soil perpendicular to the direction of travel of the tyre. The wire was connected to a spring loaded potentiometer so that when the tyre ran over the wire, the wire deformed with the soil beneath the lateral section of the tyre and the linear extension of the wire was measured and recorded on digital data logger.

Hallonborg (1996) used a colour spray for measuring the tyre surface contact area. The contact area was photographed with diapositive film with a length scale inserted. The slide was projected in appropriate scale on a checked paper and the squares were counted to determine the contact area.

Diserens *et al.* (2009, 2011) measured the contact area using a photometric method. The tyre circumference print on the ground was first sprinkled with calcium oxide

powder. Then bellows were used to distribute the powder around and beneath the tyre between the lugs so as to fill the maximum free space around and below the tyre. The contours were photographed with a digital camera. Print area was then analyzed by photometry using Adobe Photoshop Elements software.

Lu *et al.* (2010) developed envelope curve calculation algorithm for finding a pattern boundary of tyre foot print using automatic digital image processing method.

Mohsenimanesh *et al.* (2009) estimated the 3D foot print in the soil by rut depth and width across the tyre length.

Taghavifar *et al.* (2013, 2014) spread white powder on periphery of tyre soil interface to define contact area. A digital camera was used to capture image and image processing method was used to determine the contact area.

(b) Tyre contact area modelling

Contact area model can be theoretical, semi-empirical or empirical depending on the method used. In theory, the footprint of a rigid wheel on hard surface is a line, equal to the width of the tyre. Because contact length is close to zero, footprint area is also close to zero. This means, that in practice, the footprint area of a rigid wheel on hard surface becomes very small, and the contact pressure becomes high.

Sohne's (1969) stated that a decisive factor in the development of high powered tractors is the load carrying capacity of the tyres. This capacity depends both on the size and the average allowable pressure over the contact area. The contact area was expressed in terms of the tyre geometry as

$$A = 2b\sqrt{dz} \tag{2.10}$$

where, A = contact area,
z = sinkage,
b = tyre width and
d = tyre diameter.

Krick (1969) and Painter (1981) developed models for predicting the contact area of pneumatic tyre on rigid surface using dimensional analysis approach. Krick considered tyre deflection (δ) as a function of diameter (d), width (b), section height (h), inflation and carcass pressure ($P_g = p_i + p_c$) and tyre load (W). The following

relationship was suggested for contact area based on the results of the tyres tested within load range of 1.96-15.7 kN and inflation pressure between 0.6 and 2.5 atmospheres.

$$\frac{A}{h^2} = 5.3\left[\frac{p_g}{W}(d.b)\right]^{-0.8} \tag{2.11}$$

Painter (1981) considered the dimensional relationship as

$$\frac{W}{p_i\delta^2} = f\left[\frac{K}{p_i\delta}, \frac{\delta}{d}, \frac{\delta}{c_d}\right] \tag{2.12}$$

where, W = vertical load on the tyre,
p_i = tyre inflation pressure,
K = tyre elastic property,
δ = tyre deflection,
c_d = tyre cross-section equivalent diameter curvature and
d = tyre diameter at the root of tread on centre line.

The equivalent contact area was represented as,

$$A = \frac{\pi}{4} a_1 a_3 d^{a_2} c_d^{a_2} \delta^{2-(a_2+a_4)} \tag{2.13}$$

where, a_1, a_2, a_3 and a_4 are empirical constants.

Komandi (1976) suggested the following empirical relationship on the basis of the results of ten tyres ranging from 9-24 to 15-30 at inflation pressures from 39.2 to 157.0 kPa on concrete pavement.

$$A = (l_c - b_c) b_c + \frac{b_c^2 \pi}{4} \tag{2.14}$$

where, A = contact area, cm^2,
l_c = length of contact area and
b_c =width of the contact area.

The area of the tread imprints amounted to 22-24 per cent of the total area. Therefore, an average value of A_t = 0.23*A was recommended. Further, Komandi (1990) suggested that the contact surface for bias-ply tyres on deforming road surface in ploughed field as

$$A = C.W^{0.7}\left(\frac{b}{d}\right)^{0.5} p_i^{-0.45} \tag{2.15}$$

where, A = tyre contact area, m^2,
W = load on tyre, kN,
b = width of tyre, m,
d = tyre diameter, m,
p_i = inflation pressure, kPa and
C = constant depending on the surface (from Table 2.1).

The experiments were performed at pressures varying between 4×10^4 and 1.6×10^5 N/m^2.

Table 2.1: Value of constant (C) for different substrates in Komandi's model

Soil	Constant C
Rather bearing soil	0.30 - 0.32
Sandy field	0.36 – 0.38
Loose sand	0.42 – 0.44

Plackett (1984) described measurement of tyre contact area on hard surface to be an accurate and reliable method of determining mean ground pressure under static conditions. Method of overlaying a number of contact prints on the same area to overcome subjective assessment of the contact area of a tyre with lugs was also proposed.

Upadhyaya and Wulfsohn (1988) developed mathematical expressions to calculate contact area as follows,

$$A = \frac{\pi}{4} ab \left[1 - \frac{2\eta}{\pi} \right] \qquad (2.16)$$

where, $\eta = 0$, if b<w,

$$\eta = \left[2(1 - w/b) \right]^{0.5} - (w/b)\left[1 - (w/b)^2 \right]^{0.5}, \text{ if b>w}$$

Upadhyaya and Wulfsohn (1990) developed mathematical expressions for 2-D contact length, contact width and contact area of a pneumatic tyre on a rigid surface based on the geometry and deflection characteristics of the tyre. These expressions show that the 2-D contact area is elliptical when the tyre deflection is small but becomes rectangular with curved edges as the deflection increases. The model predictions were verified using experimental results obtained with 16.9 R 38, 18.4 R 38 and 24.5 R 32 tyres.

Ziani and Biarez (1990) gave the following formulae for calculating tyre contact properties (Figs. 2.2 and 2.3).

$$A = \frac{\pi}{4} b_c l_c \tag{2.17}$$

$$l_c = 2\sqrt{z(2r - z)} \tag{2.18}$$

$$b_c = 2\sqrt{z(2r_b - z)} \tag{2.19}$$

where, b_c = contact width, m,
l_c = contact length, m,
r = tyre (longitudinal) radius, m,
r_b = tyre (transversal) radius, m and
z = sinkage, m.

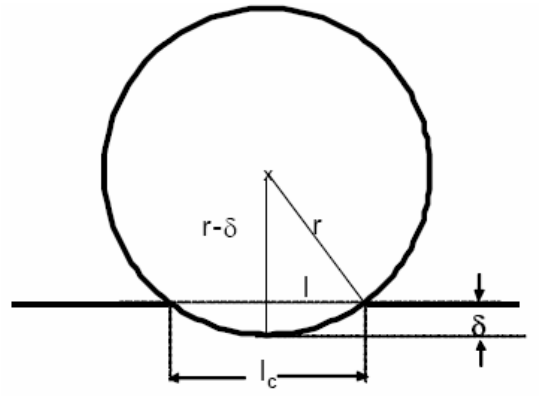

Fig. 2.2 Pneumatic tyre on hard surface

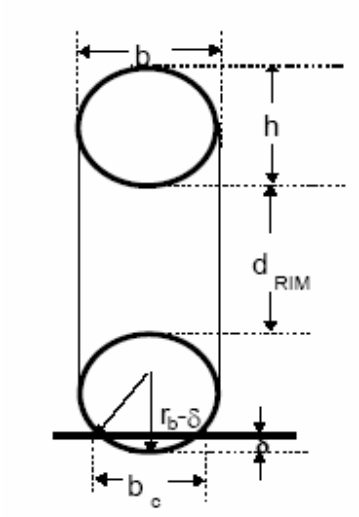

Fig. 2.3 Contact width and section height of a pneumatic tyre

Schwanghart (1991) suggested a mathematical model for calculating contact area and ground pressure under a tyre in soft soil with some assumptions. The contact lengths l_1 and l_2 can be calculated based on tyre geometry (Fig. 2.4).

The term ellipticity coefficient β of the contact area was introduced in the model as

$$A = b / \beta \tag{2.20}$$

where b = width of tyre, = $b_o + b_1 I_w$,
b_o = rated tyre width,
b_1 = 3-5 (cm/load percentage) and
I_w = W/W_{rated}, load percentage of the rated load W_{rated} due to inflation pressure.

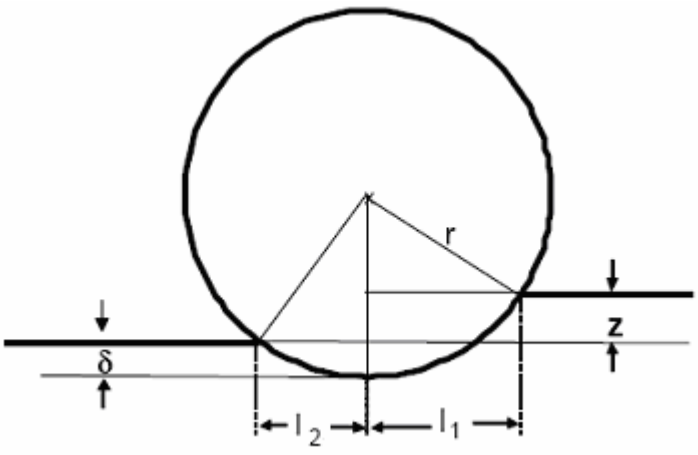

Fig. 2.4 Flexible tyre on soft ground

Contact length l_c is the function of diameter, deflection and sinkage of the tyre and was calculated by

$$l_c = l_1 + l_2 = \sqrt{\{d(z+\delta)-(z-\delta)+(d\delta-\delta^2)\}} \quad (2.21)$$

where, d = tyre diameter,
δ = tyre deflection and
z = tyre sinkage to be calculated using a simplified Bekker's equation involving soil properties.

The model was validated within an acceptable range and it was concluded that doubling the vertical load resulted in an area increase of 30-40 per cent, whereas doubling the inflation pressure caused a decrease in the contact area to 70-80 per cent of the original size.

Godbole *et al.* (1993) presented the following generalized models for contact patch length and contact area assuming h = b.

$$l_c = 2\sqrt{d\delta} \quad (2.22)$$

$$b_c = 2\sqrt{h\delta} \quad (2.23)$$

$$A = \pi\delta\sqrt{dh} \quad (2.24)$$

$$\delta = 0.54\, h\left(\frac{p_i dh}{W}\right)^{-0.79} \quad \text{for large agricultural tyres} \quad (2.25)$$

$$\delta = 1.05\, h\left(\frac{p_i dh}{W}\right)^{-1.24} \quad \text{for small agricultural tyres} \quad (2.26)$$

Grecenko (1995) presented an overview on the modelling of the footprint area and suggested the following empirical models:

$$A = 1.57(d - 2r_1)\sqrt{db} \tag{2.27}$$

$$A = \pi\delta\sqrt{db} \tag{2.28}$$

$$A = Cbd \tag{2.29}$$

where, r_1 = loaded radius, m and
C = constant (from Table 2.2).

Table 2.2 Constant C for Grecenko's footprint area model (Eqn. 2.29)

Tyre and soil type	Value of C
Hard tyre, hard ground	0.175
Flexible tyre (20% deformation), soft ground	0.245
Hard tyre, soft ground	0.270

Hallonborg (1996) stated that the super ellipse provides an excellent means for describing the shape and size of widely varying contact area ranging from circles over ellipses to squares or rectangles. It provides explicit border values for integration of ground pressure over the contact area. Thus a more accurate location of ground pressure centre is expected. In an orthogonal coordinate system, the exponent (n) is a positive real number that determines the shape, and parameters a and b determine the length of half the major and minor axes and thus, the proportions of the surface. The proposed super elliptic model is

$$\frac{x^n}{a^n} + \frac{y^n}{b^n} = 1 \tag{2.30}$$

Saarilahti (2002) stated that footprint area can be measured by pulling the tyre on a soil surface with a certain wheel load (W). Generally, the area between the lugs, even if not in full contact with the soil, specially on harder surfaces, is included in footprint area. For more exact analysis, effective area, e.g. the lug area supporting the load, is measured. Idealized footprint is some kind of overestimate, but can be used for different models, which are based on average forces. He reported that on hard surface, under narrow, large diameter tyres with high inflation pressure the contact shape is elliptical. With wider tyres the shape is more rounded. A general model for tyre footprint area is

$$A = c.l_c.b_c \tag{2.31}$$

where, c = shape parameter,

c = $\frac{\pi}{4} = 0.785$ for circle and ellipse, and

c = 1 for square and rectangle.

The form of the footprint is generally between circle and rectangle, and the estimate for c lies between 0.8 and 0.9.

Keller (2005) predicted the contact area by using the Hallonborg (1996) method and assumed that the longitudinal and transverse axis of tyre footprint were the axis of symmetry and thus

$$A = k \times b_c \times l_c \tag{2.32}$$

The value of k can be found by numerical integration as

$$kab = b \times \int_0^a \left(1 - \frac{x^n}{a^n}\right)^{1/n} dx \tag{2.33}$$

where, a and b are half axes of the supper ellipse and n is the shape parameter of the supper ellipse which can be found as follows

$$n = 2.1 \times (b \times d)^2 + 2 \tag{2.34}$$

where, A = tyre predicted contact area, m,

b_c = width of contact area, m,

l_c = length of contact area, m,

d = overall tyre diameter, m and

b = tyre width, m.

Tiwari (2006) developed the following models to predict contact surface area and ground pressure of bias-ply tyres on hard surface.

$$A = \frac{0.367 \times W^{0.554} \times \sqrt{\frac{b}{d}}}{pi^{0.418}} \tag{2.35}$$

$$P_g = 13.77 + 0.585 \times p_i + 3.4 \times W - 0.00067 \times (p_i)^2 \tag{2.36}$$

where, b = width of the tyre, m,

d = diameter of the tyre, m,

W = normal load, kN,

p_i = inflation pressure, kPa,
p_c = carcass pressure, kPa,
P_g = ($p_i + p_c$) = ground pressure (W/A), kPa and
A = tyre-surface contact area, m^2.

Diserens *et al.* (2011) proposed following regression model for calculating the contact area on firm soil for agricultural radial-ply traction tyres.

Undifferentiated $$A = 0.180 \times TS + 3.6 \times 10^{-3} \times W - 15.5 \times 10^{-5} \times p_i \quad (2.37)$$

TS < 0.6 $$A = 0.191 \times TS + 4.6 \times 10^{-3} \times W - 14.8 \times 10^{-5} \times p_i \quad (2.38)$$

TS ≥ 0.6 or < 1.2 $$A = 0.130 \times TS + 9.2 \times 10^{-3} \times W - 53.5 \times 10^{-5} \times p_i \quad (2.39)$$

TS ≥ 1.2 $$A = 0.126 \times TS + 5.9 \times 10^{-3} \times W - 75.7 \times 10^{-5} \times p_i \quad (2.40)$$

where, TS = product of section width and outer diameter of tyre,
p_i = tyre inflation pressure, kPa,
W = wheel load, kN and
A = contact area, m^2.

Based on the review presented in this section, it is noticed that the tyre deflection studies have been conducted on a hard surface to prepare the way for further study of tyre behaviour on soil with a constant numerical base. Even though, several empirical models have been developed to predict deflection and contact characteristics of tyres, none have found wide acceptance due to the fact that the real pressure and force distribution in soil depends on the form and structure of the loading surface. In the present study, the contact area under each test tyre was measured on a hard surface using the technique adopted by Tiwari (2006).

2.2 Strength of Soil

Soil type and conditions are the most important factors that influence traction. Changes in soil conditions influence tyre performance much more than changes in tyre loading and tyre dimensions. Tractive performance is affected by both the soils' normal strength and its shear strength. In general, normal strength has the most effect on motion resistance, while shear strength has the most effect on slip and gross traction.

2.2.1 Measurement of soil strength

Strength of soil is measured by cone index or stress-strain relationships using soil cohesion (c), internal soil frictional angle (ϕ), shear modulus and sinkage parameters (k) - for evaluation of traction performance.

The Bevameter technique pioneered by Bekker (1956, 1960, and 1969) is often used to obtain soil sinkage and shear characteristics. However, it is comparatively cumbersome and expensive. The cone index therefore, remains a "best guess" to estimate the soil consistency and strength for cohesive-frictional soils. The use of penetration resistance has a merit for providing a rapid assessment of soil mechanical condition on a given day (Defossez *et al.*, 2003)

Penetrometer has been widely accepted as a practical instrument for assessing soil strength (Vaz *et al.*, 2011). ASABE standard cone penetrometer for soil is shown in Fig. 2.5. Soil strength as measured by the soil cone penetrometer provides a combined measurement of soil normal strength and shear strength. This device works well only if the soil has moisture and if it has not been disturbed. Cone penetrometer (Perumpral, 1987) testing involves pushing a standard cone into the soil at a certain rate and recording the resisting force exerted by the soil on the penetrometer (ASABE Standards 2006a, S313.3,). The standard test procedure is given in ASABE standards EP542 (2006b).

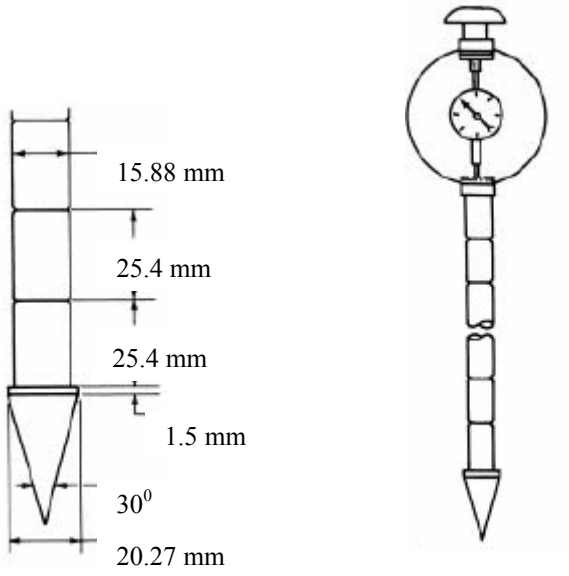

Fig 2.5 ASABE standard cone penetrometer

The force required to push the cone into the ground is recorded as a function of depth. The force divided by the area of the base of the cone provides a pressure measurement

and is referred to as cone index, commonly expressed in kN/m^2 in SI units. Cone index may be measured as deep as 500 mm when used for tillage and/or compaction measurements, but the upper 100 to 150 mm is commonly used for traction purposes.

2.2.2 Factors affecting cone index

Cone index, a measure of the penetration resistance of a soil, is considerably influenced by soil density, moisture content and soil type (Ayers and Perumpral, 1982; Busscher, 1990; Sojka *et al.*, 2001; Vaz and Hopmans, 2001; Dexter *et al.*, 2007; Santos *et al.*, 2012; Quraishi and Mouazen, 2013). Experimental studies have shown that the cone index decreases with the increasing soil moisture level (Turnage, 1970; Collins, 1971; Voorhees and Walker, 1977; Wells and Treesuwan, 1977). The logarithmic relationship between cone index and moisture content resulted in close agreement between predicted and experimental results (Collins, 1971; Wells and Treesuwan, 1977).

$$\ln(CI) = C_1 + C_2 \times \ln(MC) \tag{2.41}$$

where, Cl = soil cone index,
MC = moisture content and
C_1 and C_2 = constants based on soil type.

Past studies indicate that the soil cone index increased with increase in the density of soil (Melzer, 1971; Turnage, 1974). Results of penetration tests conducted in sandy clay loam and clay loam soils showed that the dependency of maximum penetration resistance on bulk density was greater at lower moisture levels than at higher moisture levels (Mulqueen *et al.*, 1977). Similar observations were also made by Hayes and Ligon (1977) from the results of penetration tests conducted in clay loam and loamy sand.

Ayers and Perumpral (1982) investigated the influence of density, moisture content and soil type on cone index. Five soil types were considered by mixing known quantities of Zircon sand and Fire clay. Three levels of density and eight moisture levels in the 2 to 25 per cent range were considered. Following empirical model was developed from the test results to represent the cone index as a function of density and moisture content.

$$Cl = \frac{C_1 \times \rho^{c_4}}{C_2 + (MC - C_3)^2} \tag{2.42}$$

where Cl = cone index, kPa,
ρ = dry bulk density, g/cc,
MC = moisture content, per cent, (db) and
C_1-C_4 = constants based on soil type.

Upadhyaya *et al.* (1982) developed equations for predicting cone index in certain agricultural soils of Delaware. Using dimensional analysis technique, they proposed the following prediction equation for silt loam.

$$\alpha\left(\frac{Cl}{BM}\right) = a\left(\frac{\rho}{\rho_s}\right)^n e^{-bMC} \tag{2.43}$$

where, a,b,n = soil constants,
Cl = cone index,
BM = bulk modulus,
ρ = dry bulk density,
ρ_s = soil particle density,
MC = soil moisture content and
α = non dimensional factor.

The effect of the other parameters such as base diameter of cone, apex angle of cone, size of penetrometer shaft relative to cone base diameter, surface finish of cone and penetration rate on cone index measurement have been studied in the past (Freitag, 1968a; Gill, 1968; Nowatzki and Karafiath, 1972; Perumpral, 1987). The effect of these parameters on soil cone index can be neglected by using a standard cone penetrometer.

Typical cone index values for a range of soil conditions are given in Table 2.3 (ASABE standards, 2011) and Table 2.4 (Brixius, 1987).

Table 2.3 Values of cone index under different soil conditions (ASABE standard, 2011)

Soil	CI (k Pa)
Hard	1800
Firm	1200
Tilled	900
Soft, sandy	450

Based on the review presented in this section, it is noticed that many researchers have used cone index to characterize the soil for traction performance of tractors in the

laboratory as well as in actual field conditions. The most common device to measure cone index has been manually operated cone penetrometer, even though, hydraulically operated cone penetrometers have been used by a few researchers in the field. The typical values of cone index as suggested by Brixius (1987) provide a good basis for maintaining cone index under different soil conditions.

Table 2.4 Typical cone index values (Brixius, 1987)

Soil Class	Cone Index		Typical Operating Conditions
	kN/m^2	psi	
Soft or Sandy Soil (CI = 450)	0	0	
	350	51	Rice harvest
	480	70	Disking on ploughed ground or Low-land logging
	700	101	Spring ploughing or Earthmoving on moist soil
Medium or Tilled Soil (CI = 900)	850	123	Planting, field cultivation
	1000	145	Corn Belt harvesting, fall ploughing
	1200	174	Wheat harvesting
Firm Soil (CI = 1800)	1750	254	Summer ploughing Logging in dry season Earthmoving on dry, clay soil

2.3 Techniques for Single Wheel Testing

A simple traction wheel test device requires supporting the moving wheel, applying the required torque, and measuring the developed force (net traction). However, there are various ways this can be accomplished, with varying levels of complexity. Some devices can operate only in soil bins, while others are operated in the field. In some cases, testing is done using complete vehicles, with the tractive device being the drive wheels or tracks. Tyre design is almost entirely determined by experimental methods, therefore, a number of tyre testing devices have been developed worldwide (Tiwari et al. 2009).

Zoz and Grisso (2003) has pointed out three basic devices for single wheel testing. With the single-link device (Fig. 2.6), a change in input torque results in change in vertical force reaction, which then must be measured dynamically during the test. Figure 2.7 shows a modification using two parallel links; this eliminates the weight transfer effect but may result in more difficult measurement of pull and torque. The

pull can be calculated as the sum of the reaction forces and the torque can be calculated as the difference in the forces multiplied by the distance between the arms. Most single-wheel testers use the mechanism shown in Fig. 2.8. Torque is measured at the input to the wheel. With parallel arms, there is no change in vertical reaction as torque is applied ($W = W_d$).

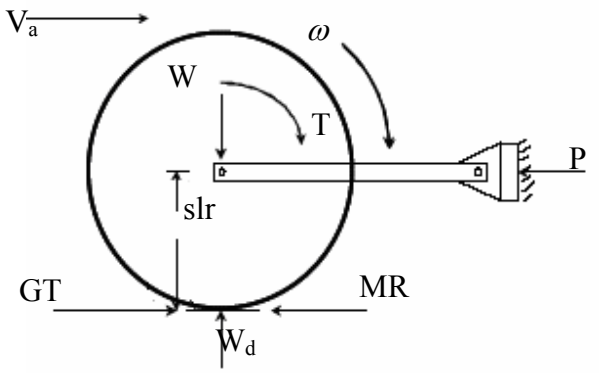

Fig. 2.6 Simplest form of single-wheel tester

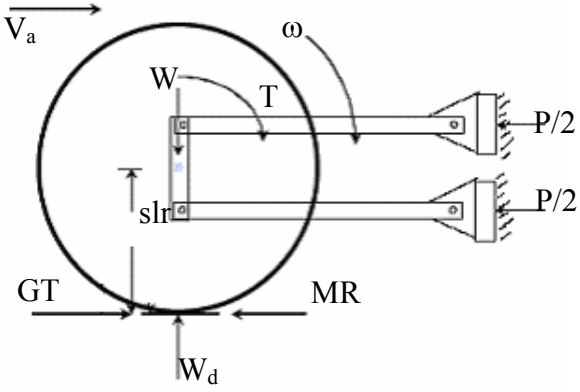

Fig. 2.7 Single-wheel tester with parallel arms

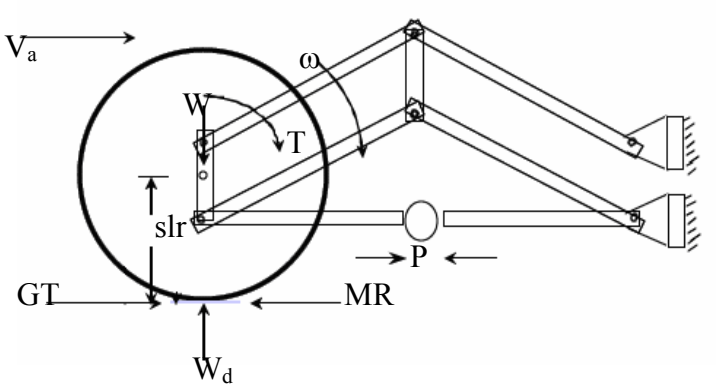

Fig. 2.8 Parallel arm single-wheel tester with direct measurement of pull

The National Soil Dynamics Laboratory developed a single wheel tester as an indoor soil bin device (Burt *et al.* 1980). The possibility of adjusting the speed of the testing

device and the angular speeds of the test tyre independently, makes the tester capable of performing either variable slip tests (while keeping the dynamic load constant) or variable dynamic load tests (while maintaining slip constant). Each major function, such as vertical load, angular velocity of the test tyres and the device's forward velocity, has its own control system. The ranges of the test tyres are from 12.4-28 to 30.5-32, the applied vertical load is up to 71.2 kN and draft force up to 44.5 kN. The NSDL unit is able to perform all necessary tyre tests with a high level of control.

The single wheel tester, developed at the University of California at Davis in the U.S.A. (Upadhyaya *et al.* 1986) was designed to perform controlled field experiments. A driven test tyre is located between the rails and is pulled by the tractor. The difference between the forward speed of the whole device and the angular speed of the test tyre provides slip. The range of the test tyres is from 0.46 to 2 m in diameter, vertical force is up to 26.7 kN and draft force is up to 13.2 kN. The Davis field single wheel tester is a combination of soil bin and field-testing devices. This tester has the advantage of operating in the field in controlled conditions. A fully instrumented device has also been developed to measure soil properties relevant to traction (Upadhyaya *et al.* 1993). The device could measure soil sinkage parameters utilizing sinkage plates, as well as shear parameters using grouser plates. This device can also be used to measure soil cone index.

Upadhyaya *et al.* (1988) emphasized on consistent test procedure and zero condition to compare tractive ability of different tyres. They reported that different testing techniques (constant slip, constant draft, varying slip, varying draft) affect scatter in traction data to different extents. The constant slip test procedure leads to repeatable and consistent results whereas a variable slip test procedure leads to considerable scatter in the data. They observed that varying slip appeared to influence the system dynamics much more than varying draft during tyre testing. They suggested the method of predicting true rolling radius and true slip for an assumed zero condition.

The tester developed at the University of Hohenheim (Ambruster and Kutzbach, 1989) was based on a rig connected to a four-wheel-trailer. The trailer was towed by a tractor during the test run. The tester was capable of accommodating tyres up to 2 m in diameter and applied vertical load of up to 40 kN. The main advantage of this tester is its capability to test driven angled wheels.

Shmulevich *et al.* (1996) developed a new field single wheel testing device to perform tyre traction tests under variable slip or vertical load conditions. The tyre-testing device was mounted at the rear of a heavy wheeled tractor that also carries a unique soil property testing device at the front. The vertical, horizontal and side forces could be measured inside a frame that holds the test wheel, while the torque was measured by a separate linkage system. The tyre testing device was capable of testing tyres up to 2 m in diameter; it could apply vertical force up to 50 kN and torque up to 31 kNm.

The review suggests that single wheel testers are capable of testing a given range of tyre sizes, normal loads, draft and speeds. A single wheel tester should be instrumented such that it is capable of giving continuous readings of the forward speed, tractive force and torque. The constant slip and constant draft test procedures yielded acceptable results; therefore, either of the two methods can be used for traction studies.

2.4 Traction Prediction Approaches

Horizontal propelling force produced by the shearing strength of the ground under a traction device is the soil thrust. A part of this thrust is wasted for overcoming motion resistance and the rest which remains as a useful force to accelerate the vehicle, climb the slope, or pull loads, is called the tractive effort or drawbar pull (Bekker, 1960).

Over the years, various approaches have been developed and adopted by different research workers to predict the traction characteristics of a wheel. In general, approaches differ in terms of characterization of terrain behaviour.

2.4.1 Stress-strain relationship approach

Based on Coulomb's equation, Bekker (1956, 1960) identified maximum thrust force required to shear the ground along the ground contact area (A) and under load (W) as

$$F = Ac + W\tan\phi + F^{/} \tag{2.44}$$

where $F^{/}$ is an additional shearing force produced by tyre treads or spuds of a track. Introducing spud action $F^{/}$ in the Eqn. (2.44) it takes the form

$$F = blc\left(1+\frac{2h_t}{b}\right) + \mathrm{W}\tan\phi\left[1+0.64\left\{\left(\frac{h_t}{b}\right)\cot^{-1}\left(\frac{h_t}{b}\right)\right\}\right] \quad (2.45)$$

where h_t is the height of the tread or grouser.

He concluded that the tread effect depends on soil type and is strongest in cohensive soils.

As soil thrust attains maximum at a certain amount of optimum slip, Bekker (1956, 1960) proposed a solution for defining the relationship among soil properties, the geometry of ground contact area, load, slippage and soil thrust in terms of distance between the front end of the ground contact area and the point where the unit thrust is to be determined.

As the proposed relationship was too complex, Janosi and Hanamoto (1961) developed a simpler equation (Fig. 2.9) for describing peripheral force or thrust as

$$F = (Ac + W\tan\phi)(1-e^{\frac{-j}{k}}) \quad (2.46)$$

where, j = soil displacement, = Sx,
K = a constant, for a particular soil,
S = slip and
x = distance from the front of contact area.

Upon integration over the whole length l of the ground contact area, the total soil thrust is given by

$$F = (Ac + W\tan\phi)\left(1+\frac{Ke^{\frac{-Sl}{K}}}{Sl}-\frac{K}{Sl}\right) \quad (2.47)$$

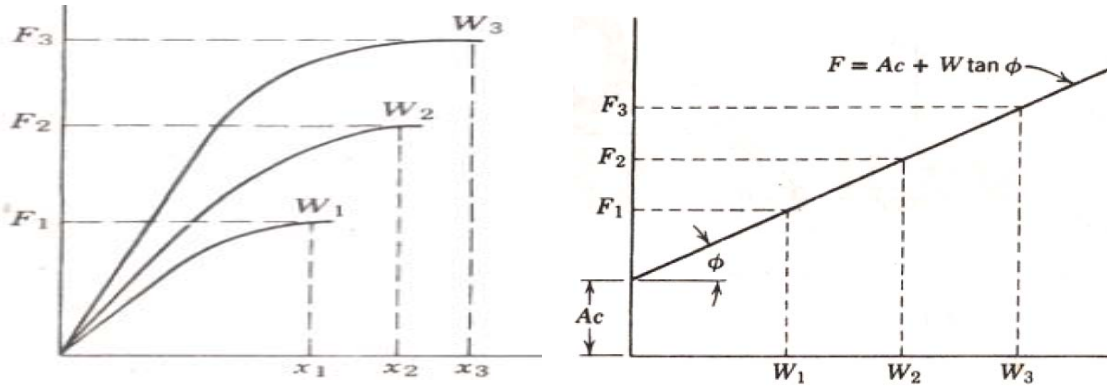

Fig. 2.9 The relationship between soil shear strength, F and soil displacement, for different values of normal load, W

Dwyer (1972) characterized the soil by c, ϕ, Bekker's sinkage displacement coefficients, bulk density, moisture content, particle size classification, soil to steel and soil to rubber friction coefficients and cone penetrometer readings to study the effect of ply rating on tyre performance on grassland, stubble and ploughed land. He concluded that ply-rating did not appear to have any important effect on the thrust obtained at normal working values of slip. However, it does have a substantial effect on rolling resistance, the stiffer higher ply rating tyres having higher rolling resistance, particularly on the softer soils.

Rosca *et al.* (2014) presented semi-empirical model for predicting the traction force for 2WD agricultural tractor, assuming that the shape of the tyre-ground contact area is a super ellipse. The best fit between model data and experimental data was achieved when the value of the super ellipse exponent was set to k = 3.5.

From the review on stress-strain relationship approach, it may be noticed that the Bekker's method of predicting tractive performance provides a good insight into the effects of different parameters and enables different ground-drive system designs to be evaluated on paper. It is valid for any soil, but is too complex for practical use. The Janosi-Hanamoto equation is simpler, but is only valid for soils which display asymptotic shear diagrams. Both equations are valid for tracked vehicles. However, Bekker (1983) amended it for pneumatic tyres. Furthermore, these equations involve tyre-soil contact area for prediction of tractive force under dynamic conditions which requires sophisticated instrumentation in field conditions. Hence, these equations are difficult to be used for a traction device with relative ease.

2.4.2 Mobility number approach

The interaction between a pneumatic tyre and terrain is very complex and is difficult to model accurately. To resolve this difficulty, empirical methods that use mobility numbers, based on dimensional analysis approach, have been developed. In general, these models are based on the test results of a number of selected pneumatic tyres over a range of terrains of interest. The measured vehicle performance is then empirically correlated with terrain conditions, usually identified by observations and simple measurements. This can lead to the establishment of a scale for evaluating vehicle mobility on the one hand and terrain traffic ability on the other.

(a) Mobility number

One of the initial empirical models for soil–tyre performance was evolved from trafficability analysis by the U.S. Army Engineer Waterways Experiment Station (WES). This analysis was based on the cone penetrometer description of soil condition and originally developed to provide a method to assess vehicle trafficability and mobility of military vehicle. The method was developed empirically from the results of numerous field tests with a variety of vehicles in fine-grained soils and is continuously being updated and validated.

The mobility number concept was first derived by Freitag (1966 and 1968b) by proposing a mobility number method based on dimensional analysis to predict the tractive performance of treadless pneumatic tyres on soft soils**.** The following two dimensionless ratios based on cone index, termed mobility numbers, one for sand and another for clay, were developed.

$$N_{CC} = \frac{CIbd}{W}\left(\frac{\delta}{h}\right)^{\frac{1}{2}} \tag{2.48}$$

$$N_S = \frac{G_{CI}(b.d)^{\frac{3}{2}}}{W}\left(\frac{\delta}{h}\right) \tag{2.49}$$

where, N_{cc} = clay mobility number,
N_s = sand mobility number,
CI = soil cone index,
G_{CI} = soil cone index gradient,
b = unloaded tyre section width,
d = unloaded overall tyre diameter,
W = dynamic load on tyre,
δ = tyre deflection and
h = tyre unloaded section height.

The cone index gradient (G_{CI}) was defined as:

$$G_{CI} = \frac{\mathrm{CI} - \mathrm{CI}_{\mathrm{surf}}}{(1/2)\,\text{depth of interest}} \tag{2.50}$$

where, CI = average soil cone index and
$\mathrm{CI}_{\mathrm{surf}}$ = soil cone index at surface.

The terrain was characterized by measuring cone index over a depth of 150mm and concluded that soil parameter CI is a satisfactory measure of soil consistency. The predicted vehicle cone index (VCI) was compared with the measured VCI for selected vehicle at different inflation pressures for validity and usefulness of the analysis technique.

Turnage (1972) analyzed the sand mobility number and clay mobility number as proposed by Freitag (1966) to cover a larger range of b/d ratio (0.05-0.88), soil strength (G_{CI} from 0.6 -7.5 MN/m^3 and CI from 55-469 kN/m^2), wheel load (450-6000 N) and tyre deflection (0.15-0.35 for sand mobility number and 0.08-0.45 for clay mobility number) and concluded that sand mobility number allows useful prediction of tyre performance for a wide range of sand conditions.

$$N_{CI} = \frac{CI.b.d}{W}\left(\frac{\delta}{h}\right)^{\frac{1}{2}}\left(1+\frac{b}{2d}\right)^{-1} \tag{2.51}$$

Further, Turnage (1972) introduced an additional modification in an attempt to compare the wheel laboratory data from vehicle field test: instead of CI, the rating penetration resistance (RCI) was used. RCI describes the soil strength that predominates during multipass tyre traffic better than any other number of soil parameters that have been investigated in WES trafficablity studies. The modified clay mobility number was defined as

$$N_{RCI} = \frac{RCI.b.d}{W}\left(\frac{\delta}{h}\right)^{\frac{1}{2}}\left(1+\frac{b}{2d}\right)^{-1} \tag{2.52}$$

Wismer and Luth (1973) used a simple wheel numeric as

$$C_n = \frac{CI.b.d}{W} \tag{2.53}$$

The Rowland's (1972) wheel numeric (N_R), used for determining the mean maximum pressure (MMP) is

$$N_R = \frac{CI.b^{0.85}.d^{1.15}}{W}.\left(\frac{\delta}{h}\right)^{0.5} \tag{2.54}$$

Maclaurin (1997) replaced the factor $\frac{\delta}{h}$ by $\frac{\delta}{d}$ in the Rowland's wheel numeric (N_R), and claimed that it is easier to use without affecting the accuracy of the model. The presented wheel numeric N_M is

$$N_M = \frac{CI.b^{0.8}.d^{0.8}.\delta^{0.4}}{W} \tag{2.55}$$

Maclaurin (1997) also tested a simple wheel numeric given by

$$W_{Ni} = \frac{CI}{p_i} \tag{2.56}$$

but found out that it was not adequate for describing the tyre/soil interaction, He concluded that a simple wheel numeric C_n, as proposed by Wismer and Luth (1973) was better.

Brixius (1987) presented different wheel numeric called mobility number (B_n). He modified the wheel numeric of Wismer and Luth (1973) by including deflection ratio (δ/h) and section width–to-diameter ratio (b/d). The proposed mobility number is

$$B_n = \left(\frac{CIbd}{W}\right)\left(\frac{1+5\frac{\delta}{h}}{1+3\frac{b}{d}}\right) \tag{2.57}$$

Out of the various mobility numbers proposed, the most cited one in the literature is the Wismer and Luth wheel numeric, C_n. As this wheel numeric, does not include deflection as an input variable, it is not suitable for tyres with different tyre inflation pressures. On this account the Brixius mobility, B_n, is better as it has wider working range.

(b) Traction models

Traction models based on mobility number approach are as follows:

(i) Models based on Turnage and Freitag mobility numbers

Turnage (1972) developed models based on military vehicle field tests and soil bin tests in 1960. Test vehicle was fitted with the military tyres and they were aimed at determining the minimum soil penetration resistance (CI) at a no-go situation. The

models may give low mobility estimates for modern vehicles, as they are based on older technology.

Field test models

$$\text{COT} = \frac{P}{W} = 0.8 - \frac{1.31}{(N_{CI} - 2.45)} \tag{2.58}$$

$$\text{MRR} = \frac{MR}{W} = 0.04 + \frac{0.20}{(N_{CI} - 2.50)} \tag{2.59}$$

Laboratory test models

$$COT = 1.51 - \frac{12.37}{(N_{CI} + 5.94)} \tag{2.60}$$

$$\text{MRR} = 0.04 + \frac{0.20}{(N_{CI} - 1.50)} \tag{2.61}$$

Dwyer *et al.* (1975) used the mobility number of Turnage (1972) to examine a range of tyres at different loads and inflation pressures operating under various field conditions. The following empirical relationships between performance parameters and mobility number were obtained and used in the development of handbook.

$$(COT)_{20\%} = 0.56 - \frac{0.47}{N_{CI}} \tag{2.62}$$

$$MRR = 0.07 - \frac{0.2}{N_{CI}} \tag{2.63}$$

$$(\text{TE})_{\max} = 78 - \frac{55}{\text{N}_{\text{CI}}} \tag{2.64}$$

$$(\text{COT})_{\text{TE(max)}} = 0.41 - \frac{0.21}{\text{N}_{\text{CI}}} \tag{2.65}$$

$$(\text{S})_{\text{TE(max)}} = 9 + \frac{19}{\text{N}_{\text{CI}}} \tag{2.66}$$

where, $(COT)_{20\%}$ = coefficient of traction at 20 per cent wheel slip,
MRR = motion resistance ratio,
TE (max) = maximum tractive efficiency,
$(COT)_{TE\ (max)}$ = coefficient of traction at maximum tractive efficiency and
$(S)_{TE\ (max)}$ = slip at maximum tractive efficiency.

Subsequently, wider ranges of data were analyzed and the following relationships were established by Gee-Clough *et al.* (1978).

$$(COT)_{\max} = 0.796 - \frac{0.92}{N_{CI}} \tag{2.67}$$

$$k(COT)_{\max} = 4.838 + 0.061 N_{CI} \tag{2.68}$$

$$COT = (COT)_{\max}\left(1 - e^{-kS}\right) \tag{2.69}$$

$$MRR = 0.049 + \frac{0.287}{N_{CI}} \tag{2.70}$$

where, COT = Coefficient of traction,
$(COT)_{\max}$ = maximum coefficient of traction,
k = a rate constant,
MRR = coefficient of rolling resistance and
N_{CI} = Turnage mobility number.

These equations were used in prediction of vehicle performance by Gee-Clough (1980) and Dwyer and Heigho (1984).

Sharma and Pandey (1998, 2001) studied bias ply tractor tyres in soil bin using sandy clay loam soil. They developed the following empirical equations based on mobility number suggested by Freitag (1966) for narrower tractor tyres (b=0.280 to 0.350 m, b/d=0.23 to 0.25) with deflection (δ/h=0.18 to 0.26).

$$COT = \frac{P}{W} = 0.76\left(1 - e^{-0.07 N_{CC}.S}\right) \tag{2.71}$$

$$GTR = \frac{T}{r.W} = 0.36\left(1 - e^{-0.35 N_{CC}.S}\right) \tag{2.72}$$

where, $N_{CC} = \frac{CIbd}{W}\left(\frac{\delta}{h}\right)^{\frac{1}{2}}$
COT = coefficient of traction,
GTR = gross traction ratio and
S = slip, decimal.

(ii) Models based on Wismer and Luth approach

Wismer and Luth (1973**)** derived empirical relationships for the tractive performance of tyres on cohesive-frictional soils. The derived equations described tractive

characteristics of both towed and driven agricultural tyres. His prediction equations are applicable for bias-ply pneumatic tyres with the conventional tread designs having b/d ratio ≈ 0.3, δ/h ratio= 0.2 and r/d ratio ≈ 0.475. The developed equations for motion resistance ratio $\left(\frac{MR}{W}\right)$ and gross traction ratio $\left(\frac{T}{rW}\right)$ are as follows

$$\frac{MR}{W} = \frac{1.2}{C_n} + 0.04 \tag{2.73}$$

$$\frac{T}{rW} = 0.75\left(1 - e^{-0.3C_nS}\right) \tag{2.74}$$

where, C_n = wheel numeric = $\frac{CIbd}{W}$,

P = wheel pull,
W = dynamic wheel load,
T = wheel torque,
r = wheel rolling radius,
MR = motion resistance force (towed force) of wheel and
S = wheel slip.

They also compared the results with WES developed equations (Turnage, 1972) which predict maximum pull at 20 per cent slip and concluded that the equations were in reasonable agreement. However, the WES relations predicted a greater change in (MR/W) or (P/W) for a given change in (CIbd/W) which was related to the generally lower strength soils tested by WES. The simplicity of the Wismer and Luth equations coupled with the need for measuring only one soil parameter (cone index) for soil strength has resulted in widespread use of these equations.

Leviticus and Reyes (1983) used a generalized form of the Wismer and Luth (1973) model to define the traction characteristics of tractors tested on the concrete surface at the University of Nebraska. The equation was the same as the Wismer and Luth equation except that the motion resistance was neglected. Also, they noted that the rubber hardness would be the cone index for a wheel operating on soil, but this factor is equivalent to 0.3 times the cone index according to Wismer and Luth's equation.

Clark (1985) proposed a modification of the Wismer and Luth (1973) model which resulted in the following two equations:

$$\frac{MR}{W} = \frac{C_1}{Cn} + C_2 \tag{2.75}$$

$$\frac{P}{W} = C_3 (1 - e^{-(C_4\ C_n\ S)}) - \left(\frac{C_1}{C_n} + C_2 \right) \tag{2.76}$$

where, $C_n = \frac{(CIbd)}{W}$ = wheel numeric, dimensionless;

MR = motion resistance of wheel, kN,
P = net pull or traction of a driving wheel, kN,
W = dynamic load on wheel, kN,
b = unloaded tyre section width, m,
d = unloaded overall tyre diameter, m,
CI = cone index, kPa,
C_1, C_2 = constants depending on soil surface,
C_3 = constant, function of the maximum net tractive ratio,
C_4 = constant, function of the soil surface and tyres and
S = wheel slip, decimal.

The generalized constants C_1, C_2, C_3 and C_4 may allow the model to be used for a broader range of actual field conditions than Wismer and Luth's equation which was only valid when the tyre deflection to the undeflected section height ratio (δ/h) was limited to a 0.20 value. Clark (1985) noted that to determine the constants C_1, C_2, C_3 and C_4 of Eqns. 2.79 and 2.80, field data with an instrumented tractor is needed. Also, he gave ranges for the values of these constants as C_1 : 0 to 0.1, C_2 : 0 to 1.5, C_3 : 0.1 to 1.5, C_4 : 0.1 to 0.5

Rummer and Ashmore (1985) developed the following rolling resistance coefficient model for skidders operating on firm soils.

$$\text{MRR} = 0.24\left(\frac{W_W}{CI.b.d} \right) + 0.06\left(\frac{W_W}{4.W_R} \right) \tag{2.77}$$

The model was modified for one wheel, with certain accuracy, as follows:

$$\text{MRR} = \frac{1.15}{C_n} + 0.06 \left(\frac{W}{W_R} \right) \tag{2.78}$$

where, W = wheel load, kN,
W_W = vehicle total weight, kN and
W_R = rated load of tyre defined by the Tyre and Rim Association.

Ashmore *et al.* (1987) developed traction equations for pneumatic log-skidder tyres tested in soil bin under different loading and soil conditions. Soil types were American clays and silts. The test tyres were 18.4 × 34 with 10-ply-rating and 24.5 × 32 with 12 ply rating. The tyre inflation pressures maintained were 103 – 172 kPa. The developed equations for gross traction ratio and motion resistance ratio are as follows:

$$GTR = 0.47\left(1 - e^{-0.20.C_n S}\right) + 0.28.\left(\frac{W}{W_R}\right) \tag{2.79}$$

$$MRR = -0.10\left(\frac{W}{W_R}\right) + \frac{0.22}{C_n} + 0.20 \tag{2.80}$$

where W = actual tyre load, kN,
W_R = nominal tyre load, rated tyre load, kN and
C_n = wheel numeric as described by Wismer and Luth (1973).

Ashmore added the dynamic load ratio (W/W_R, where W_R = rated load of the tyre), to the empirical model developed by Wismer and Luth. The dynamic load ratio accounts for varying dynamic loads frequently encountered during skidding operations. Comparing the results with Wismer and Luth (1973) they reported that both equations show similar trends but quantitative differences resulted because of testing a less flexible tyre over a range of dynamic loads. Under ideal conditions, if tyre is operated near rated load, asymptotic constant will approach 0.75 as in Wismer-Luth equation.

Wulfsohan *et al.* (1988) developed generalized forms of Wismer-Luth equations using the following empirical equations for the coefficient of traction and gross traction ratios.

$$\frac{P}{W} = C_1\left[1 - \exp\left(-C_2 S\right)\right] \tag{2.81}$$

$$\frac{T}{r.W} = C_3\left[1 - C_4 \exp\left(-C_5 S\right)\right] \tag{2.82}$$

where, C_1 to C_5 are coefficients from non-linear regression technique.

Wulfsohan *et al.* (1988) and Upadhyaya *et al.* (1988, 1989) used these equations to analyze the tractive performance of a variety of tyre sizes, inflation pressures, dynamic loads, soil conditions and loading procedures with good correlation. The

challenge to relate the traction coefficients to soil and tyre parameters was attempted with limited success. Yu and Kushwaha (1994) found that Eqns. (2.81) and (2.82) fitted their experimental data also very well.

(iii) Models based on Brixius approach

Brixius (1987) presented new equations that improved the predictions of tractive performance and extended the range of application compared to the equations of Wismer and Luth. These equations have become the most commonly accepted traction equations. Brixius models are based on the farm tractor drawbar pull tests carried out by John Deere Co. in USA. The equations were developed using a curve-fitting technique, to predict the tractive performance of bias-ply tyres operating in cohesive frictional soils. Tyre torque, motion resistance, net traction, and tractive efficiency are predicted as a function of soil strength, tyre load, travel reduction (slip), tyre size and tyre deflection. The following equations are limited to tyres with a b/d ratio ranging from 0.1 to 0.7, static radial-ply tyre deflections ranging from 10% to 30% of the undeflected tyre section height, and W/ (bd) values ranging from 15 to 55 kN/m^2 (ASABE Standards, 2011).

$$GTR = \frac{T}{rW} = 0.88\left(1 - e^{-0.1B_n}\right) \times \left(1 - e^{-7.5S}\right) + 0.04 \tag{2.83}$$

$$MRR = \frac{MR}{W} = \frac{1.0}{B_n} + 0.04 + \frac{0.5 \times S}{\sqrt{B_n}} \tag{2.84}$$

$$B_n = \left(\frac{CIbd}{W}\right) \times \left(\frac{1 + 5\frac{\delta}{h}}{1 + 3\frac{b}{d}}\right) \tag{2.85}$$

where. B_n = Mobility number,
W = dynamic wheel load, kN,
CI = cone index for the soil, kPa,
b = unloaded tyre section width, m,
d = unloaded overall tyre diameter, m,
h = tyre section height, m,
δ = tyre deflection, m,
S = slip, decimal,
T = torque applied to wheel and
MR = motion resistance.

Evans *et al.* (1991) developed a traction prediction and ballast selection model based on the traction equations of Brixius (1987) using TK Solver. The coefficients of tractive equations were modified to improve the traction predictions for a specific tractor operating on a grass surface. The slip parameter in the gross traction equation was changed from 7.5 to 4.15 and the slip parameter in the motion resistance equation was reduced from 0.5 to 0.0.

$$GTR = 0.88 \times \left(1 - e^{-0.1 B_n}\right) \times \left(1 - e^{-4.15 S}\right) + 0.04 \tag{2.86}$$

$$MRR = \frac{1.0}{B_n} + 0.04 \tag{2.87}$$

Al-Hamed *et al.* (1994) used a general form of Brixius equations. These equations include six coefficients (C_1-C_6) and two constants (K_1 & K_2) for tyres as given below.

$$B_n = \left(\frac{CIbd}{W}\right) \times \left(\frac{1 + K_1 \frac{\delta}{h}}{1 + K_2 \frac{b}{d}}\right) \tag{2.88}$$

$$GTR = C_1 \times \left(1 - e^{-C_2 B_n}\right) \times \left(1 - e^{-C_3 S}\right) + C_4 \tag{2.89}$$

$$MRR = \frac{C_5}{B_n} + C4 + \frac{C_6 S}{\sqrt{B_n}} \tag{2.90}$$

They modified the numerical values of these coefficients and constants for radial-ply tyres as shown in Table 2.5.

Table 2.5 Comparison of constants and coefficients in the generalized traction model for bias-ply and radial-ply tyres

Coefficients	Brixius (1987) for bias-ply tyres	Brixius (1987) for radial-ply tyres	Al-Hamad et al. (1994) for radial-ply tyres
K_1	5	5	5
K_2	3	3	3
C_1	0.88	0.88	0.88
C_2	0.10	0.10	0.08
C_3	7.5	8.5 to 10.5	9.5
C_4	0.04	0.03 to 0.035	0.032
C_5	1.0	0.9	0.9
C_6	0.5	0.5	0.5

These changes were made to more accurately represent the results from recent tests on radial-ply tyres.

Tiwari *et al.* (2010) proposed the following model to predict the tractive performance of bias-ply tyre used in the India.

$$GTR = 0.66 \times \left(1 - e^{-0.09 B_n}\right) \times \left(1 - e^{-5.25 S}\right) + 0.035 \tag{2.91}$$

$$MRR = \frac{1.2}{B_n} + 0.035 + \frac{0.77 S}{\sqrt{B_n}} \tag{2.92}$$

The literature suggests that the Brixius model has been widely used to predict traction performance of rear wheel driven tractors fitted with bias-ply tyres. This model has also been included in ASABE standards. However, the coefficients of this model may be amended to suit the conditions if wide variations between predicted and field results are observed.

2.5 Tyre Soil and System Parameters

Soil tyre interaction is a very complex process. Tyre tractive ability depends on tyre type (radial verses bias), tyre geometry (width, overall diameter, and section height), lug design, inflation pressure, dynamic load on axle, and soil type and conditions (Upadhyaya *et al.* 1989).

2.5.1 Effect of inflation pressure on tractive performance

Zombori (1967) determined the effect of inflation pressure on drawbar pull and tractive efficiency. Results of his study showed that at constant travel reduction a decrease in inflation pressure caused an increase in drawbar pull. When drawbar pull was held constant, a decrease in inflation pressure caused a decrease in travel reduction, which resulted in a significant increase in tractive efficiency.

Zoz (1972) concluded that improved tractive efficiency could usually be obtained by reducing the ground contact pressure. This could be accomplished by reducing weight, increasing tyre size, increasing the number of tyres (dual) or reducing the tyre pressure to the lowest permissible. He further reported that efficiencies of over 90 per cent might be obtained on a concrete surface while 50 per cent is difficult to obtain in

soft or sandy conditions. Dynamic pull-weight ratio may vary from over 0.8 at 15 per cent slip on concrete to as low as 0.30 at approximately 30 per cent slip in sand.

Wulfsohn *et al.* (1988) tested four tyres (18.4×38, 18.4×R38, 14.9×28, 14.9×R28) at two different inflation pressures and three different vertical loads in a well tilled Yolo loam soil using dimensional analysis procedure. Two models using inflation pressure and tyre deflection as variables were considered for analysis. The effect of tyre type, tyre size, tyre inflation pressure, and dynamic load on coefficient of traction at 20 per cent slip and average tractive efficiency in the 0-30 percent slip range were investigated using ANOVA technique. They reported that larger tyres performed better than the smaller tyres, increased dynamic load led to increased performance and the large radial-ply tyres resulted in an average tractive efficiency of 27.23 per cent against 25.37 per cent for the large bias ply tyres, over the 0-30 per cent slip range.

Raper *et al.* (1995) found out that tyre inflation pressure greatly affected the soil-tyre interface stresses across the surface of the tyre, particularly on the lug. Increased inflation pressure caused soil-tyre interface stresses on the lug near the centre of the tyre to also increase. The shape of the tyre contacting the soil changed with inflation pressure. Net traction and tractive efficiency were both increased when inflation pressure was correctly set according to the tyre manufacturer's specifications. Inflation pressure as low as 41 kPa has been recommended by agricultural tyre manufacturers for minimizing an oscillatory vibration problem (power hop). Other benefits of these lower inflation pressures might include decreased soil-tyre interface pressures, increased tyre performance, and decreased soil compaction.

Arvidsson and Ristic (1996) examined that the rut depth, penetration resistance and soil stress increased significantly with the increased inflation pressure. The use of low-profile tyres did not reduce compaction if not used at a lower inflation pressure. The bias-ply tyre caused a higher stress in the soil stress than the radial-ply tyres when used with the same inflation pressure, but the compaction effects in terms of rut depth and penetration resistance were not greater for this tyre than for the radial low-profile tyres.

Bailey *et al.* (1996) measured soil stresses under a radial-ply tractor tyre, operated at two levels each of dynamic load and inflation pressure. Peak soil stresses and soil bulk density increased with increases in both dynamic load and inflation pressure.

They also concluded that inflation pressure should be set at the manufacture's recommendation for the actual load on the tyre, which is the minimum acceptable inflation pressure for that load. This will minimize soil stress and compaction, and maximize efficiency.

Lee and Kim (1997) investigated the effect of inflation pressure on the tractive performance of bias-ply tyres for agricultural tractors. Traction tests were conducted at velocities of 3, 4, and 5.5 km/h under four different surface conditions using a (13.6 - 28) tyre with 6 ply-rating bias ply tyre as driving wheel of the test tractor. When the inflation pressure was reduced from 250 kPa to 40 kPa by a decrement of either 30 or 50 kPa depending upon the test surfaces, some of the test results showed that the traction coefficient and tractive efficiency were increased maximally by 14 and 6 per cent respectively, at 20 per cent slip. However, such improvements in traction were not statistically significant enough to find any rules regarding the effect of inflation pressure of bias-ply tyres on the tractive performance of tractors.

2.5.2 Effect of wheel-soil parameters on tractive performance

Taylor *et al.* (1967) studied the effect of diameter on the tractive performance of tyres. In general, increasing tyre diameter led to increased pull and tractive coefficient, at the same normal load and inflation pressure. Increasing the applied vertical load led to increased pull. Pneumatic tyres showed the greatest benefit from increasing the diameter when the additional vertical load, which the larger tyre was capable of carrying at the same deflection, was added. Moreover, they found that increasing inflation pressure for constant vertical load and diameter led to decreased pull.

Gill and Vanden Berg (1968), Zoz (1972), Burt and Lyne (1985) found out that the traction performance was not affected by the normal range of travel speeds used by farm tractors. However, after investigating the effect of speed on tractive performance of tractor tyres at speeds greater than 0.6 m/s, Greenlee *et al.* (1986) reported that net pull to dynamic weight ratio decreased as speed increased to approximately 2 m/s and then became asymptotic.

Dwyer *et al.* (1976) studied the tractive performance of tyres for different soil conditions. They found that in good tractive conditions the drawbar pull developed

could be increased by increasing the dynamic load on the driving wheels and that the increase in inflation pressure needed to accommodate the increased load would not lower performance. In poor tractive conditions, on the other hand, the increase in pull obtained by increasing the dynamic load needs to be accompanied by increased tyre size to keep the inflation pressure down (Dwyer, 1984).

Burt *et al.* (1979) investigated the effects of dynamic load on tractive efficiency. They emphasized that at constant travel reduction an increase in dynamic load resulted in an increase in tractive efficiency on compacted soil but caused a decrease in tractive efficiency on uncompacted soil. This confirms the results of Kliefoth (1966) that coefficient of traction decreased when the load on the tyre was increased on soils with a poor bearing capacity.

Gee Clough (1980) reported that for a lightly loaded axle (7 kN per wheel) there was very little benefit by increasing wheel diameter beyond 1 m in good field conditions (Cl=1500 kPa) and 1.5 m in average field conditions (Cl =700 kPa). However, in bad conditions (Cl = 200 kPa) performance was still increasing appreciably at a wheel diameter of 2.5 m at a fixed width and deflection/section height. Also, based on the experiments conducted to observe the effect of changing wheel width at wheel diameter as 1 m and deflection/section height as 0.2, he concluded that to get the same improvement in performance the diameter had to be increased by 50 per cent but the width by 60 per cent.

Dwyer and Heigho (1984) compared the tractive performance of 18.4-38, 20.8-38, 23.1-30, 23.4-38, and 25.5-38 single tyres and 13.6-38 dual tyres in a range of field conditions. The tractive performance of widest tyres was generally inferior to that of more conventional sizes. These results, however, were obtained at the same vertical load, whereas the main benefit in fitting wider tyres was to enable heavier loads to be carried. The empirical relationships based on cone penetrometer resistance did not provide a good prediction of the performance of the wide tyres, but was satisfactory for the 13.6-38 dual tyres. It appears that the relationships do not adequately take account of differences in width/diameter ratio.

The past studies conducted on bias-ply and radial-ply tyres indicate that the tractive performance of the tyres is influenced by normal load, inflation pressure (i.e. tyre

deflection), tyre size, soil condition etc. but is independent of forward speed (within normal range of travel speeds used by farm tractors). It has been emphasized by many researchers that the tyres should be loaded to match with the inflation pressure as specified by the tyre manufacturers. Keeping these recommendations in view, the experimental work in the present study has been planned.

2.6 Comparison of Radial-ply and Bias-ply Tyre

The use of radial-ply tractor drive tyres may be one of the best ways to improve tractive efficiency. Many studies have demonstrated the advantages that can be gained by using radial-ply tractor tyres instead of bias-ply tyres. These advantages are due to the construction of radial-ply tyre.

Forrest *et al.* (1962) compared the tractive performance of a radial-ply tyre with its bias-ply equivalent in three different soils and on concrete. They found that the radial-ply tyre developed 8 % more drawbar pull in sand, 23 % more in loam, 21% more in clay and a maximum of 33 % more on concrete when run in the normal operating slip range up to 30%. The tractive efficiencies of the two tyres were similar.

Worthington (1962) found that the radial-ply tyre gave consistently higher values of coefficient of traction at low slip but approximately the same values at high slip when run in an alfalfa grass field and on a hard dirt track. The radial-ply tyres gave higher coefficients of traction at all slip values when run on concrete.

Thaden (1962) reported that radial-ply tyres developed up to 29% more drawbar pull at 16 % slip than cross-ply tyres in certain soil conditions. The advantage tended to drop off at higher slip values.

Vanden Berg and Reed (1962) tested specially made 11-28 tyres, with and without lugs, with bias-ply and radial-ply carcass construction against each other. They found that the radial-ply tyres developed an average of 15% higher coefficient of traction than the bias-ply equivalent in the 0 to 30% slip range but maximum coefficients of traction were the same. The average tractive efficiency in the 0 to 30% slip range was slightly higher for the radial-ply tyres.

Taylor *et al.* (1967) conducted experiments to determine the effects of diameter on the tractive performance of tyres. At the same normal load and inflation pressure, increasing tyre diameter in general led to increased pull and tractive coefficient. Increasing the applied vertical load led to increased pull. Pneumatic tyres showed the greatest benefit from increasing the diameter when the additional vertical load, which the larger tyre is capable of carrying at the same deflection, was added. Moreover, they found that increasing inflation pressure for constant vertical load and diameter led to decreased pull.

Taylor *et al.* (1976) compared the tractive performances of a radial ply and a bias ply tyre of the same size and shape in a range of soil conditions. They concluded that the radial ply tyre had its greatest advantages on firm surfaces where most of the soil-tyre deformation took place in the tyre, and that this advantage was gradually lost as the soil became softer, causing more of the total soil-tyre deformation to take place in the soil.

Gee-Clough *et al.* (1977) found that radial ply tyres perform better than bias ply tyres in a variety of British soil conditions when the radial ply tyre was not too highly inflated. The radial-ply tyres gave an average 5-8 % increase in the coefficient of traction at 20 % slip with no difference in maximum tractive efficiencies, at low inflation pressures. When the inflation pressure was increased to the maximum permissible value there was no difference in tractive performance between radial and bias-ply tyres.

Burt *et al.* (1982) reported that radial-ply tyres perform better than bias ply tyres at an intermediate axle load and a low inflation pressure. On a drier, less dense, higher cone-index soil use of radial-ply tyres resulted in higher tractive efficiencies than bias ply tyres.

Mayfield (1983) reported that radial-ply tyres produced higher tractor drawbar power on various soil surfaces compared to bias-ply tyres. This additional performance was a result of improved tractive efficiency.

Plackett (1984) found that radial-ply tyres gave a more even distribution of ground pressure than bias ply tyres, with a 15% decrease in the peak value of ground pressure.

Hausz (1985) stated that the tractive advantages of radial-ply tyres over bias-ply tyres are usually due to a larger foot print for the same axle load, and more even ground pressure distribution over the contact area.

Mueller and Treanor (1985) tested the performance of a 4WD tractor when equipped with radial-ply or bias-ply tyres. Both tyre types were tested as singles and duals at travel speeds of 8 and 11 km/h. As singles, the radials were significantly better than the bias-ply tyres for field productivity and drawbar power. Also, the radial-ply tyres had less wheel slip. The performance of radial tyres as singles was significantly better than bias duals at 11 km/h.

Wulfsohn *et al.* (1988) used a single-wheel tester to compare two sizes of bias and radial tyres (18.4-38, 14.9-28). Each tyre was tested at two inflation pressures and three dynamic loads. They found that the larger tyre (18.4-38) performed better than the smaller tyre (14.9-28). The maximum values of the dynamic traction ratio were about 0.4 and 0.3 for the 18.4-38 and 14.9-28 tyres, respectively. The inflation pressure had no significant effect on tractive performance.

Wulfsohn *et al.* (1988) found that in a tilled Yoio loam soil an 18.4R38 radial-ply tyre performed better than an 18.4-38 bias-ply tyre with similar tread design.

The past studies conducted on bias-ply and radial-ply tyres indicate that the radial-ply tyres were significantly better than the bias-ply tyres in terms of drawbar pull, efficiency and field capacity. Also, the radial-ply tyres had less wheel slip. Such tyres are, therefore, better suited for high hp tractors being used for heavy field and haulage operations.

2.7 Concluding Remarks

The tractive characteristics of a tyre depend on the type and condition of the soil, the tyre physical parameters, and tyre loading. Soil has a greater influence on the traction capabilities than the tyre design features. However, within a given soil type and condition, tyre design has a significant effect on the tractive performance.

The past studies indicate that the stress occurring between a traction device and the supporting surface determines the amount of traction the tractive device develops. The

tyre-surface contact area defines the loading area and the intensity of applied pressure. This has been modelled by various researchers to represent static behaviour of pneumatic tyres on a hard surface.

The Mobility number approach has been adopted by a large number of researchers to predict tractive performance of tyres. This approach gives its usefulness for practical use, but being empirical in nature it has limitations of its test range. The approach predicts the tractive performance of the pneumatic tyres within the acceptable limits. However, a series of field measurements and laboratory evaluations are needed to adequately predict the tractive performance of pneumatic tyres in different conditions. Out of the various empirical models, the Brixius model developed in 1987 has been found to have wide acceptability for rear wheel driven tractors fitted with radial-ply tyres. However, a few researchers have pointed out quite discrepancies between predicted and experimental results, particularly for small size tractors. The major objective of the present study was, therefore, formulated based on this finding.

CHAPTER III

THEORETICAL CONSIDERATIONS

This chapter deals with the theoretical considerations associated with the present study under the following headings:

- Tyre parameters
- Tyre deformation and contact characteristics
- Mechanics of traction wheel
- Traction parameters
- Dimensional analysis approach
- Selection criteria of variables

3.1 Tyre Parameters

There are two distinct types of tyre construction: bias ply and radial ply. The carcass of a bias ply tyre consists of layers, or plies, set diagonally to the tread and criss-crossed at an angle called a bias angle. Radial ply tires have plies that run at right angles to the tread. A belt around the radial ply tire gives it strength and stability. The result is a tire with flexible sidewalls but a stiffer tread area. Construction of a radial-ply tyre and description of tyre parameters are shown in Figs. 3.1 and 3.2.

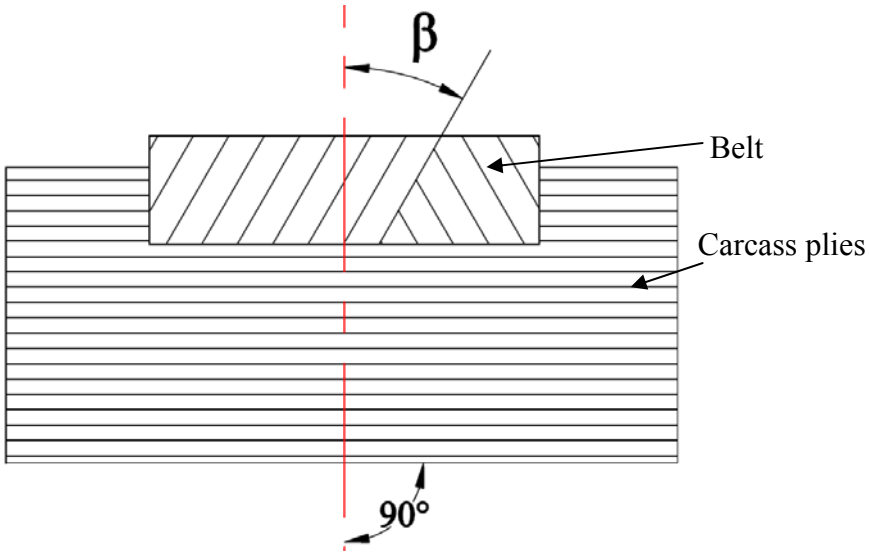

Fig. 3.1 Arrangement of belt and plies in radial-ply tyre

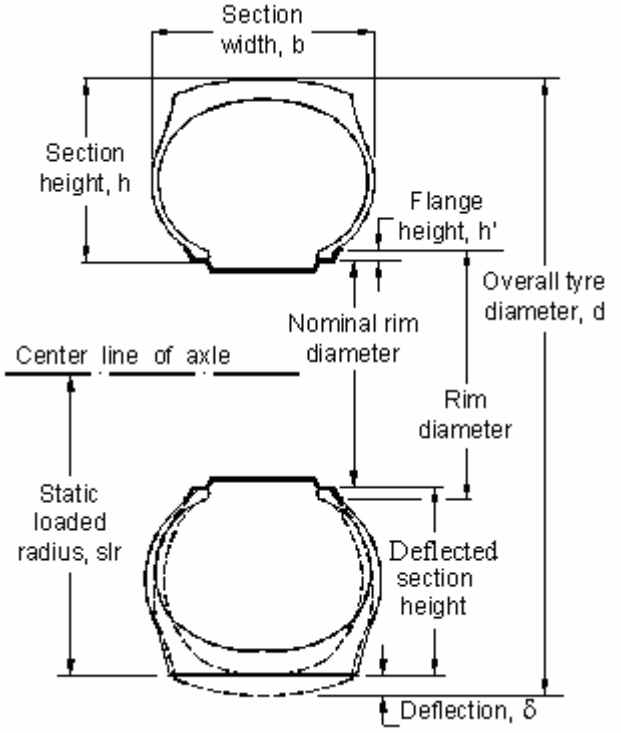

Fig: 3.2 Description of tyre parameters (Brixius, 1987)

3.1.1 Overall width (b): The undeflected width of a new tyre, including growth resulting from inflation for 24 hours is referred to as overall width of a tyre. This is the first number in a tyre size designation.

3.1.2 Overall diameter (d): The tyre circumference divided by Pi (π) gives overall diameter of a tyre. Circumference is measured over the lugs in the center plane with the tyre mounted on its recommended rim and inflated to the maximum rated inflation pressure in an unloaded condition following a 24-hour waiting period.

3.1.3 Section height (h): It can be represented as

$$h = \frac{d - \text{nominal rim diameter}}{2} \tag{3.1}$$

3.1.4 Deflection (δ): The difference between unloaded and loaded section heights of a tyre at a given load and inflation pressure is designated as tyre deflection. It can be represented as

$$\text{Deflection } (\delta) = \frac{\text{Overall diameter (d)}}{2} \text{ - static loaded radius (slr)} \tag{3.2}$$

3.1.5 Static loaded radius (slr): The distance from the tyre axle centre line to the supporting hard surface for a tyre mounted on an approved rim and carrying a load at a specific inflation pressure.

3.1.6 Deflection, per cent: The per cent deflection is defined as the ratio of tyre deflection to the portion of the tyre section height beyond the rim flange.

$$\text{Tyre deflection, per cent} = \frac{\text{Vertical tyre deflection } (\delta)}{(\text{Tyre section height } (h) - \text{Flange height})} \times 100 \qquad (3.3)$$

3.2 Tyre Deformation and Ground Contact Characteristics

The study of the deflection of a moving tyre under different inflation pressures and on various soil conditions is the first step toward understanding vehicle-soil relationship. The deformation of tyre significantly complicates the process of interaction between the wheel and the soil, since it leads to a change in the shape of the contact surface and the nature of the contact pressure distribution. When a pneumatic tyre is loaded against a flat rigid surface, it deflects to form an area of contact. This area transmits all of the forces developed between the tyre and the ground. When a pneumatic tyre is loaded against the soil, it can act in one of the two ways. (i) if the effective stiffness of the tyre is greater than the maximum sustainable normal stress for the soil, then the tyre will behave as a rigid wheel. (ii) If the effective stiffness is less, then the tyre will act as a flexible wheel. In both the cases, soil deformation results in the formation of a rut. As the rut depth decreases then the case of a wheel running on soil approaches that of a wheel running on a rigid surface (Plackett, 1984).

Tyre contact area on rigid surface can therefore, be considered to be valuable in assessing tyre ground pressure. Also from viewpoint of tyre-soil interaction, the significance of contact area determination on rigid surfaces is that it establishes a lower limit for the contact area in yielding soils. A rigid surface also has the advantage that, it is readily available standard and thus provides a basis for reliable and repeatable data. Therefore, as a reference, deflection patterns are determined on a firm surface.

3.3 Mechanics of Pneumatic Traction Wheel

The forces acting on a pneumatic wheel moving on soil surface are shown in Figs. 3.3 and 3.4. The torque (T) applied to the wheel can be assumed equal to gross traction (GT) acting at an effective moment arm (r). Part of the gross traction (GT) is required to overcome motion resistance (MR) which is the resistance to the movement of the wheel through the soil. The remainder is equal to net traction (P).

Gross traction (GT) = Motion resistance (MR) + Net traction (P) (3.4)

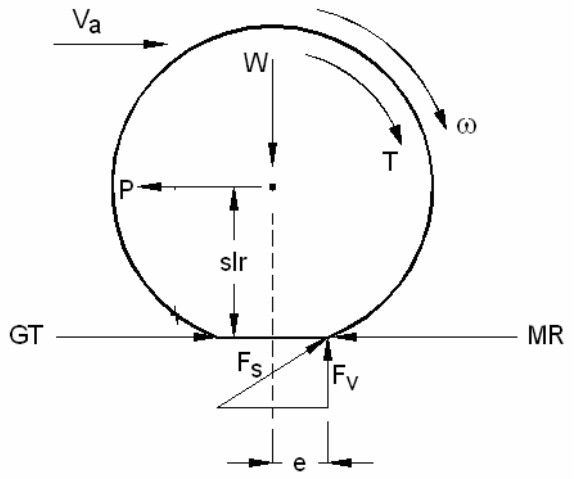

Fig. 3.3 Force diagram of a pneumatic traction wheel on hard surface

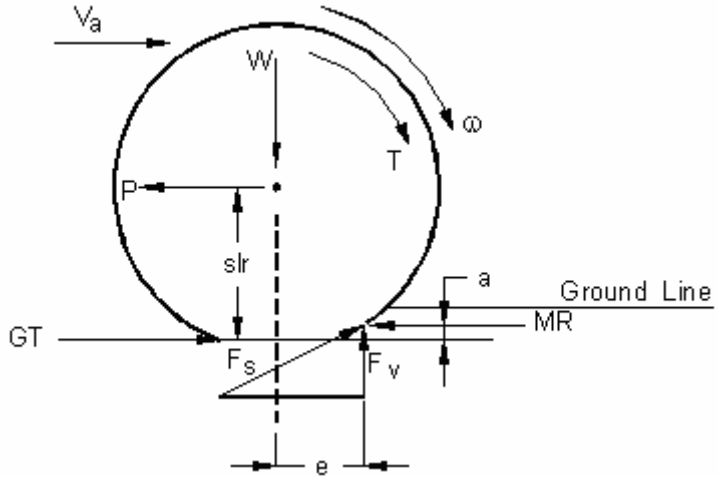

Fig. 3.4 Force diagram of a pneumatic traction wheel on deformable surface

where, a = vertical offset distance, m,
e = horizontal offset distance, m,
F_s = resultant soil reaction force, N,
F_v = vertical component of resultant soil reaction force, N,
GT = gross traction, N,
MR = motion resistance, N,
P = net traction, N,

slr = static loaded radius, m,
T = axle torque, Nm,
V_a = actual forward velocity, m/s,
W = weight on wheel, N and
ω = angular velocity, rad.

By dividing Eqn. (3.4) by the weight on the wheel (W), the following equation results

$$\frac{T}{rW} = \frac{MR}{W} + \frac{P}{W} \tag{3.5}$$

where, $\frac{T}{rW}$ = torque ratio or gross traction ratio,

$\frac{MR}{W}$ = motion resistance ratio and

$\frac{P}{W}$ = pull ratio or coefficient of traction.

For a pneumatic wheel moving on hard or soft surfaces the vertical reaction force (F_v) is not directly under the axle center line but is offset by a distance designated "e". This offset is necessary for static equilibrium. The amount of the offset on hard surface is given by

$$e = \frac{(slr \times MR)}{F_v} \tag{3.6}$$

Similarly, the offset distance on a soft surface (Fig. 3.4) is given by

$$e = \left(\frac{(slr - a) \times (MR)}{F_v} \right) \tag{3.7}$$

The amount of the horizontal offset (e) depends on the motion resistance (MR), the static loaded radius (slr), and the vertical force (F_v). The rolling radius (r) is derived from the rolling circumference. Gross traction force itself cannot be measured directly and is usually calculated from the axle torque and rolling radius. Three distinct force states are identified *i. e.* towed wheel, self-propelled wheel and driving wheel (Wismer and Luth, 1973).

A towed wheel is unpowered wheel where torque is equal to zero. A towed condition occurs when slip is less than zero. A self-propelled wheel is a traction wheel when the pull is equal to zero and gross thrust equals motion resistance. A driving wheel is a traction wheel which develops pull and it has positive slip.

3.4 Traction Parameters

Five dimensionless parameters are used to describe tractive performance

1. Gross traction ratio (GTR)
2. Net traction ratio (NTR) or pull ratio or coefficient of traction (COT)
3. Motion resistance ratio (MRR)
4. Wheel slip (S) or travel reduction ratio, expressed in per cent
5. Tractive efficiency (TE), usually in per cent

3.4.1 Wheel slip

Slip in a traction device occurs between the surfaces of the device and the medium on which it operates. This is defined as

$$S = \left(1 - \frac{V_a}{V_t}\right) \tag{3.8}$$

$$S = \left(1 - \frac{V_a}{r\omega}\right) \tag{3.9}$$

where, r = rolling radius of wheel on hard surface, m,
S = wheel slip or travel reduction, %,
V_t = theoretical travel speed, m/s,
V_a = actual travel speed, m/s and
ω = angular velocity of wheel.

Slip is a reduction in distance traveled and/or speed that occurs because of

1. flexing of the tractive device
2. shear within the soil.

From power efficiency standpoint, slip is a loss in power caused by a loss in travel distance traveled or speed. Slip occurs any time in a wheel or traction device which develops pull (net traction) (Brixius, 1987).

Rolling radius is used for calculating slip. The tyre rolling radius was determined according to the ASAE standards (1998) as the distance travelled per revolution of the wheel when operating under zero slip condition, divided by 2π. In general different zero conditions will lead to different rolling radius values and therefore to different values of slip for the same test.

Zero slip can be defined using any of the four methods (ASAE standards, 1998):

1. a self-propelled condition on a non-deforming surface.
2. a self-propelled condition on the test surface.
3. a towed condition on a non-deforming surface.
4. a towed condition on the test surface.

There are many arguments for using any of the above methods for a particular traction test. In any case, the zero condition used to define the rolling radius should always be stated (Upadhyaya *et al.*, 1988).

In the present study zero slip has been measured using a self-propelled condition (zero net traction) on a hard surface, because this method provides a repeatable test condition and data that can be replicated at other locations and test conditions.

The rolling radius (r) measured by this method can be used to calculate the theoretical speed of the wheel or tractive device:

$$V_t = \omega \, .r \tag{3.10}$$

where, ω = angular velocity of wheel.

The actual forward velocity of the vehicle or wheel is usually measured directly.

3.4.2 Pull ratio or coefficient of traction

The pull ratio is sometimes referred to as coefficient of traction, net traction ratio, or dynamic traction ratio and it is defined as the ratio of pull (P) to the dynamic weight (W) of a powered wheel.

$$\text{COT} = \frac{P}{W} \tag{3.11}$$

The dynamic weight (W) includes the effects of ballast and any weight transfer that may occur in the testing process. The net traction force (P) must be the horizontal component of force in the direction of travel and perpendicular to the reaction force (F_v). Zoz and Grisso (2003) stated that for a properly ballasted and inflated agricultural tyre, tractive efficiency tends to maximize at a coefficient of traction of approximately 0.40**.** This was also recognized by Dwyer (1984).

3.4.3 Tractive efficiency

The tractive efficiency (TE) is defined as

$$\text{TE} = \frac{\text{Output power}}{\text{Input power}} = \frac{\frac{\text{P}}{\text{W}}}{\frac{\text{T}}{\text{rW}}} \times (1 - \text{S}) \tag{3.12}$$

$$\text{TE} = \frac{COT}{GTR} \times (1 - S) \tag{3.13}$$

Loss in tractive efficiency is caused by losses in velocity and/or pull. The loss in travel speed is commonly referred to as "slip". Slip losses are visible, that is, the operator can see it happening. The other component of loss in tractive efficiency which is less visible and often overlooked, is a loss of pull, when motion resistance reduces the amount of gross traction that is converted into useful force (net traction). This is significant when a tractor is over ballasted resulting in reduced wheel slippage and increased motion resistance.

3.4.4 Torque ratio

Gross traction (GT) or thrust force (F) is sometimes referred as theoretical pull, design drawbar pull or rim pull. It is the input axle torque converted to pull force. The gross traction ratio (GTR) is the ratio of gross traction (GT) to dynamic weight on traction device (W) and is given by

$$\text{GTR} = \frac{\text{GT}}{\text{W}} = \frac{\text{T}}{\text{rW}} \tag{3.14}$$

Gross traction itself cannot be measured directly. It is usually calculated from the axle torque (T) and the rolling radius or tractive device.

3.4.5 Motion resistance ratio

The motion resistance or towed force of a pneumatic tyre is dependent on normal load, tyre size, inflation pressure, as well as on soil strength. Motion resistance or rolling resistance of a traction wheel is defined as the sum of the horizontal components of the soil reaction forces acting opposite to the direction of travel (Vandenberg *et al.*, 1961). The motion resistance ratio (MRR) is defined as the ratio of motion resistance to dynamic weight on traction device. This ratio is also represented as:

$$MRR = GTR - COT \quad (3.15)$$

The motion resistance ratio includes internal losses within the tractive device and soil forces. All energy losses beyond where the torque is measured are included in motion resistance. For example, gear losses are included if the torque is not measured directly at the input to the tractive device.

3.5 Dimensional Analysis

Dimensional analysis is the analysis of relationships between different physical quantities by identifying their fundamental dimensions. It is a powerful tool to provide a method for combining variables influencing the process and offers a method for reducing complex physical problems to the simplest forms.

3.5.1 Tyre deformation

There are six pertinent variables in the tyre deformation system as given by Eqn. 3.16. The set of parameters are shown in Table 3.1.

$$\delta = f(d, b, h, P_g, W) \quad (3.16)$$

According to Bekker (1960) and Wong (1989) the ground pressure P_g is the sum of tyre inflation pressure p_i and carcass pressure p_c.

According to Buckingham Pi theorem, four dimensionless ratios or Pi terms are needed to express a relationship among the variables in the deflection phenomena.

Table 3.1 Tyre deflection model parameters

Parameter	Symbol	Dimension
Unloaded tyre section width	b	L
Unloaded tyre diameter	d	L
Tyre deflection	δ	L
Tyre section height	h	L
Vertical wheel load	W	MLT^{-2}
Ground pressure	P_g	$ML^{-1}T^{-2}$

Assuming a product formulation eqn 3.16 can also be written as:

$$\delta = Cb^{x_1}.d^{x_2}.h^{x_3}.P_g^{\ x_4}.W^{x_5} \tag{3.17}$$

where C is a non dimensional constant.

Since the dimensions on both sides of the equation must be consistent, substitution of dimensions from Table 3.1, yields the following:

$$L = (L)^{x_1}.(L)^{x_2}.(L)^{x_3}.(ML^{-1}T^{-2})^{x_4}.(MLT^{-2})^{x_5}$$

From this equation, dimensional equality provides the following relationships:

$$L: 1 = x_1 + x_2 + x_3 - x_4 + x_5 \tag{3.18}$$

$$M: 0 = x_4 + x_5 \tag{3.19}$$

$$T: 0 = -2x_4 - 2x_5 \tag{3.20}$$

Since Eqns. 3.19 and 3.20 are identical, only two Eqns. 3.18 and 3.19 are available for solving the 5 unknowns. Solving x_3 in terms of others and x_5 in terms of x_4, we get:

$$x_3 = 1 - x_1 - x_2 + x_4 - x_5$$

and, $x_5 = -x_4$

Therefore equation (3.17) becomes,

$$\delta = Cb^{x_1}.d^{x_2}.h^{1-x_1-x_2+x_4+x_4}.P_g^{\ x_4}.W^{-x_4}$$

Collecting like terms to produce Pi terms, we get,

$$\frac{\delta}{h} = C\left(\frac{b}{h}\right)^{x_1}\left(\frac{d}{h}\right)^{x_2}\left(\frac{P_g h^2}{W}\right)^{x_4}$$

The last Pi term $\frac{P_g h^2}{W}$ can be converted to a more convenient form, by multiplying this term by other two Pi terms, $\left(\frac{b}{h}\right)$ and $\left(\frac{d}{h}\right)$ to yield $\left(\frac{P_g bd}{W}\right)$. Therefore the form of the equation becomes:

$$\frac{\delta}{h} = C\left(\frac{b}{h}\right)^{x_1}\left(\frac{d}{h}\right)^{x_2}\left(\frac{P_g bd}{W}\right)^{x_4}$$

This equation can also be written in the functional form as:

$$\frac{\delta}{h} = f\left[\left(\frac{b}{h}\right),\left(\frac{d}{h}\right),\left(\frac{P_g bd}{W}\right)\right]$$

For a given tyre, this expression can be further simplified as (b/h) and (d/h) are constant. So, this equation can be written as

$$\frac{\delta}{h} = f\left[\frac{P_g bd}{W}\right] \tag{3.21}$$

3.5.2 Traction potential of agricultural tyres

In this approach the independent parameters involving soil-tyre interaction are identified and then the manner in which they influence the dependent variables is determined. There are eleven pertinent variables and two dimensions involved in the traction study. A set of parameters are shown in the Table 3.2 and wheel torque can be written as:

$$T = f(d, b, r, \delta, h, W, S, MR, NT, CI) \tag{3.22}$$

. According to Buckingham Pi theorem, nine dimensionless ratio or Pi terms are needed to express a relationship among the variables in the traction phenomena.

Table 3.2 Wheel-soil model parameters

Parameter	Symbol	Dimension
Wheel		
Unloaded tyre section width	b	L
Unloaded tyre diameter	d	L
Tyre rolling radius	r	L
Tyre deflection	δ	L
Tyre section height	h	L
System		
Vertical wheel load	W	MLT^{-2}
Slip	S	–
Wheel torque	T	ML^2T^{-2}
Motion resistance	MR	MLT^{-2}
Net traction	NT	MLT^{-2}
Soil		
Cone index	CI	$ML^{-1}T^{-2}$

Assuming a product formulation eqn 3.22 can also be written as:

$$T = Cb^{x_1}.d^{x_2}.r^{x_3}.\delta^{x_4}.h^{x_5}.W^{x_6}.S^{x_7}.MR^{x_8}.NT^{x_9}.CI^{x_{10}} \tag{3.23}$$

where C is a non dimensional constant.

Since the dimensions on both sides of the equation must be consistent, substitution of dimensions from Table 3.2, yields the following:

$$ML^2T^{-2} = C(L)^{x_1}.(L)^{x_2}.(L)^{x_3}.(L)^{x_4}.(L)^{x_5}.(MLT^{-2})^{x_6}.(MLT^{-2})^{x_8}.(MLT^{-2})^{x_9}.(ML^{-1}T^{-2})^{x_{10}}$$

From this equation, dimensional equality provides the following relationships:

$$L: 2 = x_1 + x_2 + x_3 + x_4 + x_5 + x_6 + x_8 + x_9 - x_{10} \quad (3.24)$$

$$M: 1 = x_6 + x_8 + x_9 + x_{10} \quad (3.25)$$

$$T: -2 = -2x_6 - 2x_8 - 2x_9 - 2x_{10} \quad (3.26)$$

Since Eqns. 3.25 and 3.26 are identical, only two Eqns. 3.24 and 3.25 are available for solving the unknowns. Solving x_3 and x_6 in terms of others, we get:

$$x_3 = 1 - x_1 - x_2 - x_4 - x_5 + 2x_{10}$$

and, $x_6 = 1 - x_8 - x_9 - x_{10}$

Therefore equation (3.23) becomes,

$$T = Cb^{x_1}.d^{x_2}.r^{1-x_1-x_2-x_4-x_5+2x_{10}}.\delta^{x_4}.h^{x_5}.W^{1-x_8-x_9-x_{10}}.S^{x_7}.MR^{x_8}.NT^{x_9}.CI^{x_{10}}$$

Collecting like terms to produce Pi terms, we get,

$$\frac{T}{rW} = C\left(\frac{b}{r}\right)^{x_1}\left(\frac{d}{r}\right)^{x_2}\left(\frac{\delta}{r}\right)^{x_4}\left(\frac{h}{r}\right)^{x_5} S\left(\frac{MR}{W}\right)^{x_8}\left(\frac{NT}{W}\right)^{x_9}\left(\frac{CIr^2}{W}\right)^{x_{10}}$$

The last Pi term $\frac{CIr^2}{W}$ can be converted to a more convenient form, by multiplying this term by other two Pi terms, $\left(\frac{b}{r}\right)$ and $\left(\frac{d}{r}\right)$ to yield $\left(\frac{CIbd}{W}\right)$. Therefore the form of the equation becomes:

$$\frac{T}{rW} = C\left(\frac{b}{r}\right)^{x_1}\left(\frac{d}{r}\right)^{x_2}\left(\frac{\delta}{r}\right)^{x_4}\left(\frac{h}{r}\right)^{x_5} S\left(\frac{MR}{W}\right)^{x_8}\left(\frac{NT}{W}\right)^{x_9}\left(\frac{CIbd}{W}\right)^{x_{10}}$$

This equation can also be written in the functional form as:

$$\frac{T}{rW} = f\left[\left(\frac{b}{r}\right),\left(\frac{d}{r}\right),\left(\frac{\delta}{r}\right),\left(\frac{h}{r}\right),S,\left(\frac{MR}{W}\right),\left(\frac{NT}{W}\right),\left(\frac{CIbd}{W}\right)\right]$$

This equation can also be written as

$$\frac{T}{rW} = f\left[\left(\frac{b}{d}\right),\left(\frac{r}{d}\right),\left(\frac{\delta}{h}\right),\left(\frac{h}{d}\right),S,\left(\frac{MR}{W}\right),\left(\frac{NT}{W}\right),\left(\frac{CIbd}{W}\right)\right] \quad (3.27)$$

A similar approach was also used in the past to simplify the prediction equation for the multivariable system associated with soil-vehicle traction relations (Freitag, 1966; Freitag, 1968b; Wismer and Luth, 1973; Brixius, 1987).

However, two of the ratios can be derived from the other terms:

$$\frac{NT}{W} = \frac{T}{rW} - \frac{MR}{W}$$

$$\frac{h}{d} = \frac{1 - \frac{2r}{d}}{\frac{\delta}{h}}$$

The rolling radius ratio (r/d) is nearly constant for most agricultural tyres and thus this term may be neglected in the soil-wheel analysis. Therefore, an adequate set of dimensionless ratios for the selected variables is:

$$\left(\frac{T}{rW}\right) = f\left(\frac{CIbd}{W}, S, \frac{b}{d}, \frac{\delta}{h}\right) \tag{3.28}$$

$$\left(\frac{MR}{W}\right) = f'\left(\frac{CIbd}{W}, S, \frac{b}{d}, \frac{\delta}{h}\right) \tag{3.29}$$

in which f and f' are two separate and distinct functions.

The main purpose of the present study was to develop an empirical equation to predict the traction potential of radial-ply tyres used in rear wheel driven tractors under agro-climatic conditions of the country. The dimensionless ratios used to predict gross traction ratio and motion resistance ratio in the Eqns. 3.28 and 3.29 were utilised to develop the desired empirical equations and have been discussed in chapter V.

3.5.3 Gross traction at zero net traction on hard surface

The zero condition in the present study is defined at zero net traction on hard surface and assumed that the wheel slip is zero at zero net traction. For the prediction of gross traction at zero condition, the Eqn. 3.22 can therefore be simplified by ignoring the Pi terms $\left(\frac{CI.b.d}{W}\right)$ and S. The final form of the equation is given below.

$$\left(\frac{\mathrm{T}}{\mathrm{r} \times \mathrm{W}}\right) = \mathrm{f}\left(\frac{\mathrm{b}}{\mathrm{d}}, \frac{\delta}{\mathrm{h}}\right) \tag{3.30}$$

3.6 Criteria for Selection of Tyre, Soil and System Parameters in the Present Study

The influence of the various wheel, soil and system parameters on the traction potential of tyres was studied in the present study. Traditionally, design parameters of the tyre such as diameter, section width, section height, inflation pressure, ply rating and load deflection characteristics were considered to have varying degree of influence on the performance of the tyre. The criteria for selection of various parameters influencing the tyre performance are discussed below.

3.6.1 Tyre selection

The majority of the agricultural tractors manufactured in the country are in the power range of 18 kW to 40 kW. The sizes of traction tyres used in these tractors range from 12.4 R 28 to 16.9 R 28. Very rarely a tyre size 18.4 R 30 is adopted in tractors with P.T.O. power size greater than 50 kW. Therefore, the tyres used in the present study ranged from 12.4 R 28 to 16.9 R 28. This group represents more than 95 per cent of the tractor models manufactured in India. The selected tyres were of the same rubber compound and also had a similar tread pattern. The selected sizes of the tyres and their specified rims are given as follows.

1) 12.4 R 28 - 12 ply tyre mounted on rim size - W-11,
2) 13.6 R 28 - 12 ply tyre mounted on rim size - W-12,
3) 14.9 R 28 - 12 ply tyre mounted on rim size - W-13 and
4) 16.9 R 28 - 12 ply tyre mounted on rim size - W-15L.

3.6.2 Tyre deflection

The best single indicator of a tyre's ability to perform satisfactorily and deliver normal service life is the tyre deflection. Agricultural bias ply tyre deflection is about 20 per cent and radial ply tyre deflection is about 24 per cent under rated load and inflation pressure for normal field conditions. With the increased loads which are approved for slow speed operations, tyre deflections may approach 28 per cent. This has been found to be about the practical limit for agricultural tyres in any application where normal service life is expected. If a tyre is over-deflected as a result of overload or under inflation or a combination of these – service life will be reduced (Ellis, 1977). On the other hand, under–deflected tyre has reduced contact length with the

medium resulting in the reduced traction. Based on these facts, the tyre deflection range maintained in the present study was 20 – 28 per cent.

3.6.3 Inflation pressure and normal load

The combination of inflation pressure and normal load for each tyre was chosen to achieve the tyre deflection in the range of 20 – 28 per cent. To satisfy this criterion, the range of inflation pressure on test tyres was maintained from 41 kPa (6 psi) to 207 kPa (30 psi) and normal load from 7.36 kN (750 kg) to 19.13 kN (1950 kg). While fixing the range of inflation pressure and normal load for each tyre, it was decided to keep inflation pressure not less than 41 kPa and normal load not exceeding the higher loading capacity of the tyre.

3.6.4 Forward speed

The review of literature indicates that the traction performance in general not affected by the travel speeds used for farming operations. The heavy draft operations are usually carried out in the speed range of 2 to 5 kmph. Considering the limitations in the experimental facilities, the tests were conducted at only one forward speed which varied from 2.9 to 3.5 kmph according to the tyre size.

3.6.5 Slip

As per ASABE standard (2000), the maximum tractive efficiency is obtained with the following optimum slip ranges.

1) 4 – 8 % for concrete,
2) 8 – 10% for firm soil,
3) 11 – 13 % for tilled soil and
4) 14 – 16% for soft soils and sands.

Based on this recommendation, the tests were conducted on different sizes of tyres at different drawbar pull to ensure that the slip was in the range of 0-30 %.

3.6.6 Terrain condition

Cone index is an established satisfactory measure of soil consistency. For lateritic sandy clay loam soil, cone index in the range of 700 to 1800 kPa represents soil

conditions from loose to firm on which tractor has to operate for agricultural operations at moisture content of about 7 per cent (w.b.). In view of this the cone index values were varied as given below.

- 600–700 kPa – soft soil condition
- 1200–1300 kPa – medium soil condition
- 1700–1800 kPa – hard soil condition.

The theoretical concepts discussed in this chapter provide a sound basis for formulating the research programme as well as for developing empirical equations related to traction performance of radial ply agricultural tyres in the present study. In the next chapter, the methodology adapted to collect test data of different radial-ply tyres is discussed.

CHAPTER IV

MATERIALS AND METHODS

This chapter deals with the experimental set-up, techniques used and equipment employed for conducting the experiments. These include deflection and contact characteristics of test tyres, zero condition tests for traction tyres, and evaluation of traction performance of the test tyres

4.1 Deflection and Contact Characteristics of Test Tyres

The research plan followed to achieve this objective has been presented below.

4.1.1 Research plan

The objective of this study was to obtain vertical tyre deflection and contact area characteristics of radial ply tyres at various normal loads and inflation pressures. In order to accomplish the objective, four different sizes of radial ply tyres were tested at seven inflation pressures and six normal loads on a hard surface. The test plan is as follows:

Independent parameters:			
Tyre (radial-ply)	4	T_1-12.4 R 28 (321mm × 711mm) T_2-13.6 R 28 (358mm × 711mm) T_3-14.9 R 28 (405mm × 711mm) T_4-16.9 R 28 (452mm × 711mm)	
Inflation pressure, kPa (psi)	7	41 (6), 69 (10), 97 (14), 124 (18), 152 (22), 179 (26), 207(30)	
Normal load, kN (kgf)	6	4.905 (500), 6.377 (650), 7.848 (800), 9.32 (950), 10.791 (1100), 12.263 (1250)	- for T_1
	6	6.377 (650), 7.848 (800), 9.32 (950), 10.791 (1100) , 12.263 (1250), 13.734 (1400)	- for T_2
	6	7.848 (800), 9.81 (1000), 11.772 (1200), 13.734 (1400), 15.696 (1600) , 17.658 (1800)	- for T_3
	6	9.32 (950), 11.282 (1150), 13.244 (1350), 15.206 (1550), 17.168 (1750), 19.13 (1950)	- for T_4
Supporting surface	1	Hard surface	
Replications	3		
Dependent parameters:			
Vertical tyre deflection, mm Tyre surface contact area, cm^2 Ground pressure, kN/m^2 (kPa)			

4.1.2 Experimental tyres

As mentioned in section 3.6.1, the four different sizes of tyres which are most commonly used in Indian tractors in the power range of 18 - 40 kW were selected for the study (Fig. 4.1). The detailed specifications of the test tyres are given in Table 4.1. The lug details of a tyre are shown in Fig. 4.2 and their dimensions are given in Table 4.2.

Fig. 4.1 Test tyres used in the study

Table 4.1 Specification of the test tyres

Tyre size	Rim size	Ply rating	Section width, mm	Nominal rim. dia., mm	Flange ht., mm	Rim dia,, mm	Section ht., mm	Overall dia., mm	Lug no.
12.4 R 28 (321 mm× 711 mm)	W-11	12	321	711.2	26.5	764.2	285.5	1282.1	21
13.6 R 28 (358 mm× 711 mm)	W-12	12	358	711.2	26.5	764.2	295.2	1301.6	21
14.9 R 28 (405 mm× 711mm)	W-13	12	405	711.2	26.5	764.2	332.9	1377.0	21
16.9 R 28 (452mm× 711mm)	W-15L	12	452	711.2	26.5	764.2	367.0	1445.1	21

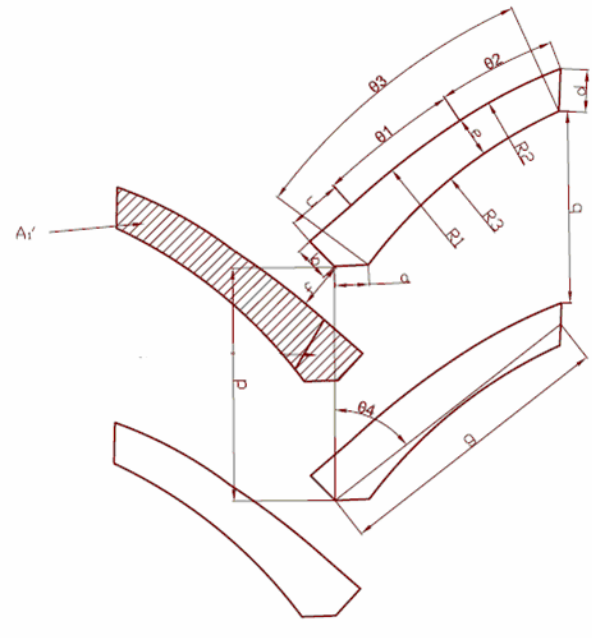

Fig. 4.2 Lug details of the test tyres

Table 4.2 Lug dimensions of the test tyres

Tyre	a mm	b mm	c mm	d mm	e mm	f mm	g mm	p mm	q mm	R_1 mm	R_2 mm	R_3 mm	θ_1 deg	θ_2 deg	θ_3 deg	θ_4 deg	A_1' mm^2
T_1	24	25	40	30	32	41	215	192	151	518	437	335	10	12	30	47	6880
T_2	25	28	42	32	33	41	220	195	153	567	443	355	10	12	30	48	7794
T_3	27	30	44	34	34	45	240	204	159	646	451	370	10	12	30	50	8560
T_4	30	32	47	37	35	50	255	212	166	713	457	425	10	12	30	52	9525

4.1.3 Experimental set-up and instrumentation

The experimental set-up consists of a tyre test carriage and an electronic platform balance. The tyre test carriage could accommodate the various sizes of the tyres and it has an arrangement to provide the free vertical movement to the test tyre under static position which helped in transferring the normal load of the test carriage solely on the wheel. The constructional details of the test carriage are discussed in section 4.3.2.

The vertical deflection of the tyre was measured with a displacement transducer and recorded by a Data Acquisition System (DAS). The transducer was rigidly fixed on the frame and was supported on the base plate attached to the side rail of the soil bin. The experimental set-up is shown in Fig. 4.3. The displacement transducer consists of a potentiometer with uniform coil of wire, whose resistance is proportional to its length and rack and pinion arrangement. The circuit diagram of the transducer is

given in Fig. 4.4. The transducer was connected to the input power supply of 10 volt. The detailed specifications of the displacement transducer are given in Appendix-A.

1. Hydraulic cylinder 2. Displacement transducer 3. Base plate 4. Side rail

Fig. 4.3 Test set-up for tyre vertical deflection measurement

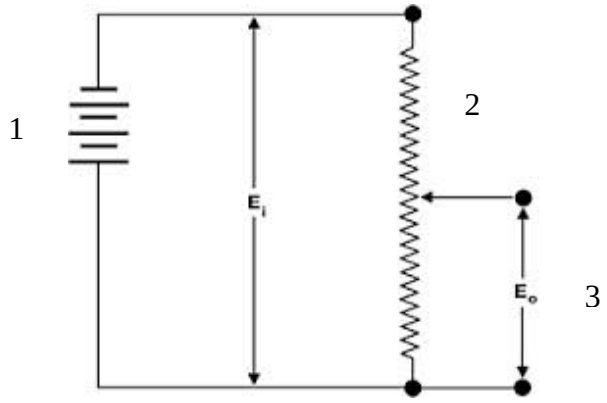

1. Power supply 2. Potentiometer 3. Signal output

Fig. 4.4 Circuit diagram of potentiometer used in displacement transducer

The transducer was calibrated before conducting the tests. First, initial reading was recorded in a DAS for a zero position of the displacement. Then using gauge blocks with dimensions corresponding to the displacement, the final output was measured in the DAS. The difference between initial and final readings of the DAS indicated the deflection.

4.1.4 Test procedure

A multiple overlay technique was used to get consistent results for the lugged tyres (Plackett, 1987; Lyasko, 1994). The test procedure followed in the present research work for deflection and contact area measurement are as follows. A steel plate, covered with white sheets with a carbon paper in between the sheets as shown in Fig. 4.5, was placed beneath the test tyre fitted in the tyre test carriage (Fig. 4.6). The paper was clamped tightly with the steel plate so that it was not displaced during the tests. The tyre with a given inflation pressure was loaded to the desired vertical load with the dead weights on a single wheel tester. The tyre was slowly brought down and allowed to rest on the paper and the transducer output was recorded for deflection measurement. Then the tyre was raised and rotated by a few degrees and pressed against the plate again. This procedure was repeated to obtain a good imprint of tyre on the white sheet (Fig. 4.7) by overlaying a number of prints on the same area. The outline of the contact area imprint was traced and area was determined using mechanical desktop software.

The mean ground pressure was represented by the normal load to contact area ratio**.** The per cent deflection was calculated using Eqn. (3.3.).

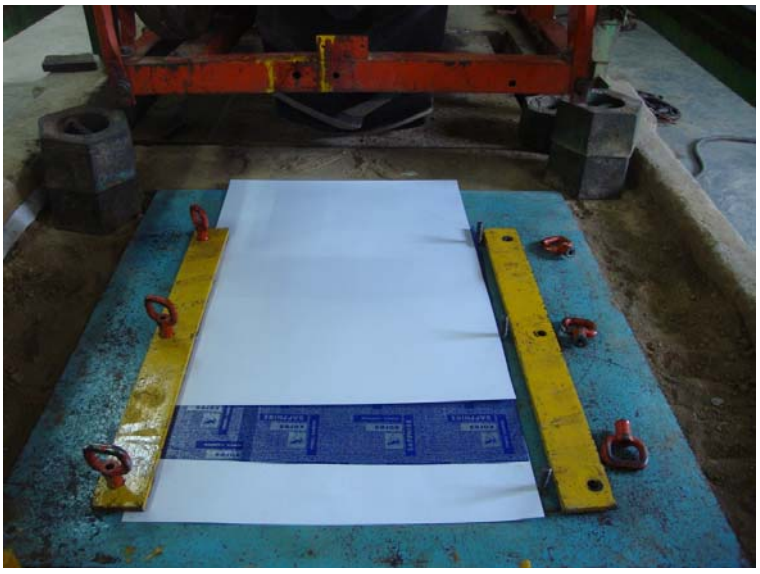

Fig. 4.5 Steel plate covered with white sheets and carbon paper

1. Steel plate 2. white sheet 3. Test tyre 4. Hydraulic cylinder

Fig. 4.6 Set-up for measurement of tyre-ground contact area

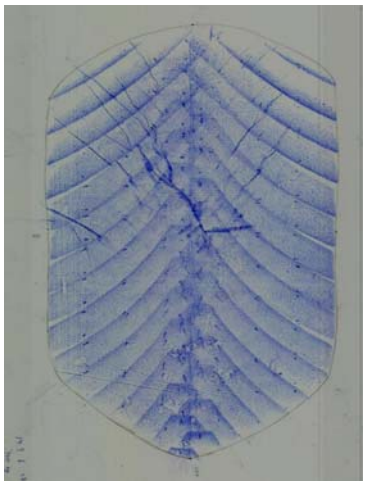

Fig. 4.7 Test tyre impression for measurement of contact area

4.2 Zero Condition Tests for Traction Tyres

The zero condition tests were conducted at zero pull. The research plan and test procedure are discussed below.

4.2.1 Research plan

The objective of this study was to obtain the characteristics of the radial ply tyres at zero condition. The zero condition selected in this study was the vehicle operating in a self-propelled condition on hard surface with zero drawbar load. In order to accomplish the objective four different radial ply tyres were tested at three normal

loads and three percent tyre deflections on a hard surface. The test plan followed is given below.

Independent parameters:			
Supporting surface	1	Hard surface	
Tyre (radial-ply)	4	T_1-12.4 R 28 (321mm × 711mm) T_2-13.6 R 28 (358mm × 711mm) T_3-14.9 R 28 (405mm × 711mm) T_4-16.9 R 28 (452mm × 711mm)	
Normal load, kN (kgf)	3	7.36 (750), 9.32 (950), 11.28 (1150)	- for T_1
	3	9.32 (950), 11.28 (1150), 13.24 (1350)	- for T_2
	3	11.28 (1150), 13.73 (1400), 16.19 (1650)	- for T_3
	3	14.22 (1450), 16.68 (1700), 19.13 (1950)	- for T_4
Tyre deflection, %	3	20, 24, 28	
Replication	3		
Dependent parameters:			
Rolling radius, m Input-torque, Nm			

4.2.2 Test procedure

The hard surface for zero condition was created by placing 10 mm thick MS sheets over the well-compacted soil in the soil bin. The input torque values for each selected conditions of load and inflation pressure were measured. Rolling radius of the tyre under each selected condition was calculated by measuring the distance traveled in one revolution of the tyre divided by 2π. Prior to each experiment the periphery of the test tyre was marked with white paint. The distance covered in one revolution of tyre was obtained by measuring the distance between the two consecutive painted marks on the hard surface while the tyre was in operation. Three replications were taken for each experiment.

4.3 Evaluation of Traction Performance of Test Tyres

To evaluate the traction performance of test tyres in the present study the experiments were conducted under controlled conditions in the soil bin as discussed below. The research plan and the experimental set-up for the present investigation are presented in the subsequent sub-sections.

4.3.1 Research plan

The objective of this study was to obtain the influence of soil, tyre and system parameters on the tractive performance of the tyres. Four different radial ply tyres were selected for tyre performance test on three terrain conditions, with three normal loads (based on the tyre size) and three percent deflections. The three terrain conditions were achieved by compacting the soil in test bed with the cone index values of 600-700 kPa, 1200-1300 kPa and 1700-1800 kPa respectively. The research plan for the present investigation is given below.

Independent parameters:			
Soil Type	1	Lateritic sandy clay loam	
Cone index, kPa	3	600 – 700 soft soil condition 1200 – 1300 medium soil condition 1700 – 1800 hard soil condition	
Tyre (Radial–ply) Size	4	T_1-12.4 R 28 (321mm × 711mm) T_2-13.6 R 28 (358mm × 711mm) T_3-14.9 R 28 (405mm × 711mm) T_4-16.9 R 28 (452mm × 711mm)	
Deflection, %	3	20, 24, 28	
System			
Normal load, kN (kgf)	3	7.36 (750), 9.32 (950), 11.28 (1150)	- for T_1
	3	9.32 (950), 11.28 (1150), 13.24 (1350)	- for T_2
	3	11.28 (1150), 13.73 (1400), 16.19 (1650)	- for T_3
	3	14.22 (1450), 16.68 (1700), 19.13 (1950)	- for T_4
Theoretical speed, km/h	1	2.9-3.5	
Drawbar pull, kN (kgf)	7	0-9.8 (0-1000)	
Replication	3		
Dependent parameters :			
Forward speed, m/s Torque, Nm Sinkage, mm			

4.3.2 Experimental set-up

The experimental set-up consists of an indoor soil bin, a soil processing trolley, a tyre test carriage, a drawbar pull loading device and control chamber. The different units of the experimental set-up are briefly described as follows. A general view of the experimental set-up is shown in Fig. 4.8.

1. Soil bin 2. Soil processing trolley 3. Tyre test carriage
4. Drawbar loading device 5. Control chamber

Fig. 4.8 A view of traction test experimental set-up at IIT Kharagpur

(a) Soil bin

The soil bin is constructed with cement concrete and bricks with 23.5 m × 1.37 m × 1.50 m overall dimensions. It is provided with 90 mm × 90 mm × 5 mm M.S. angle iron posts over. Two side rails (125 mm × 65 mm × 5 mm) of 'C' cross section were mounted 1.37 m apart along the length of the soil bin to facilitate movement of the towing trolley as well as soil processing trolley in the soil bin. An electronic plateform balance was installed at one end of the soil bin to measure the static weight on the test tyre. The bin was filled with the lateritic sandy clay loam soil. The properties of the soil are given in Appendix-B.

(b) Soil processing trolley

A soil processing trolley was used to prepare the test beds at different compaction levels in the soil bin. The soil processing trolley which is shown in Fig. 4.9 consists of a rotary tiller, a leveller blade and a compacting roller. These units were mounted on a common rectangular M.S. channel frame equipped with four rollers to facilitate the movement over the soil bin. The tiller was operated by a 3.73 kW, 3 phase, 1445

rev/min induction motor through a pulley and V-belt drive unit (1:3 and 1:1.5 ratio). The trolley was moved to and fro by means of a separate drive system (Fig. 4.10**).**

1. Main frame 2. Induction motor 3. Soil tiller
4. Soil leveler 5. Soil compacting roller

Fig. 4.9 Soil processing trolley for soil bed preparation

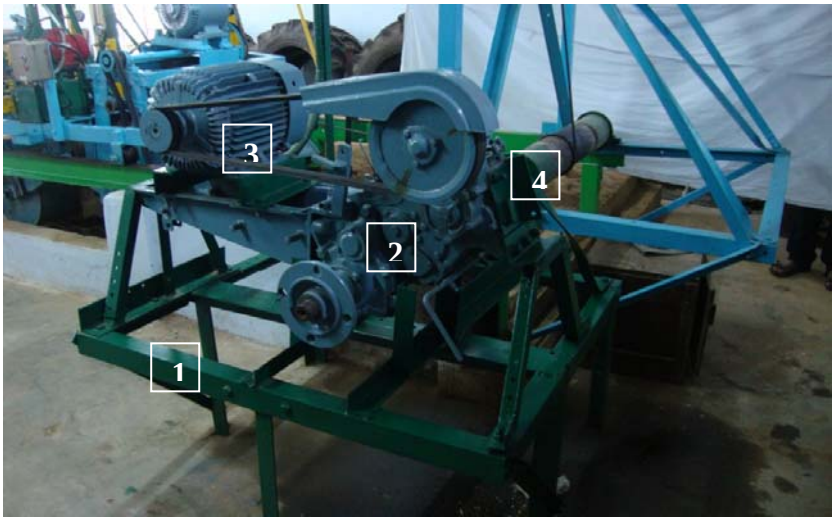

1. Main frame 2.Gear box 3. Induction motor 4. Rope drum

Fig. 4.10 Processing trolley linear motion drive unit

(c) Tyre test carriage

A tyre test carriage consists of a main frame to accommodate the various size of tyres, a loading platform, lifting arms, a parallel bar linkage system and a power transmission system. The test carriage was attached to a towing trolley through fixed

supports of parallel bar linkage. The constructional details of the test carriage are shown in Fig. 4.11.

1. Induction motor 2. Torque transducer 3. Chain drive
4. Gear box 5. Test wheel 6. Main frame
7. Loading platform 8. Towing trolley 9. Parallel bar linkage system.

Fig. 4.11 Constructional details of the tyre test carriage

A four bar parallel linkage system was attached to the tyre test carriage with the towing trolley through pin joints. This arrangement provided free vertical movement of the test carriage and helped in transferring the normal load of the test carriage solely onto the wheel.

A 7.46 kW, 3 phase, 1500 sync rev/min induction motor, mounted on the loading platform frame, was used to give driving power to the wheel. The speed of the motor was initially reduced by chain and sprocket drive arrangement (2.6:1), which was further reduced by a worm and worm gear reduction unit (50:1). The test tyre was mounted on the output shaft of the gear reduction unit through a sleeve coupling and flange arrangement. An idle shaft with a ball bearing at one end supported the far end of the sleeve coupling. Thus the final linear speed of the wheel axle was obtained between 2.9 – 3.5 km/h depending upon the tyre size and other operating conditions.

(d) Drawbar loading device

A loading device was used to vary horizontal pull of the test wheel. The drawbar-loading device is shown in Fig. 4.12. It has a steel drum of 63 cm in length and 53 cm

in diameter. This drum was mounted on a 55 mm M.S. shaft, supported on bearings at both ends. A shoe type braking arrangement was provided at one end of the shaft, which could be operated by applying downward force, by means of dead weights in a pan. A steel wire rope of 10 mm diameter was wrapped around the drum with one end of the rope attached to the drum and the other end, after passing over a set of pulleys, was tied to the ring transducer in the towing trolley. The rope unwrapped as the wheel moved forward and in turn, being a positive drive mechanism, it rotated the drum. The rotary motion of the drum was restricted by varying the braking force on the drum thus providing varying drawbar loads to the test wheel.

1. Frame 2.Drum 3.Steel wire rope
4. Braking mechanism 5.Weight pan 6.Lever arm

Fig. 4.12 Drawbar loading device

4.3.3 Instrumentation

A control chamber which houses an electrical control panel and various recording units is shown in Figs. 4.13 and 4.14. The electrical control panel was used to operate the soil processing trolley and the tyre test carriage in forward and reverse directions. The recording units included a DAS and a computer. The details of the instruments used in the present study are given in Appendix-A.

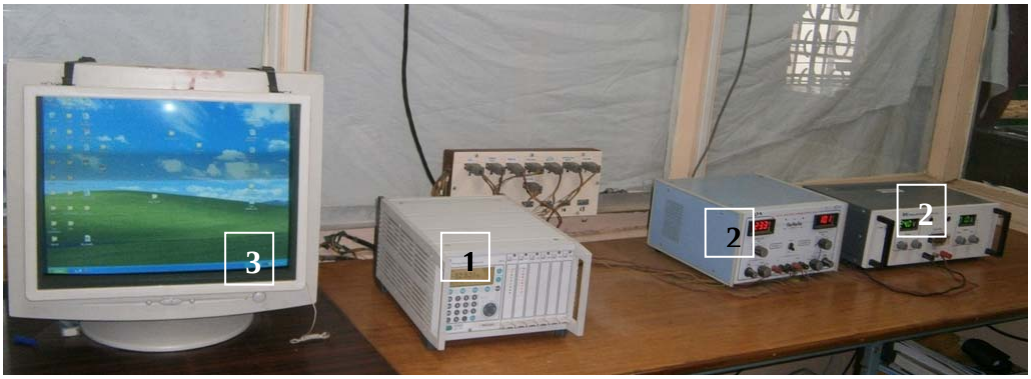

1. Data acquisition system 2. DC power supply unit 3. Computer

Fig. 4.13 Data recording system for measuring different parameters

Fig. 4.14 Electrical control panel

(a) Measurement of drawbar pull

The drawbar pull of the test tyre was measured using a ring transducer of 10 kN capacity, equipped with electrical resistance strain gauges as sensitive elements (Fig. 4.15). Four strain gauges each of 120 Ω resistances forming a Wheatstone bridge circuit were bonded on the ring transducer of 10 kN capacity **(**Fig. 4**.**15). Two couplers were fixed at both the ends of the transducer for attaching it between the towing trolley and drawbar pull loading system.

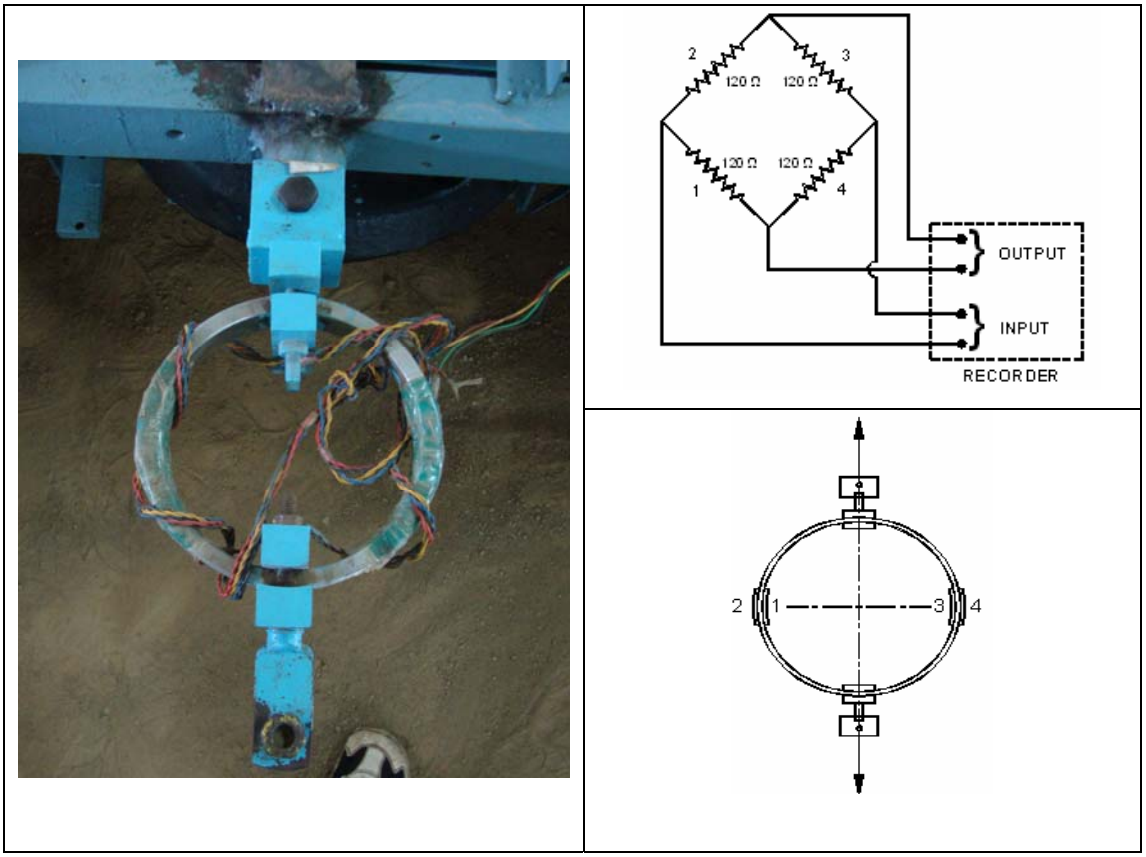

Fig. 4.15 Ring transducer & Wheatstone bridge circuit for pull measurement

The transducer was calibrated before conducting the tests. The strain gauge circuit of the transducer was connected to the DAS. The DAS supplies an excitation voltage of 5 volt DC to the transducer bridge. The tensile force in the ring transducer was gradually increased/decreased using the dead weights and the corresponding output voltage was recorded.

(b) Torque measuring system

Input torque to the wheel axle was measured by using a torque transducer and recorded in DAS. The torque transducer unit (Fig. 4.16) was connected in horizontal position in between the prime mover (a 3-phase 7.46 kW induction motor) and the load shaft (driving sprocket) through two sets of flexible coupling for continuous measurement of dynamic torque. The schematic diagram of torque measuring system is shown in Fig. 4.17. A stabilized 24 Volt DC was fed to the terminal box. The output voltage from the terminal box was recorded by the DAS.

1. Induction motor 2. Torque transducer (T20WN) 3. Couplers
4. Drive shaft 5. Terminal box (VK20)

Fig. 4.16 Torque transducer mounted on tyre test carriage

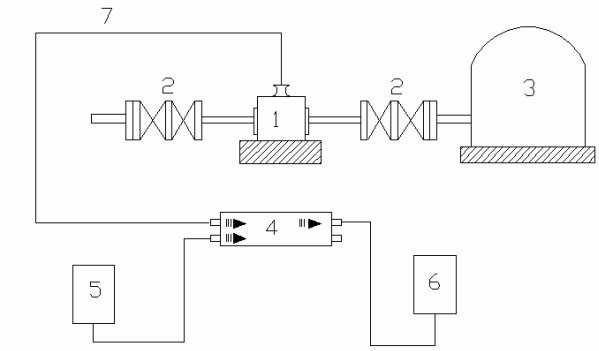

1. Torque transducer (T20WN) 2. Mounting couplings 3. Induction motor
4. Terminal box (VK20) 5. Power supply 6. Data acquisition system
7. Connecting cable

Fig. 4.17 Schematic diagram of torque measuring system

The torque transducer was calibrated under dynamic conditions to take into account the losses that might occur in power transmission system between the test wheel and the torque transducer unit. For the dynamic condition calibration, a wheel rim was used. The whole frame of the tyre-test carriage was raised and rigidly fixed so that the rim could be rotated on the wheel axle freely in the standing position. A band brake was mounted over the wheel rim and its both the ends were connected to two ring transducers as shown in Fig. 4.18. The torque was applied to the rim by varying the tensions at the tight side and measuring the corresponding tension at the loose side of the band brake.

The applied torque was calculated as follows

$$T = (t_1 - t_2) \times r \qquad (4.1)$$

where, T = applied torque, Nm,

t_1 = tension at tight side, N,

t_2 = tension at slack side, N and

r_m = radius of rim, m.

For each applied torque, the output voltage was recorded.

1. Ring transducer 2. Fixed arm 3. Band brake
4. Wheel rim 5. Loading/unloading lever

Fig. 4.18 Test set-up for dynamic calibration of torque transducer

(c) Measurement of forward speed

In order to determine the wheel slippage for each test, the actual and theoretical forward speed of the wheel was required to be measured. The actual forward speed measuring device (Fig. 4.19) consisted of a proximity switch attached to towing trolley and sensing the rotation of a roller moving over the steel rail. The radius of the roller is 0.0448 m. The number of signal pick from the proximity switch was counted using a program developed in matlab and the time corresponding to the 1st and last pick was also noted. The actual forward speed of the wheel was calculated as follows.

$$\text{Actual velocity } (V_a) = \frac{2\pi \times (N_p - 1) \times r_r}{t_t} \text{ m/s.} \quad (4.2)$$

where N_p = number of signal picks,

r_r = radius of the roller, m and

t_t = total time between 1st and last pick, s.

The theoretical forward speed of the wheel was also measured using another proximity switch, which senses the rotation of a disc connected to the wheel axle through chain and sprocket. The disk consisted of eight pegs. The theoretical forward speed measuring device is shown in Fig. 4.20. The theoretical forward speed of the wheel was calculated as follows.

$$\text{Theoretical velocity } (V_t) = \frac{2\pi \times (N_p - 1) \times r}{8 \times t_t} \text{ m/s.} \quad (4.3)$$

where, N_p = number of signal picks,

r = rolling radius of the test tyre, m and

t_t = total time between 1st and last pick, s.

Fig. 4.19 Actual forward speed measuring device

Fig. 4.20 Theoretical forward speed measuring device

(d) Measurement of tyre sinkage

A point gauge with a supporting frame, as shown in Fig. 4.21 was used to measure the surface profile of the soil bed before and after each test. The difference between initial and final readings of the soil profile indicated the tyre sinkage.

1. Prepared soil bed 2. Point gauge 3. Reference frame

Fig. 4.21 Tyre sinkage measuring device

(e) Measurement of soil parameters

The tests were conducted in lateritic sandy clay loam soil. In order to check the uniformity of the bed conditions, a few important soil parameters such as soil cone

index, bulk density and moisture content were measured before starting the experiment.

Soil cone index is used as a measure of soil strength (consistency). It is the force per unit base area required to force a cone shaped probe into the soil at a steady rate. To measure the soil cone index from zero to 150 mm depth of soil surface, a hydraulically operated cone penetrometer **(**Fig. 4.22**)** was used. It consists of a 30 degrees cone with a base area of 323 mm^2 and a circular shaft of 15.6 mm diameter attached to a ring transducer. The cone penetration depth was measured using penetration depth sensor. The cone penetration depth sensor consists of potentiometer mounted on rack and pinion arrangement.

For the measurement of bulk density of the soil, a core sampler having a 30 degree bevel edge at one end for easy penetration in to the soil was used. The core sampler was penetrated into the soil bed and carefully taken out without disturbing the soil inside the sampler. The content of the sampler was emptied and weighed for calculating the bulk density of the soil. For measurement of soil moisture content, standard oven dry method was used.

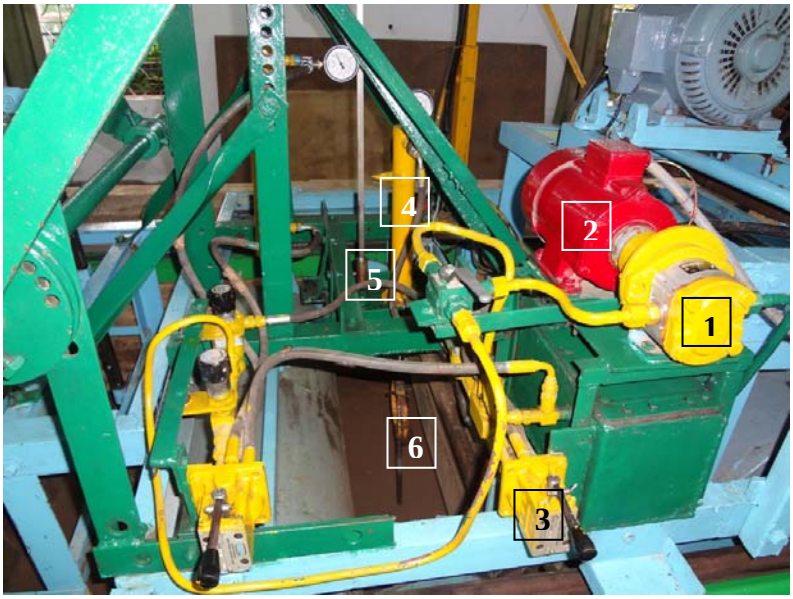

1. Hydraulic pump 2. Electric motor 3. Directional control valve
4. Hydraulic cylinder 5. Depth sensor 6. Ring transducer and cone penetrometer

Fig. 4.22 Hydraulic cone penetrometer

4.3.4 Experimental Procedure

The procedure followed for preparation of soil test bed and for evaluation of traction performance of test tyres has been described in the following sub sections.

Preparation of test bed

The soil bed was prepared using the soil processing trolley before each test. A hydraulic cone penetrometer was used to measure the soil cone index at different places upto 150 mm depth. The penetrometer was forced into the soil at a constant rate of 25 mm/s. The ring transducer signal was recorded in DAS.

The soil processing was repeated if large variation in the compaction level was observed. The tests were conducted at three compaction levels as given in the research plan. A few sample observations of soil cone index are presented in Appendix-B (Table B-3). A typical plot of depth of penetration versus average cone index is also presented in Fig. B-1.

Test procedure for evaluation of traction performance of test tyre

To evaluate the traction performance of test tyres, the tyre was mounted on tyre test carriage and was loaded with the desired normal load and inflation pressure as given in section 4.3.1. Before conducting the test the level of the soil bed at four different locations was recorded with point gauge after preparation of the test bed. Then a constant drawbar pull was applied before running the tyre on the test bed. Each test was conducted on a 16 m long soil bed. The variables recorded for each test were (i) normal load on wheel axle, (ii) tyre inflation pressure, (iii) soil compaction level, (iv) soil moisture content, (v) drawbar pull, (vi) input torque to the axle, (vii) actual forward speed, (viii) theoretical forward speed and (ix) tyre sinkage.

The tests were conducted for each tyre at different normal loads, tyre deflections, soil compaction levels and drawbar pulls. Each test was replicated thrice. The drawbar pull, forward speed and axle torque were recorded in the DAS when the wheel was in motion. The average values of the experimental observations are presented in Appendix-C and the results are discussed in chapter V.

Chapter V

RESULTS AND DISCUSSION

This chapter presents the analysis and interpretation of the experimental results obtained during the course of the study in the following sub sections.

- Deflection and contact characteristics of test tyres
- Zero condition tests for test tyres
- Effect of soil, tyre and system parameters on tractive performance of test tyres
- Development of traction prediction models

5.1 Deflection and Contact Characteristics of Test Tyres

As explained in chapter IV the vertical tyre deflection and contact area characteristics of four radial-ply tyres were studied at different inflation pressures (41 to 207 kPa) and normal loads on a hard surface. The selected radial-ply tyres are used in agricultural tractors manufactured in the country in the power range of 18 kW to 40 kW. The load and inflation pressure used for deflection study was according to Tyre and Rim Association standard yearbook 2005. The results are discussed below.

5.1.1 Calibration of displacement transducer

The displacement transducer was calibrated for measurement of vertical tyre deflection. The calibration procedure has been explained in section 4.1.3. In order to calibrate the displacement transducer the change in output voltage was recoded with respect to change in deflection. The calibration curve (Fig. 5.1) shows a linear relationship between output voltage and deflection. The calibration equation was fed to the DAS for real time measurement of vertical tyre deflection.

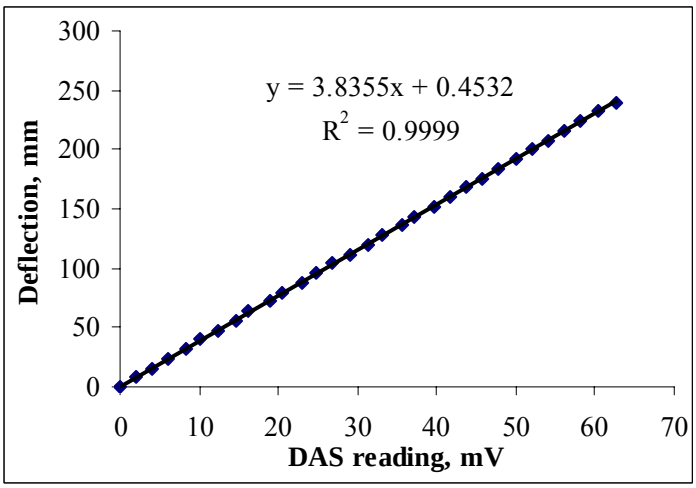

Fig. 5.1 Calibration of displacement transducer for tyre vertical deflection

5.1.2 Effect of normal load and inflation pressure on tyre deflection

The observed vertical deflection of the four test tyres at different normal loads and inflation pressures is given in Table C-1. The relationship between inflation pressure and tyre deflection ratio at different normal loads is shown in Fig. 5.2 and that between normal load and tyre deflection ratio at different inflation pressures is shown in Fig.5.3.

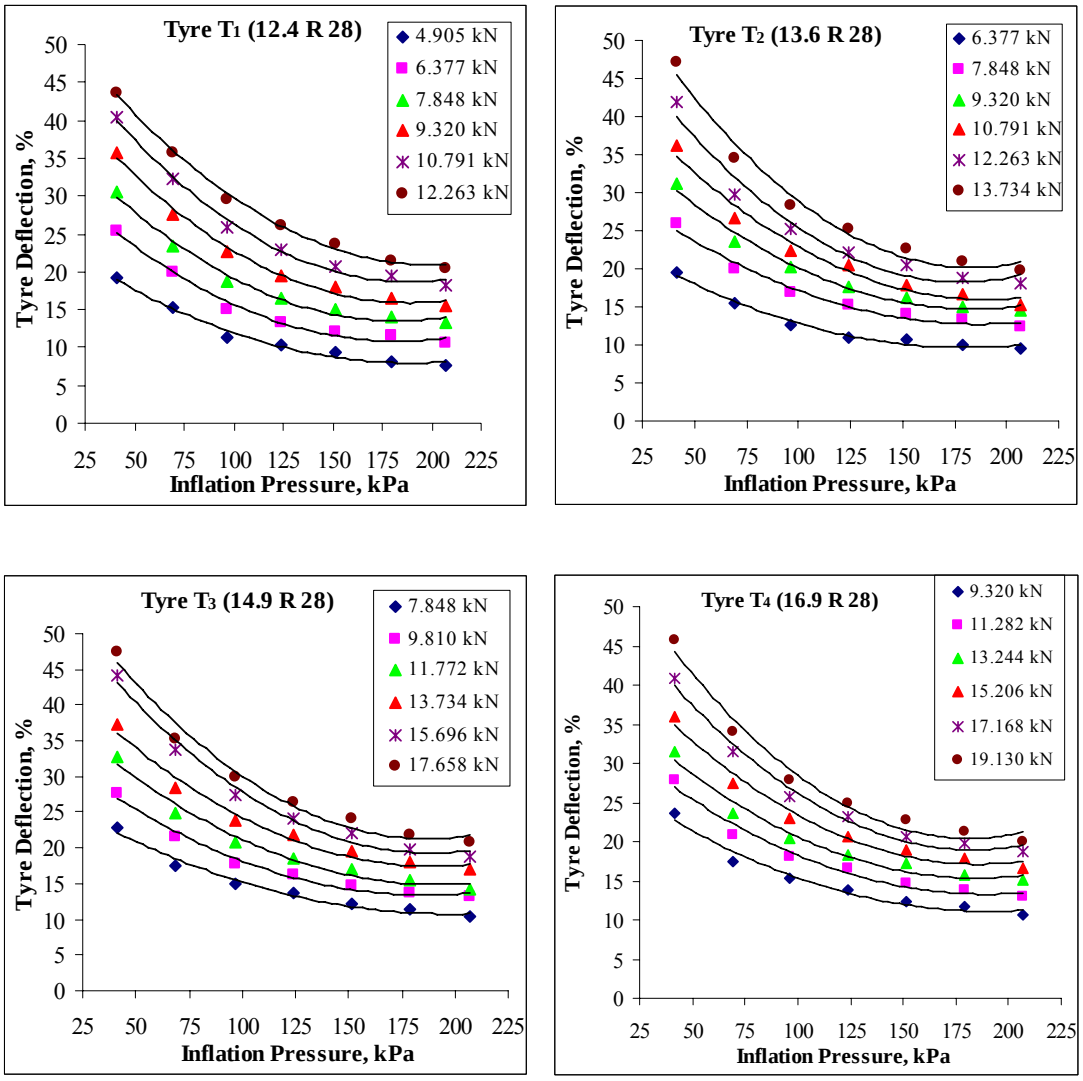

Fig. 5.2 Relationship between inflation pressure and tyre deflection at different normal loads for test tyres

The general trend shows that tyre deflection decreased non-linearly with increase in inflation pressure from 41 to 207 kPa, while it increased linearly with increase in normal load for different test tyres. A similar trend was also observed by Abeel (1976), Fujimoto (1977), Yong *et al.* (1978), Plackett (1983), Sharma and Pandey

(1996) and Tiwari (2006). It was also noticed that the rate of increase of deflection with normal load was higher at lower values of inflation pressure than at higher ones. This may be due to the fact that carcass stiffness is not a constant value but changes with inflation pressure. This finding is in accordance with Karafaith and Nawatzki (1978). He suggested that tyre carcass stiffness is influenced by its inflation pressure and it reduces with inflation pressure.

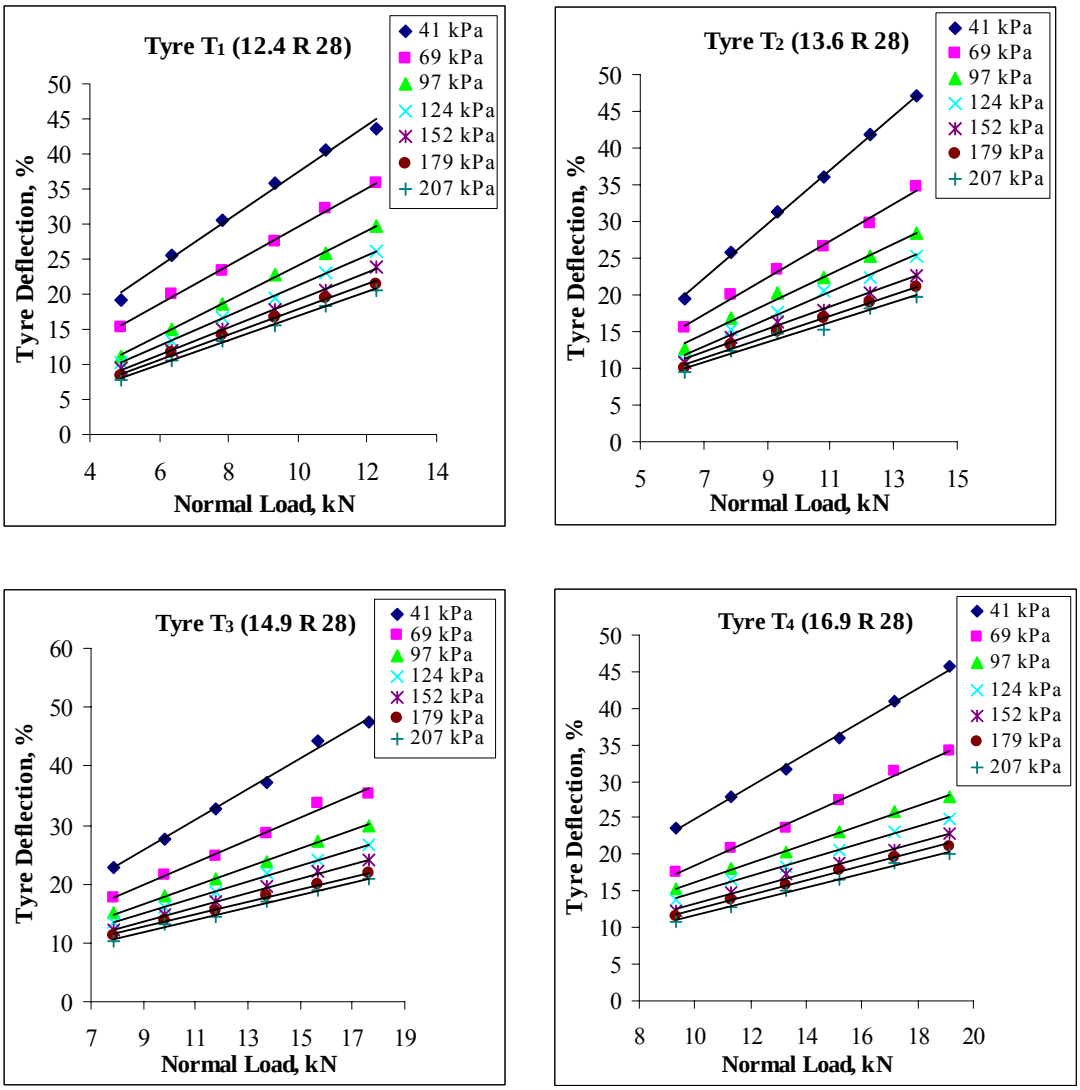

Fig. 5.3 Relationship between normal load and tyre deflection at different inflation pressures for test tyres

It is also clear from the curves that due to higher stiffness, the larger tyres yielded smaller deflection compared to smaller tyres at the same inflation pressure and normal load.

5.1.3 Deflection models

The deflection of agricultural tyres depends on their normal load, air inflation pressure and b/d ratio. The experimental data were analyzed to develop two deflection models based on regression analysis approach and dimensional analysis approach to predict deflection of agricultural tyres at different inflation pressures and normal loads.

(a) Regression analysis approach

A second degree-regression equation was found to have best fit of the experimental data as given below.

$$\frac{\delta}{h} = C_1 + C_2 \times W + C_3 \times p_i + C_4 \times \frac{b}{d} + C_5 \times W \times p_i + C_6 \times W \times \frac{b}{d} + C_7 \times p_i \times \frac{b}{d} + C_8 \times p_i^2 + C_9 \times \left(\frac{b}{d}\right)^2 \quad (5.1)$$

where, $\frac{\delta}{h}$ = deflection ratio, per cent

$\frac{b}{d}$ = width to diameter ratio of tyre,

p_i = inflation pressure, MPa

W = normal load, kN and

C_1 to C_9 = regression coefficients (Table 5.1).

The coefficients of the developed model based on regression approach are given in Table 5.1. The ANOVA for the proposed model is tabulated in Table C-2.

Table 5.1 Coefficients of the developed deflection model based on regression approach

Constants	Coefficients	Std. Error
C_1	56.38	0.2058
C_2	7.64	0.0045
C_3	-445.05	0.2801
C_4	-255.42	1.5123
C_5	-8.92	0.0061
C_6	-16.74	0.0152
C_7	829.63	1.0348
C_8	839.25	0.4140
C_9	349.16	2.8011

$R^2 = 0.98$

A high value of R^2 shows that the experimental data fit the regression very well. This model was used to calculate the load-pressure combinations to get the desired level of

20, 24 and 28 per cent tyre deflection for each test tyre. These values are given in Table 5.2 and the same were adopted to study the traction performance of test tyres under different soil conditions.

Table 5.2 Inflation pressure required to achieve 20, 24 and 28 per cent deflection at different normal loads for the test tyres (based on Eqn. (5.1))

Tyre	Load, kN (kgf)	Inflation pressure, kPa (psi)		
		At tyre deflection, %		
		20	24	28
T_1 (12.4R28)	7.36 (750)	85 (12.3)	63 (9.1)	44 (6.4)
	9.32 (950)	121 (17.5)	92 (13.4)	71 (10.3)
	11.28 (1150)	171 (24.8)	126 (18.3)	99 (14.4)
T_2 (13.6R28)	9.32 (950)	94 (13.7)	70 (10.1)	50 (7.2)
	11.28 (1150)	127 (18.4)	97 (14)	74 (10.7)
	13.24 (1350)	171 (24.8)	125 (18.1)	98 (14.2)
T_3 (14.9R28)	11.28 (1150)	103 (14.9)	76 (11)	55 (8)
	13.73 (1400)	139 (20.2)	105 (15.3)	81 (11.8)
	16.19 (1650)	194 (28.2)	137 (19.8)	108 (15.6)
T_4 (16.9R28)	14.22 (1450)	115 (16.7)	87 (12.6)	66 (9.5)
	16.68 (1700)	145 (21)	111 (16.1)	87 (12.6)
	19.13 (1950)	175 (25.4)	134 (19.4)	108 (15.6)

(b) Dimensional analysis approach

A mathematical relationship between tyre deflection and ground pressure was formulated using dimensional analysis approach as discussed in section 3.5.1. The experimental data of all the tyres were fitted to this model and the values of the constants C_1 and C_2 were determined. The generalized deflection model takes the following form,

$$\frac{\delta}{h} = C_1 \times \left[\frac{P_g}{W} (d \times b) \right]^{C_2} \tag{5.2}$$

where, δ/h = deflection ratio, per cent,
b = width of the tyre, m,
d = diameter of the tyre, m,
W = normal load, kN,
P_g = $(p_i + p_c)$,
= ground pressure (W/A), kPa,
A = tyre-surface contact area, m^2 and
C_1 and C_2 = constants (Table 5.3).

This model (Eqn. (5.2)) can be used to determine the tyre deflection in terms of ground pressure and normal load for radial-ply tyres having b/d ratio in the test range of 0.25 to 0.31. The nonlinear regression summary statistics and the coefficients of the developed deflection model (Eqn. (5.2)) are given in Table 5.3.

Table 5.3 Nonlinear regression summary statistics for the deflection model based on dimensional analysis approach

Source	**Sum of Squares**	**DF**	**Mean Square**	**F**
Regression	75307.87	2	37653.9	45273*
Residual	297.71	138	2.157	
Total	75605.58	140		
			95 % Confidence Interval	
Parameter	Estimate	Std. Error	Lower	Upper
C_1	114.43	2.564	109.361	119.499
C_2	-1.07	0.016	-1.103	-1.039

* Significant at 5 per cent level R^2 0.97

The average ground pressure P_g for a specific tyre at given normal load and inflation pressure can be derived from the so called "generalized deflection chart," normally available from tyre manufacturers. However, P_g can also be determined using a model (Eqn. (5.4)) developed in the present study.

(c) Validation and comparison of the developed model

The developed model based on regression analysis (Eqn. (5.1)) has 9 coefficients while that based on dimensional analysis (Eqn. (5.2)) has only 2 coefficients. Even though the coefficient of determination of the model based on dimensional analysis is slightly lower, it is more compact and handy. Therefore, this model was finally recommended to predict the deflection characteristics of the radial-ply tyres. The developed model was validated with the test data which were not included for developing the model of four test tyres. The predicted and the experimental deflection ratio were plotted against the dimensionless term found in section 3.5.1. From the curve (Fig. 5.4) it can be found that the model predicts the deflection ratio very well. The statistical analysis for the validation and comparison of the developed model is shown in Table.5.4.

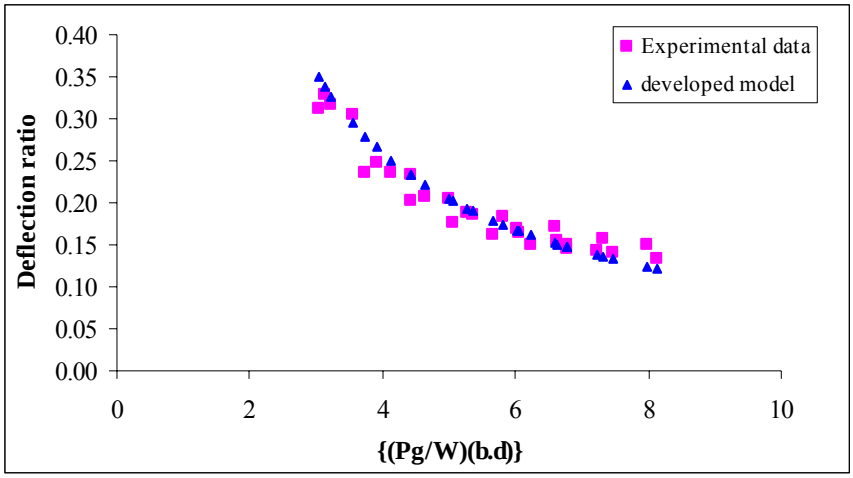

Fig. 5.4 Comparison of the developed deflection model based on dimensional analysis approach with the test data

Table 5.4 Statistical analysis for model validation and comparison

Models	Mean		RMSE %	Model Effi.	Bias %	Deviation %	R^2
	Obs.	Sim.					
Developed	0.198	0.203	1.085	0.989	-2.2	-7.6 to 8.6	0.948

R^2 = Correlation coefficient, Obs. = Observed, Sim. = Simulated

It was noticed from the analysis that the model based on dimensional analysis was suitable to predict deflection of agricultural tyres as this model has a high value of coefficient of determination (0.948) with a per cent deviation of -7.6 to 8.6 %. The model efficiency of 0.989 indicates that the developed model was acceptable. The root mean squared error (RMSE) of the developed model was 1.085 % and per cent bias was -2.2 also supported the acceptability of the developed model.

5.1.4 Contact characteristics of radial-ply tyres at different normal loads and inflation pressures

The research plan and test procedure for the study of the contact characteristics of the tyre has been discussed in section 4.1. The observed data on contact area and ground pressure under different normal loads and inflation pressures on a hard surface are given in Table C-3. The graphical representations of the experimental data are shown in Figs 5.5 and 5.6. And the results are discussed as follows.

(a) Relationship between inflation pressure and ground contact area

It is noticed from Fig. 5.5 that contact area decreased nonlinearly with increase in inflation pressure at all the normal loads studied. However, it increased with increase

in load at a constant inflation pressure. The decrease in tyre-surface contact area with increase in inflation pressure may be attributed to increase in tyre stiffness. Karafiath and Nowatzki (1978) suggested that tyre carcass stiffness is influenced by its inflation pressure and was found to reduce with inflation pressure.

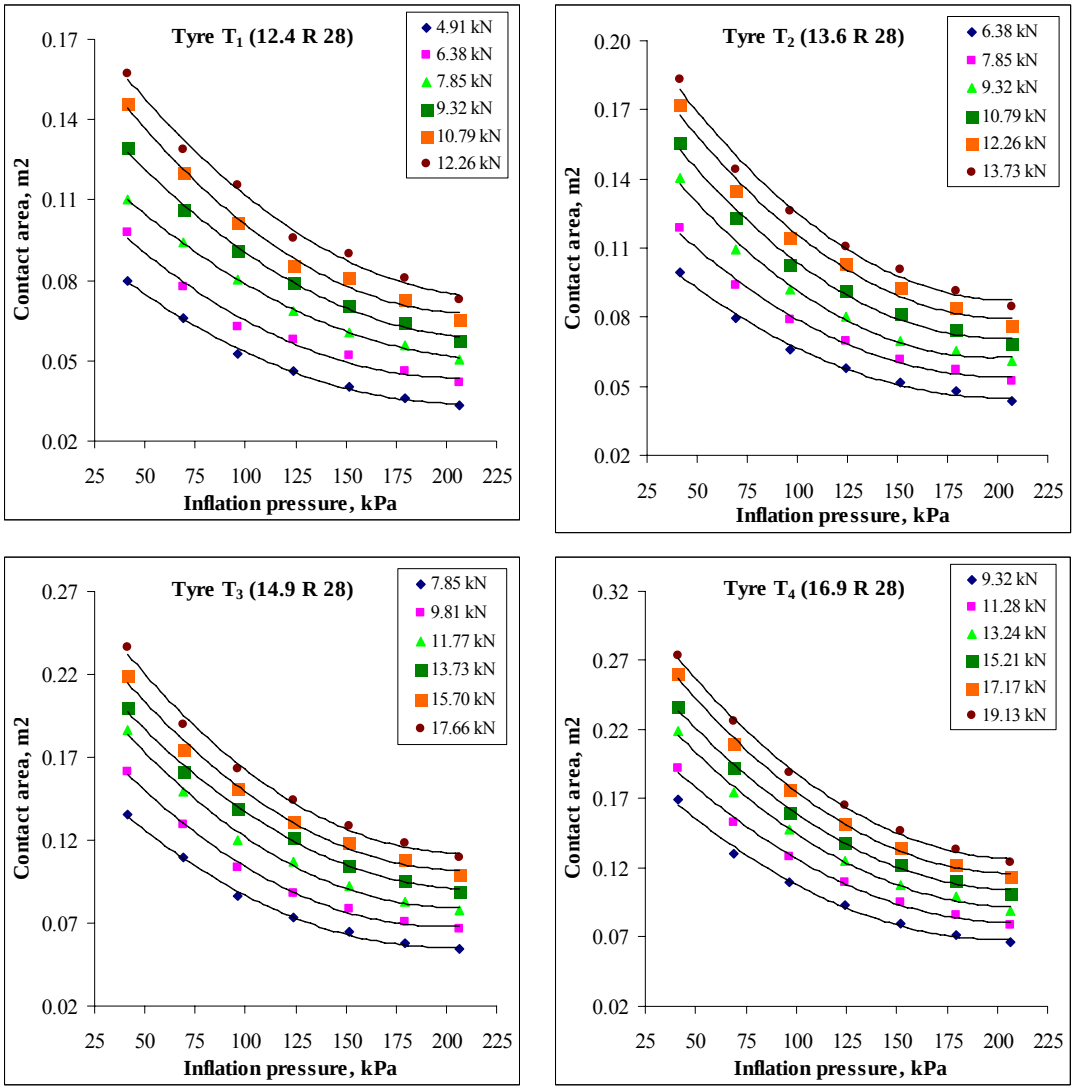

Fig. 5.5 Relationship between inflation pressure and ground contact area of the test tyres at different normal loads

(b) Relationship between inflation pressure and ground pressure

The graphical relationship between average ground pressure (P_g) and inflation pressure (p_i) for the test loads and tyres is shown in Fig. 5.6.

It was noticed from Fig. 5.6 that the average ground pressure increased with inflation pressure at all the normal loads. This was may be due to increase of tyre stiffness with inflation pressure which eventually decreased the contact area. Yong *et al.* (1978) and

Schwanghart (1991) also observed a similar trend of average ground pressure with tyre inflation pressure. The average ground pressure was also found to increase with the load at all the inflation pressures studied. This increase may be due to a lower increase in contact area compared to the increase in load.

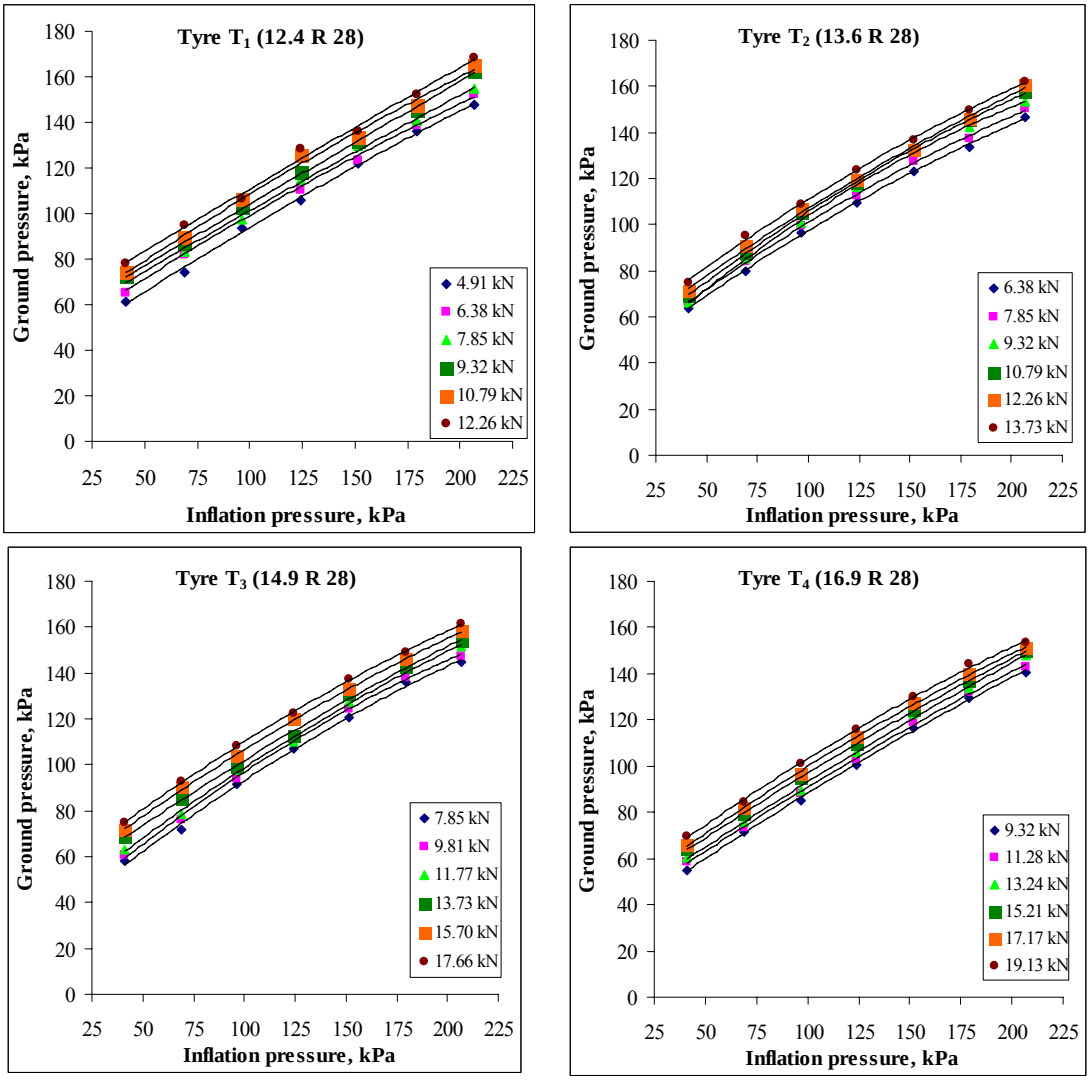

Fig. 5.6 Relationship between inflation pressure and mean ground pressure of the test tyres at different normal loads

5.1.5 Tyre contact area model

Saarilahti (2002) discussed that tyre deflection is dependent on the load applied, inflation pressure, carcass stiffness and tyre type (radial/cross-ply). So, an attempt was made to determine an empirical equation to express the tyre-surface contact area as a function of normal load, inflation pressure and tyre parameters. In the present study the following relationship was derived for tyre-surface contact area, which is of the same form as given by Komandi (1990). Nonlinear regression summary statistics for the model of tyre surface contact area is given in Table 5.5.

$$A = \frac{C_1 \times W^{C_2} \times \sqrt{\frac{b}{d}}}{p_i^{C_3}} \quad (5.3)$$

where, A = contact area, m^2,
W = normal load, kN,
p_i = inflation pressure, kPa,
$\frac{b}{d}$ = width to diameter ratio of tyre and
C_1 to C_3 = constants (Table 5.5).

Table 5.5 Nonlinear regression summary statistics for tyre surface contact area model

Source	**Sum of Squares**	**DF**	**Mean Square**	**F**
Regression	2.024	3	0.675	22500*
Residual	0.04	137	0.00003	
Total	2.028	140		
* Significant at 5 per cent level R^2 0.97				
			95 % Confidence Interval	
Constants	Estimate	Std. Error	Lower	Upper
C_1	0.27	0.012	0.245	0.292
C_2	0.84	0.013	0.815	0.865
C_3	0.5	0.007	0.486	0.513

The developed model was validated with the test data of four test tyres which were not included for developing the model and compared with the Diserens's model (2011) as shown in Fig. 5.7. The statistical analysis result for validation is given in Table 5.6. For developed contact area model, the RMSE was 0.03 %, model efficiency was 0.999, per cent bias was 5.8, per cent deviation was in the range of -9.7 to 0.15 and coefficient of determination was 0.995. Whereas for Diseren's model, the RMSE was 2.73 %, model efficiency was 0.975, per cent bias was -12.1, per cent deviation was in the range of -23 to 48 and coefficient of determination was 0.664. Thus, the developed contact area model was found suitable to predict contact area of radial-ply tyres with higher accuracy and model efficiency and lesser percent deviation.

Table 5.6 Model validation and comparison using other experimental data

Models	**Mean, m^2**		**RMSE**	**Model**	**Bias**	**Deviation**	**R^2**
	Obs.	**Sim.**	**%**	**Effi.**	**%**	**%**	
Developed	0.101	0.095	0.03	0.999	5.8	-9.7 to +0.15	0.995
Diseren's	0.101	0.113	2.73	0.975	-12.1	-23 to 48	0.664

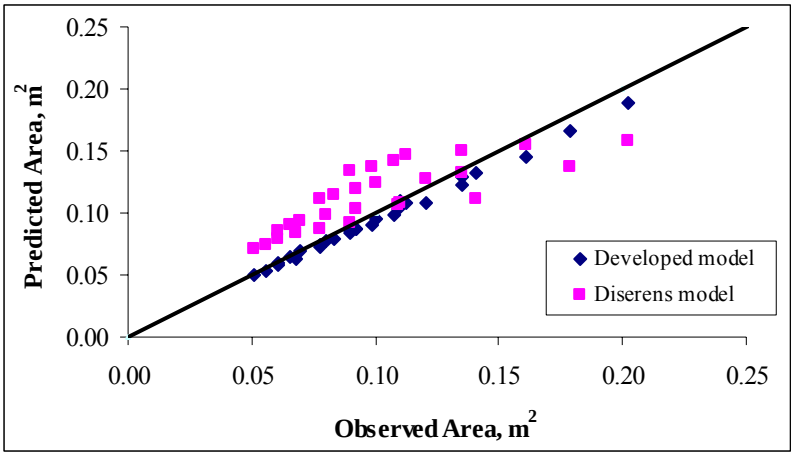

Fig. 5.7 Comparison of the developed contact area model with the Diseren's (2011) model

5.1.6 Ground pressure model

Dwyer (1983) suggested that to minimize soil compaction, it is necessary to keep ground pressure as low as possible. At present, there is no agreed standard for determining the ground pressure of loaded agricultural radial-ply tyre and there is limited information available which allows comparison to be made between different agricultural tyres. A multiple regression analysis was performed to determine the best fit equation (Eqn. (5.4)) of the experimental data to predict ground pressure in terms of normal load and inflation pressure for different tyres. The details are given in the Table 5.7 and Fig. 5.8.

$$P_g = C_1 + C_2 \times W + C_3 \times p_i + C_4 \times \frac{b}{d} + C_5 \times W \times \frac{b}{d} + C_6 \times p_i \times \frac{b}{d} + C_7 \times p_i^2 + C_8 \times \left(\frac{b}{d}\right)^2 \qquad (5.4)$$

where, P_g = ground pressure, kPa,

$\frac{b}{d}$ = width to diameter ratio of tyre,

p_i = inflation pressure, MPa,

W = normal load, kN and

C_1 to C_8 = regression coefficients (Table 5.7).

The high value of R^2 (0.99) shows that the experimental values fit the regression model very well. The developed model was validated with the test data of four test tyres which were not included for developing the model. The statistical analysis result for validation is given in Table 5.8. From analysis, it was found that the developed ground pressure model has RMSE value of 0.596 per cent, high model efficiency of 0.992, lower per cent bias of -0.279, lower percent deviation of -5 to 6 per cent and

high coefficient of determination of 0.99. Thus the developed ground pressure model was found suitable to predict the ground pressure of radial-ply agricultural tyres.

Table 5.7 ANOVA and coefficients of the model (Eqn. (5.4))

Model	Sum of Squares	DF	Mean Square	F
Regression	1897069.97	8	237133.7	87859.8 *
Residual	356.25	132	2.699	
Total	1897426.23	140		
Constants	Coefficients	P value	Std. Error	
C_1	-164.9		0.261542	
C_2	5.7	<0.001	0.005624	
C_3	696	<0.001	0.33575	
C_4	1460.6	<0.001	1.922514	
C_5	-13.7	0.0491	0.019425	
C_6	-124	0.0651	1.088762	
C_7	-554.6	<0.001	0.526927	
C_8	-2828.1	<0.001	3.564824	

* Significant at 5 per cent level $R^2 = 0.997$

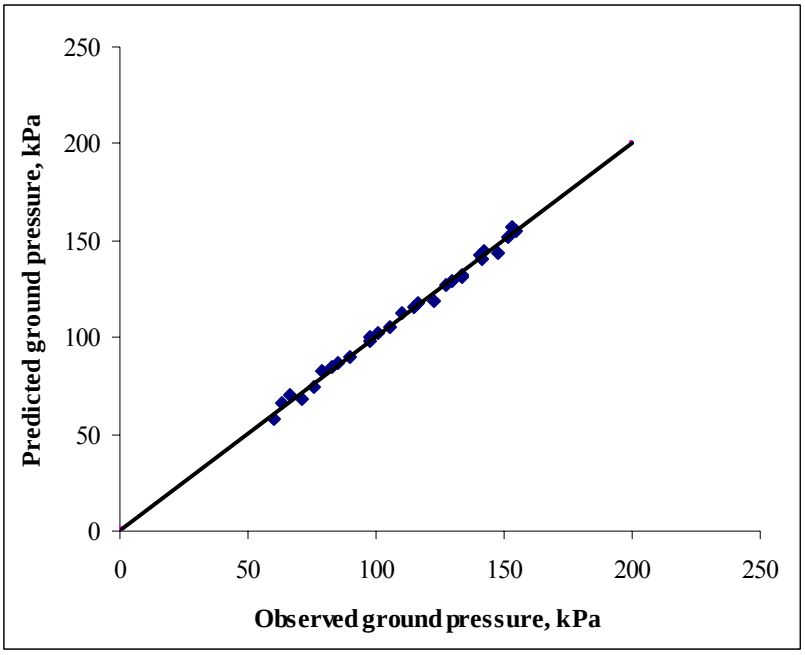

Fig. 5.8 Validation of the developed ground pressure model with experimental data

Table 5.8 Statistical analysis for ground pressure model validation

Model	Mean, kPa		RMSE	Model Effi.	Bias %	Deviation %	R^2
	Obs.	Sim.					
Developed	110.6	110.9	0.596	0.992	-0.279	-5 to +6	0.99

Based on the results discussed in this section, the following generalized models was developed to predict deflection-ratio, contact characteristics and ground pressure of radial-ply tyres having b/d ratio in the range of 0.25 to 0.31.

1) Deflection model

$$\frac{\delta}{h} = 114.43\left[\frac{P_g}{W}(d \times b)\right]^{-1.07}$$

2) Contact area model

$$A = \frac{0.27 \times W^{0.84} \times \sqrt{\frac{b}{d}}}{p_i^{0.5}}$$

3) Ground pressure model

$$P_g = -164.9 + 5.7 \times W + 696 \times p_i + 1460.6 \times \frac{b}{d} - 13.7 \times W \times \frac{b}{d} - 124 \times p_i \times \frac{b}{d} - 554.6 \times p_i - 2828.1 \times \left(\frac{b}{d}\right)^2$$

5.2 Zero Condition Tests for Traction Tyres

The traction performance parameters are wheel slip, gross traction, drawbar pull and tractive efficiency (Al-Hamed, 1994). Slip is calculated by using rolling radius. In general different zero conditions lead to different rolling radius values and therefore different values of slip. Different zero slip conditions, as per ASAE standards (1998), have been explained in section 3.4.1. The zero condition selected in this study was the vehicle operating in a self-propelled condition on hard surface with zero drawbar load. The test observations for zero condition for traction tyres are presented in Tables 5.9 and 5.10.

5.2.1 Rolling radius of traction tyres

The data (Table 5.9) revealed that at a constant tyre deflection, rolling radius of each tyre is practically constant. The constant deflection was maintained by changing the inflation pressure to support the different normal loads. The increase in tyre deflection from 20 to 28 per cent was associated with decrease in rolling radius for all the four test tyres.

The relationship between rolling radius (r) and the overall tyre diameter (d) was also determined (Fig. 5.9) and found that the r/d ratio of all the test tyres with different loads at 20 to 28 per cent deflection was nearly constant, and is given by

$$\frac{r}{d} = 0.4721 \quad (R^2 = 0.988) \qquad (5.5)$$

Brixius (1987) and Wismer and Luth (1973) found this ratio to be approx. 0.475.

Table 5.9 Rolling radius of test tyres at different normal loads and tyre deflections

Tyre	Normal load, kN (kgf)	Rolling radius, m		
		At tyre deflection, %		
		20	24	28
T_1 (12.4 R 28)	7.36 (750)	0.6084	0.6042	0.6000
	9.32 (950)	0.6089	0.6045	0.5995
	11.28 (1150)	0.6082	0.6042	0.6005
T_2 (13.6 R 28)	9.32 (950)	0.6171	0.6135	0.6094
	11.28 (1150)	0.6173	0.6133	0.6097
	13.24 (1350)	0.6166	0.6137	0.6097
T_3 (14.9 R 28)	11.28 (1150)	0.6540	0.6500	0.6455
	13.73 (1400)	0.6543	0.6502	0.6458
	16.19 (1650)	0.6540	0.6495	0.6463
T_4 (16.9 R 28)	14.22 (1450)	0.6880	0.6833	0.6803
	16.68 (1700)	0.6884	0.6837	0.6802
	19.13 (1950)	0.6879	0.6838	0.6807

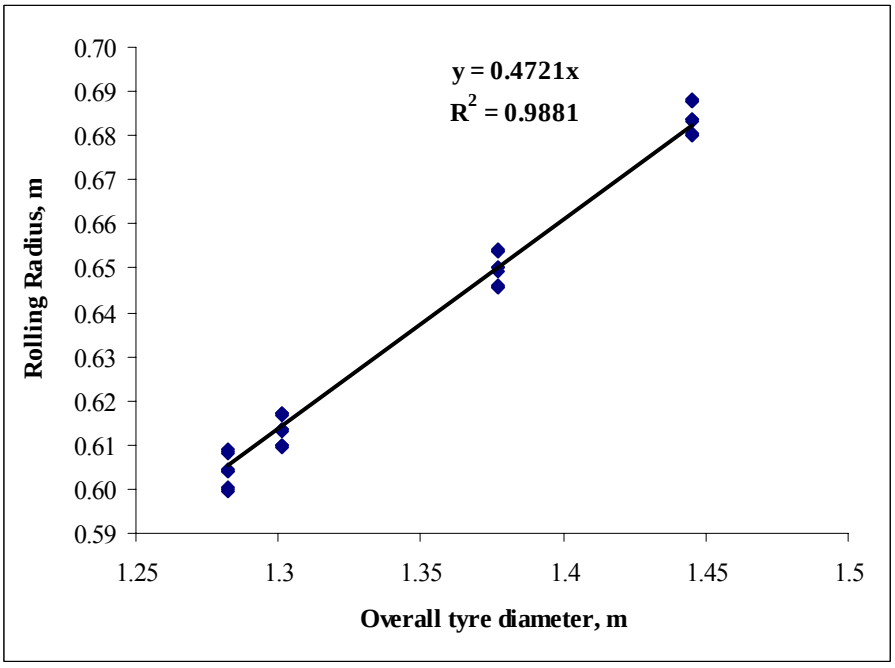

Fig. 5.9 Relationship between rolling radius and overall tyre diameter

5.2.2 Effect of b/d ratio and tyre deflection on torque ratio

The input torque requirement for all the four tyres under different conditions is given in Table 5.10.

Table 5.10 Input torque requirement for various test tyres at different normal loads and deflections

Tyre	Normal load, kN (kgf)	Input-torque, N-m		
		At tyre deflection, %		
		20	24	28
T_1 (12.4 R 28)	7.36 (750)	150.9	164.5	178.8
	9.32 (950)	192.9	207.3	224.6
	11.28 (1150)	230.5	251.5	271.0
T_2 (13.6 R 28)	9.32 (950)	192.7	209.3	226.0
	11.28 (1150)	231.9	252.5	270.3
	13.24 (1350)	273.6	294.2	318.9
T_3 (14.9 R 28)	11.28 (1150)	243.5	264.0	284.0
	13.73 (1400)	299.2	320.6	343.2
	16.19 (1650)	350.4	373.2	406.9
T_4 (16.9 R 28)	14.22 (1450)	315.1	335.3	372.6
	16.68 (1700)	374.3	395.7	434.5
	19.13 (1950)	432.9	452.6	494.8

Experimental results showed a negative linear relationship between the torque ratio and b/d ratio (Fig. 5.10). On the other hand, there is a positive linear relationship between torque ratio and the tyre deflection ratio (Fig. 5.11).

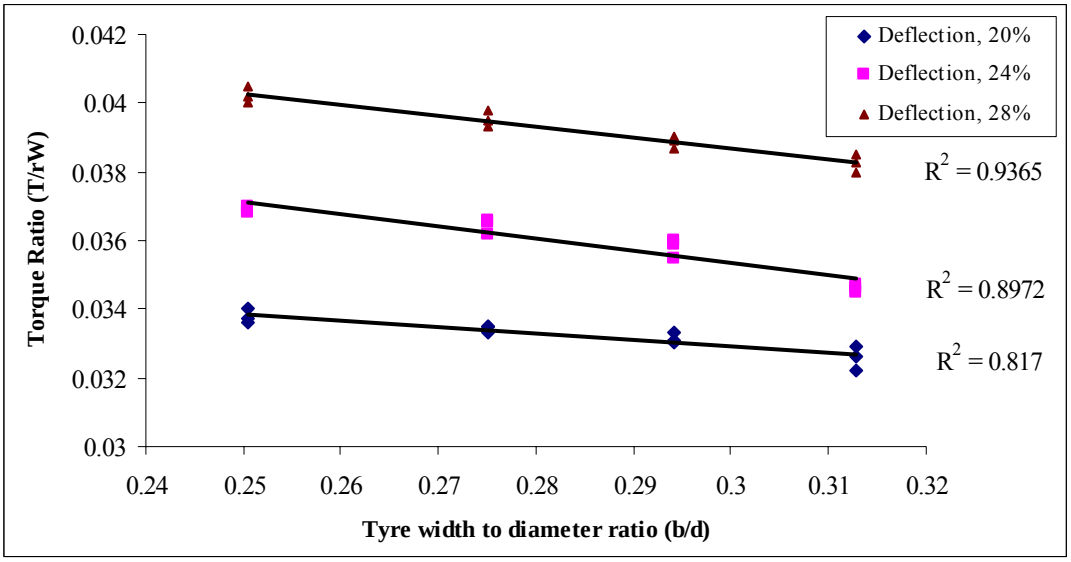

Fig. 5.10 Relationship between torque ratio and tyre size (b/d) of the test tyres at zero condition

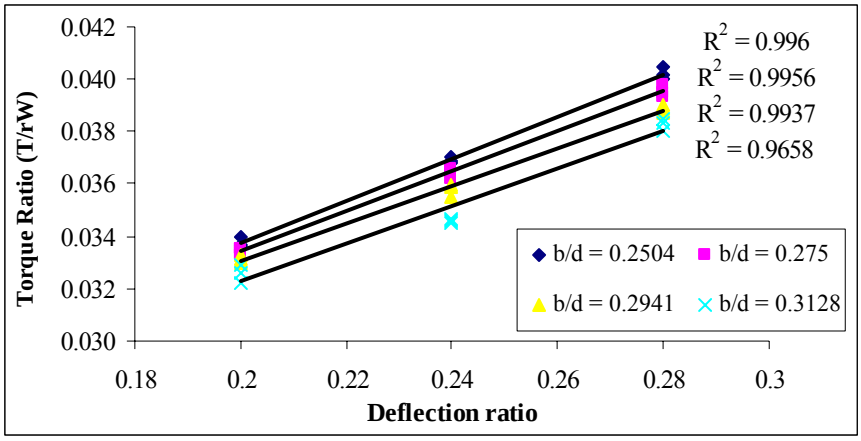

Fig. 5.11 Relationship between torque ratio and tyre deflection for different sizes of test tyre

The decrease in torque ratio with increase in overall diameter of a tyre was due to its increased rolling radius for a constant normal load. This is also in line with the findings of Sefa and Kazim (2004). The higher torque ratio for greater deflection ratio may be due to higher flexing resistance for a constant normal load which results in higher motion resistance and thereby the higher torque requirement. For a constant deflection, the larger tyre indicated lower torque ratio mainly due to its increased rolling radius as compared to smaller tyres. This behaviour is in agreement with Sharma and Pandey (1997), Sefa and Kazim (2004) and Tiwari (2006).

5.2.3 Motion resistance ratio

The minimum motion resistance ratio was determined by conducting tests on hard surface at zero net traction and at different normal loads for all the test tyres. As net traction was zero so, the recorded thrust force was equal to the motion resistance. The relationship between thrust force and normal load on hard surface is shown in Fig. 5.12.

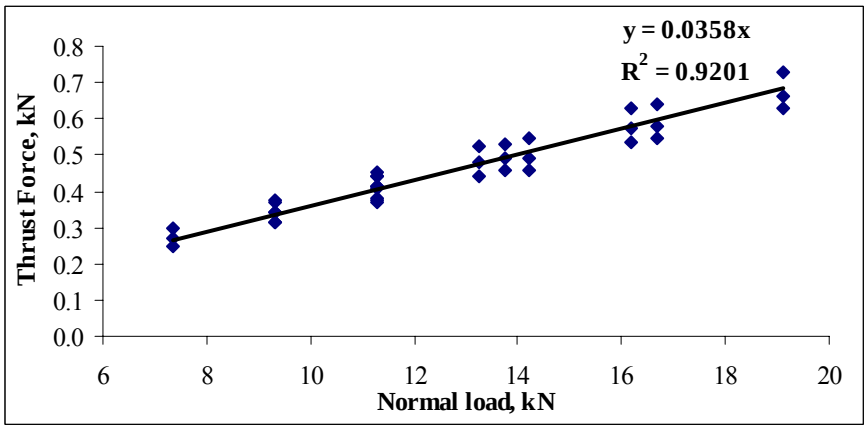

Fig. 5.12 Relationship between normal load and thrust force on a hard surface at zero net pull

From the plot it was found that thrust force was positively correlated with normal load and has linear relationship. From the relationship between thrust force and normal load on a hard surface, the minimum motion resistance ratio determined was 0.036.

5.2.4 Rolling radius model

To estimate the rolling radius of the agricultural traction tyre on hard surface Brixius (1987) proposed a model as

$$r = \frac{2.5 \times \frac{d}{2} \quad (\text{static loaded radius})}{1.5 \times \frac{d}{2} + (\text{static loaded radius})} \tag{5.6}$$

In the present study an attempt was made to develop a model to estimate the rolling radius of radial ply tractor tyre on hard surface as given below (C_1 = 2.265, C_2 = 1.24).

$$r = \frac{C_1 \times \frac{d}{2} \quad (\text{static loaded radius})}{C_2 \times \frac{d}{2} + (\text{static loaded radius})} \tag{5.7}$$

The experimental data were fitted into the regression model and constants were determined. The details are given in Table C-4. The developed rolling radius model was validated and compared with the model given by Brixius (1987) as given in Table 5.11.

Table 5.11 Validation of developed and Brixius rolling radius model (1987) with experimental data

Model	Mean, m		RMSE	Model Effi.	Bias %	Deviation %	R^2
	Obs.	Sim.					
Brixius	0.637	0.6281	0.645	0.938	0.14	-1.5 to-1.4	0.99
Developed	0.637	0.6369	0.0064	0.999	0.028	-0.09 to 0.014	0.99

From the analysis it was found that for developed rolling radius model, the RMSE was 0.0064 %, model efficiency was 0.999, per cent bias was 0.028, per cent deviation was in the range of -0.09 to 0.014 and coefficient of determination was 0.99. Whereas for Brixius rolling radius model the RMSE was 0.645 %, model efficiency was 0.938, per cent bias was 0.14, per cent deviation was in the range of -1.5 to -1.4 and coefficient of determination was 0.99. Thus the developed rolling radius model

was found suitable to predict rolling radius of radial-ply tyres with higher accuracy and model efficiency and lesser percent deviation.

5.2.5 Modelling of gross traction ratio at zero net traction on hard surface

In order to predict the gross traction at zero net traction for the test tyres on hard surface *i.e.* the minimum rolling resistance, a mathematical equation using dimensional analysis approach was developed (as discussed in section 3.5.2) by ignoring the Pi terms $\left(\frac{CI.b.d}{W}\right)$ and S. The final form of the equation (Eqn. (3.28)) is given below.

$$\left(\frac{T}{r \times W}\right) = C\, f\left(\frac{b}{d}, \frac{\delta}{h}\right)$$

The analysis of variance (ANOVA) for the test variables is presented in Table C-5. The analysis shows that the effects of tyre width to diameter (b/d) ratio and tyre deflection (δ/h) on the torque ratio were highly significant for different tyres but the interaction effect of width to diameter ratio and tyre deflection ratio was not significant.

The experimental data obtained on hard surface at zero condition were used to develop the following gross traction model.

$$\frac{\mathrm{T}}{\mathrm{r} \times \mathrm{W}} = \mathrm{C}_1 + \mathrm{C}_2 \times \frac{\delta}{\mathrm{h}} + \mathrm{C}_3 \times \frac{\mathrm{b}}{\mathrm{d}} \qquad (5.8)$$

where, $\frac{\delta}{h}$ = tyre deflection ratio,

$\frac{b}{d}$ = width to diameter ratio of tyre, and

C_1 to C_3 = regression coefficients (Table 5.12).

Table 5.12 Torque ratio model summary with coefficients

Coefficients	Value	Std. Error
C_1	0.027	0.002
C_2	0.075	0.003
C_3	- 0.031	0.005

The developed model was validated with the test data which were not included for developing the model of four test tyres. The details are given in Table 5.13.

Table 5.13 Validation of the developed torque ratio model

Model	Mean		RMSE	Model Effi.	Bias %	Deviation %	R^2
	Obs.	Sim.					
Developed	0.03612	0.03622	0.243	0.993	-0.296	-1.3 to 2.0	0.989

From the analysis it was found that for developed torque ratio model, the RMSE was 0.243 %, model efficiency was 0.993, per cent bias was -0.296, per cent deviation was in the range of -1.3 to 2.0 and coefficient of determination was 0.989. Thus the developed torque ratio model was found suitable to predict torque ratio of radial-ply tyres on hard surface at zero condition with higher accuracy and model efficiency and lesser percent deviation.

Based on the results discussed in this section the following major outcomes can be drawn.

1. The rolling radius decreased with increase in deflection for all the test tyres.
2. Torque ratio (T/rW) was found positively related with the deflection ratio (δ/h), while it had a negative linear relationship with the tyre width to diameter (b/d) ratio.
3. The minimum motion resistance ratio was found to be 0.036 for all the test tyres in the deflection range of 20 to 28 per cent on hard surface. Thus for any hard surface the minimum motion resistance ratio may be taken as 0.036.
4. The developed rolling radius model can be used for determination of rolling radius on hard surface.

$$r = \frac{2.265 \times \frac{d}{2} \times (\text{static loaded radius})}{1.24 \times \frac{d}{2} + (\text{static loaded radius})}$$

The value of rolling radius ratio for all the test tyres was found to be nearly constant on a hard surface and may be considered as

$$\frac{r}{d} \cong 0.4721$$

5. The developed torque ratio model based on dimensional analysis approach (Eqn. (5.8)) can be used to predict the gross traction at zero net traction for the agricultural traction tyres (12.4 R 28, 13.6 R 28, 14.9 R 28 and 16.9 R 28) on a hard surface.

$$\frac{T}{(r.W)} = 0.027 + 0.075 \times \left(\frac{\delta}{h}\right) - 0.031 \times \left(\frac{b}{d}\right)$$

5.3 Calibration of Different Systems

Before conducting the traction test the various sensors on the traction machine were calibrated. The calibration results are discussed in following sub sections.

5.3.1 Calibration of ring transducer for pull measurement

The ring transducer for drawbar pull measurement was calibrated as explained in section 4.3.3. In order to calibrate the ring transducer the change in output voltage was recorded with change in applied load on the transducer. The calibration curve is shown in Fig. 5.13**.** The transducer system exhibited a linear force displacement characteristic. The calibration equation was fed to DAS for real time measurement of drawbar loading.

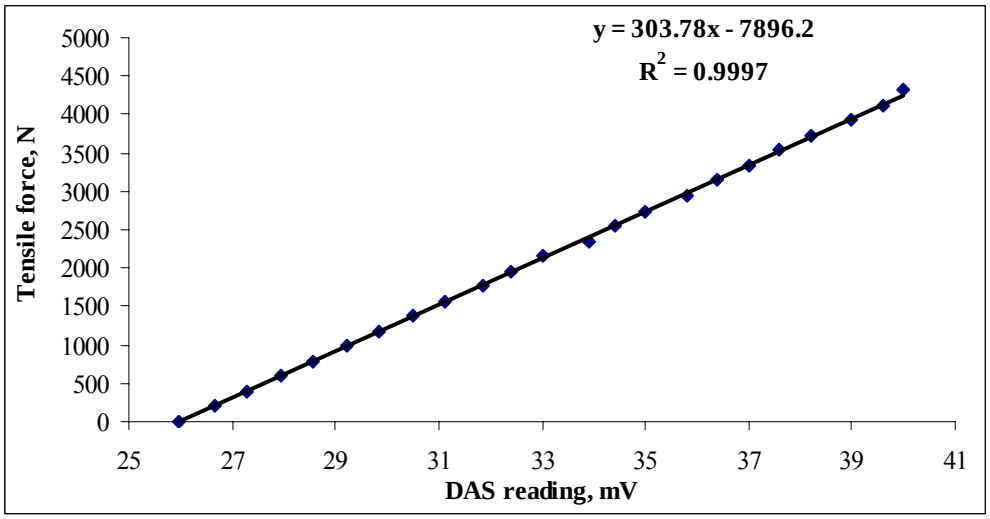

Fig. 5.13 Calibration of ring transducer for pull measurement

5.3.2 Calibration of torque transducer

The torque transducer was used to measure the wheel axle torque as explained in section 4.3.3. The calibration curve of the torque transducer is given in Fig. 5.14. The calibration equation was used to calculate the axle torque.

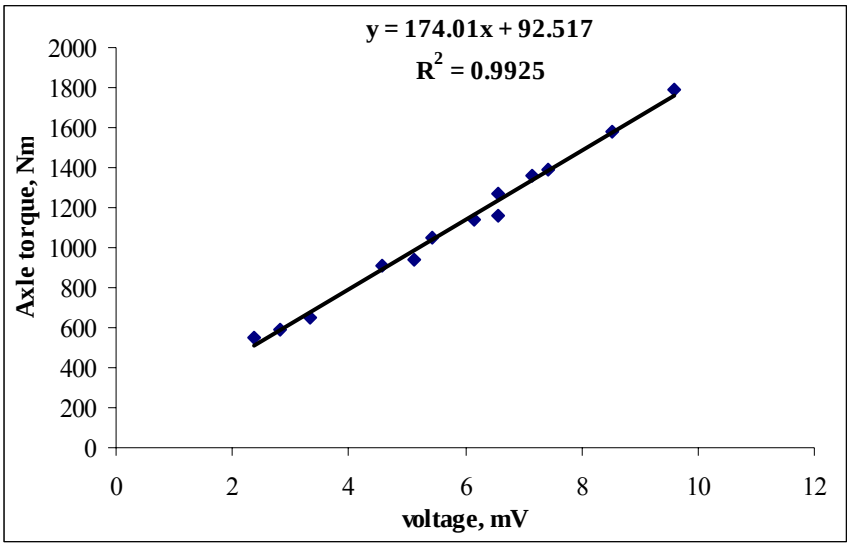

Fig. 5.14 Calibration of torque transducer

5.3.3 Calibration of ring transducer for cone index measurement

A ring transducer was used to measure the penetration force of cone penetrometer. The ring transducer was calibrated so that it gives the soil resistance in terms of force per unit base area, or cone index. The calibration curve is shown in Fig. 5.15.

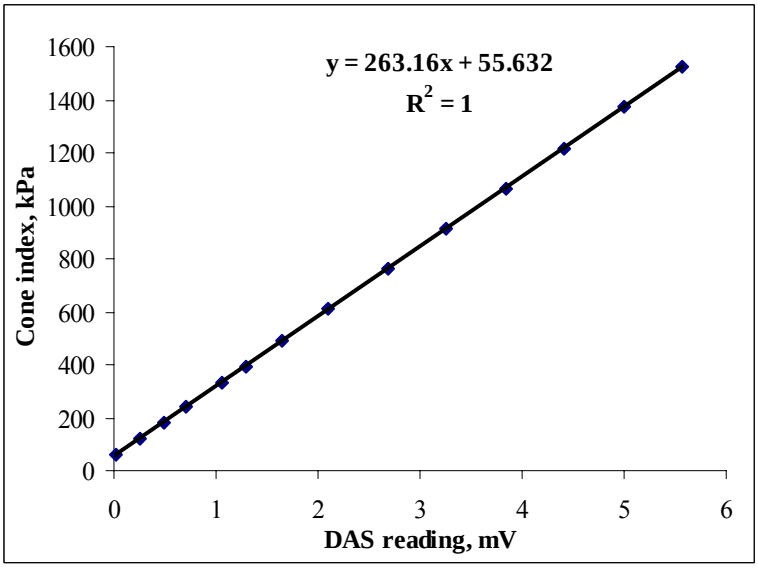

Fig. 5.15 Calibration of hydraulically operated cone penetrometer

5.3.4 Calibration of cone penetrometer depth sensor

A depth sensor was used to measure the penetration depth of cone penetrometer as explained in section 4.4.4. The calibration curve of penetration depth sensor is shown in Fig. 5.16. The calibration equation was fed to the data acquisition system to measure penetration depth in real time during operation.

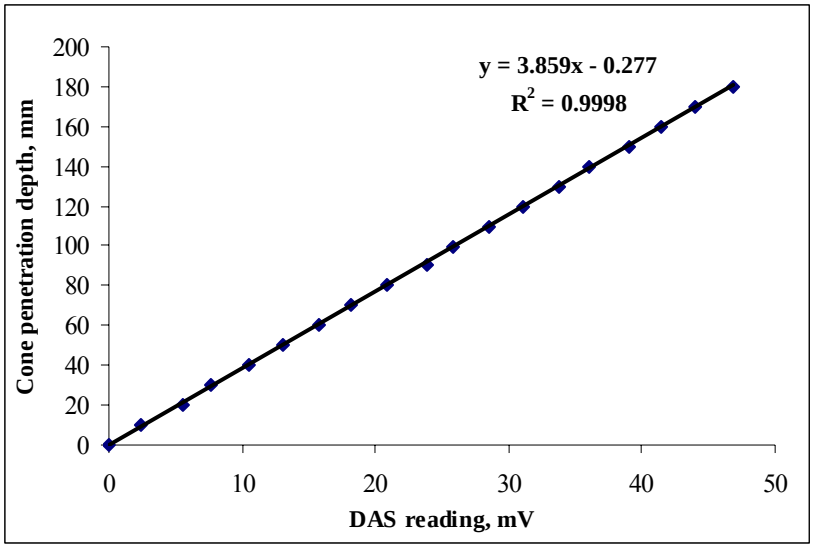

Fig. 5.16 Calibration of cone penetration depth sensor

5.4 Effect of Soil, Tyre and System Parameters on Tractive Performance of Radial-ply Tyres

In the present study the four radial-ply tyres (T_1, T_2, T_3 and T_4) were tested to study the effect of terrain condition, normal load, tyre deflection and tyre size on tyre performance. The normal load range was 7.36 kN to 19.13 kN (according to tyre sizes). Three tyre deflection range 20 to 28 per cent and three compaction levels with the soil cone index ranging from 600 to 1800 kPa were studied in this study. The recorded experimental data are given in Table C-6. Experimental design was based on factorial RBD. The experimental data were used to prepare two plots: (i) coefficient of traction (COT) versus slip (S), and (ii) coefficient of traction versus tractive efficiency (TE) for the test tyres under different operating conditions. A plot showing the variation of TE and slip with COT for a tyre is given in Fig. 5.17. Each data point on the plot represents the average value of three replications. The plot shows a large scatter of data which makes it difficult to draw meaningful conclusions. Regression analysis was, therefore, carried out to determine COT and gross traction ratio (GTR) as a function of slip as given below.

$$COT = C_1 \times \left[1 - \exp\left(-C_2 \times S\right)\right] \tag{5.9}$$

$$GTR = C_3 \times \left[1 - C_4 \times \exp\left(-C_5 \times S\right)\right] \tag{5.10}$$

where, S = slip, decimal and
C_1 to C_5 = regression coefficients.

Tractive efficiency was determined using the following equation

$$TE = \frac{COT}{GTR}\left(1 - S\right) \tag{5.11}$$

A similar relationship was also given by Upadhyaya *et al.* (1989).

A non linear regression technique was used to analyze the experimental data to obtain the values of the coefficients (Eqns. (5.9 and 5.10)). Tables C-7 to C-10 show the coefficients estimated from non linear regression. The variation of TE and slip with COT for the test tyres under different conditions are shown in Figs. 5.18 to 5.30. The general trend showed that slip increased at a slower rate in the beginning followed by a faster rate beyond a certain value of COT. This trend may be due to lower rolling resistance at lower drawbar pulls. Due to reduced slippage at lower drawbar pull, the tractive efficiency also increased in the beginning, attained a peak value at certain value of COT, beyond which it was found to decrease. Such a trend of COT and TE with wheel slip has been observed by Upadhyaya *et al.* (1989), Godbole *et al.* (1993), Zoz *et al.* (2003) and many researchers in the past.

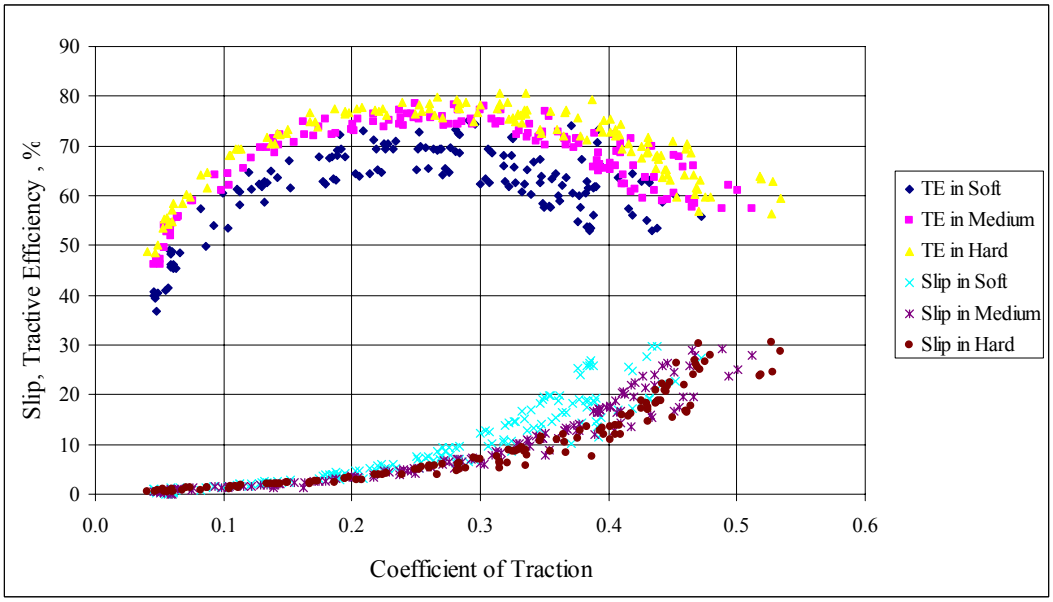

Fig. 5.17 Relationship between coefficient of traction and tractive performance under varying soil compactions for a particular tyre (13.6 R 28)

These curves have been drawn to study the effect of soil cone index, normal load and tyre deflection on tractive performance of different sizes of radial-ply tyres used in 20 to 45 kW two wheel drive tractors in the country. While discussing the effect of one parameter the data obtained at the other two parameters for a given size of tyre were used in the analysis. The results derived from these curves are discussed below.

5.4.1 Effect of soil cone index

The effect of soil cone index on tractive performance of radial-ply agricultural traction tyres are illustrated in Figs. 5.18 through 5.21. The ANOVA results are tabulated in Tables C-11 to C-14. The analysis shows that the effect of soil cone index is highly significant on tractive performance of all the test tyres. The data indicate that tractive efficiency of the tyres increased while wheel slip decreased with increase in the soil cone index from soft to hard soil conditions. It is interesting to note that all the tyres indicated peak tractive efficiency in the range of 66 to 77 per cent corresponding to a COT value of 0.30 within 8 to 11 per cent slip range. But Dwyer (1987), Brixius (1987) and Zoz *et al.* (2003) observed that tractive efficiency tends to maximize at a COT of approximately 0.4. The observed value of COT is less than that observed by Dwyer (1987), Brixius (1987) and Zoz *et al.* (2003), presumably due to lower sizes of tyres and sandy clay loam soil used in the present study. The comparative performance of the tyres under different soil conditions is given in Table 5.14. The data revealed that the performance of all the four test tyres was almost similar under each soil condition. The maximum tractive efficiency for different tyres varied from 66 to 71 percent under soft soil condition, 74 to 76 per cent under medium soil condition and 76 to 77 per cent under hard soil condition, while maintaining the value of COT as 0.28 to 0.30 at maximum TE. The efficient COT range remained approximately same (0.18 to 0.42) for each soil condition.

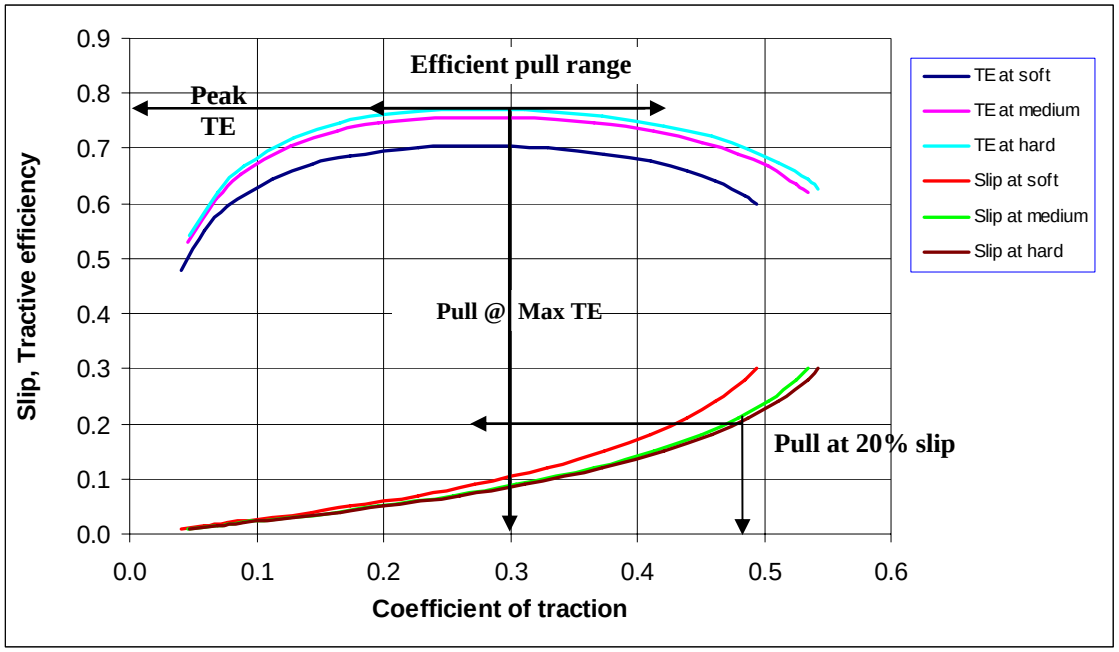

Fig. 5.18 Regression curves showing the effect of soil condition on tractive performance of T_1 (12.4 R 28) radial-ply tyre

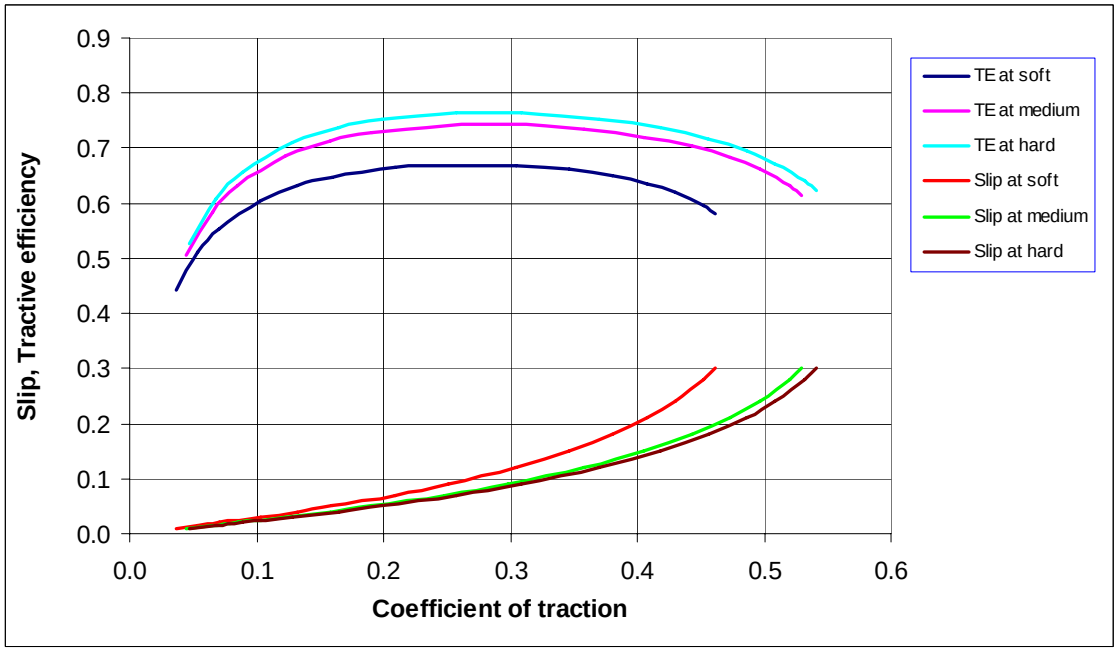

Fig. 5.19 Regression curves showing the of effect soil condition on tractive performance of T_2 (13.6 R 28) radial-ply tyre

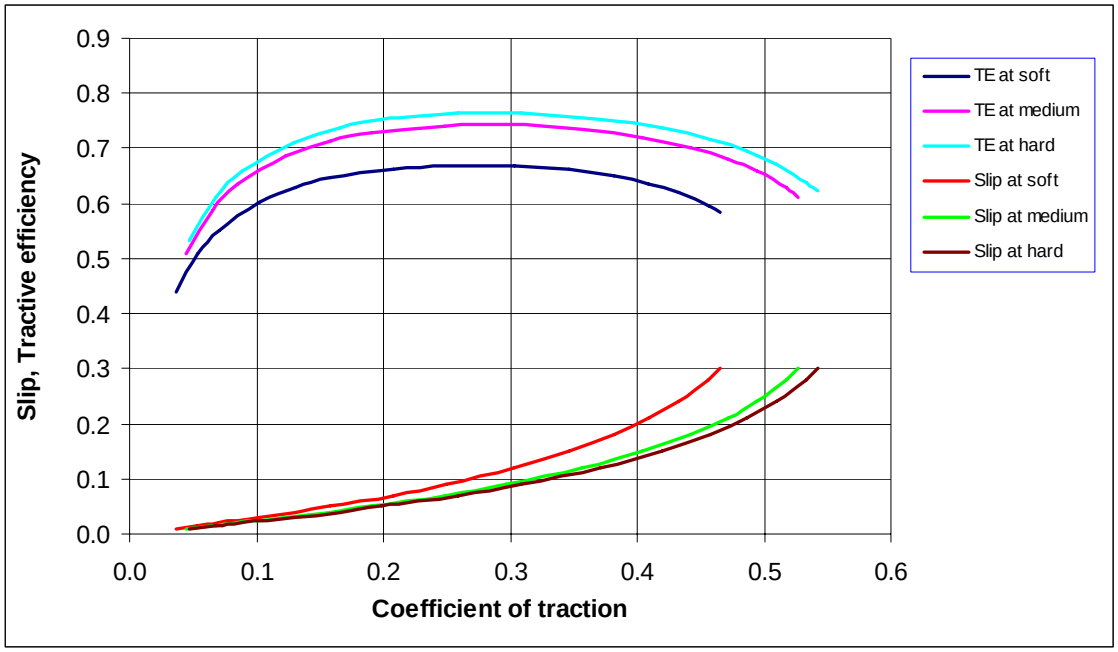

Fig. 5.20 Regression curves showing the effect of soil condition on tractive performance of T_3 (14.9 R 28) radial-ply tyre

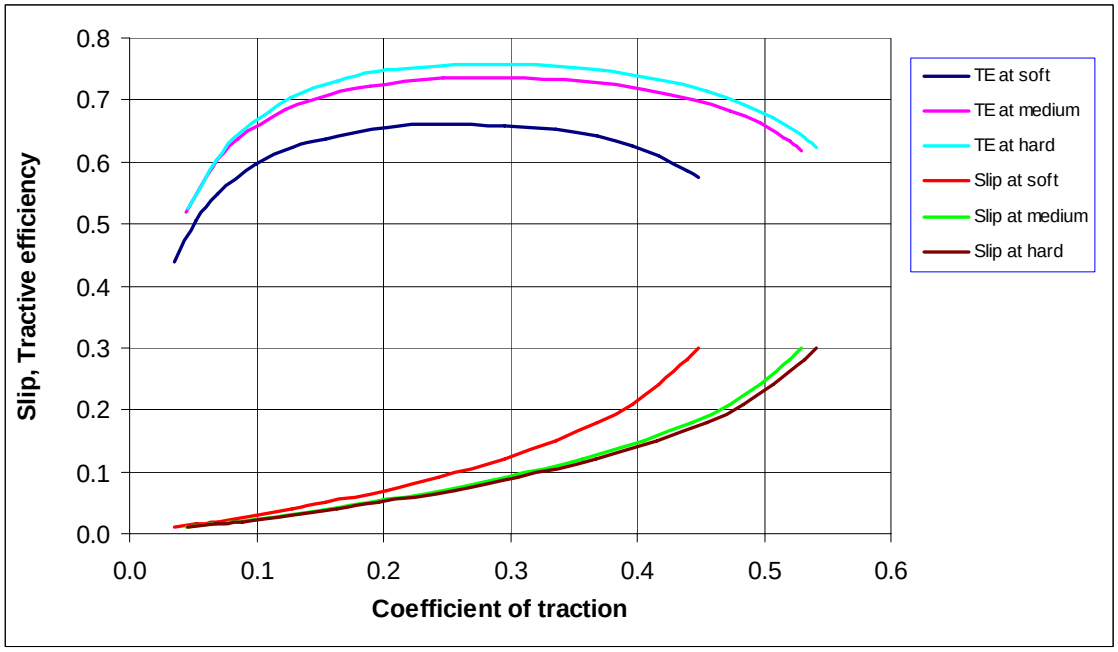

Fig. 5.21 Regression curves showing the effect of soil condition on tractive performance of T_4 (16.9 R 28) radial-ply tyre

Table 5.14 Comparative performance of the test tyres under different soil conditions

Tyre Performance	T_1 (12.4 R 28)			T_2 (13.6 R 28)			T_3 (14.9 R 28)			T_4 (16.9 R 28)		
	S	M	H	S	M	H	S	M	H	S	M	H
Max. TE (%)	71	76	77	67	74	76	67	74	76	66	74	76
COT @ Max. TE	0.29	0.30	0.30	0.29	0.30	0.30	0.29	0.30	0.30	0.28	0.29	0.29
Efficient COT range	0.18 to 0.38	0.18 to 0.42	0.18 to 0.42	0.18 to 0.38	0.18 to 0.42	0.18 to 0.42	0.18 to 0.38	0.18 to 0.42	0.18 to 0.42	0.18 to 0.38	0.18 to 0.42	0.18 to 0.42
Slip (%) @ Max. TE	10.4	8.4	8	10.8	8.4	8.0	10.6	8.4	8	10.8	8.4	8.0

S, M and H represent soft, medium and hard soil conditions respectively.

5.4.2 Effect of normal load

The effect of normal load on tractive performance of radial-ply agricultural traction tyres are illustrated in Figs. 5.22 to 5.25. The ANOVA results are tabulated in Tables C-15 to C-18. The analysis shows that the effect of normal load is highly significant on tractive performance of all the test tyres. The comparative performance of the tyres under different normal load conditions is tabulated in Table 5.15. The data indicate that tractive efficiency of the radial-ply tyres increased while wheel slip decreased with decrease in normal load from 11.3 kN to 7.4 kN for tyre T_1, 13.2 kN to 9.3 kN for tyre T_2, 16.2 kN to 11.3 kN for tyre T_3 and 19.1 kN to 14.2 kN for tyre T_4 within the range of test conditions. The increase in slip with increase in normal load for a constant coefficient of traction may be due to increase in pull in proportion to the dynamic weight. A similar COT-slip relationship at different normal loads was also found by Burt *et al.* (1979), Charles (1984) and Zoz *et al.* (2003) using COT as an independent variable.

It is interesting to note that all the test tyres indicated peak tractive efficiency in the range of 70 to 76 per cent corresponding to a COT value of 0.27 to 0.29 within 8 to 9.5 per cent slip range for the test loads. This shows that the tyre load has a major affect upon the performance and must be correct for the operation of drawbar pull. Maximum tractive efficiency was achieved at about the same coefficient of traction for each weight. If only the weight is changed, then performance may suffer from not operating condition at the optimum COT. Therefore, the optimum COT should be maintained to perform a tillage operation with a tractor at its peak tractive efficiency.

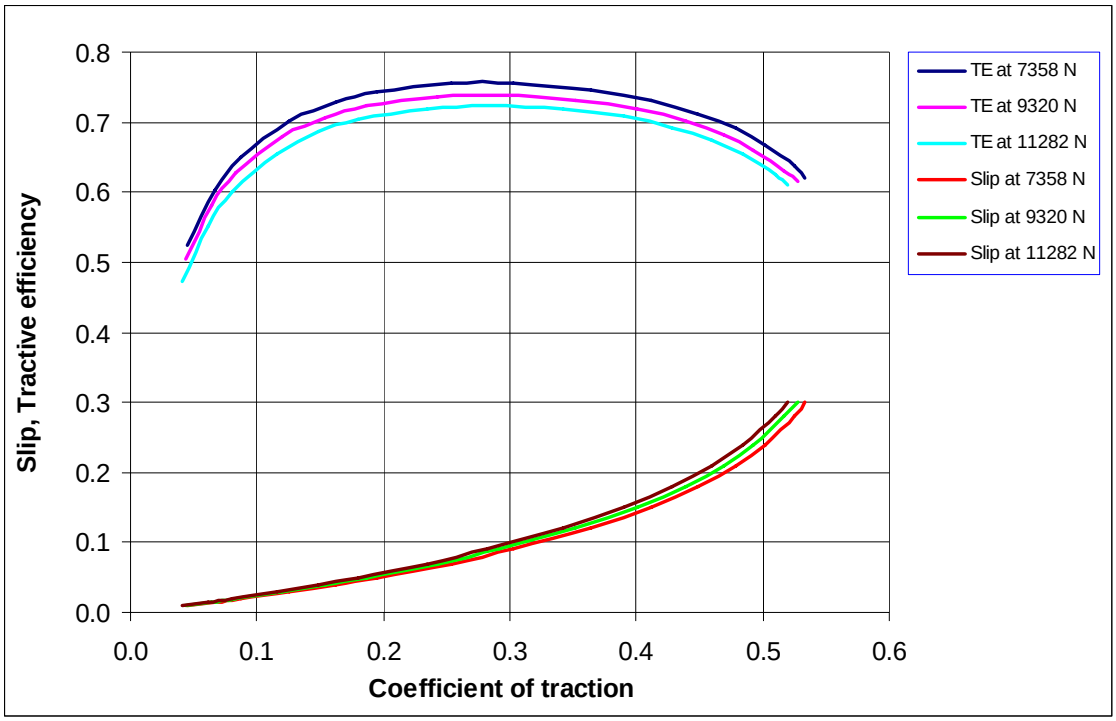

Fig. 5.22 Regression curves showing the effect of normal load on tractive performance of tyre T_1 (12.4 R 28) radial-ply tyre

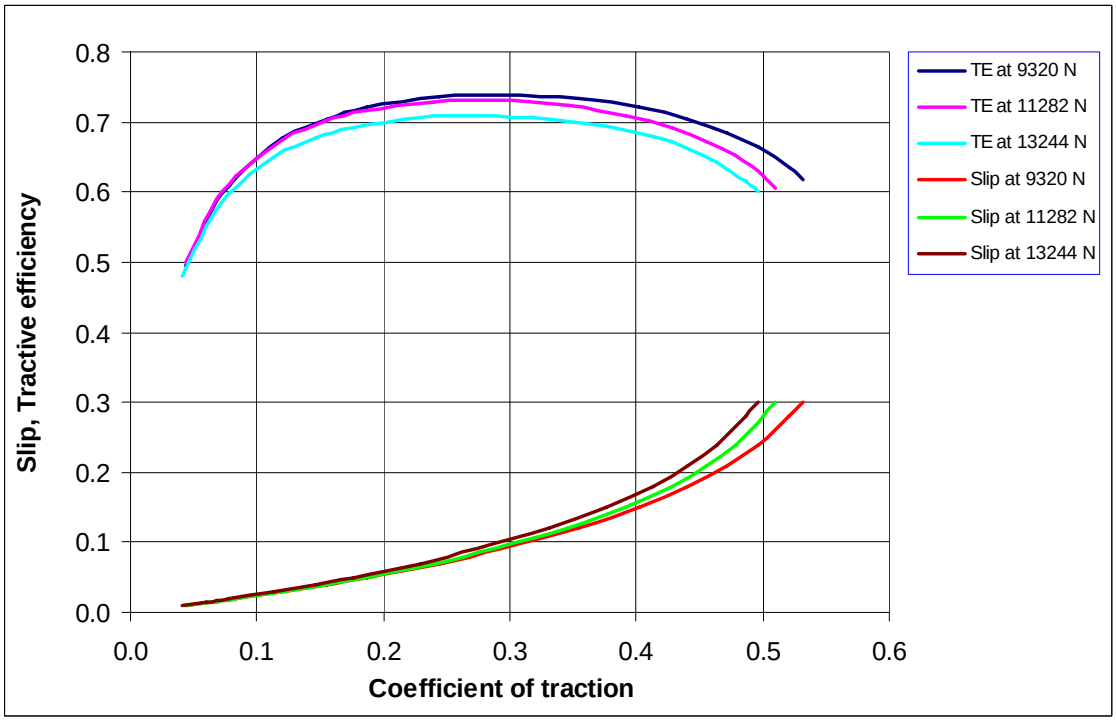

Fig. 5.23 Regression curves showing the effect of normal load on tractive performance of tyre T_2 (13.6 R 28) radial-ply tyre

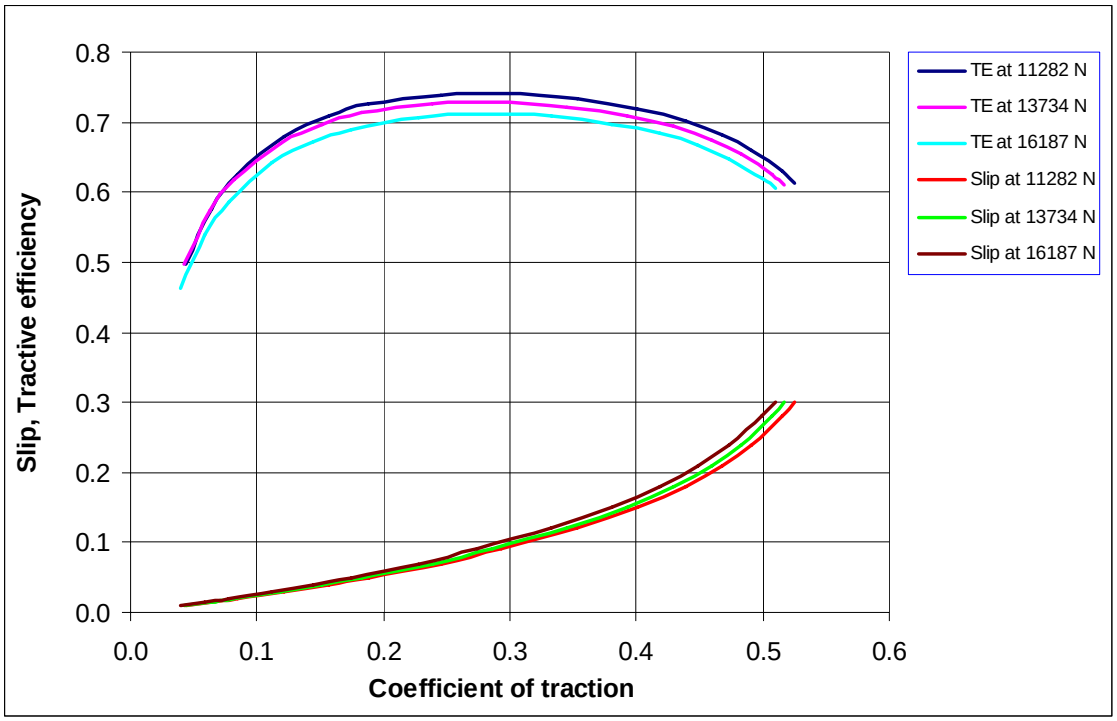

Fig. 5.24 Regression curves showing the effect of normal load on tractive performance of tyre T_3 (14.9 R 28) radial-ply tyre

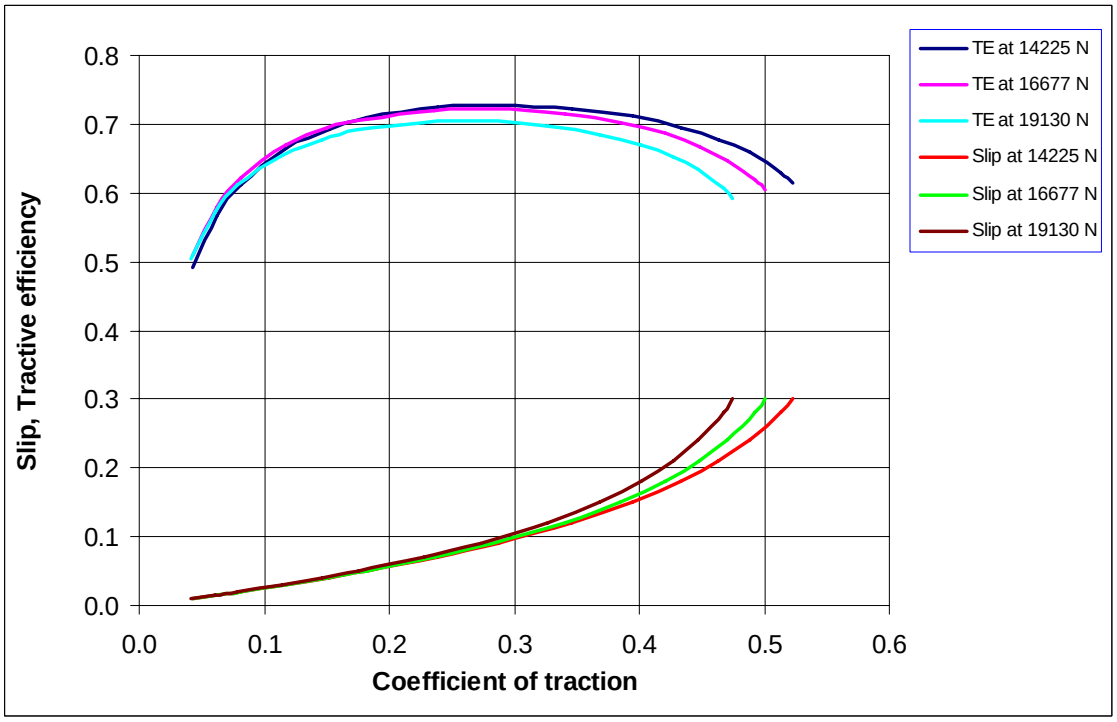

Fig. 5.25 Regression curves showing the effect of normal load on tractive performance of tyre T_4 (16.9 R 28) radial-ply tyre

Table 5.15 Comparative performance of the test tyres under different normal load conditions

Tyre Performance	T_1 (12.4 R 28)			T_2 (13.6 R 28)			T_3 (14.9 R 28)			T_4 (16.9 R 28)		
	Normal load (kN)			Normal load (kN)			Normal load (kN)			Normal load (kN)		
	7.4	9.3	11.3	9.3	11.3	13.2	11.3	13.7	16.2	14.2	16.7	19.1
Max. TE (%)	76	74	72	74	73	71	74	73	71	73	72	70
COT @ Max. TE	0.29	0.29	0.29	0.29	0.28	0.28	0.28	0.28	0.28	0.29	0.28	0.27
Efficient COT range	0.18 to 0.4	0.18 to 0.38	0.18 to 0.34	0.18 to 0.4	0.18 to 0.38	0.18 to 0.34	0.18 to 0.4	0.18 to 0.38	0.18 to 0.34	0.18 to 0.4	0.18 to 0.38	0.18 to 0.34
Slip (%) @ Max. TE	8.0	8.6	9.2	8.4	8.8	9	8.4	8.6	9.4	8.6	8.8	9.0

5.4.3 Effect of tyre deflection

The effect of tyre deflection on tractive performance of the radial-ply agricultural traction tyres are illustrated in Figs. 5.26 to 5.29. The ANOVA results are tabulated in Tables C-19 to C-22. The analysis shows that the effect of tyre deflection is significant at 5 per cent level on tractive performance of all the test tyres. The comparative performance of the tyres under different deflection conditions is given in Table 5.16.

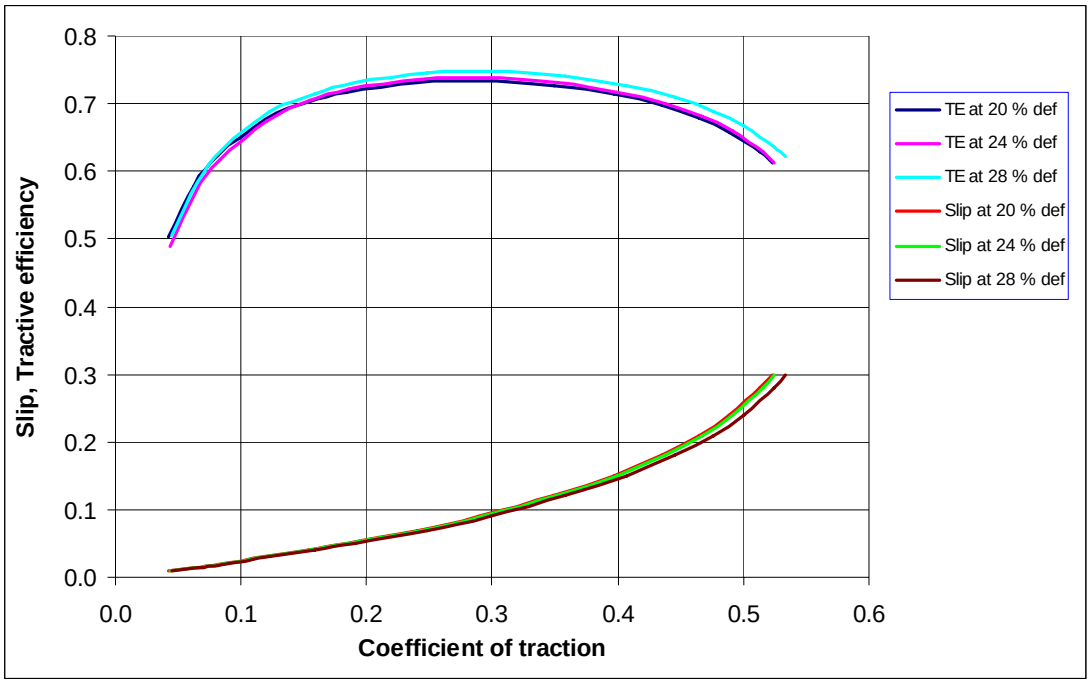

Fig. 5.26 Regression curves showing the effect of deflection on tractive performance of tyre T_1 (12.4 R 28) radial-ply tyre

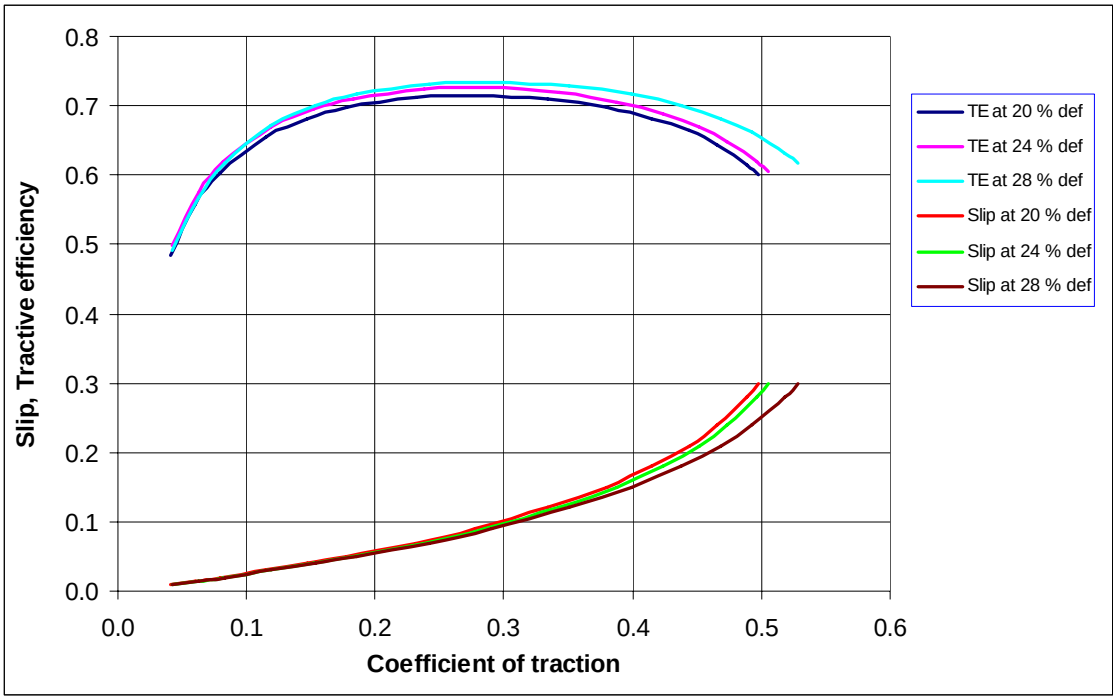

Fig. 5.27 Regression curves showing the effect of deflection on tractive performance of tyre T_2 (13.6 R 28) radial-ply tyre

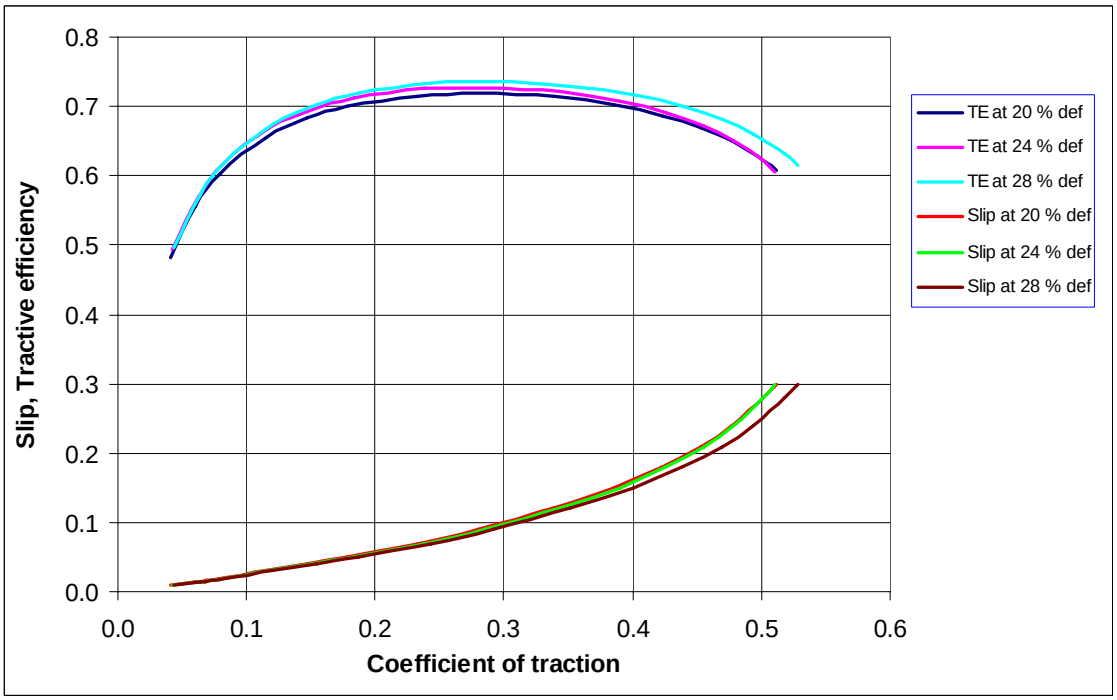

Fig. 5.28 Regression curves showing the effect of deflection on tractive performance of tyre T_3 (14.9 R 28) radial-ply tyre

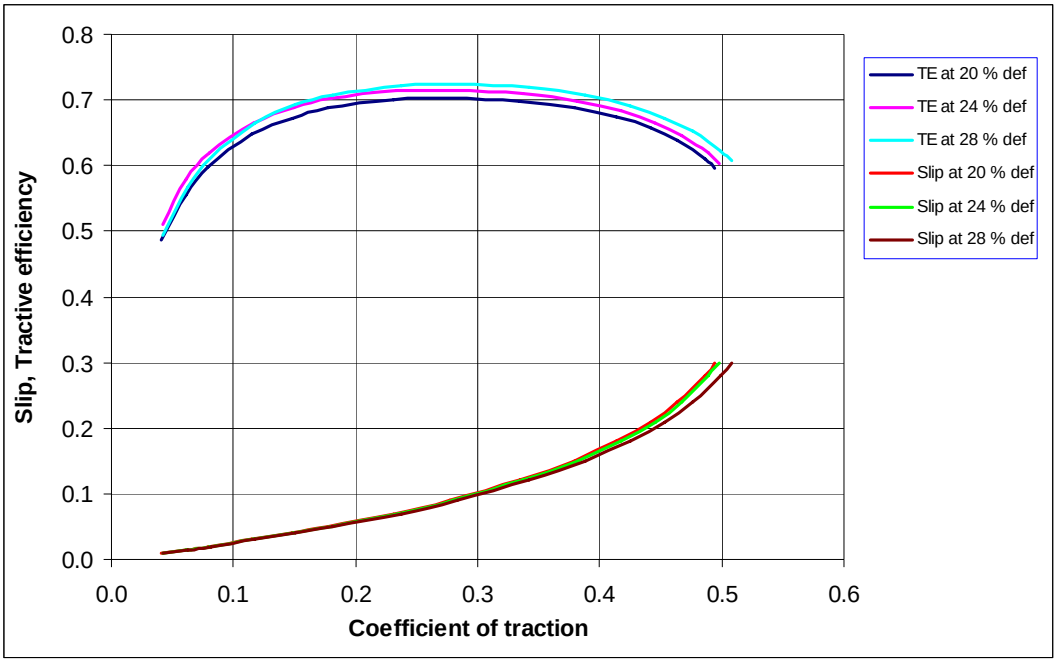

Fig. 5.29 Regression curves showing the effect of deflection on tractive performance of tyre T_4 (16.9 R 28) radial-ply tyre

The data indicate that all the tyres indicated the peak tractive efficiency of about 70 – 75 percent for the test deflection range of 20 to 28 per cent corresponding to a COT value of 0.28 at nearly 8.5 - 9 per cent slip. It is evident from the curves that the tyre performance was not affected much by changing the tyre deflection.

Table 5.16 Comparative performance of the test tyres under different levels of tyre deflection

Tyre Performance	T_1 (12.4 R 28)			T_2 (13.6 R 28)			T_3 (14.9 R 28)			T_4 (16.9 R 28)		
	Tyre deflection, %			Tyre deflection, %			Tyre deflection, %			Tyre deflection, %		
	20	24	28	20	24	28	20	24	28	20	24	28
Max. TE (%)	73	74	75	71	72	73	72	73	74	70	72	73
COT @ Max. TE	0.28	0.28	0.29	0.27	0.27	0.28	0.28	0.28	0.28	0.28	0.28	0.28
Efficient COT range	0.18 to 0.4	0.18 to 0.4	0.18 to 0.4	0.18 to 0.4	0.18 to 0.4	0.18 to 0.4	0.18 to 0.4	0.18 to 0.4	0.18 to 0.4	0.18 to 0.4	0.18 to 0.4	0.18 to 0.4
Slip (%) @ Max. TE	8.8	8.6	8.4	8.8	8.6	8.6	9.0	8.8	8.6	9.0	8.8	8.6

However, some effect could be noticed at a higher COT and some improvement in tractive performance can be expected by lowering the inflation pressure of radial-ply tyres, under soft soil conditions. The inflation pressure contributes directly to stiffness and hence controls the tyre contact area and tyre-soil ground pressure distribution,

which affect the traction capability of the tyre. These results are in agreement with those found by Taylor *et al.* (1967), Wulfsohn *et al.* (1988) and Upadhyaya *et al.* (1989). It was also noticed that at a constant COT slip decreased with decrease in tyre inflation pressure.

5.4.4 Effect of tyre size

All the four test tyres were compared in soft soil condition at 24 per cent tyre deflection (Fig. 5.30). The ANOVA results presented in Table C-23 indicate that the effect of tyre size is significant at 5 per cent level. The maximum tractive efficiency was observed with tyre T_4, which is 6, 4.4 and 1.9 per cent higher than that observed with tyres T_1, T_2 and T_3 respectively (Table 5.17). Similarly the observed slip was lower with larger diameter tyres than with smaller diameter tyres. These results are in agreement with those found by Taylor *et al.* (1967), Wulfsohn *et al.* (1988) and Zoz *et al.* (2003). The efficient range of COT is nearly same (0.18 to 0.36) for all the tyres indicating COT value of 0.30 at peak TE. The better tractive performance of the larger diameter tyres was due to their higher loading capacity and thereby their higher pulling ability for a given value of COT.

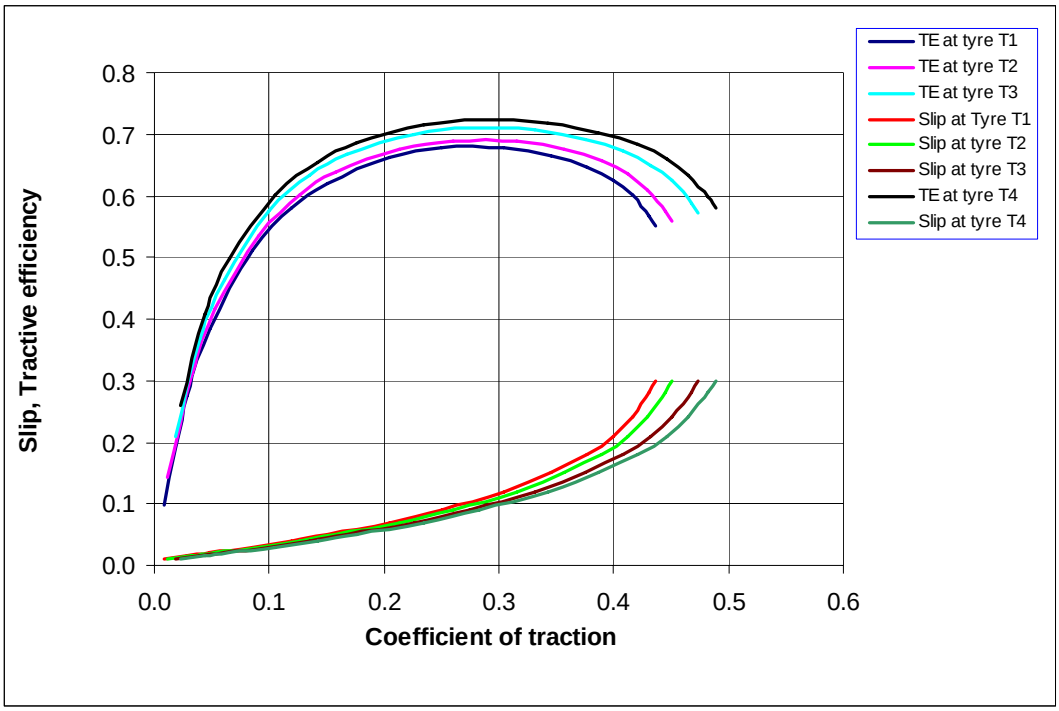

Fig. 5.30 Regression curves showing the effect of tyre size on tractive performance in soft soil condition at 24 per cent deflection

Table 5.17 Comparative performance of all test tyres under soft soil conditions at 24 per cent tyre deflection

Particular	T_1 (12.4 R 28)	T_2 (13.6 R 28)	T_3 (14.9 R 28)	T_4 (16.9 R 28)
Max. TE (%)	68.4	69.6	71.4	72.8
COT @ Max. TE	0.283	0.289	0.292	0.298
Efficient COT range	0.18 – 0.36	0.18 – 0.36	0.18 – 0.36	0.18 – 0.36
Slip (%) @ Max. TE	10.6	10.4	9.8	9.6

Based on the results discussed in this section, the following outcomes can be drawn:

1. The pulling ability of the test tyres was found to improve with increase in soil cone index and normal load within the range of test conditions. However, tyre deflection did not indicate a very strong effect on their performance.
2. Changes in soil conditions influence tyre performance much more than changes in tyre loading and dimensions. These results are in agreement with those found by Upadhyaya *et al.* (1989).
3. All the tyres were observed to have peak tractive efficiency in the range of 66 to 77 per cent within 8 to 11 per cent slip range corresponding to an optimum COT value of 0.3, when tested in the soil having cone index range in of 600 to 1800 kPa.
4. The larger diameter tyres indicated better tractive performance compared to smaller sizes of tyres under soft soil condition for a given COT.

5.5 Development of Traction Prediction Models

The aim of the present study was to develop a traction prediction model with the capability to predict the traction performance in a lateritic sandy clay loam soil for commonly used radial-ply tyres in agricultural tractors. A similar study on development of prediction models for radial-ply tyres was conducted earlier by Brixius (1987) and Al-Hamed *et al.* (1994). Out of these models, the Brixius model has been most widely used. He expressed GTR (Gross Traction Ratio) and MRR (Motion Resistance Ratio) as a function of mobility number (B_n) and wheel slip (S) and determined the dimensionless numbers in the equations using a curve-fitting technique. The following are the generalized equations he developed:

$$B_n = \frac{CI \times b \times d}{W} \times \left(\frac{1 + K_1 \times \frac{\delta}{h}}{1 + K_2 \times \frac{b}{d}} \right) \quad (5.12)$$

$$GTR = \frac{T}{r \times W} = C_1 \times \left(1 - e^{-C_2 B_n}\right) \times \left(1 - e^{-C_3 S}\right) + C_4 \quad (5.13)$$

$$MRR = \frac{MR}{W} = \frac{C_5}{B_n} + C_4 + \frac{C_6 \times S}{\sqrt{B_n}} \quad (5.14)$$

For radial-ply tyres, values of C_1, C_2, C_3, C_4, C_5, C_6, K_1, and K_2 are 0.88, 0.1, 9.5, 0.0325, 0.9, 0.5, 5 and 3, respectively (Brixius, 1987).

It was found from review that many researchers have modified the values of constants in Brixius equations for more accurate results related to their conditions (Al-Hamed *et al.*, 1994). The applicability of these equations for radial-ply tyres used in Indian soil conditions is not known. As a part of the present study, when a sample soil-bin data obtained with a 14.9 R 28 tyre was compared with the predicted results of the Brixius equations, a large variation was observed. Therefore, it was decided to modify the original equations developed by Brixius (1987) for the soil and tyre conditions prevailing in the country. Such models would be of great help in developing efficient and cost effective tractors and evaluating their drawbar performance for field as well as haulage operations.

5.5.1 Procedure adopted for model development

The experimental values of the input axle torque (T), wheel slip (S), drawbar pull (P), rolling radius (r), normal load (W), tyre deflection (δ) and tyre parameters with four different sizes of radial-ply traction tyres in lateritic sandy clay loam soil were collected and analyzed for building of traction models (gross traction ratio, GTR and motion resistance ratio, MRR). In all 2268 data points (tyre: 4; CI: 3; load/deflection: 3; deflection: 3; pull: 7; and replications: 3) were used. The values of GTR and MRR were calculated using the following equations with MATLAB programme.

$$GTR = \frac{T}{r \times W} \qquad \text{and} \qquad MRR = \frac{\left(\frac{T}{r} - P\right)}{W}$$

The mobility number (B_n) (Eqn. (5.12)), as proposed by Brixius (1987) was retained as such. The value of C_4, determined on hard surface (section 5.2.3), was taken as 0.036. Then in order to determine the values of the coefficients (C_1 to C_6) other than C_4 in Eqns (5.13 and 5.14) through non-linear regression analysis, SPSS software was used. The results of the regression analysis for prediction of GTR and MRR are given in Tables 5.18 and 5.19.

Table 5.18 Nonlinear regression summary statistics for GTR as dependent variable

Source	**DF**	**Sum of Squares**	**Mean Square**
Regression	3	242.07	80.69
Residual	2265	1.9566	0.0009
Total	2268	244.03	
Corrected Total	2267	56.49	
R^2 = 1 - Residual SS / Corrected SS = 0.965			
95 % Confidence Interval			
Parameter	Estimate	Std. Error	Lower	Upper
C1	0.62	0 .00106	0.604	0 .644
C2	0.08	0.0005	0.081	0 .083
C3	8.5	0 .033	8.41	8.59

Table 5.19 Nonlinear regression summary statistics for MRR as dependent variable

Source	**DF**	**Sum of Squares**	**Mean Square**
Regression	2	9.0395	4.5197
Residual	2266	0.03258	1.44 E-05
Total	2268	9.07207	
Corrected Total	2267	0.6568	
R^2 = 1 - Residual SS / Corrected SS = 0.95			
95 % Confidence Interval			
Parameter	Estimate	Std. Error	Lower	Upper
C5	1.08	0.0037	1.0697	1.1044
C6	0.75	0.0044	0.7425	0.7598

The higher value of coefficient of determination (R^2) indicates better agreement between observed and predicted data. The analysis shows that the parameters in the model are significantly affecting GTR and MRR. Based on this analysis the final prediction models are given as follows

$$GTR = \frac{T}{r \times W} = 0.62 \times (1 - e^{-0.08 B_n}) \times (1 - e^{-8.5S}) + 0.036 \quad (5.15)$$

$$MRR = \frac{MR}{W} = \frac{1.08}{B_n} + 0.036 + \frac{0.75 \times S}{\sqrt{B_n}} \quad (5.16)$$

where, $B_n = \left(\frac{CI \times b \times d}{W}\right) \times \left(\frac{1 + 5\frac{\delta}{h}}{1 + 3\frac{b}{d}}\right)$ (same as Eqn. (2.58))

CI = cone index, kPa
b = unloaded tyre section width, m
d = overall (unloaded) tyre diameter, m
δ = tyre deflection, m
h = tyre section height, m
r = rolling radius on hard surface, m
W = dynamic load on the tractive device, kN
S = wheel slip, decimal
M = motion resistance, kN
P = net traction or pull, kN and
T = wheel axle torque. kNm

5.5.2 Model parameters

Each of the parameters in GTR and MRR models has some significance. The significance of each term in the developed models for GTR and MRR (Eqns. (5.15 and 5.16)) as explained by Brixius (1987) is presented below.

1) Torque Ratio (T/rW): Torque ratio is same as coefficient of gross traction. It is analogous to a friction coefficient as given by

$$\frac{F}{W} = \frac{T}{r \times W}$$

where, $F = \frac{T}{r}$ is the gross thrust developed at the wheel-soil surface. The largest frictional coefficient is developed at a high slip when there is a large relative movement between the wheel and the soil.

The torque ratio $\left(\frac{T}{r \times W}\right)$, predicted by Eqn. (5.15) is plotted in Fig. 5.31 for several values of the mobility number (B_n). As B_n increases, the tractive performance of a wheel improves. The curves asymptotically approach a maximum value which is a function of B_n.

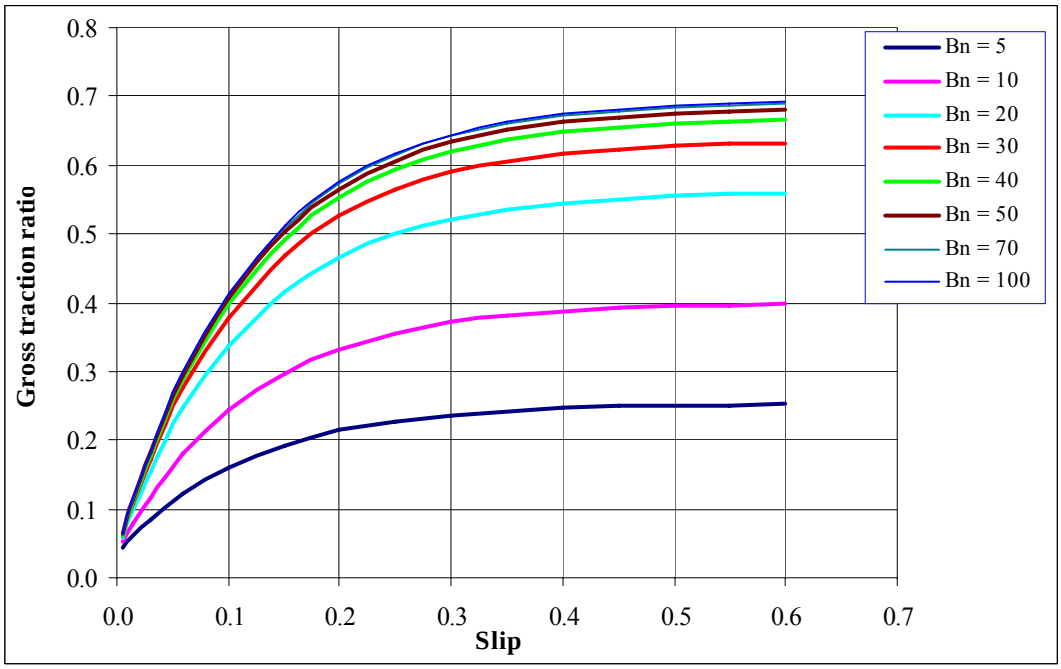

Fig. 5.31 Gross thrust of a driven wheel

2. The constant 0.62: It limits the maximum torque ratio developed by a wheel on soil to 0.656 = 0.62 + 0.036. This is obtained at high slip.

3) $e^{-0.08\ Bn}$: The wheel numeric $\left(C_n = \frac{CI \times b \times d}{W}\right)$, the deflection ratio $\left(\frac{\delta}{h}\right)$ and the width-to-diameter ratio b/d are combined in one dimensionless product called the mobility number (B_n). The mobility number is used in the equation to predict the combined effect of the soil-wheel parameters on tractive performance. The mobility number increases when

- Soil strength (CI) increases
- Tyre diameter (d) or section width (b) increases
- Load (W) decreases
- Deflection ratio (δ/h) increases
- Width-to-diameter ratio (b/d) decreases.

The constant 0.08 along with mobility number (B_n) controls the maximum value of the torque ratio which is attained at high slip.

4) $e^{-8.5S}$: The constant 8.5, which may be called a griping or surface factor, controls the rate of torque ratio increase with slip.

5) The constant 0.036: It approximates the torque ratio at zero slip for all conditions. On a hard surface, zero slip occurs when the wheel is in the self- propelled state. Under this condition torque is required only to overcome motion resistance due to tyre flexing and scrubbing. Brixius (1987) found this constant equal to 0.03 to 0.035.

6) Motion resistance ratio (MR/W): Motion resistance (MR) is caused by several factors:

- Tyre flexing and scrubbing (hard surface)
- Compaction of soil
- Bulldozing of soil to the side
- Lateral drag caused by soil adherence and viscosity

7) $1.08/B_n$: As B_n decreases, motion resistance increases, as shown in Fig. 5.32, due to increased soil compaction and sinkage. B_n decreases with decrease in wheel numeric (C_n), deflection ratio and with increase in width-to-diameter ratio. A decrease in the wheel numeric corresponds to a decrease in soil strength and/or an increase in soil-tyre contact pressure. A decrease in deflection ratio corresponds to a decrease in contact area, which increases peak pressure and therefore increases soil compaction and resistance to motion. Increase in tyre width to diameter ratio corresponds to increase in soil volume under compaction and thus increases motion resistance. Motion resistance is less for a long narrow tyre print.

8) Constant 0.036: The constant 0.036 represents the minimum value of motion resistance ratio on any surface and is equal to motion resistance ratio on a hard surface. This term is due to tyre flexing and scrubbing.

9) $0.75S/\sqrt{B_n}$: Motion resistance increases with slip due to increase in tyre sinkage and soil shearing. Towed force of a wheel can be approximated by Eqn. (5.16) by setting this term equal to zero.

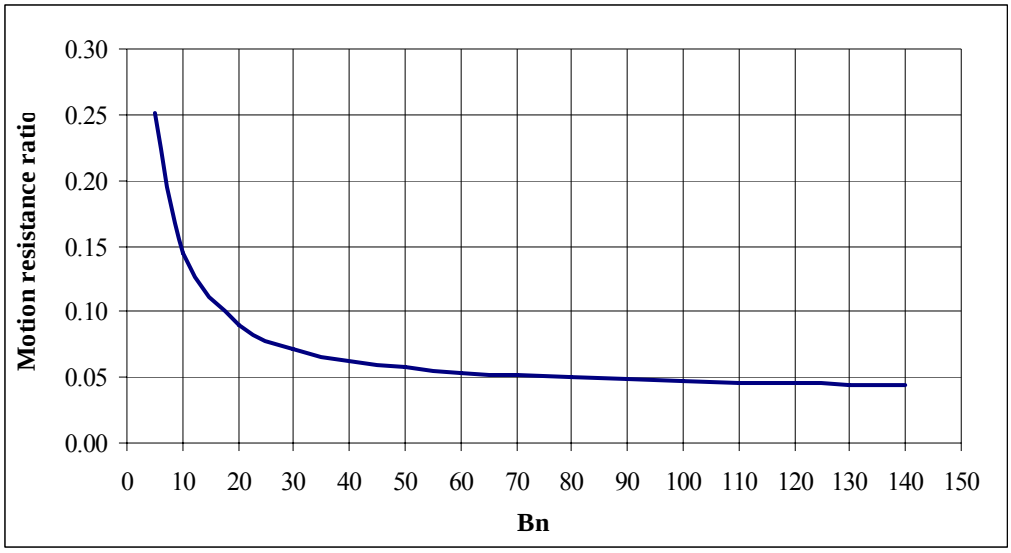

Fig.5.32 Motion resistance ratio at zero slip (Towed force ratio)

5.5.3 Pull Ratio

Pull ratio or coefficient of traction (COT) is the net pull of the wheel divided by wheel load. It is defined as

$$\frac{P}{W} = \frac{T}{r \times W} - \frac{MR}{W} \tag{5.17}$$

Similar to torque ratio, the pull ratio (also called coefficient of traction) is sensitive to B_n at high slip (Fig. 5.33). The highest pull ratio is obtained for a large value of B_n, which is associated with a large torque ratio and a small motion resistance. Pull ratio drops off sharply for B_n less than 10. This is also supported by Brixius (1987).

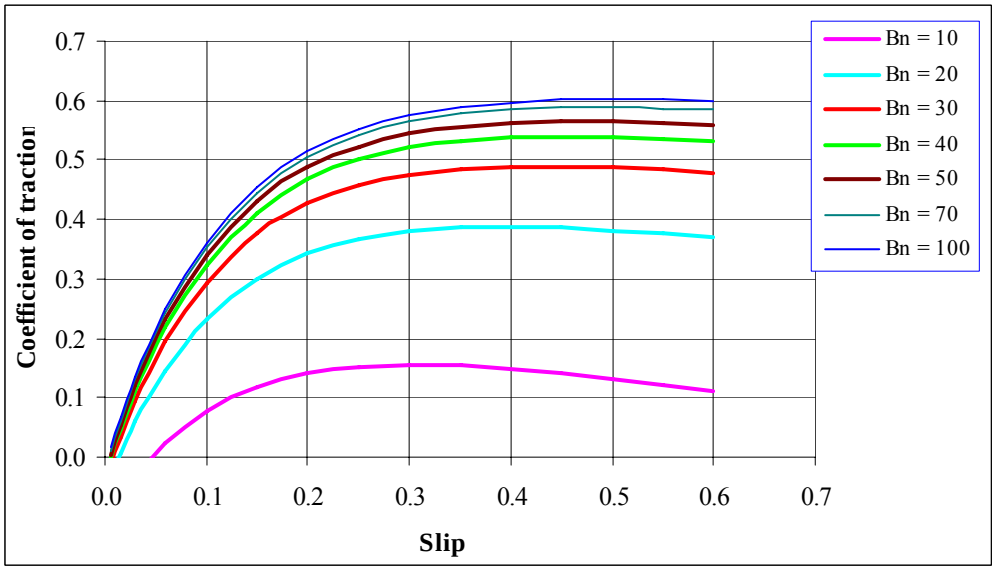

Fig. 5.33 Net pull of a driven wheel

5.5.4 Tractive Efficiency

Tractive efficiency-slip curves are shown in Fig 5.34 for several values of B_n. Peak wheel efficiency is typically obtained when the wheel operates between 5 to 20 per cent slip. For slip less than 5 per cent, a large portion of input power is required to overcome the tyre motion resistance. Above 20 per cent slip, an increasing portion of input power is lost in slip. The similar range of slip was also found by Brixius (1987).

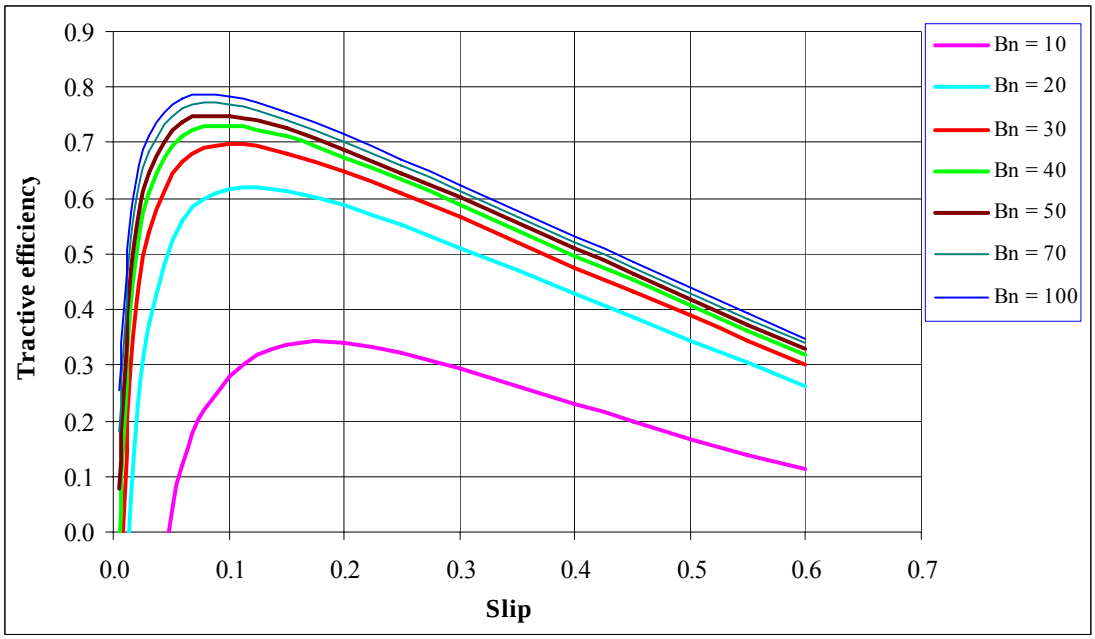

Fig. 5.34 Relationship between tractive efficiency and wheel slip

5.5.5 Comparison of the developed models with a few existing models

The developed GTR model (Eqn. (5.15)) was compared with the models developed by Brixius (1987) and Al-Hamed (1994) as shown in Fig. 5.35. Similarly, the developed MRR model (Eqn. (5.16)) was also compared with the Brixius and Al-Hamed models as shown in Fig. 5.36. The experimental data used for validating and comparing the GTR and MRR model were from separate investigation conducted with 4 test tyres under similar soil conditions. The following models were used to compare the performance of the developed models.

(a) Brixius model (1987)

$$GTR = \frac{T}{rW} = 0.88 \times \left(1 - e^{-0.1B_n}\right) \times \left(1 - e^{-9.5S}\right) + 0.0325 \qquad (5.18)$$

$$MRR = \frac{MR}{W} = \frac{0.9}{B_n} + 0.0325 + \frac{0.5 \times S}{\sqrt{B_n}} \tag{5.19}$$

$$B_n = \left(\frac{CIbd}{W}\right)\left(\frac{1+5\frac{\delta}{h}}{1+3\frac{b}{d}}\right) \tag{5.20}$$

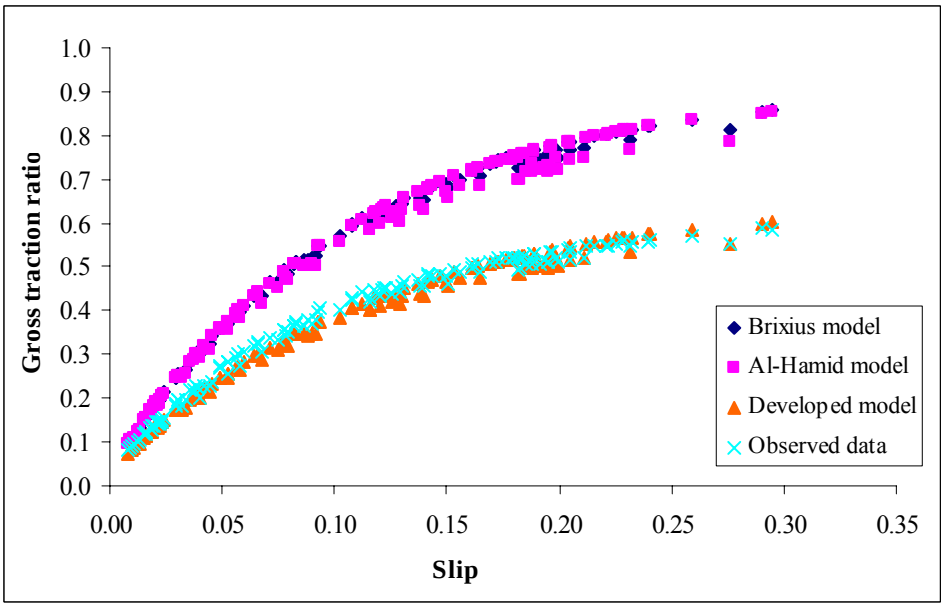

Fig. 5.35 Comparison of the developed GTR model with a few existing models

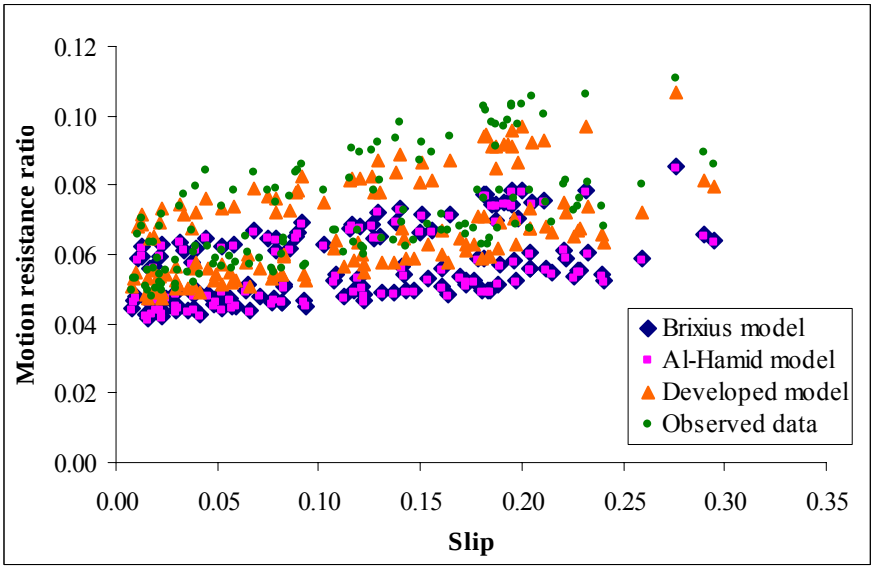

Fig. 5.36 Comparison of the developed MRR model with a few existing models

(b) Al-Hamed model (1994)

$$GTR = \frac{T}{rW} = 0.88 \times \left(1 - e^{-0.08B_n}\right) \times \left(1 - e^{-9.5S}\right) + 0.032 \quad (5.21)$$

$$MRR = \frac{MR}{W} = \frac{0.9}{B_n} + 0.032 + \frac{0.5 \times S}{\sqrt{B_n}} \quad (5.22)$$

$$B_n = \left(\frac{CIbd}{W}\right)\left(\frac{1 + 5\frac{\delta}{h}}{1 + 3\frac{b}{d}}\right) \quad (5.23)$$

(c) The developed model

$$GTR = \frac{T}{r \times W} = 0.62 \times (1 - e^{-0.08B_n}) \times (1 - e^{-8.5S}) + 0.036 \quad (5.24)$$

$$MRR = \frac{MR}{W} = \frac{1.08}{B_n} + 0.036 + \frac{0.75 \times S}{\sqrt{B_n}} \quad (5.25)$$

Based on statistical analysis (Table 5.20), the Brixius and Al-Hamed models were found to over predict the traction potential of the tyres.

Table 5.20 Comparison of the GTR and MRR models

Traction Performance	Models	Mean		Deviation %	RMSE	Model Effi.	Bias %	R^2
		Obs.	Sim.					
GTR	Brixius	0.378	0.537	17.7 to 49.3	0.905	0.976	-42.0	0.996
	Al-Hamed	0.378	0.530	16.8 to 47.7	0.833	0.979	-40.2	0.994
	Developed	0.378	0.368	-9.7 to 3.4	0.0688	0.999	2.7	0.998
MRR	Brixius	0.072	0.057	-28.9 to -9.5	0.859	0.186	28.9	0.961
	Al-Hamed	0.072	0.056	-29.4 to -10.5	0.918	0.072	21.7	0.955
	Developed	0.072	0.067	-13.4 to -3.3	0.144	0.977	6.2	0.979

This shows that both the developed models can be used effectively to predict the traction behavior of the radial-ply tyres under sandy clay loam soils.

5.5.6 Comparing traction potential of radial and bias tyres

The traction potential of radial ply tyres using the developed models and that of the bias-ply tyres using the models (Eqns. (5.26 to 5.28)) developed earlier by Tiwari *et. al.* (2010) under the similar soil conditions is shown in Fig. 5.37.

$$GTR = \frac{T}{r \times W} = 0.66 \times (1 - e^{-0.09 B_n}) \times (1 - e^{-5.25 S}) + 0.035 \quad (5.26)$$

$$MRR = \frac{MR}{W} = \frac{1.2}{B_n} + 0.035 + \frac{0.77 \times S}{\sqrt{B_n}} \quad (5.27)$$

$$B_n = \frac{CI \times b \times d}{W} \times \left(\frac{1 + K_1 \times \frac{\delta}{h}}{1 + K_2 \times \frac{b}{d}} \right) \quad (5.28)$$

The data indicate that the radial tyres with b/d ratios 0.25 to 0.31 are capable of developing 25-30% higher COT and compared to similar sizes of bias-ply tyres within 30% slip.

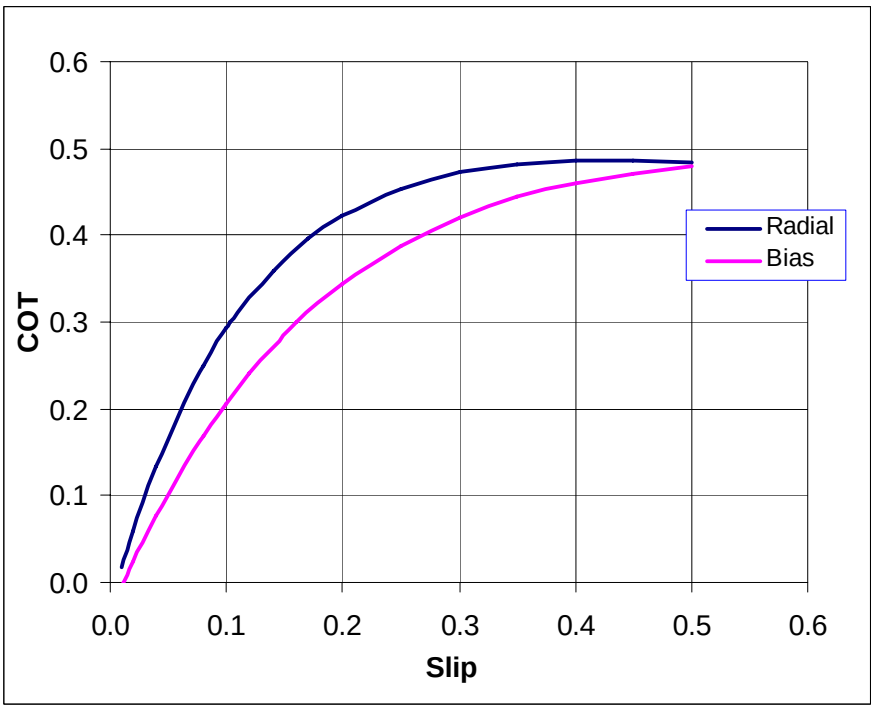

Fig. 5.37 Comparison of traction potential of radial and bias-ply tyres

5.5.7 Tractive efficiency design curve

Figure 5.38 shows relationship of COT and TE with wheel slip at different values of B_n. The values of COT and TE were calculated using the developed GTR and MRR models as given below.

$$COT = GTR - MRR \quad (5.29)$$

$$TE = \frac{COT}{GTR}(1 - S) \quad (5.30)$$

The data indicate that pull ratio (or) drawbar pull increases with wheel slip, while tractive efficiency decreases at high wheel slip. Therefore, a compromise in vehicle operation must be reached between obtaining maximum tractive efficiency and high wheel pull.

One possible tractive efficiency design curve which compromises the two values is shown in the Fig. 5.38. From this curve, the designed TE, P/W and slip for various values of B_n can be determined: *e.g.*: for B_n = 50, TE = 0.74, P/W = 0.30 and slip = 0.09. Other design curves can be chosen depending on whether high tyre pull or efficiency is desired. For the same B_n value, the tractive performance ratios found with Brixius model are comparatively higher. The type of soil used in the present study was probably responsible for getting the lower prediction as compared to Brixius model.

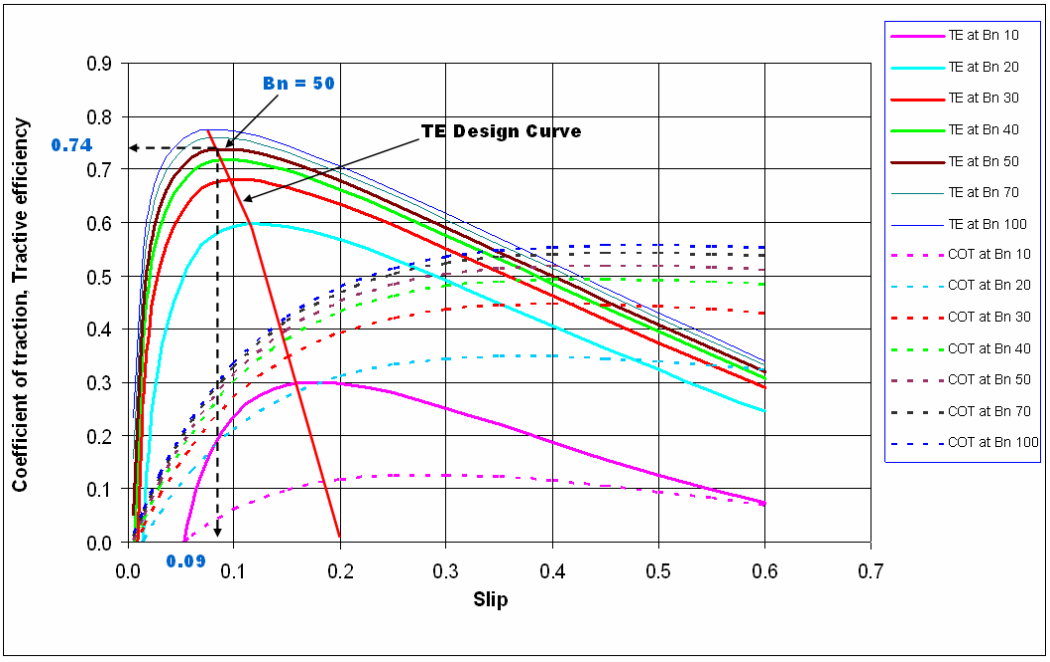

Fig.5.38 Tractive efficiency design curve

Based on the result discussed in this section, the following outcomes can be drawn.

1. The test data were utilized to develop two prediction models, one for gross traction ratio and another for motion resistance ratio for radial-ply tyres (b/d = 0.25-0.31, δ/h = 20-28 per cent) to be used under varying soil conditions in sandy clay loam soils.

2. The developed models were compared with a few existing models using a set of data which were not considered in model building in the present study. The developed models were found to perform well compared to the other models.

3. A tractive efficiency design curve has been constructed based on the developed models. These curves can be used to determine optimum tractive performance parameters of a given tyre and soil condition. Such a curve would help in economic operation of the tractors under varying soil conditions.

4. The radial tyres were found to have 24-30% greater coefficient of traction (COT) compared to similar sizes of bias-ply tyre within 30% slip range under varying compaction levels of sandy clay soil and 34-37% reduced slip at 0.3 COT.

The summary of the present investigation along with the specific conclusions are presented in the next chapter.

CHAPTER VI
SUMMARY AND CONCLUSIONS

6.1 Introduction

The total cultivated area of the country is 124.75 Mha, which yields about 259.23 Mt of food grain. The productivity of Indian farms stands at 2.06 t/ha. This has been achieved through the adoption of improved seeds, fertilizer, irrigation water, biological mechanized farming and other chemical and mechanical inputs. The availability of farm power per unit area is considered to be an important parameter in evaluating the level of farm mechanization. Based on this index the present level of mechanization in India is only 1.84 kW/ha compared to that available in some of the advanced countries such as Japan (8.75 kW/ha) and Italy (3.01 kW/ha). The predicted value of farm power availability in India for the year 2020 is 2.2 kW/ha. On the basis of net cultivated area the present level of mechanization in India is estimated to be 40-45 per cent. However, all operations are not uniformly mechanized. Operation-wise level of mechanization varies from 29 - 42 per cent. India is the largest producer of farm tractors in the world which account for 46 per cent of the total share of mechanical power used in the country (Mehta *et al.*, 2014). Past studies indicate that 20-55 per cent of the available tractor energy is wasted at the tyre-soil interface (Burt *et al.*, 1982). Interaction between soil and low pressure pneumatic tyres continues to be an inefficient means of transferring engine power to drawbar powered implements. Although considerable progress has been made in the past few decades, our understanding of the soil-wheel interaction process and our capability to quantify this interaction is far from satisfactory. The official tractor drawbar performance tests of agricultural tractors are conducted on hard surfaces that provide uniform and reproducible test conditions for comparisons. However, it does not provide a fundamental understanding of the traction process, nor does it provide a basis for the prediction of performance. The main disadvantages are that the results are not immediately applicable to normal working conditions on the farm.

6.1.1 Predicting tractive potential of radial-ply tyres

The tractive characteristics of a pneumatic tyre depend on tyre geometry (width, overall diameter, and section height), tyre type (radial verses bias), lug design,

inflation pressure, dynamic load on axle, and soil type and condition (Gill and Vandenberg, 1968 and Upadhyaya *et al.*, 1986). Tractive characteristics of tyres are usually determined by conducting either field experiments or tests under controlled laboratory soil bin conditions. A traction test under controlled soil bin conditions involves loading the test tyre to a desired dynamic load and then controlling draft or slip in some predetermined manner. The response of the system consists of input torque and draft if slip is controlled, or slip if draft is controlled.

A pre-requisite for the successful design of a traction device is a sound mathematical model for the soil-traction interaction process. These models allow researchers and designers to investigate many problems related to tractor performance under a wide range of conditions with the goal to improve tractor design, to optimize tractor operational parameters, and to improve the tractor/implement match. Relative importance of these factors affecting field performance of a tractor can be achieved without expensive field-testing. These models can also assist tractor operators to improve (fine-tune) and optimize their tractors' setup to match operating conditions.

6.1.2 Justification and objectives

The tractors used in the country are generally provided with bias-ply tyres. The use of radial tyres is limited due to their non availability in the local market and high cost. However, such tyres have been found to be more efficient than the bias-ply tyres in traction performance as well as in fuel economy (Forrest *et al.*, 1962; Thaden, 1962; Gee-Clough *et al.*, 1977; Hausz and Akins, 1980; Hauck *et al.*, 1983). In developing countries, particularly in India, the use of high hp tractors in the power segment of 40 to 50 hp and beyond has been found to increase during the last one decade. These tractors are preferred for heavy field and haulage operations where greater amount of traction power is needed. The radial tyres are expected to find greater use in such tractors to provide desired traction requirement and fuel economy as well as comfort level in haulage operations. It is essential to have suitable traction prediction models for these tyres to provide needed input for designing new tractors. In this context, many studies were conducted in the past, but the model developed by Brixius in 1987 is most widely used. This model, however, is not very useful for low hp tractors using small size tyres at reduced loading conditions. On comparing with the experimental

data obtained at IIT Kharagpur the Brixius model was found to overpredict the tractive efficiency of 14.9 R 28 tyre by 13-50% under different soil conditions. A need was, therefore, felt to study the traction potential of such tyres under the varying soil and tyre operating conditions. The major objectives of the project are as follows.

Objectives

1. To study the deflection and contact characteristics of radial-ply tractor tyres at different normal loads and inflation pressures.
2. To study the characteristics of the radial-ply tractor tyres at zero condition.
3. To study the influence of soil, tyre and system parameters on the tractive performance of the tyres.
4. To develop empirical models for drawbar performance prediction of radial-ply tractor tyres for Indian operating conditions and to compare them with the prominently used traction prediction models.

6.2 Methodology

The methodology followed to conduct the experiments has been described in the following sub sections.

6.2.1 Deflection and contact characteristics of test tyres

The best single indicator of a tyre's ability to perform satisfactorily and deliver normal service life is tyre deflection. When a tyre is over deflected as a result of over load and under inflation or a combination of these, service life will be reduced. The over deflected tyre bulges excessively at ground contact making it more subject to puncture damage. This requires that the recommended inflation pressure is maintained in all tyres and that the tyres are not subjected to load more than the recommended load. It is, therefore, essential to study the deflection characteristics of a tyre with a view to arrive at optimum combinations of load and inflation pressure for evaluating its traction performance.

The experimental facilities for deflection test included a tyre test carriage (single wheel tester), an electronic platform balance and deflection measuring device. The tyre test carriage can accommodate the various sizes of the tyres and can be raised and

lowered using a hydraulic cylinder. The vertical deflection of the tyre was measured with displacement transducer and recorded by a Data Acquisition System (DAS). The four different sizes of test tyres (12.4R28, 13.6R28, 14.9R28 and 16.9R28) were selected for the study. The tyre aspect ratio varied from 0.812 to 0.860 and b/d ratio from 0.25 to 0.31.

A multiple overlay technique was used to get consistent results for the lugged tyres. A steel plate, covered with white sheets with a carbon paper in between the sheets, was placed beneath the test tyre fitted in the tyre test carriage. The tyre with a given inflation pressure was loaded to the desired vertical load with the dead weights on a single wheel tester. The tyre was slowly brought down and allowed to rest on the paper and the transducer output was recorded for deflection measurement. The tyre was raised and rotated by a few degrees and pressed against the plate again. This procedure was repeated to obtain a good imprint of tyre on the white sheet by overlaying a number of prints on the same area. The outline of the imprint was traced and the contact area was determined using mechanical desktop software. The per cent deflection was calculated using the following formula.

$$\text{Tyre deflection, per cent} = \frac{\text{Vertical tyre deflection, } (\delta)}{(\text{Tyre section height } (h) - \text{Flange height})} \times 100 \qquad (6.1)$$

The mean ground pressure was represented by the normal load to contact area ratio. Each tyre was tested at seven inflation pressures varying from 41 kPa (6 psi) to 207 kPa (30 psi) with representative loads varying from 4.905 kN (500 kg) to 19.13 kN (1950 kg).

For the study of zero condition and tyre performance tests the load-pressure combinations to get the desired level of deflection (20, 24 and 28 per cent) for each tyre were determined by varying inflation pressure from 41 kPa (6 psi) to 207 kPa (30 psi) and normal load from 7.36 kN (750 kg) to 19.13 kN (1900 kg) according to the tyre size.

6.2.2 Tractive performance of test tyres

The experimental set-up consists of an indoor soil bin (23.5 m × 1.37 m × 1.50 m) filled with the locally available lateritic sandy clay loam soil, a soil processing trolley, a tyre test carriage (single wheel tester) and a drawbar pull loading device. The tyre test carriage was provided with a main frame to accommodate the various sizes of tyres, a loading platform, a parallel bar linkage system and a power transmission system. The test carriage was attached to a towing trolley through fixed supports of parallel bar linkage. A 7.46 kW, 3 phase, 1500 sync rev/min induction motor mounted on the loading platform frame was used to give driving power to the wheel. The speed of the motor was initially reduced by a sprocket and chain drive arrangement (2.6:1), which was further reduced by a worm and worm gear reduction unit (50:1). Thus the final linear speed of the wheel axle was obtained between 2.9 – 3.5 km/h depending upon the test tyre size and other operating conditions. To vary horizontal pull of the test wheel a drawbar-loading device with a shoe type braking arrangement was used. An electrical control panel was used to control the operations of soil processing trolley and the tyre test carriage in forward and reverse directions.

The recording units include a Data Acquisition System and a computer. The input torque to the wheel axle was measured using a 200 Nm torque transducer. A ring transducer of 10 kN capacity was used to sense the drawbar pull of the test wheel. The actual forward speed of the wheel was measured with the help of a proximity switch sensing the rotation of a roller moving over the steel rail. The theoretical forward speed of the wheel was measured with another proximity switch which sense the rotation of a disc attached to the wheel axle through chain and sprocket. A point gauge with a supporting frame was used to measure the wheel sinkage as well as surface profile of the soil bed before and after each test. A hydraulically operated standard cone penetrometer with a base diameter of 20.27 mm and apex angle of 30 degree was used to measure the cone index.

The zero condition was used to define the rolling radius to calculate the theoretical speed of the wheel. In the present study zero slip condition has been assumed at zero net traction on a hard surface (ASAE standards, 1998). The hard surface for zero condition was created by placing 10 mm thick MS sheets over the well-compacted

soil in the soil bin. The input torque values for each selected conditions of load and inflation pressure were measured. Rolling radius of the tyre under each selected condition was calculated by measuring the distance traveled in one revolution of the tyre and divided it by 2π.

To study the effect of soil, tyre and system parameters on tractive performance, the tests were conducted with four radial-ply tyres in three soil conditions (600-700 kPa, 1200-1300 kPa and 1700-1800 kPa) and at three levels of deflection (20, 24, and 28 per cent).

Before each test, the soil bed was prepared using the soil processing trolley. The soil processing was repeated, if large variation in the desired cone index value was observed. Each test was conducted on a 16 m long bed. For each level of deflection, the drawbar pull was varied till tyre indicated excessive slip beyond 25-30 per cent. The variables recorded for each test were i) drawbar pull, ii) input torque to wheel axle, iii) actual and theoretical forward speeds, and iv) wheel sinkage. Each test was replicated thrice. The recorded data were used to calculate the traction performance parameters of the tyre, namely, wheel slip, coefficient of traction and tractive efficiency.

6.3 Results and Discussion

The analysis and interpretation of the experimental results obtained during the course of study has been presented in the following sub sections.

6.3.1 Deflection and contact characteristics

The test results showed that the tyre deflection increased non-linearly with decrease in inflation pressure from 207 to 41 kPa, while it increased linearly with increase in normal load for all the test tyres. It was also noticed that the rate of increase of deflection with normal load was higher at lower values of inflation pressure than at higher ones.

The following models were developed to predict deflection, ground contact area and ground pressure of the tyres on a hard surface.

$$\frac{\delta}{h} = 114.43\left[\frac{P_g}{W}(d \times b)\right]^{-1.07} \quad (6.2)$$

$$A = \frac{0.27 \times W^{0.84} \times \sqrt{\frac{b}{d}}}{p_i^{0.5}} \quad (6.3)$$

$$P_g = -164.9 + 5.7 \times W + 696 \times p_i + 1460.6 \times \frac{b}{d} - 13.7 \times W \times \frac{b}{d} - 124 \times p_i \times \frac{b}{d} - 554.6 \times p_i^2 - 2828.1 \times \left(\frac{b}{d}\right)^2 \quad (6.4)$$

where, $\frac{\delta}{h}$ = deflection ratio, per cent,

b = width of the tyre, m,

d = diameter of the tyre, m,

W = normal load, kN,

P_g = ground pressure (W/A), kPa and

A = tyre-surface contact area, m^2.

The developed models were compared with some of the existing models available in the literature. The statistical analysis indicated that the developed models predict the behaviour of the test tyres better than the existing models.

6.3.2 Tyre behaviour under zero condition

The data obtained from zero condition tests indicated that:

1. The rolling radius decreased with increase in deflection for all the test tyres.
2. Torque ratio was found positively related with the deflection ratio (δ/h), while it had a negative linear relationship with the tyre width-to-diameter (b/d) ratio.
3. The minimum motion resistance ratio was found to be 0.036 for all the test tyres in the deflection range of 20 to 28 per cent on hard surface. Thus for any hard surface the minimum motion resistance ratio may be taken as 0.036.
4. The following rolling radius model can be used for determination of rolling radius on hard surface.

$$r = \frac{2.265 \times \frac{d}{2} \times (\text{static lodeded radius})}{1.24 \times \frac{d}{2} + (\text{static loaded radius})} \quad (6.5)$$

The value of rolling radius ratio for all the test tyres was found to be nearly constant on a hard surface and may be considered as

$$\frac{r}{d} \cong 0.4721$$

5. The developed torque ratio model based on dimensional analysis approach can be used to predict the gross traction at zero net traction for the agricultural traction tyres (12.4 R 28, 13.6 R 28, 14.9 R 28 and 16.9 R 28) on a hard surface.

$$\frac{T}{(r.W)} = 0.027 + 0.075 \times \left(\frac{\delta}{h}\right) - 0.031 \times \left(\frac{b}{d}\right) \qquad (6.6)$$

where, T = input torque to the wheel axle, Nm
r = rolling radius, m
W = normal load, kN
δ / h = deflection ratio, decimal
b = width of tyre, m and
d = diameter of tyre, m

6.3.3 Effect of soil, tyre and system parameters on tractive performance

The experimental data were used to graphically represent variations of tractive efficiency (TE) and wheel slip (s) with coefficient of traction (COT) for varying tyres under different operating conditions. From the regression analysis the following conclusions were drawn:

1. The pulling ability of the test tyres was found to improve with increase in soil cone index and normal load less within range of test conditions. However, tyre deflection did not indicate a very strong effect on their performance when COT was maintained less than 0.4.

2. The effect of soil cone index was found to be more pronounced than that of tyre size and normal load. These results are in agreement with those found by Upadhyaya and Wulfsohn (1989).

3. All the tyres were observed to have peak tractive efficiency in the range of 66 to 77 per cent within 8 to 11 per cent slip range corresponding to an optimum COT value of 0.3, when tested in the soil cone index range of 600 to 1800 kPa.

6.3.4 Development of traction prediction models

The tractive performance data of input axle torque (T), wheel slip (S), drawbar pull (P), rolling radius (r), normal load on wheel-axle (W), tyre deflection (δ), and tyre parameters of four different sizes of radial-ply traction tyres obtained in lateritic sandy clay loam soil were analysed to develop the following traction models:

$$\mathrm{GTR} = \frac{\mathrm{T}}{\mathrm{r} \times \mathrm{W}} = 0.62 \times (1 - \mathrm{e}^{-0.08\mathrm{B_n}}) \times (1 - \mathrm{e}^{-8.5\mathrm{S}}) + 0.036 \tag{6.7}$$

$$\mathrm{MRR} = \frac{\mathrm{MR}}{\mathrm{W}} = \frac{1.08}{\mathrm{B_n}} + 0.036 + \frac{0.75 \times \mathrm{S}}{\sqrt{\mathrm{B_n}}} \tag{6.8}$$

$$B_n = \frac{CI \times b \times d}{W} \times \left(\frac{1 + 5 \times \frac{\delta}{h}}{1 + 3 \times \frac{b}{d}} \right) \tag{6.9}$$

Constraints:

$b/d \approx 0.25$ to 0.31, $\delta/h \approx 0.20$ to 0.28

6.3.5 Comparison of the developed models with a few existing models

The developed GTR and MRR models were compared with the models developed by Brixius (1987) and Al-Hamed (1994) for radial farm tyres (Fig. 6.1). The experimental data used for validating and comparing the GTR and MRR models were obtained from a separate investigation conducted with 4 test tyres under similar soil conditions.

Based on statistical analysis, the Brixius and Al-Hamed models were found to over predict the traction potential of the tyres by 17 to 49 per cent, whereas, the developed model could predict within the range of -10 to 3.4 per cent. The model efficiency of the developed models was also found to be better than that of the existing models. Using the developed models a tractive efficiency design curve (Fig. 6.2) was constructed by plotting calculated values of TE and COT at different values of Bn and wheel slip. This curve can be used to evaluate drawbar performance (TE, COT and slip) of radial tyres within the specified range of mobility numbers.

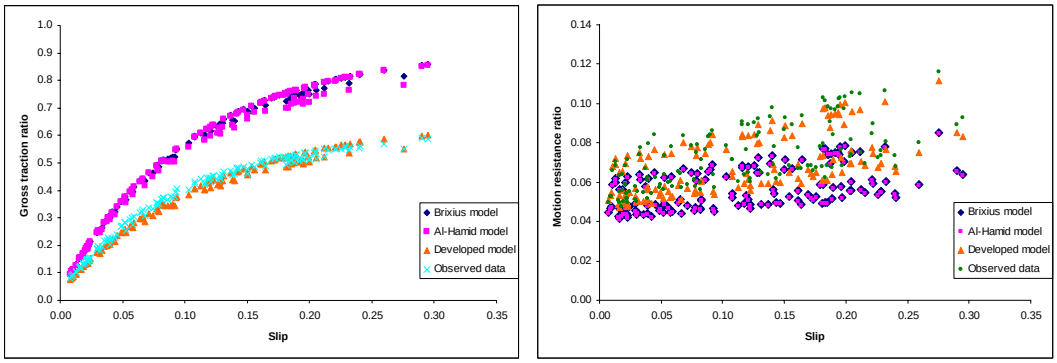

Fig. 6.1 Comparison of the developed GTR and MRR model with a few existing models

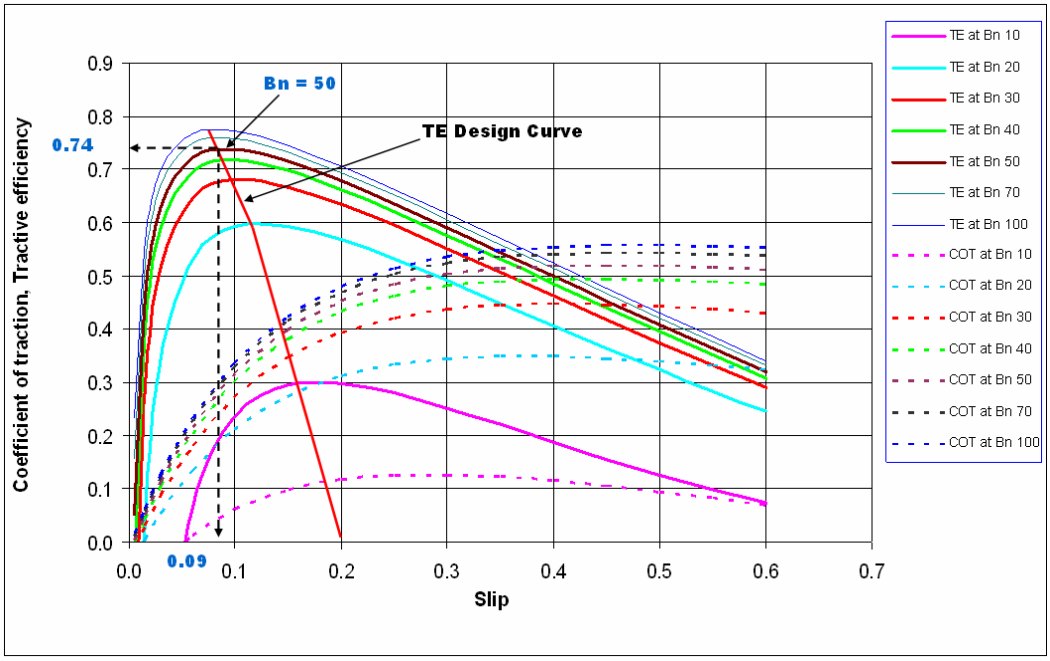

Fig. 6.2 Tractive efficiency design curve

6.3.6 Comparing traction potential of the radial and bias-ply tyres

An attempt was made to compare the traction potential of radial tyres using the developed models with that of the bias-ply tyres using the models (Eqns. 6.10 to 6.12) developed earlier by Tiwari *et al.* (2010) under similar soil conditions.

$$GTR = \frac{T}{r \times W} = 0.66 \times (1 - e^{-0.09 B_n}) \times (1 - e^{-5.25 S}) + 0.035 \qquad (6.10)$$

$$MRR = \frac{MR}{W} = \frac{1.2}{B_n} + 0.035 + \frac{0.77 \times S}{\sqrt{B_n}} \qquad (6.11)$$

$$B_n = \frac{CI \times b \times d}{W} \times \left(\frac{1 + 5 \times \frac{\delta}{h}}{1 + 3 \times \frac{b}{d}} \right) \quad (6.12)$$

The analysis indicate that the radial tyres with b/d ratios 0.25 to 0.31 developed 24-30% higher COT as compared to the similar sizes of bias-ply tyres within 0-30% slip range.

6.4 Conclusions

Based on the results of this study, the following specific conclusions can be drawn for radial-ply tyres (b/d ratio 0.25-0.31) used in the agricultural tractors.

1. The developed deflection and contact characteristics of the radial tyre (b/d ratio 0.25-0.31) can be used to optimize the tyre and system parameters to obtain desired level of tyre deflection.
2. A model to predict the gross traction ratio of radial-ply tyres at zero net traction was developed for the deflection range of 20-28 per cent on a hard surface. Such a model can be used to determine rolling resistance of the tyres on hard surface under self propelled condition.
3. The traction potential of radial tyres used in the tractor power range of 20 to 60 hp can be predicted by applying the GTR and MRR models developed in the present study under varying soil and operating conditions.
4. Based on the developed traction models, an efficient tractive efficiency design curve can be constructed by reaching a compromise between peak tractive efficiency and high drawbar pull. Such a curve will facilitate in economic operation of tractors under varying soil conditions.
5. All the tyres were observed to have peak tractive efficiency in the range of 66 to 77 per cent within 8 to 11 per cent slip range corresponding to an optimum COT value of 0.3, when tested in the soil having cone index in range of 600 to 1800 kPa. These values can be adopted to develop new tractors where sandy clay loam soil is prevalent.
6. The most significant parameter affecting the tractive performance of the radial tyre was found to be cone index followed by normal load, tyre size and deflection.

7. The radial tyres were found to have 24-30% greater coefficient of traction compared to similar sizes of bias-ply tyres within 30% slip range under varying soil conditions of sandy clay soil. Such tyres are, therefore, better suited for high hp tractors being used for heavy field and haulage operations.

SUGGESTIONS FOR FUTURE WORK

In the present study, traction prediction model for radial-ply tyre has been developed in the soil bin for sandy clay loam soil, and have laid a foundation for continued research. Here, several suggestions for further investigations are proposed. In summary, they are:

1. With a view to validate the developed models with field data, it is essential to conduct field experiments with tractors equipped with different sizes of radial-ply tyres under sandy clay loam soils. This will help to predict the drawbar performance of agricultural tractors under varied soil and load conditions.

2. The developed traction models are suitable for sandy clay loam soils prevalent in most parts of the country. However, to have generalized traction models it is desired to conduct experiments also in clay soils and suggest the models suitable for different regions where clayey and sandy soils are predominant.

REFERENCES

Abeels, P.J.F., 1976. Tyre deflection and contact studies. Journal of Terramechanics, 13(3): 183-196.

Abeels, P.J.F., 1981. Studies of agricultural and forestry tyres on testing stand, basis for data standardization. Seventh international conference of ISTVS, 16-20 August 1981, Vol. II, Calgary, Alberta: 439-453.

Abeels, P.J.F., 1989. Tyre testing: Automatic recording of the tyre deformability. ASAE paper No. 89-1051, St. Joseph, MI.

Al-Hamed, S.A., Grisso, R.D., Zoz, F.M. and Bargen, K.V., 1994. Tractor performance spread sheet for radial tyres. Computers and Electronics in Agriculture, 10(1): 45-62.

Ambruster, K. and Kutzbach, H.D., 1989. Development of a single wheel tester for measurement on driven angled wheel. Proceedings of 5th European conference of the ISTVS, Wageningen. The Netherlands: 8-14.

Anonimous, 2005. Yearbook. Tyre and Rim Association.

Arvidsson, J. and Ristic, S., 1996. Soil stress and compaction effect for four tractor tyres. Journal of Terramechanics, 33(5): 223-232.

ASAE Standards, 1998. ASAE S296.4 DEC95. General terminology for traction of agricultural tractors, self-propelled implements, and traction and transport devices. St. Joseph, Michigan: ASAE.

ASAE Standards, 2000. ASAE EP496.2 DEC99. Agricultural machinery management. St. Joseph, Michigan: ASAE.

ASABE Standards, 2006a. ASAE S313.3 FEB04. Soil cone penetrometer. St. Joseph, Michigan: ASAE.

ASABE Standards, 2006b. ASAE EP542 FEB99. Procedures for using and reporting data obtained with the soil cone penetrometer. St. Joseph, Michigan: ASAE.

ASABE Standards, 2011. ASAE D497.7 March 2011. Agricultural machinery management data. St. Joseph, Michigan: ASAE.

Ashmore, C., Burt, C. and Turner, J., 1987. An empirical equation for predicting tractive performance of log-skidder tyres. Transactions of the ASAE, 30(5): 1231-1236.

Ayers, P.D. and Perumpral, J.V., 1982. Moisture and density effect on cone index. Transactions of the ASAE, 25(5): 1169-1172.

Bailey, A.C., Raper, T.R., Burt, E.C. and Johnson, C.E., 1996. Soil stresses under a tractor tyre at various loads and inflation pressures. Journal of Terramechanics, 33(1): 1-11.

Bekker, M.G., 1956. Theory of land locomotion- The mechanics of vehicle mobility. University of Michigan Press.

Bekker, M.G., 1960. Off-the-Road Locomotion. University of Michigan Press.

Bekker, M.G., 1969. Introduction to terrain-vehicle systems. University of Michigan Press.

Bekker, M.G., 1983. Prediction of design and performance parameters in agro-forestry vehicles. National Research Council of Canada. Report No.22880.

Brixius, W.W., 1987. Traction prediction equations for bias-ply tyres. ASAE Paper No. 87-1622. St. Joseph, MI.

Burt, E.C., Bailley, A. C., Patterson, R. M. and Taylor, J. H., 1979. Combined effect of dynamic load and travel reduction on tyre performance. Transactions of the ASAE, 22(1): 40-45.

Burt, E.C., Lyne, P.W.L., Meiring, P. and Keen, J.F., 1982. Ballast and inflation pressure effects on tractive efficiency. ASAE paper No. 82-1567, St. Joseph, MI.

Burt, E.C., and Bailley, A.C., 1982. Load and inflation pressure effects on tyres. Transactions of the ASAE, 25(4): 881-884.

Burt, E.C. and Lyne, P.W.L., 1985. Velocity effects on traction performance. Transactions of the ASAE, 28(6): 1729-1730.

Burt, E.C., Reaves, C.A., Bailey, A.C. and Pickering, W.D., 1980. A machine for testing tractor tyres in soil bins. Transactions of the ASAE, 23(3): 546-547.

Busscher, W.J., 1990. Adjustment of flat-tipped penetrometer resistance data to a common water content. Transactions of the ASAE, 33(2): 519-524.

Charles, S.M., 1984. Effects of ballast and inflation pressure on tractor tire performance. Agricultural engineering, 65(2): 11-13

Clark, R.L., 1985. Tractive modeling with the modified Wismer-Luth model. ASAE Paper No. 85-1049. St. Joseph, MI.

Collins, J.G., 1971. Forecasting trafficability of soils. Technical Memo. 3-331, U.S. Army Corps of Engineers Waterways Experiment Station, Vicksburg, MS.

Defossez, P., Richard, G., Boizard, H. and Sullivan, M.F.O., 2003. Modelling change in soil compaction due to agricultural traffic as function of soil water content. Geoderma, 116(1-2): 89-105.

Dexter, A.R., Horn, R., Holloway, R., Jakobsen, B.F., 1988. Pressure transmission beneath wheels in soils on the Eyre peninsula of South Australia. Journal of Terramechanics, 25(2): 135–147.

Dexter, A.R., Czyz, E.A., Gate, O.P., 2007. A method for prediction of soil penetration resistance. Soil and Tillage Research, 93(2): 412–419.

Diserens, E., 2009. Calculating the contact area of trailer tyres in the field. Soil and Tillage Research, 103(2): 302-309.

Diserens, E., Defossez, p., Duboisset, A., and Alaoui, A., 2011. Prediction of the contact area of agricultural traction tyres on firm soil. Biosystems Engineering, 110(2): 73-82.

Dwyer, M.J., 1972. Field measurement of agricultural tractor tyre performance at the National Institute of Agricultural Engineering. Proceedings of 4th international conference of ISTVS, 24-28 April 1972, vol. 1: 39-60.

Dwyer, M.J., Evernden, D.W. and McAllister, M., 1976. Handbook of agricultural tyre performance, II Edition, NIAE report No.18. NIAE, Silsoe, Bedford, England.

Dwyer, M.J., 1983. Soil dynamics and the problems of traction and compaction, Agricultural Engineer, 38(3): 62-68.

Dwyer, M.J., 1984. The tractive performance of wheeled vehicles. Journal of Terramechanics, 21(1): 19-34.

Dwyer, M.J. and Heigho, D.P., 1984. The tractive performance of some large tractor tyres compared with dual tyres. Journal of Agricultural Engineering Research, 29(1): 43-50.

Dwyer, M.J., 1987. The tractive performance of a wide, low-pressure tyre compared with conventional tractor drive tyres. Journal of Terramechanics, 24(3): 227-234.

Ekinci, S., and Carman, K., 2011. Effects on tyre contact area of tyre structural and operational parameters. 6th International Advanced Technologies Symposium (IATS'11), 16-18 May 2011, Elazıg, Turkey.

Ellis, R.W., 1977. Agricultural tyre design requirements and selection considerations. ASAE Distinguished Lecture No.3, pp. 1-10. Winter Meeting of the American Society of Agricultural Engineers, 13 December 1977, Chicago, Illinois.

Evans, M.D., Clark, R.L. and Manor, G., 1991. An improved traction model for ballast selection. Transactions of the ASAE. 34(3): 773-780.

Forrest, P.J., Reed, 1.F. and Constantakis, G.V., 1962. Tractive characteristics of radial-ply tires, Transactions of the ASAE. 5(2): 108.

Freitag, D.R., 1966. A dimensional analysis of the performance of pneumatic tyres on clay. Journal of Terramechanics, 3(3): 51-68.

Freitag, D.R. and Smith, M.E., 1966. Centre line deflection of pneumatic tyres moving in dry sand. Journal of Terramechanics, 3(1): 31-46.

Freitag, D.R., 1968a. Penetration tests for soil measurements. Miscellaneous Report 4-284, U.S. Army Corps of Engineers Waterways Experiment Station, Vicksburg, MS.

Freitag, D.R., 1968b. Dimensional analysis of performance of pneumatic tyres on sand. Transactions of the ASAE, 11(5): 669-672.

Fujimoto, Y., 1977. Performance of elastic wheels on yielding cohesive soils. Journal of Terramechanics, 14(4): 191-210.

Gee-Clough, D., Mcallister, M. and Evernden, D. W., 1977. Tractive performance of tractor drive tires II. A comparison of radial and cross-ply carcass construction, Journal of Agricultural Engineering Research, 22(4): 385-395.

Gee-Clough, D., McAllister, M., Pearson, G. and Evernden, D. W., 1978. The empirical prediction of tractor-implement field performance. Journal of Terramechanics, 15(2): 81-94.

Gee-Clough, D., 1980. Selection of tyre sizes for agricultural vehicles. Journal of Agricultural Engineering Research, 25(3): 261-278.

Gill, W.R., 1968. Influence of compaction hardening of soil on penetration resistance. Transactions of the ASAE, 11(6): 741-745.

Gill, W.R. and Vandenberg, G.E., 1968. Soil dynamics in tillage and traction. Agricultural Handbook No. 316, U.S. Government printing office, Washington, D.C.

Godbole, R., Alcock, R. and Hettiaratchi, D., 1993. The prediction of tractive performance of on soil surfaces. Journal of Terramechanics, 30(6): 443-459.

Grecenko, A., 1995. Tyre footprint area on hard ground computed from catalogue value. Journal of Terramechanics 32(6): 325-333.

Greenlee, J.G., Summers, J.D. and Self, K.P., 1986. Effect of velocity on tractive performance of tractor tyres. ASAE paper No. 86-1539, St. Joseph, MI.

Hallonborg, U., 1996. Super ellipse as tyre-ground contact area. Journal of Terramechanics, 33(3): 125-132.

Hauck, D.D. and Kucera, H.L., 1983. Radial tractor tires. Cooperative Extension Service, North Dakota State University, Fargo, North Dakota.

Hausz, F.C. and Akins, H., 1980. Optimizing tire/vehicle relationships for best field performance. SAE Paper No. 801021.

Hausz, F.C., 1985. Traction characteristics of radial tractor tires, Proc. Int. Conf. Soil Dynamics, Auburn, AL, Vol. 4, 723-729.

Hayes, John C, and Ligon, J.T., 1977. Prediction of traction using soil physical properties. ASAE paper No. 77-1054, St. Joseph, MI.

Janosi, Z., 1961. An analysis of pneumatic tyre performance on deformable soils. First Int. Conf. on the Mechanics of Soil-Vehicle Systems. Torino-St. Vincent, Italy.

Janosi, Z. and Hanamoto, B., 1961. The analytical determination of drawbar pull as a function of slip for tracked vehicles in deformable soils. Proc. of First Inter. Conf. on Mechanics of Soil-Vehicle Systems, Torino-St. Vincent, Italy. pp. 707-736.

Karafiath, L.L., Nowatzki, E.A., 1978. Soil mechanics for off-road vehicle engineering, 1st edition, Trans Tech Publications, Germany.

Keller T., 2005. A Model for the Prediction of the Contact Area and the Distribution of Vertical Stress below Agricultural Tyres Readily Available Tyre Parameters. Biosystems Engeneering, 92(1): 85-96.

Kinght, S.J. and Green, A.J., 1962. Deflection of a moving tyre on firm to soft surfaces. Transactions of the ASAE, 5(2): 116-120.

Kliefoth, F., 1966. The determination of traction-coefficient curves synthetic farm tractor field tests. Journal of Terramechanics, 3(2): 71-84.

Komandi, G., 1976. The determination of the deflection, contact area dimensions and load carrying capacity for driven pneumatic tyres operarting on concrete pavement. Journal of Terramechanics, 13(1): 15-21.

Komandi, G., 1990. Establishment of soil-mechanical parameters which determine traction on deforming soil. Journal of Terramechanics, 27(2): 115-124.

Krick, G., 1969. Radial and shear stress distribution under rigid wheels and pneumatic tyres operating on yielding soils with consideration of tyre deformation. Journal of Terramechanics, 6(3): 73-98.

Lee, D.R. and Kim, K., 1997. Effect of inflation pressure on tractive performance of bias-ply tyres. Journal of Terramechanics, 34(3): 187-208.

Leviticus, L.I. and Reyes, J.F., 1983. Traction on concrete-I, dynamic ratio and traction quotient. ASAE paper No. 83-1558, St. Joseph, MI.

Li, Y., Whang, Z.H., Qui-Xi-Ding and Wang, Q.N., 1985. Distribution of stress beneath a drive pneumatic tyre and prediction of its tractive performance on sand. Proc. of Int. Conf. of Soil Dynamics. Auburn, AL, Vol. 4 : 738-755.

Lines, J.A. and Murphy, K., 1991. The stiffness of agricultural tractor tyres. Journal of Terramechanics, 28 (1): 49-64.

Lu, R. S., Liu, N., Li, Q, and Chen, X., 2010. Measurement of Vehicle Tire Footprint Pattern and Pressure Distribution Using Piezoresistive Force Sensor Mat and Image Analysis. Key Engineering Materials, Vol. 437: 467-471.

Lyasko, M.I., 1994. The determination of deflection and contact characteristics of a pneumatic tyre on a rigid surface. Journal of Terramechanics, 31(4): 239-246.

Maclaurin, E.B., 1997. The use of mobility numbers to predict the tractive performance of wheeled and tracked vehicles in soft cohesive soils. Proc. of the 7th European ISTVS Conf., Ferrara, Italy, 8-10 October 1997: 391-398.

Mayfield, W.D., 1983. An independent testing: radial tires increase tractor power efficiency. USDA Ext. Agric. Eng., 642300-4/83.

Mehta, C.R., Chandel, N.S., Senthilkumar, T. and Singh, K.K. 2014. Trends of agricultural mechanization in India. CSAM policy brief, June, 2014.

Melzer, K.J., 1971. Relative density and cone penetration resistance. Technical report 3-652, U.S. Army Corps of Engineers Waterways Experiment Station, Vicksburg, MS.

Mohsenimanesh, A., Ward, S.M. and Gilchrist, M.D., 2009. Stress analysis of a multi-laminated tractor tyre using non-linear 3D finite element analysis, Material and Design, 30(4): 1124-1132.

Mueller, J.P. and Treanor, R.R., 1985. Performance of a four wheel drive tractor equipped with radial tires. ASAE paper No. 85-1048, St. Joseph, MI.

Mulqueen, J., Stafford, J.V. and Tanner, D.W., 1977. Evaluation of penetrometers for measuring soil strength. Journal of Terramechanics, 14(3): 137-157.

Nowatzki, E.A. and Karafiath, L.L., 1972. Effect of cone angle on penetration resistance. Highway Research Record, 405: 51-59.

Painter, D.J., 1981. A simple deflection model for agricultural tyres. Journal of Agricultural Engineering Research, 26(1): 9-20.

Perumpral, J.V., 1987. Cone penetrometer applications- A review. Transactions of the ASAE, 30(4): 939-944.

Plackett, C.W., 1983. Hard surface contact area measurement for agricultural tyres, National Institute of Agricultural Engineering, Divisional Note DN 1200, England.

Plackett, C.W., 1984. The ground pressure of some agricultural tyres at low load with zero sinkage. Journal of Agricultural Engineering Research, 29(2): 159-166.

Porterfield, J.W. and Carpenter, T.G., 1986. Soil compaction: an index of potential compaction for agricultural tyres. Transactions of the ASAE, 29(4): 917-922.

Quraishi, M.Z. and Mouazen, A.M., 2013. A prototype sensor for the assessment of soil bulk density. Soil and Tillage Research, 134: 97-110.

Raper, T.R., Bailey, A.C., Burt, E.C., Way, T. R., and Liberati, P., 1995. The effects of reduced inflation pressure on soil-tyre interface stresses and soil strength. Journal of Terramechanics, 32(1): 43-51.

Rashidi, M., Sheikhi, M., Razavi, S., Niyazadeh, M. and Arkian, M., 2013. Prediction of radial-ply tire deflection based on section width, overall unloaded diameter, inflation pressure and vertical load. World Applied Sciences Journal, 21(12): 1804-1811.

Romano, E., Cutini, M. and Bisaglia, C., 2008. Agricultural tyre footprint shape correlation to treads penetration in different soils. International Conference. 15-17 September, Ragusa – Italy

Rosca, R., Carlescu, P. and Tenu, L., 2014. A semi-empirical traction prediction model for an agricultural tyre, based on the super ellipse shape of the contact surface. Soil and Tillage Research, 141: 10-18.

Rowland, D., 1972. Tracked vehicle ground pressure and its effect on soft ground performance. Proceedings of the 4th International ISTVS Conference, 24-28 April 1972, Stockholm-Kiruna, Sweden, 1: 353-384

Rummer, R. and Ashmore, C., 1985. Factors affecting the rolling resistance of rubber-tyred skidders. ASAE paper No. 85-1611, St. Joseph, MI.

Saarilahti, M., 2002. Soil Interaction Model Appendix Report No. 5. Quality of Life and Management of Living Resources Contract. No. QLK5-1999-00991.

Santos, F.L., Jesus, V.P.M. and Valente, D.S.M., 2012. Modeling of soil penetration resistance using statistical analyses and artificial neural networks. Acta Scientiarum. Agronomy, 34: 219-224.

Schwanghart, H., 1991. Measurement of contact area, contact pressure and compaction under tyres in soft soil. Journal of Terramechanics, 28(4): 309-318.

Sefa T. and Kazim C., 2004. Modeling the torque and power requirements of traction tyres of horticultural tractors using dimensional analysis. Mathematical and Computational Applications, 9(3): 427-434.

Sharma, A.K. and Pandey, K.P., 1996. The deflection and contact characteristics of some agricultural tyres with zero sinkage. Journal of Terramechanics, 33(6): 293-299.

Sharma, A.K. and Pandey, K.P., 1997. Modelling power requirement for traction tyres with zero sinkage. Journal of Terramechanics, 34(1): 13-21.

Sharma, A.K. and Pandey, K.P., 1998. Traction data analysis in reference to a unique zero condition. Journal of Terramechanics, 35(3): 179-188.

Sharma, A.K. and Pandey, K.P., 2001. Matching tyre size to weight, speed and power available for maximising pulling ability of agricultural tractors. Journal of Terramechanics, 38(2): 89-97.

Shmuleviuch, I., Ronai, D. and Wolf, D., 1996. A new field single wheel tester. Journal of Terramechanics, 33(3): 133-141.

Söhne, W., 1969. Agricultural engineering and Terramechanics. Journal of Terramechanics, 6(4): 9-30.

Sojka, R.E., Busscher, W.J. and Lehrsch, G.A., 2001. In situ strength, water content and water content relationships of a durinodic xeric haplocalcid soil. Soil Science, 166: 220-229.

Taghavifar, H. and Mardani, A., 2013. Potential of functional image processing technique for the measurements of contact area and contact pressure of a radial ply tire in a soil bin testing facility. Measurement, 46(10): 4038-4044.

Taghavifar, H. and Mardani, A., 2014. Fuzzy logic system based prediction effort: A case study on the effects of tire parameters on contact area and contact pressure. Applied Soft Computing, 14(C): 390-396.

Taylor, J.H., Vadenberg, G.E. and Reed, I.F., 1967. Effect of diameter on performance of powered tractor wheels. Transactions of the ASAE, 10(6): 838-842.

Taylor, J.H. and Burt, E.C., 1975. Track and tyre performance in agricultural soils. Transactions of the ASAE, 18(1): 3-6.

Taylor, J.H., Burt, E. C. and Bailey, A.C., 1976. Radial tire performance in firm and soft soils, Transaction of the ASAE, 19(6): 1062-1064.

Taylor, J.H., 1988. Effect of total load on subsurface soil compaction. Transactions of the ASAE, 23(3): 568-570.

Taylor, R.K., Bashford, L.L. and Schrock, M.D., 2000. Methods for measuring vertical tyre stiffness. Transactions of the ASAE, 43(6): 1415-1419.

Thaden, T.J., 1962. Operating characteristics of radial-ply tractor tires**.** Transactions of the ASAE, 5(2): 109-110.

Tiwari V.K., 2006. The deflection and contact area characteristics of bias-ply tyres, unpublished PhD thesis.

Tiwari V.K., Pandey K. P. and Sharma A. K., 2009. Development of a tyre traction test facility. Journal of Terramechanics, 46(6): 293-298.

Tiwari V.K., Pandey K. P. and Pranav P. K., 2010. A review on traction prediction equations. Journal of Terramechanics, 47(3): 191-199.

Turnage, G.W., 1970. Effects of velocity, size and shape of probes on penetration resistance of fine-grained soils. Technical report No. 3-652, U. S. Army Corps of Engineers Waterways Experiment Station, Vicksberg, MS.

Turnage, G.W., 1972. Tyre selection and performance prediction for off-road wheeled-vehicle operations. Proceedings of the 4th International ISTVS Conference, Stockholm-Kiruna, Sweden, April 24-28, 1972. I: 62- 82.

Turnage, G.W., 1972. Using dimensionless prediction terms to describe off-road wheel vehicle performance. ASAE paper No. 72-634, St. Joseph, MI.

Turnage, G.W., 1974. Resistance of coarse-grained soils to high-speed penetration. Technical report No.3-652, U. S. Army Corps of Engineers Waterways Experiment Station, Vicksberg, MS.

Upadhyaya, S.K., Kemble, L.L., Collins, N.E. and Williams, T.H., 1982. Cone index prediction equations for Delaware soils. ASAE paper No. 82-1542, St. Joseph, MI.

Upadhyaya**,** S.K., Mehkschau, J., Wulfsohn, D. and Glancey, J.L., 1986. Development of a unique mobile single wheel traction testing machine. Transactions of the ASAE, 29(5): 1243-1246.

Upadhyaya, S.K., Wulfsohn, D. and Jubbal, G., 1987. Traction prediction equations for radial-ply tyres. Journal of Terramechanics, 26(2): 149-175.

Upadhyaya, S.K. and Wulfsohn, D., 1988. Relationship between tyre deflection characteristics and soil tyre contact area. ASAE paper No. 88-1005, St. Joseph, MI.

Upadhyaya, S.K., Chancellor, W.J., Wulfsohn, D. and Glancey, J.L., 1988. Sources of variability in traction data. Journal of Terramechanics, 25(4): 249-272.

Upadhyaya, S.K., Wulfsohn, D. and Jubbal, G., 1989. Traction prediction equation for radial-ply tyres. Journal of Terramechanics, 26(2): 149-175.

Upadhyaya, S.K. and Wulfsohn, D., 1990. Review of traction prediction equations. ASAE paper No. 90-1573, St. Joseph, MI.

Upadhyaya, S.K. and Wulfsohn, D., 1990. Relationship between tyre deflection characteristics and 2-D tyre contact area. Transactions of the ASAE, 33(1): 25-30.

Upadhyaya, S.K., Wulfsohn, D., and Mehlschau, 1993. An instrumented device to obtain traction related parameters. Journal of Terramechanics, 30(1): 1-20.

Vanden Berg, G.E., Reed, I.F., and Cooper, A.W., 1961. Evaluating and improving performance of traction devices. Proceedings of the First International Conference on the Mechanics of Soil Vehicle Systems. Italy.

Vanden Berg, G.E. and Reed, I.F., 1962. Tractive performance of radial-ply and conventional tractor tires. Transactions of the ASAE, 5 (2): 126-129.

Vaz, C.M.P. and Hopmans, J.W., 2001. Simultaneous measurement of soil penetration resistance and water content with a combined penetrometer–TDR Moisture Probe. Alliance of Crop, Soil and Environmental Science Societies, 65, 4-12.

Vaz, C.M.P., Manieri, J.M., Maria, I.C. and Tuller, M., 2011. Modeling and correction of soil penetration resistance for varying soil water content. Geoderma, 166(1): 92-101.

Voorhees, M.L. and Walker, P.N., 1977. Tractionability as a function of soil moisture. Transactions of the ASAE, 20(5): 806-809.

Wells, L.G. and Treesuwan, O., 1977. The response of various soil strength indices to changing water content. ASAE paper No. 77-1055, St. Joseph, MI.

Wismer, R.D. and Luth, H.J., 1973. Off-road traction prediction for wheeled vehicles. Journal of Terramechanics, 10(2): 49-61.

Wong, J.Y., 1989. Terramechanics and off-road vehicles. Elsevier Science Publishers B.V. Sara Burgerhartstraat 25, P.O. Box 211, 1000 A.E. Amsterdam, the Netherlands.

Wong, J.Y., 2001. Theory of ground vehicles (3rd edition). John Wiley and Sons, Inc. Professional/ Trade Division, 605 Third Avenue, New York, N. Y. 10158-0012.

Worthington, W.H., 1962. A discussion of performance characteristics of radial-ply tractor tires, Transactions of the ASAE, 5(2): 113.

Wulfsohn, D., Upadhyaya, S.K. and Chancellor, W.J., 1988. Tractive characteristics of radial-ply and bias-ply tyres in a California soil. Journal of Terramechanics, 25(2): 111-134.

Wulfsohn, D. and Upadhyaya, S.K., 1992. Determination of dynamic three dimensional soil-tyre contact profile. Journal of Terramechanics, 29(4): 433-464.

Yong, R.N., Boonsinsuk, P. and Fattah, E.A., 1978. Analysis and prediction of tyre soil interaction and performance using finite elements. Journal of Terramechanics, 15(1): 43-63.

Yu Gu and Kushwaha, R.L., 1994. Dynamic load distribution and tractive performance of a model tractor. Journal of Terramechanics, 31(1): 21-39.

Zbigniew**,** B., 1990. A method for the determination of the contact area between a tyre and the ground. Journal of Terramechanics, 27(4): 263-282.

Ziani, F. and Biarez, 1990. Pressure sinkage relationship for tyres on very loose sand. Journal of Terramechanics, 27(3): 167-177.

Zombori, J., 1967. Drawbar pull tests of various traction devices on sandy soils. Journal of Terramechanics, 4(1): 9-17.

Zoz, F.M., 1972. Predicting tractor field performance. Transactions of the ASAE, 15(2): 249-255.

Zoz, F.M. and Grisso, R.D., 2003. Traction and tractor performance. ASAE Distinguished Lecture No. 27. Agricultural Equipment Technology Conference, 9-11 February 2003, Louisville, Kentucky U.S.A.

APPENDIX–A

SPECIFICATIONS OF INSTRUMENTS AND ACCESSORIES

Table A-1 Potentiometer for displacement transducer

i.	Type	: multi turn
ii.	Resistance	: 10 k-ohms
iii.	Tolrence	: $\pm$ 5 per cent
iv.	Operating temperature range	: - 40 to +125 ^{o}C
v.	Power	: 2 watts
vi.	Number of turns	: 10
vii.	Terminals	: solder lugs
viii.	Actuator type	: slotted shaft
ix.	Dimensions of the electronics module	: 102 * 32 * 13.5 mm
x.	Manufacturer	: BOURNS

Table A-2 Data acquisition system

i.	Model	: MGC Plus AB22A
ii.	Measurement	: D.C. voltage, A.C. voltage, resistance, frequency
iii.	No of channels	: 16
iv.	Maximum input	: 300 V
v.	DC Power supply	: 24 V
vi.	Measurement rate	: 1600 readings / sec
vii.	Manufacturer	: HBM Inc. 19 Bartlett Street, Marlborough MA 01752, U.S.A.

Table A-3 Torque transducer

i.	Type	: T20WN – VK20
ii.	Supply voltage range	: 14 to 30 V
iii.	Power consumption	: maximum 9 W
iv.	Torque	: -10 to +10V
v.	Load-carrying capacity	: 200 Nm
vi.	Accuracy class	: 0. 2
vii.	Maximum rotational speed	: up to 10 000 per min for torque measurement : up to 3000 per min for rotational speed measurement
viii.	Manufacturer	: Hottinger Baldwin Messtechnik Postfach 10 0151, D-64201 Darmstadt.

Table A-4 Strain gauge for ring transducer

i.	Type	: Foil
ii.	Resistance	: 120 ohms
iii.	Gauge factor	: 2.1
iv.	Grid size	: 5 * 2.5 mm
v.	Gauge material	: Constantan
vi.	Grid style	: Flat grid
vii.	Temperature limit	: -150 to 100 ^{o}C
viii.	Ring transducer capacity	: 10 kN
ix.	Manufacturer	: Hytech Micri Measurements Pvt. Ltd C-24, Shivalik, New Delhi - 110017, India.

Table A-5 Cone penetrometer

i.	Type	: Hydraulically operated proving ring
ii.	Capacity	: 1000 N
iii.	Cone angle	: 30 Deg
iv.	Cone base area	: 322 mm^2
v.	Manufacturer	: IIT Kharagpur

APPENDIX–B
SOIL PROPERTIES

Table B-1 Properties of experimental soil

Soil type	Lateritic sandy clay loam
Composition	
- Course sand	34.35 per cent
- Fine sand	22.31 per cent
- Silt	19.88 per cent
- Clay	23.05 per cent
- Organic matter	0.41 per cent
Upper plastic limit	17.0 4 per cent
Lower plastic limit	12.01 per cent
Particle density	2.66 gm/cc
Moisture content (w. b.)	7.02-7.12 per cent
Cohesion	0.12 kg/cm^2
Friction	22^0

Table B-2 Some observations of moisture content and bulk density of soil in the soil bin

Soil condition	Test No.	Moisture content, % (w.b.)	Bulk density, g/cc
Soft	1	7.57	1.32
	2	7.86	1.34
	3	7.76	1.37
	4	7.75	1.33
	5	7.55	1.40
	6	7.51	1.52
	7	7.47	1.51
	8	7.62	1.46
Average		**7.64**	**1.41**
Medium	1	7.67	1.72
	2	7.72	1.74
	3	7.97	1.80
	4	7.05	1.85
	5	7.38	1.90
	6	6.78	1.89
	7	6.92	1.90
	8	6.82	1.79
Average		**7.29**	**1.82**
Hard	1	7.62	2.11
	2	7.68	2.08
	3	7.26	2.21
	4	6.82	2.24
	5	6.88	2.08
	6	7.46	2.09
	7	7.50	2.20
	8	7.52	2.19
Average		**7.34**	**2.15**

Table B-3 A few observations of soil cone index in the soil bin

Soil condition	S. No.	Cone index values at different depths (mm), kPa							
		0	**25.4**	**50.8**	**76.2**	**101.6**	**127**	**152.4**	**Mean**
Soft	1	57.40	184.92	353.53	599.22	727.95	768.01	956.21	626.50
	2	57.26	179.73	329.39	574.73	739.35	852.96	976.44	641.61
	3	48.01	188.14	373.06	596.51	736.93	942.78	991.42	671.92
	4	46.32	189.02	370.58	592.35	755.73	964.35	1065.59	699.58
	5	47.74	204.45	359.25	560.11	704.09	930.20	1148.30	699.77
	6	43.38	208.85	376.85	518.29	698.68	821.82	1041.37	622.66
	7	57.57	217.42	339.83	506.84	758.12	827.16	1037.17	699.32
	8	52.13	215.04	347.30	504.49	750.00	919.85	1140.58	698.09
	Avg.	**51.23**	**198.45**	**356.22**	**556.57**	**733.86**	**878.39**	**1044.64**	**669.93**
Medium	1	115.11	386.77	631.40	999.56	1444.04	1745.74	1956.65	1273.70
	2	111.78	375.97	629.39	994.06	1378.99	1534.16	1792.11	1298.33
	3	106.79	391.16	660.60	988.07	1363.68	1574.05	1796.05	1295.95
	4	113.88	410.08	596.65	964.24	1361.68	1529.18	1791.04	1280.59
	5	106.52	395.42	637.18	872.70	1367.59	1643.97	1919.68	1222.07
	6	123.49	401.98	683.16	1139.48	1398.51	1477.63	1719.91	1248.21
	7	107.63	413.84	626.53	964.16	1300.21	1512.32	1862.53	1207.97
	8	110.40	375.16	648.03	1165.90	1392.44	1487.29	1663.50	1209.55
	Avg.	**111.95**	**393.80**	**639.12**	**1011.02**	**1375.89**	**1563.04**	**1812.68**	**1254.55**
Hard	1	207.01	736.02	1068.99	1777.53	2263.79	2369.47	2469.05	1790.89
	2	186.67	744.11	1013.94	1612.97	2218.09	2424.04	2547.41	1762.59
	3	193.52	664.91	1111.49	1803.28	2240.13	2292.73	2385.69	1754.96
	4	193.22	733.39	1085.08	1583.04	2213.28	2384.32	2539.94	1753.23
	5	180.85	727.59	1078.05	1727.24	2190.34	2369.50	2483.56	1772.76
	6	202.84	730.72	1063.15	1638.82	2141.01	2343.57	2454.76	1738.85
	7	207.78	676.09	1005.75	1742.45	2241.40	2334.56	2449.01	1769.71
	8	190.63	672.80	1129.28	1844.57	2161.06	2269.29	2401.60	1759.80
	Avg.	**195.32**	**710.70**	**1069.47**	**1716.24**	**2208.64**	**2348.43**	**2466.38**	**1762.85**

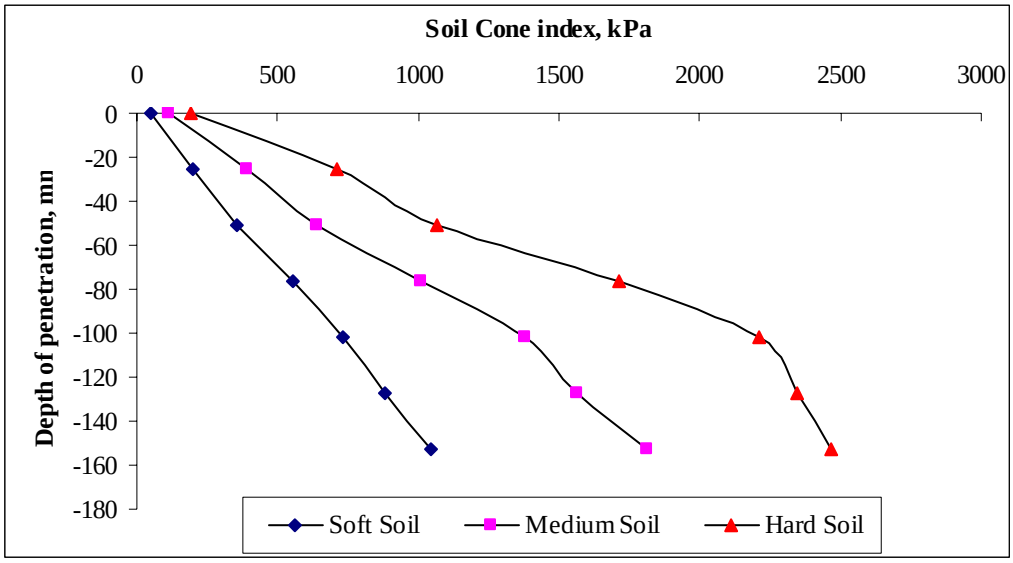

Fig. B-1 Typical plot of soil cone index versus depth at different soil compaction levels

APPENDIX-C
TEST OBSERVATIONS

Table C-1 Tyre deflection at different normal loads and inflation pressures for the test tyres

Tyre T_1 (12.4 R 28)							
Normal load, kN (kgf)	**Inflation pressure kPa (psi**	**Deflection, mm**					**Deflection ratio, %**
		Rep 1	**Rep 2**	**Rep 3**	**Rep 4**	**Mean**	
4.905 (500)	41.4 (6)	49.7	49.8	49.6	49.8	49.7	19.20
	68.9 (10)	39.2	39.3	39.4	39.2	39.3	15.17
	96.5 (14)	29.0	29.1	29.1	29.1	29.0	11.22
	124.1 (18)	26.8	26.8	26.8	26.9	26.8	10.36
	151.7 (22)	24.4	24.2	24.2	24.2	24.2	9.36
	179.3 (26)	21.1	21.2	21.3	21.5	21.3	8.23
	206.8 (30)	20.0	20.1	20.0	19.9	20.0	7.72
6.377 (650)	41.4 (6)	65.7	65.8	65.9	66.0	65.9	25.43
	68.9 (10)	51.7	51.8	51.9	51.9	51.8	20.02
	96.5 (14)	38.7	39.0	38.7	38.9	38.8	14.98
	124.1 (18)	34.6	34.7	34.7	34.8	34.7	13.39
	151.7 (22)	31.1	31.2	31.3	31.3	31.2	12.07
	179.3 (26)	30.0	29.7	29.8	30.0	29.9	11.53
	206.8 (30)	27.9	27.7	27.2	27.5	27.6	10.65
7.848 (800)	41.4 (6)	78.8	79.1	79.3	79.5	79.2	30.58
	68.9 (10)	60.4	60.7	60.5	60.9	60.6	23.41
	96.5 (14)	48.3	48.4	48.5	48.6	48.5	18.72
	124.1 (18)	42.7	42.9	43.0	42.7	42.8	16.54
	151.7 (22)	38.7	38.7	38.6	38.6	38.6	14.92
	179.3 (26)	36.4	36.5	36.5	36.5	36.5	14.08
	206.8 (30)	34.5	34.5	34.6	34.6	34.5	13.34
9.320 (950)	41.4 (6)	92.3	92.5	92.7	92.9	92.6	35.76
	68.9 (10)	71.0	71.3	71.3	71.5	71.3	27.52
	96.5 (14)	58.7	59.0	58.8	58.9	58.9	22.73
	124.1 (18)	50.4	50.5	50.7	50.5	50.5	19.51
	151.7 (22)	46.1	46.3	46.4	46.4	46.3	17.88
	179.3 (26)	42.6	42.9	43.0	43.0	42.9	16.55
	206.8 (30)	40.2	40.3	40.1	40.1	40.2	15.51
10.791 (1100)	41.4 (6)	104.8	104.9	104.9	104.7	104.8	40.48
	68.9 (10)	83.2	83.3	83.4	83.2	83.3	32.16
	96.5 (14)	66.6	66.9	67.0	67.2	66.9	25.85
	124.1 (18)	59.2	59.4	59.6	59.8	59.5	22.98
	151.7 (22)	53.2	53.3	53.3	53.3	53.3	20.57
	179.3 (26)	50.3	50.3	50.3	50.1	50.3	19.41
	206.8 (30)	47.5	47.4	47.5	47.6	47.5	18.34
12.263 (1250)	41.4 (6)	113.9	113.3	113.1	113.5	113.5	43.72
	68.9 (10)	92.4	92.6	92.9	92.8	92.7	35.78
	96.5 (14)	76.6	76.8	76.6	76.7	76.7	29.60
	124.1 (18)	67.3	67.6	67.7	67.5	67.5	26.08
	151.7 (22)	61.5	61.6	61.5	61.6	61.5	23.77
	179.3 (26)	55.6	55.5	55.7	55.8	55.7	21.49
	206.8 (30)	53.1	53.0	53.1	53.2	53.1	20.50

Contd…

Tyre T_2 (13.6 R 28)							
Normal load, kN (kgf)	**Inflation pressure kPa (psi)**	**Deflection, mm**					**Deflection ratio, %**
		Rep 1	**Rep 2**	**Rep 3**	**Rep 4**	**Mean**	
6.377 (650)	41.4 (6)	52.6	52.6	52.7	52.5	52.6	19.57
	68.9 (10)	41.4	41.6	41.4	41.6	41.5	15.44
	96.5 (14)	33.6	33.8	33.8	33.7	33.7	12.54
	124.1 (18)	29.7	29.6	29.5	29.7	29.6	11.03
	151.7 (22)	28.7	28.6	28.7	28.7	28.7	10.67
	179.3 (26)	27.3	27.1	27.1	27.2	27.2	10.11
	206.8 (30)	25.7	25.6	25.5	25.6	25.6	9.53
7.848 (800)	41.4 (6)	69.5	69.4	69.5	69.6	69.5	25.86
	68.9 (10)	53.7	53.7	53.8	53.9	53.8	20.01
	96.5 (14)	45.3	45.4	45.4	45.5	45.4	16.89
	124.1 (18)	40.7	40.9	40.9	41.0	40.9	15.21
	151.7 (22)	37.8	37.9	37.9	38.0	37.9	14.10
	179.3 (26)	35.7	35.7	35.5	35.8	35.7	13.27
	206.8 (30)	33.2	33.3	33.4	33.1	33.2	12.37
9.320 (950)	41.4 (6)	83.7	83.9	83.9	84.0	83.9	31.21
	68.9 (10)	63.1	63.3	63.2	63.1	63.2	23.50
	96.5 (14)	54.2	54.3	54.4	54.5	54.3	20.22
	124.1 (18)	47.3	47.4	47.4	47.4	47.4	17.63
	151.7 (22)	43.7	43.6	43.8	43.7	43.7	16.26
	179.3 (26)	40.3	40.2	40.3	40.4	40.3	15.00
	206.8 (30)	39.6	39.1	39.2	39.3	39.3	14.63
10.791 (1100)	41.4 (6)	97.0	97.0	97.3	97.2	97.1	36.15
	68.9 (10)	71.4	71.5	71.7	71.6	71.6	26.63
	96.5 (14)	60.1	60.1	60.3	60.3	60.2	22.41
	124.1 (18)	55.0	55.0	55.2	55.2	55.1	20.51
	151.7 (22)	48.0	48.1	48.1	48.2	48.1	17.89
	179.3 (26)	45.0	45.1	45.1	45.1	45.1	16.77
	206.8 (30)	41.1	41.1	41.2	41.1	41.1	15.30
12.263 (1250)	41.4 (6)	112.4	112.1	112.3	112.6	112.4	41.81
	68.9 (10)	79.6	79.9	79.7	79.7	79.7	29.67
	96.5 (14)	67.5	67.7	67.8	68.0	67.7	25.21
	124.1 (18)	59.7	59.8	60.0	59.7	59.8	22.26
	151.7 (22)	54.7	54.7	54.8	54.6	54.7	20.36
	179.3 (26)	50.7	50.8	50.7	50.8	50.8	18.89
	206.8 (30)	48.8	48.9	48.8	48.9	48.8	18.17
13.734 (1400)	41.4 (6)	126.3	126.4	126.6	126.8	126.5	47.09
	68.9 (10)	93.0	93.1	93.0	93.2	93.1	34.64
	96.5 (14)	76.3	76.2	76.2	76.2	76.2	28.36
	124.1 (18)	67.3	67.9	67.9	67.8	67.7	25.20
	151.7 (22)	60.9	61.2	61.0	61.1	61.0	22.71
	179.3 (26)	56.6	56.5	56.6	56.7	56.6	21.07
	206.8 (30)	53.0	52.9	53.0	53.1	53.0	19.73

Contd…

Tyre T_3 (14.9 R 28)							
Normal load, kN (kgf)	**Inflation pressure kPa (psi**	**Deflection, mm**					**Deflection ratio, %**
		Rep 1	**Rep 2**	**Rep 3**	**Rep 4**	**Mean**	
7.848 (800)	41.4 (6)	69.4	70.0	70.1	70.2	69.9	22.82
	68.9 (10)	53.7	53.9	53.7	53.9	53.8	17.56
	96.5 (14)	45.7	45.9	46.1	46.0	45.9	14.99
	124.1 (18)	41.3	41.5	41.8	41.8	41.6	13.58
	151.7 (22)	37.4	37.6	37.7	37.6	37.6	12.27
	179.3 (26)	34.9	34.5	34.5	34.6	34.6	11.30
	206.8 (30)	31.6	31.6	31.7	31.4	31.6	10.30
9.810 (1000)	41.4 (6)	84.5	84.7	84.7	84.8	84.7	27.63
	68.9 (10)	65.7	65.9	66.0	66.0	65.9	21.51
	96.5 (14)	54.7	54.7	54.9	54.8	54.8	17.87
	124.1 (18)	49.3	49.4	49.5	49.7	49.5	16.14
	151.7 (22)	45.0	45.1	45.0	45.3	45.1	14.72
	179.3 (26)	42.3	42.1	42.5	42.4	42.3	13.82
	206.8 (30)	40.4	40.4	40.5	40.5	40.5	13.20
11.772 (1200)	41.4 (6)	99.9	100.4	100.6	100.7	100.4	32.76
	68.9 (10)	76.0	76.1	76.3	76.2	76.1	24.85
	96.5 (14)	63.6	63.8	63.9	63.9	63.8	20.82
	124.1 (18)	57.1	57.1	57.2	57.2	57.1	18.65
	151.7 (22)	51.9	51.8	51.8	51.9	51.9	16.92
	179.3 (26)	47.6	47.5	47.7	47.7	47.6	15.55
	206.8 (30)	43.7	43.8	43.9	43.9	43.8	14.30
13.734 (1400)	41.4 (6)	113.9	114.2	114.5	113.7	114.1	37.23
	68.9 (10)	87.3	87.4	87.0	87.7	87.3	28.51
	96.5 (14)	72.8	72.7	72.6	73.0	72.8	23.75
	124.1 (18)	66.5	66.2	66.6	66.7	66.5	21.70
	151.7 (22)	59.9	59.9	60.0	60.2	60.0	19.58
	179.3 (26)	54.7	54.9	54.9	55.0	54.9	17.90
	206.8 (30)	52.0	52.1	51.8	52.1	52.0	16.97
15.696 (1600)	41.4 (6)	135.2	135.3	135.7	135.1	135.3	44.17
	68.9 (10)	103.6	103.7	103.9	103.3	103.6	33.82
	96.5 (14)	84.0	83.7	84.0	84.2	84.0	27.40
	124.1 (18)	73.9	73.7	74.0	74.1	73.9	24.12
	151.7 (22)	66.8	67.8	67.9	67.7	67.5	22.04
	179.3 (26)	60.9	60.9	61.0	61.0	61.0	19.89
	206.8 (30)	57.6	57.7	57.7	57.9	57.7	18.84
17.658 (1800)	41.4 (6)	145.5	145.7	145.9	145.2	145.6	47.51
	68.9 (10)	107.9	108.2	108.3	107.8	108.1	35.26
	96.5 (14)	91.7	91.6	91.7	91.8	91.7	29.92
	124.1 (18)	81.0	81.1	81.2	81.3	81.2	26.49
	151.7 (22)	73.4	73.4	73.6	73.8	73.5	24.00
	179.3 (26)	66.6	66.5	66.7	66.8	66.7	21.75
	206.8 (30)	63.9	64.1	64.3	64.2	64.1	20.92

Contd…

Tyre T_4 (16.9 R 28)							
Normal load, kN (kgf)	**Inflation pressure kPa (psi**	**Deflection, mm**					**Deflection ratio, %**
		Rep 1	**Rep 2**	**Rep 3**	**Rep 4**	**Mean**	
9.320 (950)	41.4 (6)	79.9	80.1	80.3	80.5	80.2	23.54
	68.9 (10)	59.4	59.5	59.9	59.9	59.7	17.53
	96.5 (14)	52.0	52.2	52.3	52.4	52.2	15.33
	124.1 (18)	47.0	47.2	47.0	47.2	47.1	13.84
	151.7 (22)	41.8	41.9	42.0	42.0	41.9	12.31
	179.3 (26)	39.5	39.6	39.8	39.4	39.6	11.62
	206.8 (30)	36.4	36.2	36.5	36.7	36.5	10.71
11.282 (1150)	41.4 (6)	94.5	94.9	95.2	95.7	95.1	27.93
	68.9 (10)	71.2	71.7	71.4	71.1	71.3	20.95
	96.5 (14)	61.3	61.8	61.4	61.0	61.4	18.02
	124.1 (18)	56.5	56.7	56.9	56.2	56.6	16.62
	151.7 (22)	50.0	50.2	49.9	50.3	50.1	14.71
	179.3 (26)	46.8	46.7	46.9	46.5	46.7	13.73
	206.8 (30)	43.7	43.9	44.1	44.1	43.9	12.91
13.244 (1350)	41.4 (6)	107.3	107.1	107.7	107.9	107.5	31.58
	68.9 (10)	80.4	80.7	80.4	80.7	80.6	23.66
	96.5 (14)	69.3	69.2	69.3	69.5	69.3	20.36
	124.1 (18)	62.2	62.2	62.5	62.5	62.3	18.31
	151.7 (22)	58.6	58.6	58.7	58.8	58.7	17.23
	179.3 (26)	53.7	53.8	53.3	53.8	53.6	15.75
	206.8 (30)	51.0	51.1	51.2	51.2	51.1	15.01
15.206 (1550)	41.4 (6)	122.3	122.4	122.7	122.9	122.6	36.00
	68.9 (10)	93.5	93.5	93.7	93.6	93.6	27.49
	96.5 (14)	78.1	78.1	79.2	78.4	78.4	23.03
	124.1 (18)	70.1	70.4	70.5	70.6	70.4	20.68
	151.7 (22)	64.0	64.3	64.8	64.5	64.4	18.91
	179.3 (26)	61.0	61.1	61.1	60.8	61.0	17.92
	206.8 (30)	56.7	56.5	56.7	56.8	56.7	16.65
17.168 (1750)	41.4 (6)	139.2	139.7	139.5	139.1	139.4	40.94
	68.9 (10)	106.9	106.5	107.2	107.2	107.0	31.41
	96.5 (14)	87.6	87.6	87.8	87.9	87.7	25.76
	124.1 (18)	78.7	78.5	78.7	78.8	78.7	23.11
	151.7 (22)	70.3	70.4	70.9	70.5	70.5	20.71
	179.3 (26)	66.9	67.0	67.0	67.2	67.0	19.68
	206.8 (30)	63.7	63.9	63.9	63.6	63.8	18.73
19.130 (1950)	41.4 (6)	155.4	155.7	155.9	156.2	155.8	45.76
	68.9 (10)	115.7	115.9	116.2	116.4	116.1	34.09
	96.5 (14)	95.1	95.2	95.2	95.4	95.2	27.97
	124.1 (18)	85.0	84.2	84.4	84.4	84.5	24.82
	151.7 (22)	77.5	77.5	77.7	77.7	77.6	22.79
	179.3 (26)	72.1	72.2	72.3	72.4	72.2	21.22
	206.8 (30)	68.2	68.3	68.5	68.7	68.4	20.10

Table C-2 ANOVA of the deflection model (Eqn. 5.1)

Model def.	Sum of Squares	DF	Mean Square	F
Regression	75387.3	9	8376.37	5016 *
Residual	218.3	131	1.67	
Total	75605.6	140		

* Significant at 5 per cent level, $R^2 = 0.98$

Table C-3 Tyre surface contact area and mean ground pressure at different normal loads and inflation pressures for test tyres

Tyre T_1 (12.4 R 28)						
Normal load, kN (kgf)	**Inflation pressure, kPa (psi)**	**Contact Area, cm^2**				**Mean ground pressure, kPa**
		Rep 1	**Rep 2**	**Rep 3**	**Mean Area, cm^2**	
4.905 (500)	41.4 (6)	796	798	803	799	61.43
	68.9 (10)	658	654	662	658	74.51
	96.5 (14)	523	525	529	526	93.28
	124.1 (18)	463	462	464	463	105.87
	151.7 (22)	405	400	397	401	122.23
	179.3 (26)	360	362	361	361	136.01
	206.8 (30)	335	332	331	333	147.46
6.377 (650)	41.4 (6)	984	975	978	979	65.13
	68.9 (10)	772	785	775	777	82.10
	96.5 (14)	623	627	632	627	101.68
	124.1 (18)	581	574	578	578	110.26
	151.7 (22)	513	517	524	518	123.01
	179.3 (26)	464	459	456	460	138.65
	206.8 (30)	418	414	425	419	152.30
7.848 (800)	41.4 (6)	1098	1101	1102	1100	71.32
	68.9 (10)	942	942	947	944	83.17
	96.5 (14)	803	800	806	803	97.71
	124.1 (18)	681	685	684	683	114.83
	151.7 (22)	603	606	607	605	129.67
	179.3 (26)	567	554	552	558	140.74
	206.8 (30)	502	506	512	507	154.94
9.320 (950)	41.4 (6)	1293	1293	1295	1294	72.01
	68.9 (10)	1072	1065	1063	1067	87.37
	96.5 (14)	908	908	909	908	102.63
	124.1 (18)	790	793	791	791	117.86
	151.7 (22)	705	703	712	707	131.87
	179.3 (26)	654	641	632	642	145.09
	206.8 (30)	571	573	574	573	162.70
10.791 (1100)	41.4 (6)	1461	1465	1453	1460	73.92
	68.9 (10)	1200	1207	1203	1203	89.70
	96.5 (14)	1012	1015	1018	1015	106.34
	124.1 (18)	862	858	857	859	125.59
	151.7 (22)	806	805	808	806	133.85
	179.3 (26)	731	732	728	730	147.75
	206.8 (30)	652	652	658	654	164.90
12.263 (1250)	41.4 (6)	1571	1572	1575	1573	77.96
	68.9 (10)	1295	1287	1287	1290	77.96
	96.5 (14)	1150	1154	1158	1154	106.22
	124.1 (18)	959	956	957	957	128.08
	151.7 (22)	901	902	895	899	136.43
	179.3 (26)	805	808	804	806	152.15
	206.8 (30)	728	721	733	727	168.59

Cont…

Tyre T_2 (13.6 R 28)						
Normal load, kN (kgf)	**Inflation pressure, kPa (psi)**	**Contact Area, cm^2**				**Mean ground pressure, kPa**
		Rep 1	**Rep 2**	**Rep 3**	**Mean Area, cm^2**	
6.377 (650)	41.4 (6)	997	995	1001	998	63.92
	68.9 (10)	794	796	804	798	79.89
	96.5 (14)	657	661	663	660	96.56
	124.1 (18)	578	580	584	581	109.75
	151.7 (22)	515	515	521	517	123.38
	179.3 (26)	467	479	486	477	133.74
	206.8 (30)	434	432	436	434	146.87
7.848 (800)	41.4 (6)	1188	1189	1188	1188	66.06
	68.9 (10)	933	933	941	936	83.86
	96.5 (14)	789	790	784	788	99.54
	124.1 (18)	693	692	703	696	112.81
	151.7 (22)	611	621	618	617	127.13
	179.3 (26)	574	573	570	572	137.32
	206.8 (30)	524	521	521	522	150.25
9.320 (950)	41.4 (6)	1400	1407	1413	1407	66.23
	68.9 (10)	1093	1091	1097	1094	85.16
	96.5 (14)	916	926	923	922	101.04
	124.1 (18)	800	804	795	800	116.51
	151.7 (22)	694	703	700	699	133.31
	179.3 (26)	654	653	660	656	142.04
	206.8 (30)	604	609	608	607	153.42
10.791 (1100)	41.4 (6)	1564	1563	1556	1561	69.12
	68.9 (10)	1234	1232	1233	1233	87.54
	96.5 (14)	1025	1027	1031	1028	104.99
	124.1 (18)	917	911	909	912	118.32
	151.7 (22)	813	814	817	815	132.41
	179.3 (26)	742	743	746	744	145.13
	206.8 (30)	684	685	686	685	157.51
12.263 (1250)	41.4 (6)	1723	1722	1727	1724	71.14
	68.9 (10)	1354	1350	1346	1350	90.80
	96.5 (14)	1143	1141	1147	1144	107.18
	124.1 (18)	1026	1031	1031	1029	119.18
	151.7 (22)	922	921	928	924	132.68
	179.3 (26)	840	841	839	840	146.07
	206.8 (30)	765	766	762	764	160.55
13.734 (1400)	41.4 (6)	1832	1832	1829	1831	75.01
	68.9 (10)	1445	1448	1440	1444	75.01
	96.5 (14)	1262	1265	1256	1261	108.92
	124.1 (18)	1108	1107	1108	1108	123.98
	151.7 (22)	1004	1004	1008	1005	136.63
	179.3 (26)	915	916	917	916	149.86
	206.8 (30)	843	849	849	847	162.19

Cont…

Tyre T_3 (14.9 R 28)						
Normal load, kN (kgf)	**Inflation pressure, kPa (psi)**	**Contact Area, cm^2**				**Mean ground pressure, kPa**
		Rep 1	**Rep 2**	**Rep 3**	**Mean Area, cm^2**	
7.848 (800)	41.4 (6)	1351	1354	1350	1352	58.03
	68.9 (10)	1099	1095	1096	1097	71.52
	96.5 (14)	865	857	858	860	91.27
	124.1 (18)	732	736	728	732	107.20
	151.7 (22)	658	646	646	650	120.68
	179.3 (26)	578	576	580	578	135.87
	206.8 (30)	542	545	541	543	144.48
9.810 (1000)	41.4 (6)	1614	1614	1617	1615	60.73
	68.9 (10)	1295	1293	1293	1294	75.83
	96.5 (14)	1042	1043	1036	1041	94.28
	124.1 (18)	882	883	879	881	111.35
	151.7 (22)	785	785	790	787	124.62
	179.3 (26)	712	715	704	710	138.15
	206.8 (30)	665	664	666	665	147.41
11.772 (1200)	41.4 (6)	1862	1861	1864	1862	63.21
	68.9 (10)	1493	1494	1492	1493	78.84
	96.5 (14)	1200	1202	1206	1203	97.85
	124.1 (18)	1071	1073	1065	1070	110.03
	151.7 (22)	921	920	924	922	127.71
	179.3 (26)	832	831	830	831	141.58
	206.8 (30)	779	778	776	778	151.32
13.734 (1400)	41.4 (6)	2000	2001	2005	2002	68.62
	68.9 (10)	1610	1612	1616	1613	85.12
	96.5 (14)	1387	1389	1385	1387	99.02
	124.1 (18)	1217	1219	1218	1218	112.79
	151.7 (22)	1049	1047	1046	1047	131.20
	179.3 (26)	965	965	960	963	142.67
	206.8 (30)	893	890	897	893	153.72
15.696 (1600)	41.4 (6)	2189	2190	2190	2190	71.68
	68.9 (10)	1744	1743	1746	1744	90.00
	96.5 (14)	1512	1511	1513	1512	103.82
	124.1 (18)	1306	1308	1310	1308	119.96
	151.7 (22)	1176	1184	1181	1180	133.00
	179.3 (26)	1076	1075	1078	1076	145.90
	206.8 (30)	991	990	997	993	158.10
17.658 (1800)	41.4 (6)	2368	2367	2366	2367	74.60
	68.9 (10)	1900	1900	1902	1901	74.60
	96.5 (14)	1630	1634	1624	1629	108.38
	124.1 (18)	1444	1443	1447	1445	122.24
	151.7 (22)	1287	1284	1290	1287	137.25
	179.3 (26)	1183	1185	1183	1184	149.15
	206.8 (30)	1092	1091	1099	1094	161.38

Cont…

Tyre T_4 (16.9 R 28)						
Normal load, kN (kgf)	**Inflation pressure, kPa (psi)**	**Contact Area, cm^2**				**Mean ground pressure, kPa**
		Rep 1	**Rep 2**	**Rep 3**	**Mean Area, cm^2**	
9.320 (950)	41.4 (6)	1692	1691	1693	1692	55.08
	68.9 (10)	1297	1299	1305	1300	71.70
	96.5 (14)	1096	1103	1099	1099	84.82
	124.1 (18)	927	926	931	928	100.40
	151.7 (22)	796	798	799	798	116.75
	179.3 (26)	714	717	726	719	129.67
	206.8 (30)	660	661	665	662	140.77
11.282 (1150)	41.4 (6)	1917	1919	1919	1918	58.82
	68.9 (10)	1531	1531	1536	1533	73.59
	96.5 (14)	1281	1282	1283	1282	87.98
	124.1 (18)	1091	1093	1097	1094	103.17
	151.7 (22)	948	947	948	948	118.96
	179.3 (26)	856	855	855	855	131.95
	206.8 (30)	784	788	790	787	143.29
13.244 (1350)	41.4 (6)	2190	2188	2188	2189	60.49
	68.9 (10)	1743	1747	1744	1745	75.89
	96.5 (14)	1477	1479	1480	1479	89.57
	124.1 (18)	1250	1251	1252	1251	105.84
	151.7 (22)	1079	1077	1078	1078	122.90
	179.3 (26)	985	993	988	989	133.94
	206.8 (30)	890	899	899	896	147.85
15.206 (1550)	41.4 (6)	2364	2370	2370	2368	64.21
	68.9 (10)	1916	1916	1918	1917	79.30
	96.5 (14)	1603	1605	1608	1605	94.74
	124.1 (18)	1386	1384	1380	1383	109.92
	151.7 (22)	1219	1229	1220	1223	124.37
	179.3 (26)	1109	1110	1113	1111	136.92
	206.8 (30)	1014	1016	1018	1016	149.72
17.168 (1750)	41.4 (6)	2603	2604	2597	2601	66.01
	68.9 (10)	2097	2098	2101	2099	81.79
	96.5 (14)	1769	1771	1773	1771	96.92
	124.1 (18)	1523	1525	1518	1522	112.83
	151.7 (22)	1354	1343	1348	1348	127.37
	179.3 (26)	1227	1228	1224	1226	140.07
	206.8 (30)	1136	1138	1134	1136	151.11
19.130 (1950)	41.4 (6)	2735	2732	2739	2735	69.95
	68.9 (10)	2257	2254	2259	2257	69.95
	96.5 (14)	1891	1892	1895	1893	101.05
	124.1 (18)	1650	1651	1652	1651	115.84
	151.7 (22)	1466	1472	1476	1471	130.00
	179.3 (26)	1332	1330	1326	1329	143.95
	206.8 (30)	1246	1245	1247	1246	153.51

Table C-4 Non-linear regression summary statistics for the model of rolling radius

Source	**DF**	**Sum of Squares**	**Mean Square**	**F**
Regression	2	14.68576	7.34288	1631751*
Residual	34	1.53E-05	4.5E-07	
Total	36	14.68578		
			95 % Confidence Interval	
Parameter	Estimate	Std. Error	Lower	Upper
C_1	2.265	0.0811	2.06	2.39
C_2	1.24	0.0782	1.08	1.39

Table C-5 Analysis of variance for effect of tyre width to diameter (b/d) ratio and deflection on torque ratio at zero condition

Source	**Sum of Squares**	**DF**	**Mean Square**	**F**
b/d	5.534E-05	3	1.845E-05	18.71 *
δ/h	6.545E-04	2	3.273E-04	331.92 *
(b/d)×(δ/h)	7.772E-06	6	1.287E-06	1.31
Error	9.268E-05	94	9.86E-07	

* Significant at 5 per cent level

Table C-6 Tractive performances of the test tyres

Tyre T_1 (12.4 R 28)										
Normal load N(kgf)	Tyre def. ratio	Cone index kPa	Rut depth cm	Drawbar Pull N	Slip %	Axle Torque N-m	Gross Traction Ratio	Motion Resis. Ratio	Tractive Eff. %	Mobility Number
W	**(δ/h)**	**CI**	**R_d**	**P**	**S**	**T**	**GTR**	**MRR**	**TE**	**B_n**
7358 (750)	0.20	696	3.4	222.7	1.2	404.8	0.090	0.060	33.1	44.44
		626	3.4	1025.1	4.1	922.6	0.206	0.067	64.8	40.03
		672	3.7	1930.4	8.5	1497.2	0.334	0.072	71.8	42.93
		700	3.9	2871.4	14.2	2085.4	0.466	0.076	71.9	44.71
		699	4.3	3100.7	18.7	2245.1	0.502	0.080	68.3	44.66
		623	4.2	3329.6	24.8	2443.2	0.546	0.093	62.4	39.78
		699	4.6	3598.0	27.7	2588.0	0.578	0.089	61.1	44.68
	0.24	605	3.3	353.6	1.6	490.7	0.110	0.062	42.8	42.54
		658	3.3	1242.0	4.9	1041.5	0.234	0.065	68.5	46.24
		669	3.7	2255.6	10.1	1682.9	0.379	0.072	72.8	47.05
		689	4.3	2655.8	13.0	1930.2	0.434	0.073	72.3	48.44
		679	3.4	3054.2	16.9	2181.8	0.491	0.076	70.3	47.74
		677	4.1	3490.5	21.7	2465.6	0.555	0.080	67.0	47.58
		666	4.5	3481.2	24.8	2492.9	0.561	0.088	63.5	46.81
	0.28	689	2.6	182.7	1.0	360.1	0.082	0.057	30.1	52.85
		699	3.0	1583.7	5.8	1233.7	0.279	0.064	72.5	53.59
		677	3.4	2214.4	8.7	1613.8	0.366	0.065	75.1	51.91
		656	3.6	2566.7	12.2	1858.0	0.421	0.072	72.8	50.27
		699	3.6	3153.2	15.8	2202.0	0.499	0.070	72.3	53.59
		661	4.2	3512.1	21.0	2447.0	0.554	0.077	68.0	50.64
		684	4.2	3651.5	23.5	2544.5	0.576	0.080	65.9	52.46

Cont…..

Tyre T_1 (12.4 R 28)										
W	**(δ/h)**	**CI**	**R_d**	**P**	**S**	**T**	**GTR**	**MRR**	**TE**	**B_n**
9320 (950)	0.20	600	4.1	238.4	1.4	550.1	0.097	0.071	26.0	30.28
		684	4.7	1662.0	5.3	1445.6	0.255	0.076	66.3	34.47
		699	4.2	2286.7	8.3	1833.4	0.323	0.078	69.7	35.26
		668	5.0	3249.1	14.3	2464.5	0.434	0.086	68.8	33.68
		654	4.8	3585.6	16.3	2705.4	0.477	0.092	67.6	32.97
		699	4.6	4017.0	20.0	2957.7	0.521	0.090	66.2	35.26
		693	4.8	4085.3	23.7	3030.6	0.534	0.096	62.6	34.95
	0.24	627	3.7	245.1	1.2	541.7	0.096	0.070	27.0	34.79
		682	4.0	1706.1	5.7	1443.5	0.256	0.073	67.4	37.82
		651	3.4	2263.7	8.0	1805.5	0.320	0.078	69.7	36.09
		652	4.5	3097.6	12.9	2324.3	0.413	0.080	70.2	36.18
		652	4.2	3815.8	20.1	2825.5	0.502	0.092	65.2	36.15
		690	4.7	4380.0	24.6	3185.2	0.565	0.095	62.7	38.28
		655	4.3	4365.8	27.2	3191.0	0.566	0.098	60.2	36.36
	0.28	639	3.1	324.3	1.2	549.4	0.089	0.064	35.0	38.66
		656	2.8	1517.1	4.5	1299.8	0.212	0.070	66.8	39.71
		681	3.7	2712.1	9.8	2052.5	0.305	0.076	71.4	41.24
		633	3.3	3502.4	14.9	2547.9	0.358	0.080	70.1	38.31
		683	3.6	3879.0	17.2	2790.4	0.373	0.083	69.0	41.34
		667	4.1	4054.0	19.2	2913.9	0.388	0.087	67.4	40.36
		660	4.5	4343.6	25.8	3108.9	0.423	0.090	62.1	39.95

Cont…..

Tyre T_1 (12.4 R 28)										
Normal load N(kgf)	Tyre def. ratio	Cone index kPa	Rut depth cm	Drawbar Pull N	Slip %	Axle Torque N-m	Gross Traction Ratio	Motion Resis. Ratio	Tractive Eff. %	Mobility Number
W	**(δ/h)**	**CI**	**R_d**	**P**	**S**	**T**	**GTR**	**MRR**	**TE**	**B_n**
11282 (1150)	0.20	605	5.0	241.7	1.5	710.4	0.104	0.082	20.4	25.23
		678	4.5	1805.4	5.5	1648.3	0.240	0.080	63.0	28.26
		647	5.5	2786.7	9.2	2301.5	0.335	0.088	66.8	26.96
		682	5.4	3628.2	13.6	2852.6	0.416	0.094	66.8	28.44
		699	4.6	4358.2	18.6	3322.3	0.484	0.098	65.0	29.12
		692	5.3	4222.7	19.5	3319.4	0.484	0.109	62.3	28.82
		699	5.1	4676.0	25.6	3577.2	0.521	0.107	59.2	29.12
	0.24	622	4.5	224.0	1.3	670.9	0.098	0.079	19.9	28.53
		699	4.6	674.3	2.2	888.7	0.130	0.071	44.8	32.05
		699	4.7	1879.2	5.3	1678.5	0.246	0.080	64.1	32.04
		699	4.7	3292.9	9.9	2564.1	0.376	0.084	69.9	32.04
		615	5.5	3295.3	12.3	2655.0	0.390	0.097	65.8	28.19
		620	4.9	4456.4	18.9	3395.0	0.498	0.103	64.3	28.42
		641	5.0	4712.9	26.2	3569.4	0.524	0.106	58.9	29.39
	0.28	647	3.6	260.2	1.2	644.7	0.095	0.072	23.9	32.34
		672	4.4	1756.2	4.5	1572.2	0.232	0.076	64.0	33.59
		634	4.0	2582.4	7.7	2106.4	0.311	0.082	68.0	31.72
		698	5.2	3591.8	12.5	2721.1	0.402	0.083	69.4	34.89
		675	4.2	4275.2	17.2	3170.3	0.468	0.089	67.1	33.72
		688	4.9	4600.0	20.0	3394.4	0.501	0.093	65.1	34.40
		699	4.5	5067.9	23.5	3684.6	0.544	0.095	63.2	34.95

Cont…..

Tyre T_1 (12.4 R 28)										
W	**(δ/h)**	**CI**	**R_d**	**P**	**S**	**T**	**GTR**	**MRR**	**TE**	**B_n**
7358 (750)	0.20	1274	1.7	282.8	1.2	405.0	0.090	0.052	42.0	81.37
		1298	2.6	1800.7	6.6	1343.8	0.300	0.055	76.1	82.93
		1201	3.0	2569.7	10.5	1831.6	0.409	0.060	76.4	76.73
		1201	3.1	3136.5	14.6	2182.4	0.488	0.061	74.7	76.73
		1222	3.2	3566.1	20.2	2481.6	0.554	0.070	69.7	78.07
		1204	3.7	3642.1	23.4	2538.1	0.567	0.072	66.9	76.92
		1205	3.9	3941.9	29.1	2727.2	0.609	0.073	62.3	76.98
	0.24	1208	1.8	461.0	1.6	505.3	0.114	0.051	54.2	84.89
		1203	1.7	1296.0	4.2	1010.8	0.227	0.051	74.2	84.54
		1290	2.2	2120.0	7.8	1527.2	0.344	0.055	77.4	90.66
		1209	2.8	3010.4	13.7	2085.5	0.469	0.060	75.3	84.96
		1298	3.3	3526.5	19.4	2416.6	0.544	0.064	71.1	91.22
		1258	3.6	3538.0	21.3	2424.5	0.545	0.065	69.4	88.42
		1278	4.1	3757.9	25.7	2581.0	0.581	0.070	65.3	89.84
	0.28	1290	1.0	422.0	1.3	459.8	0.104	0.047	54.3	98.86
		1274	2.0	1599.5	5.4	1189.8	0.270	0.052	76.3	97.69
		1297	2.3	1902.8	7.2	1381.1	0.313	0.054	76.8	99.46
		1241	2.4	2751.9	12.3	1901.4	0.431	0.057	76.2	95.14
		1208	3.2	3168.3	15.2	2161.2	0.490	0.059	74.6	92.61
		1200	3.6	3463.7	19.9	2357.8	0.534	0.063	70.6	92.03
		1282	3.7	3681.8	21.7	2497.5	0.566	0.0653	69.3	98.30

Cont…..

Tyre T_1 (12.4 R 28)										
Normal load N(kgf)	Tyre def. ratio	Cone index kPa	Rut depth cm	Drawbar Pull N	Slip %	Axle Torque N-m	Gross Traction Ratio	Motion Resis. Ratio	Tractive Eff. %	Mobility Number
W	**(δ/h)**	**CI**	**R_d**	**P**	**S**	**T**	**GTR**	**MRR**	**TE**	**B_n**
9320 (950)	0.20	1246	1.7	581.5	1.7	657.5	0.116	0.053	52.9	62.82
		1247	2.8	1625.7	4.8	1329.1	0.234	0.060	70.9	62.89
		1224	3.0	2938.8	9.0	2136.8	0.377	0.061	76.2	61.75
		1252	3.0	3625.0	12.8	2579.0	0.454	0.066	74.6	63.14
		1257	3.8	3950.7	16.3	2784.9	0.491	0.067	72.3	63.40
		1253	4.0	4435.3	20.2	3116.1	0.549	0.073	69.2	63.19
		1202	3.6	4654.8	24.1	3286.6	0.579	0.080	65.5	60.63
		1294	3.3	4770.8	28.5	3352.7	0.591	0.079	61.9	65.29
	0.24	1234	1.9	541.7	1.6	622.2	0.110	0.052	51.8	68.49
		1209	1.7	1742.4	4.6	1372.3	0.244	0.057	73.2	67.08
		1227	2.8	3046.1	9.5	2185.3	0.388	0.061	76.2	68.10
		1289	3.3	4043.4	15.9	2813.3	0.499	0.066	73.1	71.51
		1278	22.6	4543.3	20.4	3123.5	0.554	0.067	70.0	70.91
		1250	3.3	4612.4	23.9	3195.5	0.567	0.072	66.4	69.32
		1223	4.0	4798.8	25.9	3320.9	0.589	0.075	64.8	67.85
	0.28	1298	1.2	375.8	1.2	505.1	0.090	0.050	44.1	78.56
		1296	2.1	1559.4	4.3	1244.0	0.223	0.055	71.9	78.44
		1191	1.7	2915.7	9.5	2071.7	0.371	0.058	76.4	72.07
		1230	2.6	3379.8	11.0	2353.6	0.421	0.059	76.6	74.44
		1282	2.8	4079.1	15.6	2788.0	0.499	0.061	74.0	77.61
		1204	2.5	4699.1	22.5	3219.7	0.576	0.072	67.8	72.90
		1209	3.1	4719.0	26.2	3244.6	0.581	0.074	64.4	73.17

Cont…..

Tyre T_1 (12.4 R 28)										
W	**(δ/h)**	**CI**	**R_d**	**P**	**S**	**T**	**GTR**	**MRR**	**TE**	**B_n**
11282 (1150)	0.20	1264	2.7	793.6	2.0	893.4	0.130	0.060	52.9	52.65
		1201	3.7	2545.6	6.4	1983.5	0.289	0.063	73.1	50.04
		1246	3.5	3766.0	11.5	2756.2	0.402	0.068	73.5	51.91
		1255	4.2	4445.3	14.8	3205.8	0.467	0.073	71.9	52.29
		1270		4930.9	17.2	3502.6	0.510	0.073	70.9	52.90
		1295	3.9	5165.8	21.2	3668.6	0.535	0.077	67.5	53.94
		1299	4.3	5596.3	24.5	3973.8	0.579	0.083	64.7	54.12
	0.24	1239	2.8	541.6	1.4	706.5	0.104	0.056	45.7	56.78
		1298	2.9	1524.2	3.6	1321.5	0.194	0.059	67.2	59.49
		1217	3.6	3028.9	7.6	2268.3	0.333	0.064	74.5	55.79
		1263	3.1	4232.0	12.5	3025.3	0.444	0.069	73.9	57.90
		1284	4.2	4598.2	15.3	3260.1	0.478	0.071	72.2	58.87
		1233	4.3	5070.1	19.1	3563.8	0.523	0.073	69.5	56.50
		1256	3.6	5521.4	22.8	3879.5	0.569	0.080	66.4	57.56
	0.28	1292	3.4	440.9	1.2	612.9	0.090	0.051	42.7	64.60
		1238	2.3	1763.0	4.2	1436.3	0.212	0.056	70.6	61.89
		1290	3.7	3392.4	9.1	2444.5	0.361	0.060	75.7	64.50
		1225	4.7	4153.9	11.9	2931.4	0.433	0.065	75.0	61.24
		1242	3.5	4881.1	17.0	3391.5	0.501	0.068	71.8	62.09
		1298	3.5	5470.3	21.3	3787.9	0.559	0.074	68.3	64.90
		1296	4.0	5887.4	26.1	4055.0	0.599	0.077	64.4	64.82

Cont…..

Tyre T_1 (12.4 R 28)										
Normal load N(kgf)	Tyre def. ratio	Cone index kPa	Rut depth cm	Drawbar Pull N	Slip %	Axle Torque N-m	Gross Traction Ratio	Motion Resis. Ratio	Tractive Eff. %	Mobility Number
W	**(δ/h)**	**CI**	**R_d**	**P**	**S**	**T**	**GTR**	**MRR**	**TE**	**B_n**
7358 (750)	0.20	1791	1.2	475.9	1.6	493.9	0.110	0.046	57.7	114.41
		1763	1.3	1352.8	4.3	1041.8	0.233	0.049	75.6	112.61
		1799	2.2	2472.9	10.1	1742.9	0.389	0.053	77.6	114.93
		1753	2.4	3126.4	14.5	2146.5	0.480	0.055	75.8	112.01
		1773	2.4	3317.5	17.6	2286.0	0.511	0.060	72.8	113.26
		1739	1.7	3637.7	22.7	2491.6	0.557	0.062	68.6	111.09
		1799	2.5	4017.5	29.8	2733.5	0.611	0.065	62.8	114.93
	0.24	1770	1.1	646.9	1.9	591.4	0.133	0.045	64.8	124.37
		1743	1.1	1263.0	4.3	979.9	0.220	0.049	74.6	122.52
		1757	1.7	1685.3	6.2	1240.0	0.279	0.050	77.0	123.46
		1781	2.2	2725.2	11.2	1874.2	0.422	0.051	78.0	125.19
		1754	2.5	3240.5	16.4	2200.6	0.495	0.055	74.4	123.23
		1769	2.3	3508.0	20.4	2376.7	0.535	0.058	71.0	124.33
		1759	2.6	3866.2	24.1	2612.0	0.588	0.062	67.9	123.60
	0.28	1757	0.5	452.8	1.4	472.3	0.107	0.045	56.7	134.73
		1726	0.8	1191.4	4.0	929.7	0.211	0.049	73.8	132.29
		1730	1.1	2243.3	8.3	1566.5	0.355	0.050	78.8	132.60
		1737	1.6	3005.8	14.1	2034.5	0.461	0.052	76.2	133.19
		1750	1.7	3501.4	18.3	2350.7	0.532	0.057	73.0	134.17
		1756	2.9	3748.6	22.4	2513.3	0.569	0.060	69.5	134.62
		1731	2.7	3846.3	26.4	2573.2	0.583	0.060	66.0	132.72

Cont…..

Tyre T_1 (12.4 R 28)										
W	**(δ/h)**	**CI**	**R_d**	**P**	**S**	**T**	**GTR**	**MRR**	**TE**	**B_n**
9320 (950)	0.20	1770	1.4	386.6	1.2	512.9	0.090	0.049	45.4	89.27
		1767	2.0	1716.6	4.5	1347.0	0.237	0.053	74.1	89.14
		1768	2.1	3019.8	9.8	2159.9	0.381	0.057	76.8	89.19
		1735	3.0	3896.8	15.0	2724.8	0.480	0.062	74.1	87.51
		1730	3.6	4294.1	18.9	2968.5	0.523	0.062	71.4	87.23
		1757	3.2	4539.5	20.3	3118.4	0.550	0.062	70.6	88.60
		1715	3.7	4758.9	23.9	3287.9	0.579	0.069	67.1	86.50
	0.24	1739	1.5	634.2	1.7	652.9	0.116	0.048	57.7	96.46
		1743	1.2	1408.9	3.7	1127.7	0.200	0.049	72.8	96.68
		1748	2.2	2616.2	8.0	1881.9	0.334	0.053	77.4	96.96
		1776	2.5	3299.1	11.1	2312.8	0.411	0.057	76.6	98.52
		1723	2.3	4186.1	16.4	2868.4	0.509	0.060	73.8	95.61
		1754	3.1	4459.1	20.5	3046.3	0.541	0.062	70.3	97.33
		1780	3.4	5045.2	28.8	3432.2	0.609	0.068	63.3	98.75
	0.28	1732	1.2	592.2	1.6	616.2	0.110	0.047	56.7	104.83
		1737	1.5	1511.1	4.2	1184.9	0.212	0.050	73.3	105.13
		1762	1.4	3107.1	9.4	2166.0	0.388	0.054	77.9	106.65
		1766	2.4	3708.3	12.7	2539.0	0.454	0.057	76.5	106.91
		1758	2.0	4211.1	17.6	2853.6	0.511	0.059	72.9	106.41
		1718	2.6	4478.4	20.4	3020.8	0.541	0.060	70.7	103.99
		1758	3.2	4942.4	28.3	3329.9	0.596	0.066	63.8	106.42

Cont…..

Tyre T_1 (12.4 R 28)										
Normal load N(kgf)	Tyre def. ratio	Cone index kPa	Rut depth cm	Drawbar Pull N	Slip %	Axle Torque N-m	Gross Traction Ratio	Motion Resis. Ratio	Tractive Eff. %	Mobility Number
W	**(δ/h)**	**CI**	**R_d**	**P**	**S**	**T**	**GTR**	**MRR**	**TE**	**B_n**
11282 (1150)	0.20	1767	2.3	822.7	1.8	851.8	0.124	0.051	57.7	73.63
		1772	2.7	1702.0	3.9	1415.3	0.206	0.055	70.3	73.81
		1728	3.1	3279.0	8.5	2405.0	0.351	0.060	75.8	72.00
		1795	3.7	4493.3	13.9	3160.0	0.461	0.062	74.4	74.78
		1744	3.2	4889.3	15.5	3422.7	0.499	0.065	73.4	72.67
		1741	3.8	5364.0	21.5	3742.6	0.545	0.070	68.5	72.55
		1792	3.0	5575.8	24.0	3893.0	0.567	0.073	66.2	74.65
	0.24	1756	1.9	693.9	1.6	767.4	0.113	0.051	53.7	80.49
		1727	2.5	1688.3	3.9	1383.3	0.203	0.053	70.9	79.17
		1795	2.0	3082.3	7.9	2254.7	0.331	0.058	76.1	82.28
		1760	2.6	4566.0	13.5	3175.0	0.466	0.061	75.2	80.69
		1730	3.2	4909.9	15.9	3404.9	0.500	0.064	73.2	79.30
		1728	3.2	5263.6	20.0	3641.4	0.534	0.068	69.8	79.19
		1703	3.4	5815.3	24.1	4004.6	0.588	0.072	66.6	78.06
	0.28	1727	1.4	829.2	1.8	829.9	0.123	0.049	58.9	86.36
		1759	2.2	2363.6	5.5	1780.2	0.263	0.053	75.3	87.96
		1749	2.3	3759.8	9.5	2627.6	0.388	0.055	77.8	87.46
		1746	2.3	4303.1	12.0	2975.6	0.439	0.058	76.4	87.28
		1752	2.7	4696.9	15.1	3240.8	0.478	0.062	73.9	87.62
		1748	3.7	5160.6	18.6	3527.9	0.521	0.063	71.5	87.38
		1784	3.5	5534.4	22.2	3767.6	0.556	0.066	68.6	89.19
		1781	3.7	6090.7	29.8	4132.9	0.610	0.070	62.1	89.06

Cont…..

Tyre T_1 (13.6 R 28)										
W	**(δ/h)**	**CI**	**R_d**	**P**	**S**	**T**	**GTR**	**MRR**	**TE**	**B_n**
9320 (950)	0.20	634	2.6	255.1	1.2	547.7	0.095	0.068	28.4	34.74
		696	2.7	1217.0	4.0	1153.1	0.200	0.070	62.5	38.13
		600	3.8	1323.0	4.4	1256.1	0.218	0.076	62.2	32.87
		602	4.1	1979.7	6.9	1663.2	0.289	0.077	68.4	32.98
		676	5.1	2644.7	9.2	2067.1	0.359	0.076	71.7	37.04
		609	4.5	3239.4	14.4	2497.7	0.434	0.087	68.5	33.37
		671	3.9	3926.5	18.5	2928.1	0.509	0.088	67.4	36.76
		602	4.1	3883.4	22.2	2947.3	0.512	0.096	63.2	32.98
	0.24	670	3.8	307.2	1.2	551.0	0.096	0.063	33.8	40.38
		639	4.1	1622.1	5.3	1401.4	0.245	0.071	67.2	38.51
		606	3.9	2481.9	8.6	1966.4	0.344	0.078	70.8	36.52
		682	5.1	3627.1	14.7	2682.3	0.469	0.080	70.8	41.10
		602	5.5	3669.1	17.0	2735.3	0.478	0.085	68.3	36.28
		664	5.5	3960.3	19.3	2919.0	0.511	0.086	67.2	40.02
		655	5.6	4395.0	27.5	3243.0	0.567	0.096	60.3	39.48
	0.28	646	3.7	193.8	1.0	466.0	0.082	0.061	25.1	42.47
		610	2.5	975.5	3.1	967.4	0.170	0.066	59.6	40.11
		693	3.7	2174.0	6.4	1697.9	0.299	0.066	73.0	45.56
		667	4.4	3051.5	10.3	2264.1	0.399	0.071	73.7	43.85
		636	4.4	3391.2	13.6	2502.6	0.441	0.077	71.3	41.82
		671	4.2	4096.7	19.0	2963.3	0.522	0.082	68.3	44.12
		665	4.4	4242.8	22.6	3071.9	0.541	0.086	65.2	43.72

Cont…..

Tyre T_1 (13.6 R 28)										
Normal load N(kgf)	Tyre def. ratio	Cone index kPa	Rut depth cm	Drawbar Pull N	Slip %	Axle Torque N-m	Gross Traction Ratio	Motion Resis. Ratio	Tractive Eff. %	Mobility Number
W	**(δ/h)**	**CI**	**R_d**	**P**	**S**	**T**	**GTR**	**MRR**	**TE**	**B_n**
11282 (1150)	0.20	698	4.1	229.9	1.3	644.7	0.093	0.072	21.7	31.59
		686	4.2	1412.1	4.2	1398.5	0.201	0.076	59.7	31.05
		630	4.5	2426.2	7.8	2093.0	0.301	0.085	66.0	28.51
		636	5.4	3466.9	12.7	2788.7	0.400	0.093	67.0	28.79
		692	4.7	4254.0	16.3	3268.3	0.469	0.092	67.2	31.32
		650	5.0	4316.5	19.0	3346.3	0.481	0.098	64.5	29.42
		658	5.2	4709.0	24.8	3642.6	0.523	0.106	60.0	29.78
	0.24	620	3.6	318.8	1.3	688.7	0.100	0.071	28.0	30.87
		668	4.5	1382.8	3.6	1348.4	0.195	0.072	60.6	33.26
		689	4.2	3128.2	9.8	2465.1	0.356	0.079	70.2	34.30
		670	4.3	3698.2	13.1	2853.0	0.412	0.085	69.1	33.36
		610	4.4	4093.7	16.5	3156.9	0.456	0.093	66.4	30.37
		633	4.6	4541.8	18.9	3453.5	0.499	0.097	65.5	31.52
		634	4.8	5082.5	27.7	3869.3	0.559	0.109	58.2	31.57
	0.28	679	2.5	277.7	1.2	621.1	0.090	0.066	26.9	36.88
		683	2.9	1409.5	3.5	1333.6	0.194	0.069	62.2	37.10
		608	3.7	2410.9	7.0	1998.1	0.290	0.077	68.4	33.02
		652	4.2	3388.7	10.7	2602.6	0.378	0.078	70.9	35.41
		699	4.2	4269.5	15.5	3169.4	0.461	0.082	69.4	37.97
		663	4.8	4611.5	19.3	3444.5	0.501	0.092	65.9	36.01
		680	4.8	5279.3	25.5	3890.6	0.566	0.098	61.7	36.93

Cont…..

Tyre T_1 (13.6 R 28)										
W	**(δ/h)**	**CI**	**R_d**	**P**	**S**	**T**	**GTR**	**MRR**	**TE**	**B_n**
13244 (1350)	0.20	639	4.2	255.3	1.50	812.4	0.099	0.080	19.1	24.64
		642	4.4	1517.1	4.37	1634.6	0.200	0.086	54.7	24.75
		651	4.2	2753.2	7.50	2440.9	0.299	0.091	64.3	25.10
		641	4.8	3831.3	12.22	3177.5	0.389	0.100	65.3	24.71
		699	5.2	4549.3	17.08	3638.6	0.446	0.102	63.9	26.95
		648	4.7	4760.2	19.93	3816.4	0.467	0.108	61.6	24.98
		600	5.4	5005.2	26.42	4085.6	0.500	0.122	55.6	23.13
	0.24	661	3.8	195.5	1.3	734.7	0.090	0.076	16.1	28.03
		698	4.2	1580.7	3.8	1610.3	0.198	0.079	57.9	29.60
		637	4.8	2742.7	7.6	2379.7	0.293	0.086	65.3	27.02
		662	4.8	4210.4	12.7	3333.6	0.410	0.092	67.7	28.08
		602	5.2	4411.4	16.6	3530.6	0.434	0.101	64.0	25.53
		666	4.4	5238.7	19.8	4053.8	0.499	0.103	63.6	28.25
		686	5.2	5512.2	25.3	4251.1	0.523	0.107	59.4	29.09
	0.28	642	3.6	207.3	1.2	719.1	0.089	0.073	17.4	29.70
		687	2.8	1539.4	3.9	1556.4	0.193	0.077	57.9	31.79
		670	4.0	2903.4	7.3	2432.9	0.301	0.082	67.5	31.00
		673	4.7	3712.3	9.8	2952.8	0.366	0.085	69.2	31.14
		616	4.5	4378.4	14.5	3415.8	0.423	0.092	66.8	28.50
		649	4.7	5155.4	18.2	3940.1	0.488	0.099	65.3	30.03
		609	4.2	5587.0	25.9	4303.5	0.533	0.111	58.6	28.18

Cont…..

Tyre T_1 (13.6 R 28)										
Normal load N(kgf)	Tyre def. ratio	Cone index kPa	Rut depth cm	Drawbar Pull N	Slip %	Axle Torque N-m	Gross Traction Ratio	Motion Resis. Ratio	Tractive Eff. %	Mobility Number
W	**(δ/h)**	**CI**	**R_d**	**P**	**S**	**T**	**GTR**	**MRR**	**TE**	**B_n**
9320 (950)	0.20	1209	3.0	440.5	1.2	572.8	0.100	0.052	46.9	66.24
		1203	3.4	1348.4	4.0	1157.6	0.201	0.057	69.0	65.91
		1292	2.8	2267.7	6.2	1719.6	0.299	0.056	76.3	70.79
		1290	3.2	3666.6	12.9	2615.1	0.455	0.061	75.4	70.68
		1256	3.7	3958.4	15.9	2820.0	0.490	0.066	72.9	68.82
		1293	3.2	4304.3	19.6	3052.3	0.531	0.069	69.9	70.84
		1276	3.9	4864.2	27.8	3448.2	0.600	0.078	62.8	69.91
	0.24	1259	1.5	443.1	1.2	569.9	0.100	0.052	47.1	75.88
		1280	2.5	1660.0	4.6	1318.0	0.231	0.052	73.7	77.14
		1222	2.2	2864.8	8.8	2099.7	0.367	0.060	76.3	73.65
		1220	2.7	3771.5	14.2	2670.1	0.467	0.062	74.3	73.53
		1210	4.0	4210.0	17.4	2969.4	0.519	0.068	71.8	72.93
		1214	4.2	4726.0	23.8	3312.0	0.579	0.072	66.7	73.17
		1280	3.7	4733.6	25.0	3305.0	0.578	0.070	65.9	77.14
	0.28	1269	1.8	557.6	1.5	629.6	0.111	0.051	53.2	83.43
		1287	2.5	1572.3	4.1	1260.4	0.222	0.053	72.9	84.62
		1284	2.3	1888.6	5.3	1448.0	0.255	0.052	75.3	84.42
		1288	2.1	2367.7	6.7	1757.6	0.309	0.055	76.6	84.68
		1292	3.8	3782.1	13.5	2645.4	0.466	0.060	75.4	84.95
		1243	3.9	4085.2	16.8	2843.4	0.501	0.062	72.8	81.72
		1288	4.0	4996.2	29.2	3460.7	0.609	0.073	62.3	84.68

Cont…..

Tyre T_1 (13.6 R 28)										
W	**(δ/h)**	**CI**	**R_d**	**P**	**S**	**T**	**GTR**	**MRR**	**TE**	**B_n**
11282 (1150)	0.20	1273	2.7	588.5	1.5	764.6	0.110	0.058	46.8	57.62
		1284	3.5	2111.8	4.8	1721.0	0.247	0.060	72.1	58.12
		1295	3.1	2988.6	7.3	2277.7	0.327	0.062	75.1	58.61
		1211	3.3	3747.5	10.0	2777.0	0.399	0.067	74.9	54.81
		1230	3.5	4254.6	13.9	3106.4	0.446	0.069	72.8	55.67
		1202	3.5	4925.6	17.5	3558.5	0.511	0.074	70.5	54.40
		1231	4.5	5719.3	25.9	4102.6	0.589	0.082	63.8	55.72
	0.24	1224	3.0	216.6	0.8	516.5	0.075	0.055	25.5	60.94
		1232	3.0	1828.0	4.4	1527.9	0.221	0.059	70.1	61.34
		1244	3.5	3364.9	8.6	2486.9	0.359	0.061	75.9	61.94
		1271	3.8	4037.8	11.1	2914.7	0.421	0.063	75.5	63.28
		1235	3.8	4391.6	13.1	3147.3	0.455	0.066	74.4	61.49
		1282	3.7	5312.4	21.4	3772.2	0.545	0.074	67.9	63.83
		1246	4.6	5628.9	27.8	4005.6	0.579	0.080	62.2	62.04
	0.28	1269	2.7	396.3	0.9	594.1	0.086	0.051	40.3	68.92
		1231	3.7	1501.6	3.3	1304.3	0.190	0.057	67.9	66.86
		1206	3.3	2510.2	6.0	1928.1	0.280	0.058	74.6	65.50
		1249	4.2	3179.8	8.3	2344.2	0.341	0.059	75.9	67.84
		1295	4.7	4528.8	12.9	3196.5	0.465	0.063	75.2	70.34
		1258	4.1	4832.3	16.4	3404.8	0.495	0.067	72.3	68.33
		1240	3.5	5333.0	19.7	3739.9	0.544	0.071	69.8	67.35
		1220	3.6	5556.7	22.0	3891.8	0.566	0.073	67.9	66.26
		1253	3.9	5846.0	28.9	4099.5	0.596	0.078	61.8	68.06

Cont…..

Tyre T_1 (13.6 R 28)										
Normal load N(kgf)	Tyre def. ratio	Cone index kPa	Rut depth cm	Drawbar Pull N	Slip %	Axle Torque N-m	Gross Traction Ratio	Motion Resis. Ratio	Tractive Eff. %	Mobility Number
W	**(δ/h)**	**CI**	**R_d**	**P**	**S**	**T**	**GTR**	**MRR**	**TE**	**B_n**
13244 (1350)	0.20	1231	3.7	193.6	0.8	609.1	0.075	0.060	19.4	47.46
		1257	3.1	1540.5	3.1	1449.3	0.177	0.061	63.5	48.46
		1222	4.6	3023.5	6.7	2408.3	0.295	0.067	72.2	47.12
		1219	4.0	4341.2	10.2	3256.7	0.399	0.071	73.8	47.00
		1272	4.4	4778.4	12.3	3535.2	0.433	0.072	73.1	49.04
		1210	4.2	5739.3	17.3	4166.1	0.510	0.077	70.3	46.65
		1266	4.6	5966.6	20.3	4332.2	0.531	0.080	67.7	48.81
		1231	4.6	6418.6	23.7	4647.4	0.569	0.084	65.0	47.46
	0.24	1292	3.0	491.4	1.2	760.9	0.094	0.057	39.2	54.80
		1257	2.8	1724.2	3.5	1537.5	0.189	0.059	66.4	53.31
		1235	2.8	3142.9	6.5	2435.4	0.300	0.062	74.0	52.38
		1210	3.3	4304.2	10.6	3192.7	0.393	0.068	74.0	51.32
		1251	3.8	5524.8	16.4	3986.5	0.490	0.073	71.1	53.06
		1255	4.3	6459.2	22.5	4597.4	0.566	0.078	66.9	53.23
		1265	4.5	6444.7	25.7	4639.8	0.571	0.084	63.3	53.65
	0.28	1293	2.7	325.0	0.9	638.0	0.079	0.054	30.8	59.82
		1298	3.1	1767.8	3.4	1527.8	0.189	0.056	68.1	60.05
		1246	3.8	3461.0	7.1	2596.1	0.322	0.060	75.5	57.65
		1287	4.4	4880.9	12.7	3506.0	0.434	0.066	74.1	59.55
		1273	3.6	5572.5	16.4	3963.1	0.491	0.070	71.7	58.90
		1259	4.2	6342.3	20.6	4476.3	0.554	0.075	68.6	58.25
		1277	4.4	6612.1	24.0	4675.4	0.579	0.080	65.6	59.08

Cont…..

Tyre T_1 (13.6 R 28)										
W	**(δ/h)**	**CI**	**R_d**	**P**	**S**	**T**	**GTR**	**MRR**	**TE**	**B_n**
9320 (950)	0.20	1763	1.5	379.4	1.0	503.2	0.087	0.047	46.1	96.59
		1742	1.4	1034.4	2.6	919.7	0.160	0.049	67.6	95.44
		1756	2.4	2219.1	6.3	1669.7	0.290	0.052	76.8	96.21
		1771	3.3	3546.5	12.0	2508.4	0.436	0.056	76.8	97.03
		1714	3.2	3866.4	14.7	2730.4	0.475	0.060	74.6	93.91
		1710	3.4	4182.5	17.8	2938.4	0.511	0.062	72.2	93.69
		1730	3.8	5133.8	30.6	3571.2	0.621	0.070	61.6	94.79
	0.24	1789	1.1	247.2	0.7	418.4	0.073	0.047	36.0	107.82
		1758	1.5	1131.2	2.9	973.2	0.170	0.049	69.2	105.95
		1740	1.8	2862.0	8.4	2048.9	0.358	0.051	78.5	104.87
		1723	1.4	3434.8	11.9	2418.9	0.423	0.055	76.7	103.84
		1789	3.0	4127.4	16.8	2862.7	0.501	0.058	73.6	107.82
		1722	4.2	4766.5	24.6	3287.0	0.575	0.063	67.1	103.78
	0.28	1725	1.0	261.6	0.8	424.1	0.075	0.047	37.3	113.42
		1735	1.3	956.3	2.5	853.8	0.150	0.048	66.6	114.07
		1796	2.6	2198.9	6.2	1623.7	0.286	0.050	77.4	118.08
		1745	3.8	3348.5	10.9	2346.1	0.413	0.054	77.5	114.73
		1778	3.4	4140.5	16.5	2841.7	0.500	0.056	74.1	116.90
		1748	4.3	4816.8	23.9	3290.9	0.579	0.063	67.9	114.93
		1771	4.3	4992.0	28.7	3408.5	0.600	0.065	63.7	116.44

Cont…..

Tyre T_1 (13.6 R 28)										
Normal load N(kgf)	Tyre def. ratio	Cone index kPa	Rut depth cm	Drawbar Pull N	Slip %	Axle Torque N-m	Gross Traction Ratio	Motion Resis. Ratio	Tractive Eff. %	Mobility Number
W	**(δ/h)**	**CI**	**R_d**	**P**	**S**	**T**	**GTR**	**MRR**	**TE**	**B_n**
11282 (1150)	0.20	1724	3.9	227.1	0.7	488.7	0.070	0.050	28.5	78.03
		1717	2.6	1108.2	2.3	1033.6	0.148	0.050	64.7	77.71
		1702	2.9	3475.4	8.6	2547.5	0.366	0.058	76.9	77.03
		1716	2.9	3840.4	10.6	2787.8	0.400	0.060	76.0	77.67
		1729	3.0	4386.9	13.6	3140.7	0.451	0.062	74.5	78.26
		1762	3.4	5509.8	22.3	3873.6	0.556	0.068	68.2	79.75
		1746	3.8	5955.0	26.7	4172.0	0.599	0.071	64.6	79.03
	0.24	1702	1.1	351.7	0.9	554.3	0.080	0.049	38.6	84.74
		1780	2.3	1802.5	3.9	1459.2	0.211	0.051	72.8	88.62
		1736	2.7	3437.7	8.8	2492.8	0.360	0.056	77.1	86.43
		1745	3.4	4589.3	13.4	3222.3	0.466	0.059	75.6	86.88
		1743	3.5	5168.4	17.4	3593.5	0.519	0.061	72.9	86.78
		1740	3.4	5452.8	22.0	3812.0	0.551	0.068	68.5	86.63
		1788	3.8	5952.3	30.3	4157.2	0.601	0.073	61.2	89.02
	0.28	1740	2.0	572.6	1.2	678.2	0.099	0.048	50.9	94.51
		1731	2.3	1798.9	4.0	1448.0	0.211	0.051	72.7	94.02
		1703	2.3	3399.6	8.6	2440.3	0.355	0.053	77.6	92.50
		1719	2.4	4643.1	13.8	3228.7	0.469	0.058	75.6	93.37
		1710	2.8	5271.9	18.3	3642.0	0.529	0.062	72.1	92.88
		1796	3.5	5569.4	20.8	3817.2	0.555	0.061	70.5	97.55
		1750	3.3	5978.2	27.9	4125.6	0.600	0.070	63.7	95.05

Cont…..

Tyre T_1 (13.6 R 28)										
W	**(δ/h)**	**CI**	**R_d**	**P**	**S**	**T**	**GTR**	**MRR**	**TE**	**B_n**
13244 (1350)	0.20	1764	1.9	376.1	0.8	650.5	0.080	0.051	35.4	68.01
		1783	2.4	2098.2	4.2	1755.5	0.215	0.057	70.6	68.75
		1711	2.8	3966.9	8.6	2936.2	0.360	0.060	76.1	65.97
		1727	3.6	4752.4	12.1	3455.6	0.423	0.064	74.6	66.59
		1794	3.5	5748.1	16.1	4080.1	0.500	0.066	72.9	69.17
		1794	3.3	6340.3	22.1	4498.6	0.551	0.072	67.7	69.17
		1752	3.5	6928.3	26.4	4889.4	0.599	0.076	64.3	67.55
	0.24	1786	1.4	501.2	1.0	731.2	0.090	0.052	41.6	75.75
		1768	2.3	2187.8	4.0	1784.7	0.220	0.054	72.2	74.98
		1714	2.9	3071.7	6.1	2353.4	0.290	0.058	75.2	72.69
		1776	3.6	4215.5	9.1	3062.7	0.377	0.059	76.8	75.32
		1716	3.9	5466.4	13.7	3869.1	0.476	0.063	74.9	72.78
		1727	4.0	6293.3	18.8	4412.6	0.543	0.068	71.1	73.24
		1747	4.3	6716.2	25.6	4717.4	0.580	0.073	65.0	74.09
	0.28	1785	1.4	796.0	1.5	889.3	0.110	0.050	53.7	82.59
		1715	1.6	1808.5	3.3	1532.5	0.190	0.053	69.6	79.35
		1768	2.9	2800.6	5.2	2146.4	0.266	0.054	75.4	81.80
		1779	2.6	3543.7	7.6	2609.1	0.323	0.056	76.5	82.31
		1787	2.8	4674.0	11.3	3316.8	0.411	0.058	76.2	82.68
		1760	3.7	5798.2	17.2	4046.7	0.501	0.063	72.3	81.43
		1704	3.9	6759.4	23.9	4678.3	0.579	0.069	67.0	78.84
		1799	4.2	6750.5	26.1	4689.4	0.581	0.071	64.9	83.23

Cont…..

Tyre T_1 (14.9 R 28)										
Normal load N(kgf)	Tyre def. ratio	Cone index kPa	Rut depth cm	Drawbar Pull N	Slip %	Axle Torque N-m	Gross Traction Ratio	Motion Resis. Ratio	Tractive Eff. %	Mobility Number
W	**(δ/h)**	**CI**	**R_d**	**P**	**S**	**T**	**GTR**	**MRR**	**TE**	**B_n**
11282 (1150)	0.20	662	4.1	283.8	1.2	695.3	0.094	0.069	26.4	34.77
		697	3.4	1183.4	3.1	1284.8	0.174	0.069	58.4	36.61
		671	4.7	2689.8	7.5	2324.4	0.315	0.077	70.0	35.24
		601	4.1	3424.2	11.1	2873.3	0.389	0.086	69.3	31.57
		695	4.7	4067.5	13.6	3274.3	0.444	0.083	70.2	36.50
		613	4.9	4279.3	17.1	3471.7	0.471	0.091	66.8	32.20
		645	5.3	4807.7	20.8	3848.7	0.522	0.095	64.7	33.88
		669	4.6	5131.4	26.9	4101.7	0.556	0.101	59.9	35.14
	0.24	635	3.8	204.9	1.1	629.5	0.086	0.068	20.9	36.69
		681	4.6	1574.4	3.9	1520.6	0.207	0.068	64.7	39.35
		608	4.6	2414.1	6.4	2112.4	0.288	0.074	69.5	35.13
		636	4.5	3199.8	9.6	2642.5	0.360	0.077	71.2	36.75
		655	4.8	4061.7	13.7	3227.7	0.440	0.080	70.6	37.84
		634	4.4	4952.4	20.6	3879.8	0.529	0.090	65.9	36.63
		646	4.6	5237.5	24.7	4101.2	0.559	0.095	62.5	37.32
	0.28	627	3.8	241.0	1.0	628.5	0.086	0.065	24.5	39.52
		613	2.8	1695.6	4.4	1603.8	0.220	0.070	65.2	38.64
		620	2.9	2688.0	7.4	2259.8	0.310	0.072	71.1	39.08
		611	3.8	3742.9	11.5	2989.9	0.411	0.079	71.5	38.51
		675	4.2	4300.1	13.9	3343.2	0.459	0.078	71.5	42.54
		641	4.4	4702.5	19.0	3651.0	0.501	0.085	67.3	40.40
		691	4.4	5411.0	25.1	4147.7	0.570	0.090	63.1	43.55

Cont…..

Tyre T_1 (14.9 R 28)										
W	**(δ/h)**	**CI**	**R_d**	**P**	**S**	**T**	**GTR**	**MRR**	**TE**	**B_n**
13734 (1400)	0.20	607	4.2	270.2	1.4	886.9	0.099	0.079	19.7	26.19
		670	3.8	1909.6	4.7	1960.9	0.218	0.079	60.7	28.91
		699	4.0	3562.5	9.7	3102.9	0.345	0.086	67.8	30.16
		655	3.7	4241.7	11.9	3585.0	0.399	0.090	68.2	28.26
		650	4.4	4904.0	16.0	4086.8	0.455	0.098	66.0	28.04
		677	4.8	5084.3	17.8	4198.9	0.467	0.097	65.1	29.21
		613	4.1	5598.0	24.7	4685.7	0.521	0.114	58.9	26.45
	0.24	610	3.6	214.4	1.1	801.9	0.090	0.074	17.2	28.95
		693	3.9	1736.5	3.8	1782.6	0.200	0.073	60.9	32.89
		640	4.1	3396.6	8.8	2951.1	0.330	0.083	68.2	30.37
		679	3.8	4189.3	11.8	3491.1	0.391	0.086	68.8	32.22
		672	4.2	5438.8	19.2	4380.5	0.491	0.095	65.3	31.89
		629	5.2	5466.5	22.1	4476.3	0.501	0.103	61.9	29.85
		645	4.7	5738.4	24.7	4673.0	0.523	0.105	60.1	30.61
		664	4.9	6290.3	29.5	5054.2	0.566	0.108	57.0	31.51
	0.28	689	3.2	275.4	1.1	770.0	0.087	0.067	22.8	35.67
		673	3.3	1765.1	3.8	1771.3	0.200	0.071	61.9	34.84
		675	3.6	3580.3	8.5	3010.8	0.339	0.079	70.3	34.95
		690	4.1	4267.1	11.3	3465.7	0.391	0.080	70.5	35.72
		681	3.8	4995.8	14.0	3966.3	0.447	0.083	69.9	35.26
		611	3.8	5402.2	19.0	4339.7	0.489	0.096	65.1	31.63
		663	4.5	5867.5	22.8	4641.3	0.523	0.096	63.0	34.33
		616	4.9	6306.0	29.3	5046.9	0.569	0.110	57.1	31.89

Cont…..

Tyre T_1 (14.9 R 28)										
Normal load N(kgf)	Tyre def. ratio	Cone index kPa	Rut depth cm	Drawbar Pull N	Slip %	Axle Torque N-m	Gross Traction Ratio	Motion Resis. Ratio	Tractive Eff. %	Mobility Number
W	**(δ/h)**	**CI**	**R_d**	**P**	**S**	**T**	**GTR**	**MRR**	**TE**	**B_n**
16187 (1650)	0.20	677	4.6	196.5	1.3	986.5	0.093	0.081	12.9	24.78
		615	4.4	1827.3	4.8	2168.4	0.205	0.092	52.5	22.51
		618	4.9	2620.6	6.3	2701.2	0.255	0.093	59.4	22.62
		670	4.2	4030.2	10.5	3651.9	0.345	0.096	64.6	24.53
		663	5.0	4954.9	13.7	4310.1	0.407	0.101	64.9	24.27
		631	5.6	5855.6	21.4	5053.5	0.477	0.116	59.5	23.10
		655	5.0	6148.4	26.1	5311.6	0.502	0.122	55.9	23.98
	0.24	610	4.0	265.0	1.4	1025.9	0.098	0.081	16.5	24.56
		631	4.2	1510.9	3.7	1872.9	0.178	0.085	50.5	25.41
		660	4.2	3367.3	7.7	3121.7	0.297	0.089	64.6	26.58
		618	5.0	4627.1	12.6	4045.4	0.385	0.099	64.9	24.89
		695	5.4	6099.7	17.8	5012.9	0.477	0.100	64.9	27.99
		621	5.4	6103.8	20.9	5121.4	0.487	0.110	61.2	25.01
		654	4.5	6409.3	25.7	5371.3	0.511	0.115	57.6	26.34
	0.28	699	3.5	345.7	1.3	978.7	0.094	0.072	22.5	30.71
		665	2.9	2042.8	4.1	2146.4	0.205	0.079	59.0	29.21
		699	3.5	4444.9	9.8	3761.3	0.360	0.085	68.9	30.71
		651	4.3	4903.9	12.4	4130.9	0.395	0.092	67.2	28.60
		603	5.0	6049.8	18.5	4988.2	0.477	0.103	63.9	26.49
		692	5.4	6781.7	24.4	5471.7	0.523	0.104	60.6	30.40

Cont…..

Tyre T_1 (14.9 R 28)										
W	**(δ/h)**	**CI**	**R_d**	**P**	**S**	**T**	**GTR**	**MRR**	**TE**	**B_n**
11282 (1150)	0.20	1286	2.0	240.7	0.8	550.5	0.075	0.053	28.4	67.54
		1258	3.5	1739.4	3.8	1555.1	0.211	0.057	70.3	66.07
		1263	3.6	2786.0	6.9	2257.1	0.306	0.059	75.2	66.34
		1261	3.4	3613.8	9.8	2807.1	0.380	0.060	75.9	66.23
		1289	2.9	4477.0	14.3	3400.9	0.461	0.064	73.8	67.70
		1293	3.8	5221.7	18.7	3930.7	0.533	0.070	70.6	67.91
		1206	4.0	5557.1	21.9	4173.5	0.566	0.073	68.0	63.34
		1268	3.9	5661.1	25.8	4267.5	0.578	0.077	64.4	66.60
	0.24	1287	2.3	479.7	1.2	686.2	0.094	0.051	44.9	74.36
		1246	2.1	2131.8	4.4	1782.3	0.243	0.054	74.3	71.99
		1280	2.7	3360.3	8.3	2602.8	0.355	0.057	76.9	73.95
		1268	3.5	5027.1	16.4	3740.7	0.510	0.065	73.0	73.26
		1203	4.0	5236.4	20.0	3916.7	0.534	0.070	69.5	69.50
		1269	3.2	5712.7	22.7	4227.0	0.576	0.070	67.9	73.32
	0.28	1261	1.9	404.3	1.0	625.4	0.086	0.050	41.3	79.48
		1228	2.3	1885.4	3.9	1609.8	0.221	0.054	72.7	77.40
		1209	2.8	3137.5	8.3	2438.3	0.335	0.057	76.2	76.20
		1274	3.3	4809.6	14.5	3549.2	0.487	0.061	74.8	80.30
		1251	3.3	5279.9	18.4	3878.1	0.533	0.065	71.7	78.85
		1259	2.9	5271.9	20.1	3890.6	0.534	0.067	69.9	79.35
		1207	3.3	5600.1	24.1	4132.6	0.567	0.071	66.4	76.07

Cont…..

Tyre T_1 (14.9 R 28)										
Normal load N(kgf)	Tyre def. ratio	Cone index kPa	Rut depth cm	Drawbar Pull N	Slip %	Axle Torque N-m	Gross Traction Ratio	Motion Resis. Ratio	Tractive Eff. %	Mobility Number
W	**(δ/h)**	**CI**	**R_d**	**P**	**S**	**T**	**GTR**	**MRR**	**TE**	**B_n**
13734 (1400)	0.20	1273	3.3	809.2	1.7	1042.0	0.116	0.057	49.9	54.92
		1281	4.2	2057.7	3.9	1885.0	0.210	0.060	68.7	55.27
		1238	3.5	4031.2	8.5	3226.1	0.359	0.065	74.8	53.41
		1279	3.5	5144.2	12.4	3985.1	0.443	0.069	74.0	55.18
		1234	3.6	5732.7	16.5	4400.8	0.490	0.072	71.1	53.24
		1259	3.8	6146.0	19.9	4704.4	0.524	0.076	68.5	54.32
		1265	4.0	6938.5	24.8	5278.5	0.587	0.082	64.6	54.58
	0.24	1249	1.9	474.3	1.0	799.7	0.090	0.055	38.2	59.28
		1219	2.1	2249.8	4.2	1981.5	0.222	0.058	70.8	57.85
		1299	3.4	3532.8	7.0	2842.0	0.318	0.061	75.2	61.65
		1227	3.4	4598.0	10.8	3576.5	0.401	0.066	74.6	58.23
		1211	3.7	5337.8	14.3	4078.7	0.457	0.068	72.9	57.47
		1225	3.5	6321.2	20.6	4771.6	0.534	0.074	68.4	58.14
		1233	5.5	6714.8	25.2	5070.7	0.568	0.079	64.4	58.52
	0.28	1249	2.9	368.4	0.8	708.4	0.080	0.053	33.3	64.66
		1254	2.4	2127.6	3.9	1870.9	0.211	0.056	70.6	64.92
		1237	2.7	4315.0	8.8	3334.8	0.376	0.062	76.2	64.04
		1216	2.5	4905.9	11.3	3739.2	0.422	0.064	75.2	62.96
		1219	3.5	5208.8	13.6	3954.6	0.446	0.067	73.5	63.11
		1260	3.4	6225.7	17.6	4625.4	0.522	0.068	71.6	65.23
		1257	3.3	6484.5	21.1	4833.5	0.545	0.073	68.4	65.08
		1255	5.4	7160.9	25.8	5307.1	0.598	0.077	64.7	64.97

Cont…..

Tyre T_1 (14.9 R 28)										
W	**(δ/h)**	**CI**	**R_d**	**P**	**S**	**T**	**GTR**	**MRR**	**TE**	**B_n**
16187 (1650)	0.20	1229	2.5	611.5	1.3	1055.6	0.100	0.062	37.4	44.99
		1243	3.0	1897.1	3.3	1908.0	0.180	0.063	62.9	45.50
		1219	3.1	3934.3	7.5	3303.1	0.312	0.069	72.1	44.62
		1229	3.8	5981.8	12.8	4695.8	0.444	0.074	72.6	44.99
		1214	3.6	6468.8	16.2	5066.4	0.479	0.079	70.0	44.44
		1201	4.5	7420.9	21.3	5758.0	0.544	0.085	66.3	43.97
		1283	6.5	8058.9	26.3	6220.9	0.588	0.090	62.5	46.97
	0.24	1207	2.9	868.0	1.7	1205.1	0.115	0.061	46.0	48.60
		1291	3.1	2184.9	3.5	2050.3	0.195	0.060	66.8	51.99
		1223	3.7	3793.7	6.8	3157.1	0.300	0.066	72.7	49.25
		1236	3.5	5037.0	9.5	3976.7	0.378	0.067	74.5	49.77
		1224	4.0	6545.9	16.1	5034.9	0.479	0.075	70.9	49.29
		1296	4.6	7205.4	20.5	5508.3	0.524	0.079	67.6	52.19
		1259	3.6	8128.9	25.6	6177.9	0.588	0.085	63.5	50.70
	0.28	1242	2.5	707.0	1.4	1050.3	0.100	0.057	42.9	54.56
		1285	2.9	2041.0	3.4	1945.2	0.186	0.060	65.5	56.45
		1294	3.7	4040.1	7.5	3269.6	0.313	0.063	73.9	56.84
		1263	3.5	5425.6	11.2	4197.8	0.401	0.066	74.2	55.48
		1250	3.6	5924.8	13.2	4550.1	0.435	0.069	73.0	54.91
		1232	3.4	7704.8	21.3	5803.6	0.555	0.079	67.5	54.12
		1234	4.6	8180.7	25.1	6146.6	0.588	0.082	64.4	54.21

Cont…..

Tyre T_1 (14.9 R 28)										
Normal load N(kgf)	Tyre def. ratio	Cone index kPa	Rut depth cm	Drawbar Pull N	Slip %	Axle Torque N-m	Gross Traction Ratio	Motion Resis. Ratio	Tractive Eff. %	Mobility Number
W	**(δ/h)**	**CI**	**R_d**	**P**	**S**	**T**	**GTR**	**MRR**	**TE**	**B_n**
11282 (1150)	0.20	1735	1.5	910.1	1.9	957.0	0.130	0.049	61.0	91.13
		1715	1.4	1435.1	3.2	1314.5	0.178	0.051	69.2	90.08
		1751	2.2	4645.6	14.7	3473.7	0.471	0.059	74.6	91.97
		1783	2.4	5188.8	17.0	3844.1	0.521	0.061	73.2	93.65
		1703	2.9	5313.6	19.8	3940.5	0.534	0.063	70.7	89.45
		1762	3.7	5655.5	23.7	4185.8	0.567	0.066	67.4	92.55
	0.24	1742	1.1	737.8	1.5	837.3	0.114	0.049	56.4	100.64
		1734	1.7	2463.4	5.7	1981.8	0.270	0.052	76.2	100.18
		1799	1.9	3769.8	9.5	2845.2	0.388	0.054	77.9	103.94
		1795	2.4	4732.9	13.9	3494.1	0.476	0.057	75.8	103.71
		1722	3.0	4627.7	14.8	3431.9	0.468	0.058	74.7	99.49
		1772	3.0	5218.3	19.4	3839.9	0.524	0.061	71.2	102.38
		1730	2.7	5900.1	23.3	4304.5	0.587	0.064	68.4	99.95
		1713	3.2	5886.0	27.8	4324.5	0.590	0.068	63.9	98.97
	0.28	1701	1.1	659.4	1.3	765.7	0.105	0.047	54.9	107.21
		1729	1.2	1833.0	3.8	1533.2	0.211	0.048	74.3	108.98
		1739	1.3	3427.4	8.3	2584.3	0.355	0.051	78.5	109.61
		1751	2.6	4993.6	15.3	3631.7	0.499	0.056	75.2	110.36
		1790	2.5	5343.2	18.4	3878.3	0.533	0.059	72.6	112.82
		1766	3.4	5916.1	24.2	4279.7	0.588	0.063	67.6	111.31
		1703	2.9	5916.1	27.3	4292.8	0.589	0.065	64.7	107.34

Cont…..

Tyre T_1 (14.9 R 28)										
W	**(δ/h)**	**CI**	**R_d**	**P**	**S**	**T**	**GTR**	**MRR**	**TE**	**B_n**
13734 (1400)	0.20	1756	2.0	607.5	1.1	856.0	0.095	0.051	45.9	75.76
		1710	2.3	2786.1	5.1	2312.8	0.257	0.055	74.8	73.78
		1726	2.5	3643.6	7.7	2904.4	0.323	0.058	75.8	74.47
		1777	2.8	5228.7	12.9	3961.4	0.441	0.060	75.2	76.67
		1790	3.0	5990.2	16.4	4494.7	0.500	0.064	72.9	77.23
		1794	2.8	6610.3	20.0	4935.3	0.549	0.068	70.1	77.40
		1717	3.7	7111.3	25.0	5293.0	0.589	0.071	66.0	74.08
	0.24	1772	1.0	745.8	1.4	935.0	0.105	0.050	51.1	84.10
		1773	1.6	2036.2	3.9	1796.4	0.201	0.053	70.8	84.14
		1742	1.8	3374.3	6.9	2689.4	0.301	0.055	75.9	82.67
		1771	2.0	5435.2	12.9	4061.2	0.455	0.059	75.8	84.05
		1708	3.3	6002.6	17.4	4477.8	0.501	0.064	72.0	81.06
		1722	3.2	6834.2	21.5	5050.0	0.566	0.068	69.1	81.72
		1753	3.4	6988.2	26.3	5169.3	0.579	0.070	64.8	83.19
	0.28	1781	1.0	505.8	1.0	760.8	0.086	0.049	42.5	92.21
		1777	1.2	2202.9	4.0	1866.9	0.210	0.050	73.2	92.00
		1791	1.4	3668.0	7.0	2832.8	0.319	0.052	77.8	92.73
		1762	2.7	5283.4	12.1	3933.0	0.443	0.059	76.2	91.22
		1800	3.8	5754.4	15.5	4248.0	0.479	0.060	73.9	93.19
		1799	2.9	6894.1	20.9	5011.7	0.565	0.063	70.3	93.14
		1740	3.9	7141.5	24.7	5214.6	0.588	0.068	66.6	90.08

Cont…..

Tyre T_1 (14.9 R 28)										
Normal load N(kgf)	Tyre def. ratio	Cone index kPa	Rut depth cm	Drawbar Pull N	Slip %	Axle Torque N-m	Gross Traction Ratio	Motion Resis. Ratio	Tractive Eff. %	Mobility Number
W	**(δ/h)**	**CI**	**R_d**	**P**	**S**	**T**	**GTR**	**MRR**	**TE**	**B_n**
16187 (1650)	0.20	1722	2.0	904.3	1.5	1173.1	0.111	0.055	49.7	63.04
		1741	2.6	2504.6	3.8	2231.4	0.211	0.056	70.6	63.73
		1746	1.8	4178.4	6.9	3367.2	0.318	0.060	75.5	63.92
		1755	3.2	5982.4	11.8	4580.3	0.433	0.063	75.3	64.25
		1783	3.6	6407.9	14.3	4879.7	0.461	0.065	73.6	65.27
		1792	3.7	7467.0	17.4	5622.9	0.531	0.070	71.8	65.60
		1731	5.0	7949.8	23.8	6003.2	0.567	0.076	66.0	63.37
		1730	3.7	8435.8	27.5	6343.7	0.599	0.078	63.1	63.33
	0.24	1797	2.0	1089.2	1.8	1264.1	0.120	0.053	55.0	72.36
		1793	1.7	2533.1	4.0	2213.5	0.211	0.054	71.3	72.20
		1722	2.7	4620.8	8.5	3631.2	0.345	0.060	75.6	69.34
		1783	2.7	6018.3	11.9	4550.8	0.433	0.061	75.7	71.80
		1764	2.6	6438.2	14.1	4844.7	0.461	0.063	74.1	71.03
		1725	3.2	7503.7	18.5	5598.2	0.532	0.069	71.0	69.46
		1749	3.8	7997.9	23.6	5961.5	0.567	0.073	66.6	70.43
		1796	3.6	8505.3	25.8	6292.4	0.599	0.073	65.1	72.32
	0.28	1778	1.9	1039.0	1.6	1217.2	0.116	0.052	54.3	78.10
		1765	1.8	2401.1	3.8	2099.1	0.201	0.052	71.1	77.53
		1708	2.4	4297.1	7.1	3363.6	0.322	0.056	76.7	75.03
		1745	3.0	6031.7	11.9	4528.6	0.433	0.060	75.9	76.66
		1789	3.5	7071.1	14.9	5210.7	0.498	0.061	74.6	78.59
		1728	5.0	7373.5	19.2	5475.5	0.523	0.068	70.3	75.91
		1718	3.5	7889.7	22.6	5820.8	0.556	0.069	67.8	75.47
		1727	3.5	8512.6	25.0	6256.8	0.598	0.072	65.9	75.86

Cont…..

Tyre T_1 (16.9 R 28)										
W	**(δ/h)**	**CI**	**R_d**	**P**	**S**	**T**	**GTR**	**MRR**	**TE**	**B_n**
14225 (1450)	0.20	633	4.5	573.6	1.7	1122.4	0.115	0.074	34.6	29.99
		652	4.0	1615.9	3.9	1864.5	0.191	0.077	57.3	30.89
		644	4.3	2995.4	7.3	2845.0	0.291	0.080	67.2	30.51
		627	4.3	4434.7	12.8	3923.0	0.401	0.089	67.8	29.71
		630	4.3	5286.8	17.6	4573.3	0.467	0.096	65.5	29.85
		638	4.6	5686.7	21.3	4901.7	0.501	0.101	62.8	30.23
		636	3.8	5913.3	25.0	5121.4	0.523	0.108	59.6	30.13
	0.24	697	3.7	468.2	1.5	988.2	0.102	0.069	31.9	36.33
		641	3.9	1759.7	3.7	1905.2	0.196	0.072	60.8	33.41
		602	3.9	3106.1	7.3	2919.6	0.300	0.082	67.4	31.38
		698	4.4	4685.3	11.6	3987.8	0.410	0.081	71.0	36.38
		670	4.6	5102.9	15.1	4331.5	0.446	0.087	68.4	34.92
		689	4.4	5834.3	17.7	4850.9	0.499	0.089	67.7	35.91
		670	4.7	6219.3	24.1	5192.9	0.534	0.097	62.2	34.92
	0.28	674	3.4	639.8	1.7	1068.5	0.110	0.065	40.0	38.32
		612	3.3	1365.5	3.1	1617.0	0.167	0.071	55.7	34.80
		694	3.5	2799.0	6.2	2591.9	0.268	0.071	68.9	39.46
		625	4.0	3935.5	9.8	3450.2	0.357	0.080	70.0	35.54
		665	3.4	4715.9	12.7	3992.1	0.413	0.081	70.2	37.81
		677	4.0	5618.8	16.4	4626.5	0.478	0.083	69.1	38.49
		663	3.8	6709.7	24.4	5468.8	0.565	0.093	63.1	37.70

Cont…..

Tyre T_1 (16.9 R 28)										
Normal load N(kgf)	Tyre def. ratio	Cone index kPa	Rut depth cm	Drawbar Pull N	Slip %	Axle Torque N-m	Gross Traction Ratio	Motion Resis. Ratio	Tractive Eff. %	Mobility Number
W	**(δ/h)**	**CI**	**R_d**	**P**	**S**	**T**	**GTR**	**MRR**	**TE**	**B_n**
16677 (1700)	0.20	683	5.0	295.4	1.2	1078.0	0.094	0.076	18.6	27.60
		697	4.5	1615.2	3.3	2009.6	0.175	0.078	53.5	28.17
		658	5.0	3552.8	7.8	3445.7	0.300	0.087	65.4	26.59
		648	5.1	4921.1	11.9	4467.6	0.389	0.094	66.8	26.19
		685	4.4	5599.1	14.2	4962.5	0.432	0.097	66.7	27.68
		639	4.6	5846.7	18.0	5235.3	0.456	0.105	63.0	25.82
		604	5.2	6393.0	22.2	5725.7	0.499	0.115	59.8	24.41
		671	5.2	6705.0	25.7	5881.8	0.512	0.110	58.3	27.12
	0.24	682	4.5	289.1	1.1	1022.1	0.090	0.072	19.1	30.32
		643	4.8	2159.4	4.2	2388.2	0.209	0.080	59.2	28.58
		649	4.6	4094.0	8.4	3785.5	0.332	0.087	67.8	28.85
		671	5.2	5323.5	12.3	4664.8	0.409	0.090	68.4	29.83
		626	5.3	6172.2	17.2	5349.1	0.469	0.099	65.3	27.83
		668	5.1	6498.2	20.1	5594.5	0.491	0.101	63.4	29.70
		624	4.0	6955.5	24.7	6032.6	0.529	0.112	59.4	27.74
	0.28	647	4.0	310.1	1.1	1017.4	0.090	0.071	20.5	31.38
		673	3.9	2407.8	4.7	2499.7	0.220	0.076	62.5	32.64
		696	4.0	4395.5	8.5	3896.2	0.343	0.080	70.2	33.75
		664	4.9	5082.6	10.7	4399.5	0.388	0.083	70.2	32.20
		639	4.3	5563.2	14.3	4805.2	0.424	0.090	67.5	30.99
		625	4.0	6678.6	18.2	5650.5	0.498	0.098	65.7	30.31
		624	5.2	6684.3	21.3	5681.9	0.501	0.100	62.9	30.26
		689	4.8	7083.9	24.0	5942.1	0.524	0.099	61.6	33.41

Cont…..

Tyre T_1 (16.9 R 28)										
W	**(δ/h)**	**CI**	**R_d**	**P**	**S**	**T**	**GTR**	**MRR**	**TE**	**B_n**
19130 (1950)	0.20	623	4.0	248.3	1.5	1312.5	0.100	0.087	12.8	21.95
		656	4.4	2108.1	4.5	2634.2	0.200	0.090	52.6	23.11
		656	4.5	3920.9	8.8	3961.1	0.301	0.096	62.1	23.11
		640	6.0	5652.2	14.4	5265.4	0.400	0.105	63.2	22.55
		619	5.6	6258.0	17.9	5836.9	0.444	0.116	60.6	21.81
		685	5.3	6898.6	21.3	6197.4	0.471	0.110	60.2	24.13
		640	5.6	7167.1	24.5	6565.4	0.499	0.124	56.7	22.55
	0.24	699	4.6	207.8	1.2	1150.1	0.088	0.077	12.2	27.09
		658	4.1	1582.0	3.1	2171.3	0.166	0.083	48.3	25.50
		683	4.0	3505.3	6.7	3534.3	0.270	0.087	63.3	26.47
		634	4.5	4791.9	10.2	4531.6	0.346	0.096	65.0	24.57
		690	4.9	6391.8	14.1	5648.5	0.432	0.098	66.5	26.74
		610	4.9	6551.0	18.8	5893.7	0.451	0.108	61.7	23.64
		638	5.4	7331.5	22.5	6528.8	0.499	0.116	59.5	24.73
		657	5.4	7399.4	25.8	6559.6	0.501	0.115	57.3	25.46
	0.28	649	4.0	313.0	1.2	1227.5	0.094	0.078	17.1	27.44
		653	4.2	2075.2	3.4	2441.2	0.187	0.079	55.9	27.61
		612	4.5	4005.3	7.6	3896.9	0.299	0.090	64.7	25.87
		609	4.4	5626.3	12.0	5067.8	0.389	0.095	66.5	25.75
		663	4.9	6857.9	15.8	5919.5	0.455	0.096	66.4	28.03
		667	5.4	7701.4	20.8	6575.4	0.505	0.102	63.1	28.20
		679	5.4	8294.4	27.0	7080.1	0.544	0.110	58.2	28.71

Cont…..

Tyre T_1 (16.9 R 28)										
Normal load N(kgf)	Tyre def. ratio	Cone index kPa	Rut depth cm	Drawbar Pull N	Slip %	Axle Torque N-m	Gross Traction Ratio	Motion Resis. Ratio	Tractive Eff. %	Mobility Number
W	**(δ/h)**	**CI**	**R_d**	**P**	**S**	**T**	**GTR**	**MRR**	**TE**	**B_n**
14225 (1450)	0.20	1232	2.7	903.4	1.8	1177.7	0.120	0.057	51.8	58.37
		1292	2.8	2391.6	4.2	2204.0	0.225	0.057	71.5	61.22
		1222	3.3	3683.2	6.9	3140.3	0.321	0.062	75.1	57.90
		1273	3.4	4487.1	9.9	3704.1	0.378	0.063	75.1	60.32
		1237	3.6	5343.0	12.2	4337.9	0.443	0.068	74.4	58.61
		1202	2.9	6080.5	15.5	4878.6	0.499	0.071	72.5	56.95
		1259	3.2	6414.3	19.1	5118.3	0.523	0.072	69.7	59.65
		1219	2.5	7105.0	24.6	5670.1	0.579	0.080	65.0	57.76
	0.24	1229	2.3	1020.5	1.9	1222.8	0.126	0.054	55.9	64.05
		1300	2.4	2557.7	4.7	2292.2	0.236	0.056	72.7	67.75
		1293	2.7	4389.5	9.0	3591.5	0.370	0.061	76.0	67.39
		1291	3.4	6130.4	15.4	4846.0	0.499	0.068	73.2	67.28
		1258	3.5	6286.0	17.9	4965.0	0.511	0.069	71.0	65.56
		1264	4.2	6741.4	21.2	5298.4	0.545	0.071	68.5	65.88
	0.28	1295	1.7	697.2	1.3	970.6	0.100	0.051	48.2	73.63
		1289	2.5	2476.2	4.2	2207.5	0.228	0.054	73.1	73.29
		1206	2.7	4517.8	9.0	3645.3	0.377	0.059	76.7	68.57
		1282	3.1	5398.5	12.9	4264.9	0.441	0.061	75.0	72.89
		1245	3.1	6158.6	16.8	4844.1	0.501	0.068	72.0	70.79
		1211	3.0	6555.2	20.2	5153.3	0.533	0.072	69.1	68.85
		1299	3.6	7343.1	23.8	5683.0	0.587	0.071	67.0	73.86

Cont…..

Tyre T_1 (16.9 R 28)										
W	**(δ/h)**	**CI**	**R_d**	**P**	**S**	**T**	**GTR**	**MRR**	**TE**	**B_n**
16677 (1700)	0.20	1249	2.3	693.7	1.2	1144.2	0.100	0.058	41.2	50.48
		1278	2.7	2626.5	4.1	2518.9	0.219	0.062	68.9	51.65
		1246	3.4	4793.2	8.3	4067.9	0.354	0.067	74.4	50.35
		1295	3.8	5853.2	12.1	4832.1	0.421	0.070	73.3	52.33
		1221	4.0	6885.6	14.9	5594.0	0.487	0.074	72.1	49.34
		1257	4.7	7590.3	20.7	6131.0	0.534	0.079	67.6	50.80
		1209	4.0	7894.8	24.0	6388.7	0.556	0.083	64.6	48.86
	0.24	1241	2.7	447.8	0.9	955.5	0.084	0.057	31.8	55.17
		1244	2.9	2329.3	3.6	2275.7	0.200	0.060	67.5	55.30
		1240	2.9	4320.8	7.7	3683.2	0.323	0.064	74.0	55.12
		1289	3.6	5598.1	10.9	4569.3	0.401	0.065	74.6	57.30
		1212	3.8	6507.7	13.5	5237.0	0.459	0.069	73.5	53.88
		1243	3.8	7473.2	16.9	5932.2	0.520	0.072	71.6	55.26
		1236	3.1	7815.1	19.1	6188.0	0.543	0.074	69.9	54.95
		1239	3.6	7947.0	23.4	6344.6	0.556	0.080	65.6	55.08
	0.28	1293	2.1	847.9	1.5	1200.2	0.106	0.055	47.4	62.70
		1231	2.8	2060.1	3.3	2048.2	0.181	0.057	66.2	59.70
		1209	3.0	3833.9	6.1	3283.9	0.289	0.060	74.6	58.63
		1277	3.2	5613.0	9.9	4522.3	0.399	0.062	76.1	61.93
		1254	4.0	6484.5	14.2	5181.5	0.457	0.068	73.0	60.81
		1209	3.4	7070.0	16.7	5615.3	0.495	0.071	71.4	58.63
		1273	3.7	8041.1	20.6	6289.9	0.554	0.072	69.0	61.73
		1266	4.2	8193.6	24.4	6436.5	0.567	0.076	65.5	61.39

Cont…..

Tyre T_1 (16.9 R 28)										
Normal load N(kgf)	Tyre def. ratio	Cone index kPa	Rut depth cm	Drawbar Pull N	Slip %	Axle Torque N-m	Gross Traction Ratio	Motion Resis. Ratio	Tractive Eff. %	Mobility Number
W	**(δ/h)**	**CI**	**R_d**	**P**	**S**	**T**	**GTR**	**MRR**	**TE**	**B_n**
19130 (1950)	0.20	1236	2.2	963.3	1.6	1479.4	0.112	0.062	44.1	43.55
		1262	2.9	2520.9	3.7	2576.9	0.196	0.064	64.8	44.46
		1209	3.7	5324.8	8.9	4612.6	0.351	0.072	72.3	42.59
		1204	3.8	6842.3	12.5	5694.8	0.433	0.075	72.3	42.42
		1225	3.7	7478.0	15.7	6195.4	0.471	0.080	70.0	43.16
		1269	3.8	8435.8	18.2	6856.5	0.521	0.080	69.2	44.71
		1257	3.7	8788.7	23.3	7178.3	0.545	0.086	64.6	44.29
	0.24	1219	2.3	835.4	1.5	1369.8	0.105	0.061	41.1	47.24
		1226	2.5	3051.9	4.2	2902.2	0.222	0.062	68.9	47.51
		1279	3.1	4339.1	6.7	3805.4	0.291	0.064	72.8	49.57
		1223	3.3	6368.8	10.7	5284.3	0.404	0.071	73.6	47.40
		1244	3.8	7686.7	14.2	6229.1	0.476	0.074	72.4	48.21
		1230	4.2	8834.5	19.7	7100.6	0.543	0.081	68.4	47.67
		1229	4.6	9024.4	24.7	7283.5	0.557	0.085	63.8	47.63
	0.28	1296	2.0	1143.2	1.7	1521.0	0.117	0.057	50.3	54.79
		1269	2.5	2469.9	3.4	2462.1	0.189	0.060	65.9	53.65
		1276	2.9	4925.8	7.5	4174.3	0.321	0.063	74.3	53.95
		1241	2.7	6780.7	12.5	5514.8	0.424	0.069	73.3	52.47
		1267	3.2	8150.3	16.2	6502.1	0.499	0.073	71.5	53.57
		1210	4.6	8914.2	19.3	7067.0	0.543	0.077	69.3	51.16

Cont…..

Tyre T_1 (16.9 R 28)										
W	**(δ/h)**	**CI**	**R_d**	**P**	**S**	**T**	**GTR**	**MRR**	**TE**	**B_n**
14225 (1450)	0.20	1768	1.2	1010.0	1.7	1194.3	0.122	0.051	57.2	83.77
		1728	0.9	2249.1	4.1	2056.9	0.210	0.052	72.2	81.87
		1769	2.1	3343.8	6.4	2842.8	0.290	0.055	75.8	83.82
		1764	2.6	4871.3	10.2	3909.6	0.399	0.057	77.0	83.58
		1741	2.6	6077.9	14.4	4769.8	0.487	0.060	75.0	82.49
		1749	3.0	6509.7	18.9	5119.3	0.523	0.065	70.9	82.87
		1785	3.3	6966.4	22.6	5445.8	0.556	0.067	68.1	84.57
	0.24	1792	1.2	850.5	1.5	1048.4	0.108	0.048	54.6	93.40
		1787	1.3	2198.2	3.8	1988.6	0.205	0.050	72.7	93.14
		1721	2.0	3555.8	6.5	2945.0	0.303	0.053	77.1	89.70
		1789	2.4	4887.1	11.0	3899.3	0.401	0.058	76.2	93.24
		1729	2.7	5814.7	14.7	4547.2	0.468	0.059	74.5	90.11
		1781	3.3	6986.0	19.9	5386.0	0.554	0.063	71.0	92.82
		1733	3.3	7124.1	24.6	5519.4	0.568	0.067	66.5	90.32
	0.28	1728	0.5	669.4	1.1	911.0	0.094	0.047	49.4	98.25
		1773	1.2	2215.1	3.8	1990.3	0.206	0.050	72.8	100.81
		1718	1.6	3787.7	7.0	3080.3	0.318	0.052	77.8	97.68
		1700	2.5	5170.9	11.6	4068.4	0.420	0.057	76.5	96.66
		1786	3.0	6273.6	15.4	4827.3	0.499	0.058	74.8	101.55
		1729	1.3	6712.3	19.8	5168.2	0.534	0.062	70.8	98.30
		1763	2.9	7001.8	22.7	5386.3	0.557	0.064	68.3	100.24
		1700	3.7	7573.8	25.6	5791.8	0.599	0.066	66.2	96.66

Cont…..

Tyre T_1 (16.9 R 28)										
Normal load N(kgf)	Tyre def. ratio	Cone index kPa	Rut depth cm	Drawbar Pull N	Slip %	Axle Torque N-m	Gross Traction Ratio	Motion Resis. Ratio	Tractive Eff. %	Mobility Number
W	**(δ/h)**	**CI**	**R_d**	**P**	**S**	**T**	**GTR**	**MRR**	**TE**	**B_n**
16677 (1700)	0.20	1707	2.2	1060.9	1.6	1349.3	0.118	0.054	53.3	68.98
		1722	2.2	2420.3	3.9	2307.9	0.201	0.056	69.4	69.59
		1700	2.0	4048.0	6.5	3441.7	0.300	0.057	75.7	68.70
		1725	2.1	5478.7	9.4	4449.9	0.388	0.059	76.8	69.71
		1715	3.6	6518.5	12.9	5221.2	0.455	0.064	74.8	69.31
		1757	3.3	7397.2	16.7	5860.4	0.510	0.067	72.4	71.01
		1704	3.6	8065.8	20.5	6366.8	0.555	0.071	69.3	68.86
		1773	3.2	8261.5	24.1	6514.3	0.567	0.072	66.3	71.65
	0.24	1768	1.4	799.1	1.3	1117.4	0.098	0.050	48.3	78.59
		1755	1.4	2774.0	4.2	2511.6	0.220	0.054	72.3	78.02
		1790	2.2	4569.4	7.9	3773.1	0.331	0.057	76.2	79.57
		1730	3.0	6209.0	11.7	4931.5	0.433	0.060	76.0	76.91
		1701	3.2	6901.3	15.0	5451.8	0.478	0.064	73.6	75.62
		1795	3.2	7953.1	18.5	6187.9	0.543	0.066	71.6	79.79
		1714	4.3	8299.0	24.5	6473.6	0.568	0.070	66.2	76.19
	0.28	1730	1.1	1020.1	1.3	1250.8	0.110	0.049	54.7	83.90
		1793	1.1	2298.0	3.1	2131.3	0.188	0.050	71.1	86.95
		1783	2.3	4825.3	7.8	3899.1	0.344	0.054	77.6	86.47
		1782	2.7	6446.4	13.3	5053.2	0.445	0.059	75.3	86.42
		1759	3.4	7294.7	16.0	5667.0	0.500	0.062	73.6	85.30
		1741	3.0	7781.4	19.4	6019.6	0.531	0.064	70.8	84.43
		1774	3.7	8670.8	24.4	6667.3	0.588	0.068	66.9	86.03

Cont…..

Tyre T_1 (16.9 R 28)										
W	**(δ/h)**	**CI**	**R_d**	**P**	**S**	**T**	**GTR**	**MRR**	**TE**	**B_n**
19130 (1950)	0.20	1799	1.4	859.8	1.2	1312.9	0.100	0.055	44.5	63.38
		1786	2.2	3222.6	4.3	2979.0	0.226	0.058	71.2	62.92
		1717	2.6	6225.6	9.4	5099.7	0.388	0.062	76.0	60.49
		1749	3.1	7228.7	12.5	5840.4	0.444	0.066	74.5	61.62
		1763	3.7	8449.8	17.1	6721.5	0.511	0.069	71.7	62.11
		1732	4.2	8990.7	21.8	7177.7	0.545	0.075	67.4	61.02
	0.24	1757	1.2	885.9	1.3	1311.0	0.100	0.054	45.6	68.09
		1799	1.3	3196.9	4.5	2917.9	0.223	0.056	71.6	69.72
		1739	1.7	5445.8	8.5	4516.5	0.345	0.061	75.5	67.39
		1762	2.7	7051.8	12.5	5637.1	0.431	0.062	74.9	68.29
		1795	3.2	8283.0	15.6	6526.7	0.499	0.066	73.2	69.56
		1735	3.6	8843.6	18.2	6961.2	0.532	0.070	71.1	67.24
		1755	4.0	9438.5	21.4	7395.1	0.565	0.072	68.6	68.01
	0.28	1757	2.0	705.8	1.1	1145.1	0.088	0.051	41.5	74.28
		1747	2.5	2633.8	3.6	2483.9	0.191	0.053	69.6	73.86
		1748	2.9	4694.1	7.0	3925.5	0.301	0.056	75.7	73.90
		1754	3.0	6277.4	9.2	5040.7	0.387	0.059	77.0	74.16
		1777	3.3	6749.7	11.9	5376.6	0.413	0.060	75.3	75.13
		1763	4.0	8728.0	16.6	6775.7	0.520	0.064	73.1	74.54
		1767	4.1	8525.6	18.5	6675.2	0.513	0.067	70.8	74.71
		1785	4.4	9102.8	21.8	7106.6	0.546	0.070	68.2	75.47

Table C-7 Regression coefficients for prediction of tyre performance under varying soil cone index

Tyre	**Type of soil**	**GTR Model**				**COT Model**		
		C_3	**C_4**	**C_5**	**R^2**	**C_1**	**C_2**	**R^2**
12.4 R 28	Soft	0.622	0.944	8.614	0.980	0.551	7.58	0.972
12.4 R 28	Medium	0.653	0.946	8.522	0.975	0.586	8.142	0.980
12.4 R 28	Hard	0.655	0.946	8.527	0.979	0.593	8.249	0.970
13.6 R 28	Soft	0.595	0.941	8.793	0.975	0.518	7.368	0.977
13.6 R 28	Medium	0.652	0.943	8.432	0.973	0.584	7.911	0.982
13.6 R 28	Hard	0.656	0.944	8.481	0.984	0.592	8.174	0.985
14.9 R 28	Soft	0.603	0.941	8.524	0.972	0.528	7.118	0.975
14.9 R 28	Medium	0.652	0.944	8.430	0.982	0.581	7.945	0.978
14.9 R 28	Hard	0.658	0.945	8.481	0.982	0.593	8.178	0.976
16.9 R 28	Soft	0.586	0.942	8.782	0.978	0.504	7.327	0.971
16.9 R 28	Medium	0.643	0.949	8.783	0.981	0.585	7.856	0.984
16.9 R 28	Hard	0.654	0.945	8.539	0.981	0.594	8.044	0.983

Table C-8 Regression coefficients for prediction of tyre performance under varying normal load

Tyre	Load (N)	GTR Model				COT Model		
		C_3	C_4	C_5	R^2	C_1	C_2	R^2
12.4 R 28	7358	0.649	0.945	8.537	0.981	0.585	8.095	0.976
12.4 R 28	9320	0.650	0.945	8.339	0.982	0.586	7.665	0.980
12.4 R 28	11282	0.648	0.940	8.149	0.982	0.584	7.353	0.961
13.6 R 28	9320	0.652	0.942	8.286	0.983	0.592	7.593	0.978
13.6 R 28	11282	0.633	0.943	8.645	0.977	0.560	8.021	0.972
13.6 R 28	13244	0.623	0.943	8.603	0.985	0.552	7.644	0.953
14.9 R 28	11282	0.648	0.941	8.371	0.984	0.579	7.869	0.981
14.9 R 28	13734	0.641	0.945	8.437	0.979	0.574	7.673	0.966
14.9 R 28	16187	0.642	0.940	8.121	0.984	0.576	7.198	0.953
16.9 R 28	14225	0.644	0.944	8.411	0.986	0.585	7.486	0.972
16.9 R 28	16677	0.621	0.948	8.901	0.983	0.551	8.001	0.948
16.9 R 28	19130	0.596	0.949	9.359	0.978	0.518	8.295	0.931

Table C-9 Regression coefficients for prediction of tyre performance under varying tyre deflection

Tyre	Deflection (%)	GTR Model				COT Model		
		C_3	C_4	C_5	R^2	C_1	C_2	R^2
12.4 R 28	20	0.646	0.946	8.395	0.980	0.582	7.635	0.968
12.4 R 28	24	0.651	0.940	8.215	0.982	0.583	7.692	0.973
12.4 R 28	28	0.651	0.943	8.386	0.985	0.591	7.782	0.984
13.6 R 28	20	0.624	0.943	8.619	0.976	0.551	7.775	0.955
13.6 R 28	24	0.628	0.944	8.722	0.982	0.555	8.007	0.971
13.6 R 28	28	0.650	0.942	8.293	0.985	0.589	7.548	0.981
14.9 R 28	20	0.639	0.943	8.344	0.985	0.572	7.471	0.953
14.9 R 28	24	0.637	0.943	8.466	0.978	0.565	7.804	0.962
14.9 R 28	28	0.651	0.943	8.319	0.984	0.588	7.614	0.980
16.9 R 28	20	0.651	0.945	8.944	0.979	0.546	7.881	0.939
16.9 R 28	24	0.617	0.950	8.981	0.982	0.549	7.919	0.944
16.9 R 28	28	0.630	0.943	8.621	0.977	0.562	7.822	0.960

Table C-10 Regression coefficients to study the effect of tyre size at constant deflection of 24 per cent

Tyre	Type of soil	GTR Model				COT Model		
		C_3	C_4	C_5	R^2	C_1	C_2	R^2
12.4 R 28	Soft	0.627	0.939	8.294	0.981	0.550	7.354	0.976
13.6 R 28		0.607	0.941	8.500	0.985	0.528	7.227	0.983
14.9 R 28		0.596	0.941	8.748	0.983	0.512	7.532	0.976
16.9 R 28		0.582	0.942	8.857	0.982	0.497	7.359	0.974

Table C-11 Univariate analysis of variance to see the effect of cone index (CI) and coefficient of traction (COT) on slip (S) and tractive efficiency (TE) for tyre tyre T_1 (12.4 R 28)

Source	DF	Dependent Variables					
		Slip (S)			Tractive efficiency (TE)		
		Sum of Squares	Mean Square	F	Sum of Squares	Mean Square	F
COT	14	1.315	0.094	677.164 *	6.070	0.434	1.064E3*
CI	2	0.048	0.024	173.082 *	0.486	0.243	595.541*
COT×CI	28	0.031	0.001	7.906 *	0.009	0.000	0.749
Error	360	0.050	0.000		0.147	0.000	

* Significant at 5 per cent level

Table C-12 Univariate analysis of variance to see the effect of cone index (CI) and coefficient of traction (COT) on slip (S) and tractive efficiency (TE) for tyre T_2 (13.6 R 28)

Source	DF	Dependent Variables					
		Slip (S)			Tractive efficiency (TE)		
		Sum of Squares	Mean Square	F	Sum of Squares	Mean Square	F
COT	14	1.472	0.105	394.293 *	6.025	0.430	841.964 *
CI	2	0.088	0.044	164.956 *	0.648	0.324	634.082 *
COT×CI	28	0.065	0.002	8.738 *	0.024	0.001	1.669 *
Error	360	0.096	0.000		0.184	0.001	

* Significant at 5 per cent level

Table C-13 Univariate analysis of variance to see the effect of cone index (CI) and coefficient of traction (COT) on slip (S) and tractive efficiency (TE) for tyre T_3 (14.9 R 28)

Source	DF	Dependent Variables					
		Slip (S)			Tractive efficiency (TE)		
		Sum of Squares	Mean Square	F	Sum of Squares	Mean Square	F
COT	14	1.537	0.110	416.403 *	5.990	0.428	771.023 *
CI	2	0.110	0.055	208.762 *	0.733	0.367	660.738 *
COT×CI	28	0.078	0.003	10.498 *	0.029	0.001	1.839 *
Error	360	0.095	0.000		0.200	0.001	

* Significant at 5 per cent level

Table C-14 Univariate analysis of variance to see the effect of cone index (CI) and coefficient of traction (COT) on slip (S) and tractive efficiency (TE) for tyre T_4 (16.9 R 28)

Source	DF	Dependent Variables					
		Slip (S)			Tractive efficiency (TE)		
		Sum of Squares	Mean Square	F	Sum of Squares	Mean Square	F
COT	14	1.702	0.122	339.695 *	5.929	0.423	699.196 *
CI	2	0.164	0.082	229.647 *	0.902	0.451	744.493 *
COT×CI	28	0.130	0.005	12.956 *	0.059	0.002	3.463 *
Error	360	0.129	0.000		0.218	0.001	

* Significant at 5 per cent level

Table C-15 Univariate analysis of variance to see the effect of normal load (W) and coefficient of traction (COT) on slip (S) and tractive efficiency (TE) for tyre T_1 (12.4 R 28)

Source	DF	Dependent Variables					
		Slip (S)			Tractive efficiency (TE)		
		Sum of Squares	Mean Square	F	Sum of Squares	Mean Square	F
COT	14	1.315	0.094	305.078 *	6.070	0.434	282.162 *
W	2	0.010	0.005	16.452 *	0.085	0.042	27.564 *
COT×W	28	0.008	0.000	0.892	0.003	0.000	0.068
Error	360	0.111	0.000		0.553	0.002	

* Significant at 5 per cent level

Table C-16 Univariate analysis of variance to see the effect of normal load (W) and coefficient of traction (COT) on slip (S) and tractive efficiency (TE) for tyre T_2 (13.6 R 28)

Source	DF	Dependent Variables					
		Slip (S)			Tractive efficiency (TE)		
		Sum of Squares	Mean Square	F	Sum of Squares	Mean Square	F
COT	14	1.472	0.105	171.545 *	6.025	0.430	202.063 *
W	2	0.015	0.007	11.921 *	0.083	0.041	19.426 *
COT×W	28	0.014	0.000	0.813	0.007	0.000	0.111
Error	360	0.221	0.001		0.767	0.002	

* Significant at 5 per cent level

Table C-17 Univariate analysis of variance to see the effect of normal load (W) and coefficient of traction (COT) on slip (S) and tractive efficiency (TE) for tyre T_3 (14.9 R 28)

Source	DF	Dependent Variables					
		Slip (S)			Tractive efficiency (TE)		
		Sum of Squares	Mean Square	F	Sum of Squares	Mean Square	F
COT	14	1.537	0.110	157.633 *	5.990	0.428	179.463 *
W	2	0.018	0.009	12.720 *	0.097	0.049	20.380 *
COT×W	28	0.014	0.001	0.720	0.006	0.000	0.093
Error	360	0.251	0.001		0.858	0.002	

* Significant at 5 per cent level

Table C-18 Univariate analysis of variance to see the effect of normal load (W) and coefficient of traction (COT) on slip (S) and tractive efficiency (TE) for tyre T_4 (16.9 R 28)

Source	DF	Dependent Variables					
		Slip (S)			Tractive efficiency (TE)		
		Sum of Squares	Mean Square	F	Sum of Squares	Mean Square	F
COT	14	1.702	0.122	113.696 *	5.929	0.423	140.703 *
W	2	0.020	0.010	9.312 *	0.086	0.043	14.205 *
COT×W	28	0.018	0.001	0.608	0.010	0.000	0.114
Error	360	0.385	0.001		1.083	0.003	

* Significant at 5 per cent level

Table C-19 Univariate analysis of variance to see the effect of deflection (δ / h) and coefficient of traction (COT) on slip (S) and tractive efficiency (TE) for tyre T_1 (12.4 R 28)

Source	DF	Dependent Variables					
		Slip (S)			Tractive efficiency (TE)		
		Sum of Squares	Mean Square	F	Sum of Squares	Mean Square	F
COT	14	1.315	0.094	271.976 *	6.070	0.434	250.406 *
δ / h	2	0.002	0.001	3.341 *	0.017	0.008	4.793 *
COT× δ / h	28	0.002	7.2E-5	0.209	0.001	3.2E-5	0.018
Error	360	0.124	0.000		0.623	0.002	

* Significant at 5 per cent level

Table C-20 Univariate analysis of variance to see the effect of tyre deflection (δ / h) and coefficient of traction (COT) on slip (S) and tractive efficiency (TE) for tyre T_2 (13.6 R 28)

Source	DF	Dependent Variables					
		Slip (S)			Tractive efficiency (TE)		
		Sum of Squares	Mean Square	F	Sum of Squares	Mean Square	F
COT	14	1.472	0.105	158.12 *	6.025	0.430	186.799 *
δ / h	2	0.005	0.002	3.609 *	0.024	0.012	5.236 *
COT$\times \delta / h$	28	0.005	0.000	0.270	0.003	9.2E-5	0.040
Error	360	0.239	0.001		0.829	0.002	

* Significant at 5 per cent level

Table C-21 Univariate analysis of variance to see the effect of tyre deflection (δ / h) and coefficient of traction (COT) on slip (S) and tractive efficiency (TE) for tyre T_3 (14.9 R 28)

Source	DF	Dependent Variables					
		Slip (S)			Tractive efficiency (TE)		
		Sum of Squares	Mean Square	F	Sum of Squares	Mean Square	F
COT	14	1.537	0.110	144.777 *	5.990	0.428	165.052 *
δ / h	2	0.005	0.003	3.450 *	0.027	0.013	5.113 *
COT$\times \delta / h$	28	0.004	0.000	0.201	0.002	6.9E-5	0.027
Error	360	0.273	0.001		0.933	0.003	

* Significant at 5 per cent level

Table C-22 Univariate analysis of variance to see the effect of tyre deflection (δ / h) and coefficient of traction (COT) on slip (S) and tractive efficiency (TE) for tyre T_4 (16.9 R 28)

Source	DF	Dependent Variables					
		Slip (S)			Tractive efficiency (TE)		
		Sum of Squares	Mean Square	F	Sum of Squares	Mean Square	F
COT	14	1.702	0.122	107.224 *	5.929	0.423	133.545 *
δ / h	2	0.008	0.004	3.490 *	0.033	0.017	5.270 *
COT$\times \delta / h$	28	0.007	0.000	0.219	0.004	0.000	0.041
Error	360	0.408	0.001		1.142	0.003	

* Significant at 5 per cent level

Table C-23 Univariate analysis of variance to see the effect of tyre size (b/d) and coefficient of traction (COT) on slip (S) and tractive efficiency (TE) under soft soil condition at 22 per cent tyre deflection

Source	DF	Dependent Variables					
		Slip (S)			Tractive efficiency (TE)		
		Sum of Squares	Mean Square	F	Sum of Squares	Mean Square	F
COT	14	6.012	0.429	618.306 *	24.007	1.715	735.504 *
(b/d)	3	0.018	0.006	8.476 *	0.104	0.035	14.893 *
COT × (b/d)	42	0.014	0.000	0.487	0.006	0.000	0.061
Error	1560	1.083	0.001		3.637	0.002	

* Significant at 5 per cent level

APPENDIX-D

TERMS USED IN THE STATISTICAL ANALYSIS

1. Percent deviation measures the degree to which the predicted value differs from the observed value.

$$D = \frac{s - o}{o} \times 100$$

2. Model efficiency (E): The Model efficiency is a normalized statistic that determines the relative magnitude of the residual variance ("noise") compared to the measured data variance. It indicates how well the plot of observed versus simulated data fits the 1:1 line. It is computed as:

$$E = 1 - \frac{\sum_{i=1}^{N} (o_i - s_i)^2}{\sum_{i=1}^{N} \left(o_i - o_{avg}\right)^2}$$

Model efficiency ranges between $-\infty$ and 1, with E = 1 being the optimal value. Values between 0.0 and 1.0 are generally viewed as acceptable levels of performance, whereas values <0.0 indicates that the mean observed value is a better predictor than the simulated value, which indicates unacceptable performance.

3. Percent Bias (PBIAS) measures the average tendency of the simulated data to be larger or smaller than their observed counterparts. The optimal value of PBIAS is 0.0, with low-magnitude values indicating accurate model simulation. Positive values indicate model underestimation bias, and negative values indicate model overestimation bias. It is computed as:

$$PBIAS = \frac{\sum_{i=1}^{N} \left(o_i - s_i\right)}{\sum_{i=1}^{N} o_i} \times 100$$

4. Root mean squared error - The RMSE measures the average magnitude of the error. It is the difference between observed and corresponding predicted values are each squared and then averaged over the sample. Finally, the square root of the

average is taken. Since the errors are squared before they are averaged, the RMSE gives a relatively high weight to large errors. This means the RMSE is most useful when large errors are particularly undesirable. It is computed as:

$$RMSE = \frac{\sqrt{\frac{\sum_{i=1}^{N}(o_i - s_i)^2}{N}}}{o_{avg}} \times 100$$

5. Coefficient of determination (R^2) describes the degree of collinearity between simulated and measured data. The coefficient of determination describes the proportion of the variance in measured data explained by the model. R^2 ranges from 0 to 1, with higher values indicating less error variance. It is computed as

$$R^2 = \left(\frac{\sum_{i=1}^{N}\left[o_i - o_{avg}\right]\left[s_i - s_{avg}\right]}{\left[\sum_{i=1}^{N}\left(o_i - o_{avg}\right)^2\right]^{0.5}\left[\sum_{i=1}^{N}\left(s_i - s_{avg}\right)^2\right]^{0.5}} \right)^2$$

where, s = simulated value,

o = observed value and

N = no. of observations.